Novel Biomarkers in Cyclophosphamide and Mycophenolic Acid Therapy of SLE

Minghan Yong

A thesis submitted in fulfilment of the requirements for the degree of
Doctor of Philosophy in Biomedical Science,
The University of Auckland, 2023.

Abstract

Systemic lupus erythematosus (SLE) pathogenesis is a cycle of inflammation and immune complex formation with damage to tissues such as the kidneys, resulting in lupus nephritis (LN). Cyclophosphamide and mycophenolic acid (MPA) are used to control disease flares but drug choice remains arbitrary. This thesis aims to assess both drugs *in vitro* to understand the factors which could influence inter-individual differences in patient response and potentially guide the initial treatment choice.

Conversion of cyclophosphamide intermediate 4-hydroxycyclophosphamide (4-OHCP) to the DNA-alkylating metabolite phosphoramide mustard (PAM) is assumed to occur spontaneously via chemical hydrolysis. Using a quantitative PCR-block (QPCR-block) assay to detect PAM-induced DNA adducts, enzyme catalysis of this reaction was shown in peripheral blood mononuclear cells (PBMC). Human cAMP-phosphodiesterase 4B2 was identified as a candidate for this catalysis *in vitro* (increased gDNA alkylation, $p = 0.0406$).

Differences in repair of PAM-induced DNA adducts could also influence therapeutic response to cyclophosphamide. A small clinical study of the extent of PAM-induced DNA damage between healthy individuals and LN patients was undertaken using the QPCR-block assay. LN patients (n = 16) were significantly ($p = 0.0319$) more sensitive to PAM than healthy individuals (n = 13), and four LN patients were particularly sensitive.

MPA prevents lymphocyte proliferation by inosine monophosphate dehydrogenase (IMPDH) inhibition. Assessment of radiolabelled MPA transport and kinetics into a T-cell line (Jurkat) demonstrated partially sodium-dependent active uptake (V_{max} 8540 ± 1180 pmol.min^{-1}.10^6 cells^{-1}, K_m 478 ± 116 µM). IMPDH inhibition was quantified through HPLC (optimised and validated here). Despite intracellular MPA accumulation, there were clear time-dependent rebounds in IMPDH activity. The EC_{50} increased more than 40-fold in 20-minute incubations, and by 240 minutes there was no inhibition.

Database analyses were undertaken to explore determinants of variable *IMPDH* expression. Females were found to have higher expression of *IMPDH1* in whole blood ($p < 0.01$) but lower expression in spleen ($p < 0.01$) compared to males. Higher *IMPDH1* than *IMPDH2* in myeloid cells but vice versa in lymphoid were observed. The *in vitro* behaviours observed for both drugs at their respective targets have identified potential sources of biomarkers which could be used to select a drug for patients.

Acknowledgements

First and foremost, I would like to express my deepest gratitude to my supervisor, Associate Professor Nuala Helsby, without whom this thesis would not be possible. Her passion, enthusiasm and perseverance have kept me going even when I thought I could not.

I would also like to thank my other supervisors Dr Kathryn Burns, whose unwavering support and belief in me has been invaluable, and Dr Janak de Zoysa, whose encouragement and nurturing attitude have immensely helped. None of the work in this thesis would have been completed without them.

I am very grateful for the support of Dr Tze-Liang Goh. His commitment to the REPAIR study as well as his interest in the MPA portion of this thesis have been very helpful. My thanks also to Professor Malcolm Tingle and Dr Jacqueline Hannam, whose help with the HPLC and suggestions for research direction have aided in my progress. Thank you to Susan Pullen, whose help with Jurkat cells and with materials in the QPCR assay has been indispensable.

Thank you to the Helsby and Tingle labs for being the best support network anyone could ask for. In particular, thanks to Soo Hee, Maia, Juno, Rachael, Kim, Umaiyaall, Ellen, Philippa, James and Conor for their friendship, advice and help in my experiments. I would also not have been able to conduct any experiments without the tremendous help from Mike and Sree in the lab, thank you.

Thank you to the patients and volunteers who have participated in the REPAIR study, their enthusiasm and support for my work have been one of the reasons I have been able to push through.

I would also like to express my greatest gratitude to my family and friends, who have supported me throughout these years, especially Matthew, Christian and Jez. Above everything, thank you to Darrel, Mum, Hanting and Yuanyun, this would not have been possible without you.

Table of Contents

List of Figures

List of Tables

List of Abbreviations and Definitions

[drug]	drug concentration
[Inhibitor]	inhibitor concentration
°C	degrees Celsius
λDNA	lambda DNA standard
γH2Ax	gamma histone family member X
µCi	microCurie
µg	microgram
µL	microlitre
µM	micromolar
µm	micrometre
4-OHCP	4-hydroxycyclophosphamide
4-OOHCP	4-hydroperoxycyclophosphamide
8-oxoGua	8-oxo-7,8-dihydroguanine
A_{avg}	average IMPDH activity
ABC	ATP-binding casette
AcMPAG	acyl glucuronide mycophenolic acid
ADP	adenosine diphosphate
AEC	area under the effect curve
AICc	small sample-corrected Akaike information criterion
ALDH	aldehyde dehydrogenase
AMP	adenosine monophosphate
ANCA	antineutrophilic cytoplasmic antibody
ANOVA	analysis of variance
API	application programming interface
ARCHS4	All RNA-seq and ChIP-seq sample and signature search database
ATM	ataxia-telangiectasia mutated
ATP	adenosine triphosphate
AUC	area under curve
AUEC	area under the time-effect curve
BLK	b lymphocyte kinase
BLM	bloom syndrome
BRCA	breast cancer
$CaCl_2$	calcium chloride
Caco-2	*cancer coli* "colon cancer"
cAMP	cyclic adenosine monophosphate
CAR-T	chimeric antigen receptor-T cell
CD25(+/-)	cluster of differentiation 25 (positive/negative)
CD4(+/-)	cluster of differentiation 4 (postive/negative)
CD8(+/-)	cluster of differentiation 8 (positive/negative)
CES	carboxylesterase
cGMP	cyclic guanosine monophosphate
C_{max}	maximum concentration
C_{min}	minimum or trough concentration
CO_2	carbon dioxide
COMET	single cell gel electrophoresis assay
CPD	cyclobutene pyrimidine dimers
CsA	cyclosporin A

CYP	cytochrome P450
DAMP	damage associated molecular patterns
dATP	deoxyadenosine triphosphate
dGTP	deoxyguanosine triphosphate
DNA	deoxyribonucleic acid
DPM	disintegrations per minute
dsDNA	double-stranded DNA
E. coli	*Escherichia coli*
EC_{50}	half maximal effect concentration
EDTA	ethylenediaminetetraacetic acid
E_{max}	maximal effect
eQTL	expression quantitative trait loci
ERCC	excision repair cross complentation group
E-XMP*	enzyme-bound thiomidate intermediate
FANC	Fanconi anaemia
FANG5	functional annotation of mammalian genomes 5
FBS	foetal bovine serum
G	gravitational acceleration force
G(1/2)	growth (1/2)
gDNA	genomic DNA
GDP	guanosine diphosphate
GI	gastrointestinal
GluMPA	mycophenolic acid-phenyl glucoside
GMP	guanosine monophosphate
GST	glutathione S-transferase
GTEx	Genotype-Tissue Expression database
H	hours
H_2O	water
HCl	hydrochloric acid
HEK293	human embryonic kidney 293
HEPES	N-2-hydroxyethylpiperazine-N-2-ethane sulfonic acid
HPA	Human Protein Atlas
HPLC	high performance liquid chromatography
HSCT	haematopoietic stem cell transplant
IC_{50}	half maximal inhibitory concentration
ICOS	inducible T-cell costimulator
ID	identity
IFN-γ	interferon gamma
Ig	immunoglobulin
IL	interleukin
IMP	inosine monophosphate
IMPDH	inosine monophosphate dehydrogenase
INT	iodonitrotetrazolium
IQR	inter-quartile range
ITGAM	integrin subunit alpha M
ITGAX	integrin alpha X
Kb	kilobases
K_{cat}	first order catalytic rate constant
KCl	potassium chloride
kDa	kilodalton

KH_2PO_4	potassium dihydrogen phosphate
K_i	inhibitor constant
K_m	substrate concentration at half maximal velocity
KU70	XRCC6 gene
LCMS	liquid chromatography-mass spectrometry
LLOQ	lower limit of quantification
LN	lupus nephritis
M	molar
MAIT	mucosal-associated invariant T-cells
mCi	milliCurie
MEMα	minimum essential media alpha
mg	milligram
$MgSO_4$	magnesium sulphate
MHC	major histocompatibility complex
MilliQ	water purified with Milli-Q water purification system
min	minutes
mL	millilitre
mM	millimolar
mm	millimetre
MMF	mycophenolate mofetil
MPA	mycophenolic acid
MPAG	mycophenolic acid-7-O-glucuronide
mRNA	messenger RNA
MRP2	multidrug resistance-associated protein 2
n/N	number of replicates/individuals
NaCl	sodium chloride
NAD^+	nicotinamide adenine dinucleotide
NADH	nicotinamide adenine dinucleotide hydrogen
NaH_2PO_4	sodium dihydrogen phosphate
NaOH	sodium hydroxide
ND	not determined
NER	nucleotide excision repair
NET	neutrophil extracellular traps
NETosis	formation of NET
Ng	nanogram
nM	nanomolar
Nm	nanometre
nmol	nanomole
NOD	non-obese diabetic
NZ	New Zealand
OATP	organic anion transporting polypeptides
p	*p*-value
P	probability
PAM	phosphoramide mustard
PARP	poly (ADP-ribose) polymerase
PBMC	peripheral blood mononuclear cells
PBS	phosphate-buffered saline
PCR	polymerase chain reaction
PDE	phosphodiesterase
PD-L	programmed death ligand

P-gp	p-glycoprotein
pmol	picomole
P-O-C	phosphoester bond
POLB	DNA polymerase beta
PTCy	post-transplant cyclophosphamide
pTPM	protein-coding transcripts per million
PTPN22	protein tyrosine phosphatase non-receptor type 22
QPCR-block	quantitative PCR-block
QQ	quantile-quantile
r^2	coefficient of determination
RNA	ribonucleic acid
ROS	reactive oxygen species
S	seconds
S	synthesis
SD	standard deviation
SDS	sodium dodecyl sulphate
SLC	solute carrier
SLE	systemic lupus erythematosus
SNP	single nucleotide polymorphisms
sQTL	splicing quantitative trait loci
TBAS	tetrabutylammonium hydrogen sulphate
TCI	target concentration intervention
TDM	therapeutic drug monitoring
TLC	thin layer chromatography
TNF	tumour necrosis factor
TPM	transcripts per million
T_{reg}	regulatory T-cell
TREX1	three prime exonuclease 1
Tris	Tris base
UGT	uridine diphosphate-glucuronosyltransferase
UV	ultraviolet
V	version
v/v	volume to volume
Vmax	maximal velocity
Vs	versus
XMP	xanthosine monophosphate
XP(C/F/G)	xeroderma pigmentosum complementation group (C/F/G)
XRCC	X-ray repair cross complemention group

Chapter 1: Introduction

1.1. Autoimmune disease

Autoimmune diseases are characterised by abnormal immune response to tissues and include diseases such as systemic lupus erythematosus (SLE), vasculitis and membranous nephropathy. The involvement of the immune system results in a complex and multifactorial nature of these diseases. SLE is widely considered to be the prototypical autoimmune disease, due to its complex nature and because many of its symptoms are shared with other autoimmune diseases. In particular, SLE has proven to be a difficult disease to treat, often progressing to more serious complications such as kidney damage, known as lupus nephritis. The exact cause of SLE is not known but SLE is believed to arise from complex interactions between genetic and environmental factors. Globally, SLE affects 43.7 in 100,000 persons, although this varies substantially between countries and ethnicities.

In a recent study of SLE epidemiology in Aotearoa (Lao et al., 2023), SLE has a similar prevalence as in European countries. However, there were notable disparities between different ethnicities. The prevalence of SLE in Pasifika was the highest and was three times higher than in Europeans who had the lowest SLE prevalence. In contrast, Māori and Asian SLE prevalence was twice that of Europeans.

The increased prevalence of SLE in both Māori and Pasifika contributes to the disproportionately larger burden of disease experienced by both ethnic groups compared to other ethnicities (Gurney et al., 2020), which in turn leads to substantially worse health outcomes. Hence, investigation of factors which influence therapeutic outcomes in SLE especially in Aotearoa's most vulnerable populations could address some of these inequities.

1.1.1. Hallmarks of SLE

Clinical manifestations of SLE include inflammatory skin rashes, arthritis, haematologic disorders such as leukopenia, as well as kidney damage (lupus nephritis) (Lahita, 2011). The aetiology of these symptoms is the formation and deposition of immune complexes in tissues. These immune complexes, which are comprised of autoantibodies (antibodies specific to the body's own proteins) and self-antigens (complexes of normal protein present in the body), invariably trigger pro-inflammatory cytokine cascades, leading to inflammation and tissue damage (Podolska et al., 2015). The production of autoantibodies and self-antigens are therefore central hallmarks of SLE.

The exact pathogenesis of SLE has not been elucidated and is thought to be a combination of genetic predisposition and numerous environmental factors including UV (sun) exposure. Abnormal function of genes that have been implicated in SLE pathogenesis include genes involved in B- and T-cell signalling and maturation such as *PTPN22* (Al-Awadhi et al., 2018) and *BLK* (Harley et al., 2008), immune function such as *ITGAM* and *ITGAX* (Hom et al., 2008), and DNA damage recognition and repair such as *XPC* (Souliotis et al., 2016), *PARP* (Cerboni et al., 2009; Sibley et al., 1989), *POLB* (Senejani et al., 2014) and various *XRCC* isoforms (Jahantigh et al., 2015).

Abnormal lymphocyte maturation can lead to an overactive immune system and a loss in tolerance, which has been thought to be a trigger in SLE. For example, *PTPN22* has been extensively researched and is implicated in the pathogenesis of numerous autoimmune diseases including SLE. *PTPN22* encodes a lymphoid cytoplasmic phosphatase which inhibits T-cell receptor signalling (Chung & Criswell, 2007). A gain of function polymorphism for *PTPN22* (rs2476601) has been associated with SLE patients and is speculated to result in suppression of T_{reg} production, allowing autoreactive T- and B-cells to circulate (Bottini et al., 2006).

Variation in genes such as *ITGAM* may also aid in the development of SLE through enhancement of innate immune response. *ITGAM* produces a membrane protein that mediates adhesion between numerous immune cells such as neutrophils. Increased production of this protein may enhance the immune response in SLE and autoimmunity. In SLE patients, elevated *ITGAM* expression has been observed in the neutrophils (Buyon et al., 1988).

The role for impaired DNA damage-repair efficiency in the pathogenesis of SLE has only been elucidated relatively recently. Defective DNA damage recognition and repair may accelerate the production of self-antigens, exacerbating immune complex formation. Various studies have also observed associations with gene variants of the numerous proteins involved in the pathways of recognition and repair of damaged DNA (Lee et al., 2011; *reviewed in* Mireles-Canales et al., 2018). This is supported, in part, by the hypothesis that UV exposure and its subsequent DNA damage in the skin is an important environmental stimulus for SLE manifestation.

Based on wavelength, solar UV radiation can be classified into UV-A (315-400 nm), UV-B (280-315 nm) and UV-C (<280 nm) (Sinha & Häder, 2002). However, the majority of solar UV-B and all of UV-C radiation is absorbed by the ozone layer (Madronich et al., 1998). These different classes of UV radiation also damage DNA differently. Relative to UV-B and UV-C, UV-A radiation is absorbed poorly by native DNA (Sutherland & Griffin, 1981). Instead, UV-A mostly indirectly damages DNA through the generation of reactive oxygen species (ROS) such as hydrogen peroxide (Petersen et al., 2000), singlet molecular oxygen and hydroxyl radicals (Cadet et al., 2009). The predominant lesions observed in UV-A-induced DNA damage are thymine-thymine cyclobutene pyrimidine dimers (CPD) formed by direct absorption of UV-A (Girard et al., 2011) and 8-oxo-7,8-dihydroguanine (8-oxoGua) formed by ROS reaction (Cadet et al., 2009). In contrast, UV-B and UV-C radiation is readily absorbed by native DNA. The DNA damage caused by UV-B and UV-C is thus mainly in the form of CPDs between

cytosine and thymine as well as 6-4 pyrimidine-pyrimidone photoproducts (Rastogi et al., 2010). Of these UV-induced lesions, the CPD and 6-4 pyrimidine-pyrimidone photoproducts are mainly repaired (in mammals) by the nucleotide excision repair (NER) system (Marteijn et al., 2014). Repair of this type of DNA damage is initiated by either transcription coupled repair or global genome repair, the latter process is considered to be predominant in skin keratinocytes.

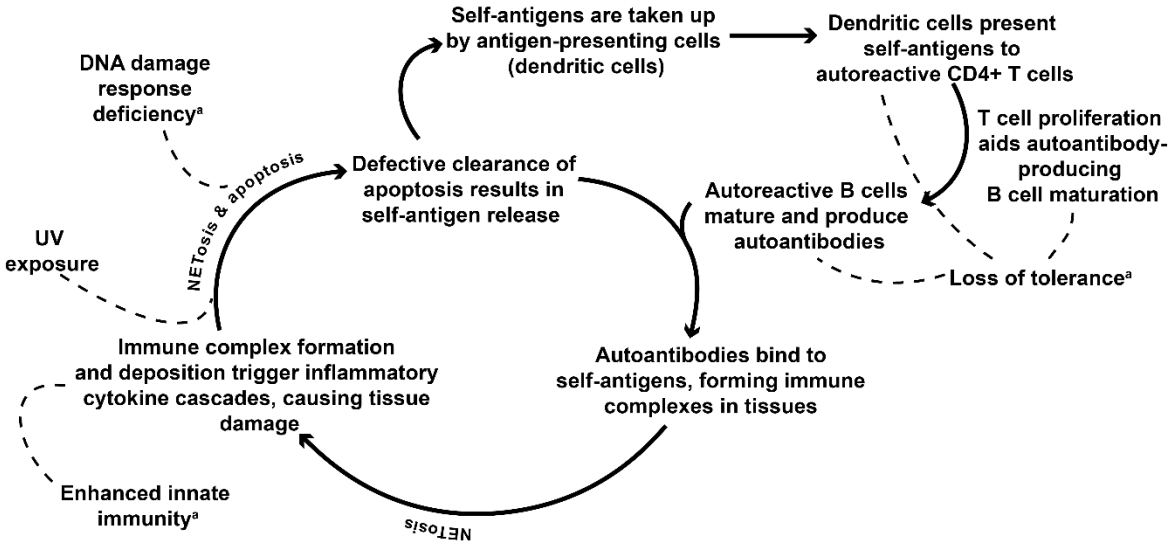

Figure 1-1. Genetic predisposition and environmental factors such as UV exposure serve as entry points into the self-propagating cycle of autoimmunity in SLE. SLE patients possess genetic factors that aid the production of autoantibodies and self-antigens. Environmental factors such as UV exposure cause tissue damage that persists in SLE patients. [a]Genetic predisposition factors

Hence, environmental factors such as UV exposure combined with genetic predisposition may provide entry into the self-propagating autoimmune cycle in SLE (Figure 1-1). UV exposure results in DNA damage, which might persist in SLE patients due to impaired DNA damage repair capacity. Persistent DNA damage in cells could then result in production of self-antigens due to defective apoptotic processes. The presentation of self-antigens ultimately triggers production of autoantibodies to nuclear material, due to a loss of tolerance. This leads to the deposition of immune complexes in tissues with subsequent inflammation and organ damage. This damage results in the further production of self-antigens.

The abnormal production of self-antigens is an important step in the SLE cycle. These self-antigens are produced through insufficient immune clearance. Apoptosis is a controlled cell death process which utilises phagocytic activity to remove cell debris and avoid activation of the immune system (Kerr et al., 1972). It is postulated that in SLE, the apoptotic process of cells is impaired (Bijl et al., 2001; Gaipl et al., 2007; Munoz et al., 2008). This has been

observed in SLE cells (Shao & Cohen, 2011). Furthermore, these apoptotic cells were demonstrated to be pro-inflammatory in the presence of autoantibodies, leading to additional production of autoantibodies and inflammatory cytokines. After apoptosis, these cells were not cleared. Instead, this leads to necrosis, resulting in an accumulation of cellular debris no longer bound by membranes. Accumulation of these damage associated molecular patterns (DAMP) aids the activation of dendritic cells, which take up antigenic material, such as DNA, and presents to $CD4^+$ T-cells (Choi et al., 2012; Fransen et al., 2010). The T-cells are then activated and trigger the proliferation of autoreactive B-cells, ultimately leading to autoantibody production specific to the antigen presented by dendritic cells.

Autoantibodies range from anti-DNA antibodies (Rekvig et al., 2004) to anti-RNA-protein antibodies (Lerner & Steitz, 1979). These antibodies are antinuclear antibodies which have become a mainstay of serological testing criteria for SLE diagnosis (Tan et al., 1982). The production of autoantibodies in SLE can be attributed to the loss of tolerance in the immune system, leading to an increase of autoreactive B-cells. These autoreactive B-cells produce autoantibodies which then form immune complexes with self-antigens. The deposition of immune complexes in tissues then leads to tissue and organ damage.

A key process involved in the autoimmunity observed in SLE is the formation of neutrophil extracellular traps (NETosis). NETosis in healthy patients is a mechanism used by neutrophils to bind foreign agents such as bacteria or viruses and kill them. The process involves the release of granular protein and chromatin from the neutrophils to form an extracellular network (Brinkmann et al., 2004). This traps the microorganisms and prevents them from spreading. Due to the release of DNA into extracellular fluid, NETosis is tightly regulated in physiological conditions. In SLE, a pathological subpopulation of neutrophils, known as low-density granulocytes, have been observed to possess an increased capacity for NETosis (Villanueva et al., 2011). These NET mediate inflammatory pathways through increased release of

inflammatory cytokines such as IL-17 and activating inflammasomes which eventually result in the release of cytokines such as IL-1β and IL-18 (Kahlenberg et al., 2013). NETosis has also been observed to contribute to clonal expansion of autoreactive T- and B-cells through release of self-antigens. Sustained NETosis can result in the escape of self-antigens such as double-stranded DNA (dsDNA) from the trap, leading to increased selection of autoreactive lymphocytes. NETosis also contributes to autoantibody production through activation of plasmacytoid dendritic cells. In SLE, plasmacytoid dendritic cells are activated through immune complexes containing anti-microbial peptides from neutrophils such as LL-37. These dendritic cells then release type I interferon, sustaining differentiation of mature dendritic cells (Lande et al., 2011). SLE patients have also been observed to possess impaired ability to remove NET, leading to sustained autoimmunity and clinical manifestations such as lupus nephritis (Hakkim et al., 2010).

1.1.2. Lupus nephritis

A common complication of SLE is lupus nephritis, which is characterised by inflammation in the kidney. Up to 60% of SLE patients experience varying degrees of renal injury in relation to the disease (Maroz & Segal, 2013). In a recent meta-analysis, biopsy-proven lupus nephritis was found to occur in 29% of lupus patients globally (Wang et al., 2017). Higher rates have been observed in certain ethnicities, for example 40 to 82% in Asians (Bastian et al., 2002; Jakes et al., 2012). Furthermore up to 22% of lupus nephritis patients develop end stage renal disease (Tektonidou et al., 2016), which has been associated with a higher risk of mortality in SLE patients (Yap et al., 2012). Importantly, kidney failure as a result of lupus nephritis frequently requires dialysis and renal transplantation. Transplantation is not only associated with better survival but also a risk reduction in two other major mortality factors – cardiovascular disease and infection (Jorge et al., 2019).

1.1.3. Treatment of SLE

Management of SLE tends to rely on immunosuppression and anti-inflammatory agents. Current treatment of SLE is typically biphasic and consists of induction therapy to control acute disease flares followed by maintenance therapy. The choice of drugs used has remained controversial with no clear advantageous drug despite various available options (Table 1-1).

Mild SLE is usually treated with hydroxychloroquine, which is ineffective against severe SLE flares. Glucocorticoids, such as prednisone, are commonly used at the start of flares to curb excessive inflammation and tissue damage. However, corticosteroid treatment has been associated with severe adverse effects, requiring the moderation of corticosteroid use. Antimetabolites such as mycophenolic acid (MPA), azathioprine as well as cyclophosphamide, a cytotoxic DNA-alkylating drug, are also used to treat SLE to curb T- and B-cell proliferation. Recent advances have led to the increasing use of B-cell depleting therapies such as the chimeric monoclonal antibody rituximab, with varying degrees of success in SLE (Yildirim-Toruner & Diamond, 2011). Alternative treatments for SLE have been suggested, including anti-cytokine therapies such as anti-TNF or anti-IL1 therapies.

Currently, in combination with steroids, MPA or cyclophosphamide are the mainstay of induction therapy and either MPA or azathioprine utilised for long-term maintenance therapy.

	Severity of flares		
	Mild	**Severe**	
Therapy Phase	-	**Induction**	**Maintenance**
Drugs and common regimens used	Hydroxychloroquine[a] ± glucocorticoids (GC)[a]	Mycophenolic acid[b] ± GC Cyclophosphamide [c] ± GC Rituximab[d] ± GC Tacrolimus[e] ± GC Tacrolimus + Mycophenolic acid ± GC Cyclophosphamide + Cyclosporin A[e]	Mycophenolic acid Azathioprine[b] Rituximab Cyclophosphamide Tacrolimus Cyclosporin A Mycophenolic acid + Tacrolimus Cyclophosphamide + Tacrolimus

Table 1-1. Commonly used drugs and regimens for SLE. [a]Anti-inflammatory drug, [b]Antimetabolite drug (disrupts *de novo* purine biosynthesis in B- and T-cells), [c]Cytotoxic (alkylates DNA and causes inter-strand crosslinks in B- and T-cells), [d]Cytotoxic monoclonal antibody (binds to CD20 on B-cells and triggers cell death), [e]Calcineurin inhibitor (decreases T-cell production of pro-inflammatory cytokines). Abbreviations: glucocorticoids (GC).

1.2. Mycophenolic Acid

MPA is an important drug in treating SLE. Besides its role as a prominent immunosuppressant in both induction and maintenance therapy of SLE, MPA is also widely used as an immunosuppressive drug after renal transplantation to prevent graft-versus-host disease. In 2017, MPA formulated either as mycophenolate mofetil (MMF) or MPA, was administered to 97% of primary renal transplant recipients in New Zealand (*ANZDATA Registry, 42nd Report, Chapter 7: Transplantation.*, 2019). However, the substantial graft rejection rate (19%) experienced 6 months after renal transplantation suggests a considerable amount of variability in patient response to immunosuppression via MPA. This inter-individual variability in response to MPA is even more important when considering therapeutic outcomes in SLE patients with kidney failure. Since these patients are likely to have been previously treated with MPA for severe SLE, prior to further use post-renal transplantation, understanding factors which influence inter-individual variation in therapeutic response to MPA in the context of SLE and renal transplantation could aid in improving outcomes for both.

MPA was first developed for use in kidney transplant recipients in 1981 (Allison & Eugui, 1993). Discovery of the immunosuppressive properties and development of MPA for clinical use was borne out of the need to avoid genotoxic effects of the predecessor drugs such as cyclophosphamide, methotrexate and cyclosporin A. Another motivation was the desire for rapid reversibility of the immunosuppression after treatment withdrawal, which other drugs do not possess.

1.2.1. Mechanism of action

The basis of lymphocyte selectivity of MPA is the dependence of T- and B-lymphocytes on the *de novo* purine synthesis pathway. A key mechanism of the adaptive immune system is lymphocyte proliferation, which involves mitosis, and this DNA replication requires purine

synthesis. Two metabolic pathways are important in this process, the salvage pathway and the *de novo* pathway. These pathways ultimately produce deoxyguanosine triphosphate (dGTP) and deoxyadenosine triphosphate (dATP) which are substrates of DNA polymerases and allow the cell to replicate DNA during mitosis. The salvage pathway synthesises these nucleotides from guanine and adenine nucleobases and this is catalysed by hypoxanthine-guanine phosphoribosyltransferase (Murray, 1971). However, in the *de novo* pathway, inosine monophosphate is first synthesised from ribose-5-phosphate and ATP. This is catalysed by 5-phosphoribosyl-1-pyrophosphate synthetase. Inosine monophosphate is then converted to guanosine monophosphate by inosine monosphosphate dehydrogenase (IMPDH) and subsequently to dGTP (Kornberg et al., 1955). Lymphocytes rely heavily on the *de novo* pathway for purine synthesis and do not require the salvage pathway (Allison et al., 1977). In contrast, other cell types derive purines mainly through salvage pathways.

MPA is a non-competitive and reversible inhibitor of IMPDH, thereby targeting the *de novo* pathway to allow selective depletion of lymphocytes over other proliferating cells. Importantly, there are two isoforms of IMPDH: type 1 and 2. MPA has a lower K_i for type 2 than type 1 (Carr et al., 1993). IMPDH1 is expressed in most tissues and is thought to be constitutively expressed as a housekeeping isoform of IMPDH. IMPDH2 is also expressed in most tissues, with relatively low expression in peripheral blood mononuclear cells (PBMC) compared with *IMPDH1* expression (Nagai et al., 1992; Jain et al., 2004). However, IMPDH2 mRNA and protein levels have been found to increase substantially in mitogen stimulated PBMC and immortalised cell lines (Nagai et al., 1992; Jain et al., 2004). Hence, MPA possesses a two-step selectivity for it inhibits the *de novo* synthesis of purines, the exclusive pathway for these nucleotides in these immune cells and has a high affinity for IMPDH2 that has increased expression in proliferating lymphocytes. Ultimately, this depletion of purine synthesis leads to inhibition of DNA replication, G_1-S arrest and quiescence of stimulated lymphocytes.

1.2.2. Pharmacokinetics

MPA is often administered orally in the form of the ester prodrug mycophenolate mofetil (MMF), which is hydrolysed by carboxylesterases (CES- 1 and CES-2) in the GI tract and liver (Fujiyama et al., 2010) to form the pharmacologically active MPA. However, more than 90% of the administered dose is eliminated in the urine (Bullingham et al., 1998). Most of the MPA that is excreted in the urine is in the glucuronidated form as MPA-7-O-glucuronide (MPAG), which is the main metabolite formed. Furthermore, the majority of circulating MPA and MPAG is bound to plasma proteins (Langman et al., 1994). Additionally, after ^{14}C-labelled MPA administration to whole blood *ex vivo* and separation into plasma, PBMC and erythrocyte fractions, 0.01% of the dose was found in the PBMC (Nowak & Shaw, 1995). Hence, it appears that only a small portion of the dose is taken up by PBMC.

MPA undergoes phase II glucuronidation by UDP-glucuronosyltransferases (UGT) that are present mainly in the liver, as well as the kidney and intestine. Three MPA metabolites are formed through this process, namely MPAG, acyl glucuronide MPA (AcMPAG) and MPA-phenyl glucoside (GluMPA) (Figure 1-2).

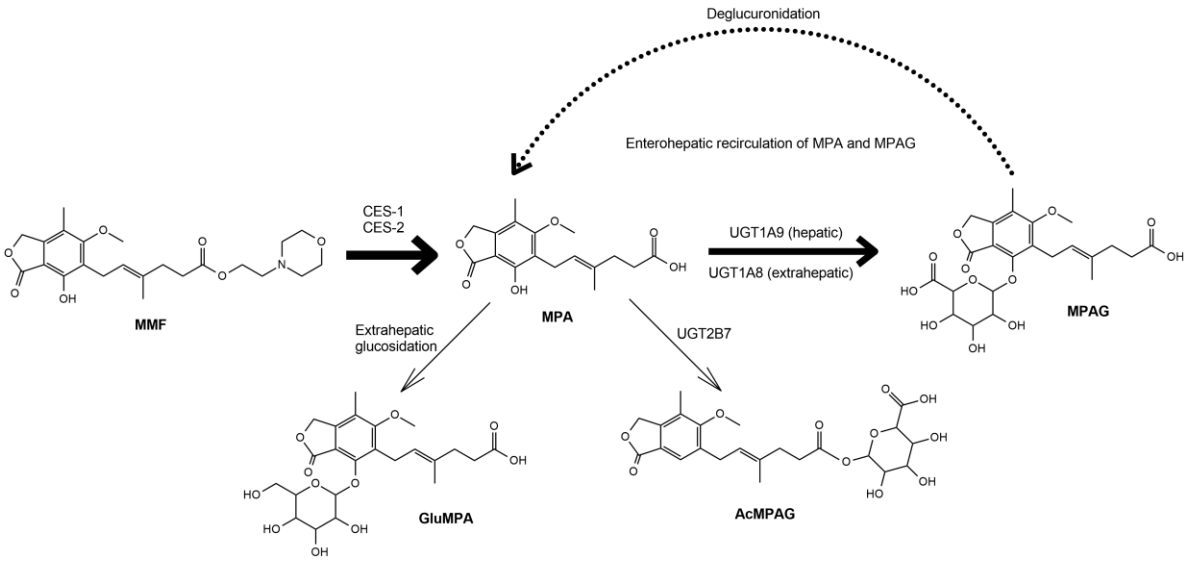

Figure 1-2. Metabolic pathways of MPA to its three metabolites when administered as MMF. The thickness of the arrows represents the relative amount of conversion from one metabolite to the next. Most of MMF is converted to MPA, which then forms the major metabolite MPAG, whilst relatively little MPA is converted to GluMPA and AcMPAG.

MPAG is the major metabolite formed and is catalysed mainly by the hepatic enzyme UGT1A9 and by UGT1A8 extrahepatically (Bernard & Guillemette, 2004). It is important to note that MPAG and GluMPA are not pharmacologically active. In contrast, the minor metabolite AcMPAG, whose formation is catalysed by UGT2B7, is an active metabolite and can act as a non-competitive inhibitor of IMPDH2 (Gensburger et al., 2009), although AcMPAG has a 10-fold higher K_i (511 nM) compared to MPA (57.7 nM) and is thus not as clinically relevant. It has also been suggested that AcMPAG induces cytokine release (Wieland et al., 2000). This active metabolite, once eliminated in the bile, may therefore be responsible for mediating the GI toxicity observed with this drug.

The concentration-time profile of oral administered MPA exhibits a C_{max} 1 hour after dose, with secondary peaks occurring 6 to 12 hours after dose (Bullingham et al., 1996). This is attributed mainly to enterohepatic cycling of MPAG. After delivery to the liver via the portal vein, MPAG is actively transported into hepatocytes by the basolaterally localised anionic

transporters organic anion transporting polypeptides 1B1 (OATP1B1) and OATP1B3 (Picard et al., 2010). The apical canalicular efflux transporter, multidrug resistance-associated protein 2 (MRP2) then secretes MPAG into bile (Patel et al., 2013). It is then thought that MPAG undergoes de-glucuronidation into MPA in the intestine (possibly catalysed by gut flora) before reabsorption. Enterohepatic recirculation of MPAG is estimated to contribute 40% of the overall plasma AUC of MPA (Bullingham et al., 1998) and thus is important when considering MPA plasma concentrations.

1.2.3. MPA Dose Adjustment

When first introduced as a therapeutic drug, MPA was billed a "one size fits all" drug, leading to the initial fixed dosing regimen. However, fixed dosing has proven to be suboptimal, exhibiting large inter-individual variability in terms of MPA exposure when measured as trough concentrations (C_{min}) or area under curve for MPA concentration over the first 12 hours (AUC_{0-12}). Numerous studies of cohorts have observed an association between either MPA AUC_{0-12} or C_{min} trough concentration with acute graft rejection in the first 3 months post-transplant (Gaston et al., 2009; Okamoto et al., 2005; Takahashi et al., 1995). However, it is important to note that apart from acute failure or toxicity, there seems to be no clear relationship between MPA exposure and overall therapeutic response (Le Meur et al., 2011). Thus, there is a clear need for precision dosing of MPA to achieve suitable immunosuppression for long term renal transplant success.

Currently, two methods of precision dosing are in use: therapeutic drug monitoring (TDM) and target concentration intervention (TCI). Either AUC_{0-12} or C_{min} trough concentrations of MPA are used for TDM and TCI guided dosage adjustments (Kuypers et al., 2010). TDM is used when dosing to a therapeutic range (MPA AUC_{0-12} between 30 to 60 mg h/L) whereas TCI is used to achieve a target concentration (MPA AUC_{0-12} = 40 mg h/L).

There have been a number of randomised controlled trials to determine the benefits of TDM or TCI for MPA dosing. Two such trials have demonstrated a decreased acute rejection rate in optimised TCI groups compared to fixed dosing groups or groups with lower MPA exposure (11.5% vs 27.5% and 7.7% vs 24.6% respectively) (Hale et al., 1998; Le Meur et al., 2007). A TDM trial demonstrated a slightly lower (22%) rejection rate compared to fixed dosing (28%) groups, although this was not significant (Gaston et al., 2009).

1.2.4. MPA in blood leukocytes

Whilst there have been promising developments and results in understanding how MPA exposure impacts beneficial outcomes, there is little consensus. Indeed, even in trials which report the benefits of controlling MPA exposure by appropriate dosage adjustments, there is still a substantial proportion of patients who have suboptimal response. This means that even with optimal MPA exposure (optimal MPA $AUC_{0\text{-}12}$), these patients do not respond. A possible explanation for this is how MPA exposure is measured. The $AUC_{0\text{-}12}$ is derived from determining MPA concentrations from at least 8 blood plasma samples of the patient over the first 12 hours of administration. Therefore, the MPA concentrations determined are the concentrations of MPA in plasma. However, the concentrations of MPA in the target site (i.e. lymphocytes) may differ from plasma MPA concentrations.

A recent study (Dom et al., 2018) found that MPA concentrations within peripheral blood mononuclear cells (PBMC) independently correlated with early transplant rejection whereas plasma unbound MPA concentrations did not. The authors concluded that measurement of MPA concentrations within PBMC could be used to facilitate TCI or TDM based dosage adjustment and thereby decrease rejection. Thus, intracellular MPA concentrations in lymphocytes may be an overlooked but important parameter for MPA precision dosing.

The transport of MPA into cells, specifically PBMC, is thus an important question to answer. There has been little research into the uptake transport of MPA into these cells. Instead, the focus has mostly been identification of the transporters for the movement of the glucuronidated metabolites of MPA into and out of hepatocytes. Using transfected HEK293 cell lines, it was demonstrated that MPAG was a substrate for the OATP1B1 and OATP1B3 uptake transporters and that neither MPA or AcMPAG could be transported by either OATP transporters (Picard et al. 2010). There is little known about the role of OATP transporters in the uptake transport of MPA into PBMC.

1.3. Cyclophosphamide

Cyclophosphamide is a prodrug that has a long history as a chemotherapeutic drug and was first approved for use in 1959. It is still a key part of the treatment of various cancers including breast and lymphoid. Along with the cytotoxic effects on cancer cells, cyclophosphamide also possesses immunomodulatory properties (Brock & Wilmanns, 1958) and has since been used in the treatment of autoimmune diseases such as SLE and minimal change nephrotic syndrome in children. Additionally, cyclophosphamide is frequently utilised in myeloablative treatment before haematopoietic stem cell transplantation (McCune et al., 2009).

1.3.1. Mechanism of action

Cyclophosphamide exerts its cytotoxic effects through the metabolite phosphoramide mustard (PAM). PAM is a bifunctional, alkylating nitrogen mustard (Figure 1-3) and can alkylate DNA, RNA and protein. However, it is mainly through DNA alkylation that PAM is cytotoxic (Masta et al., 1995).

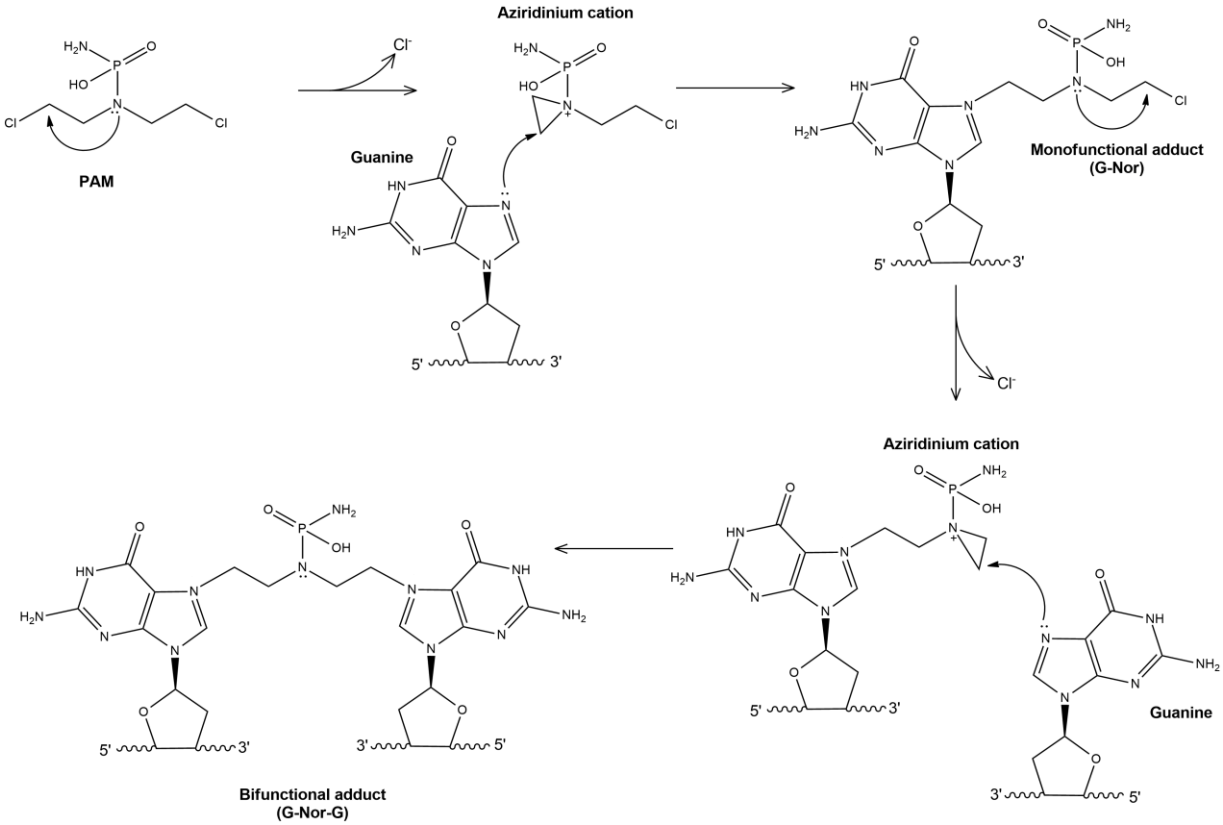

Figure 1-3. Mechanism of bifunctional adduct (G-Nor-G) formation. The intramolecular cyclisation of PAM forms the aziridinium cation which then alkylates DNA, creating a monofunctional adduct, then a bifunctional adduct with both "arms" of the mustard moiety.

PAM first undergoes intramolecular cyclisation through nucleophilic attack of the nitrogen atom on the last carbon on an "arm" of the mustard, eliminating a chloride anion. This results in the formation of an aziridinium cation with a single free mustard "arm". The reactive aziridinium cation then creates an adduct with a guanine base through electrophilic attack on N_7 of the imidazole ring (this is known as a monofunctional-adduct). The free "arm" of PAM in these monofunctional adducts can then undergo similar nucleophilic attack by the nitrogen of PAM as before, forming the aziridinium cation once again. This cation then reacts with another guanine base, forming a G-nor-G adduct (Povirk & Shuker, 1994). This results in inter-strand DNA crosslinks, where two guanine bases in opposite DNA strands are crosslinked. Due to the molecular size and steric hindrance of PAM, these inter-strand crosslinks induced

by PAM occur at 3'-GNC-5' sequences. Intra-strand crosslinks can also occur but are thought to possess no cytotoxic effect (Bauer & Povirk, 1997).

Most adducts formed by PAM are mono-functional adducts and inter-strand crosslinks make up only around 6% of all adducts formed by cyclophosphamide (Maccubbin et al., 1991). However, the inter-strand crosslinks are thought to be responsible for the cytotoxicity of cyclophosphamide. In an inter-strand crosslink induced by cyclophosphamide, the two opposite strands of DNA are covalently bound by PAM. This results in the mechanical distortion of DNA and the inability of replication complexes to form. This leads to the slowing of DNA replication, as has been observed by the retardation of S-phase growth in mouse embryos treated with cyclophosphamide (Chernoff et al., 1989). The accumulated DNA damage eventually culminates in a S-G_2 arrest of the cell.

Importantly, inter-strand crosslinks can be repaired by the cell. The damage to DNA is thought to be recognised by the cell through the stalling of DNA replication and transcription. Repair proteins are then recruited to excise the adduct and the resulting broken DNA strands are subsequently re-ligated. After recognition, repair is carried out through specific DNA damage repair pathways such as nucleotide excision repair (NER). The NER proteins ERCC-1 and ERCC-4/XPF form an endonuclease complex around the crosslink, making an incision at the 3' end of the nucleotide sequence containing the crosslink (Laat et al., 1998). XPG makes the incision at the 5' end of the nucleotide sequence (Friedberg et al., 2005). These incisions free the crosslink and results in a double strand break. The cell then repairs this double strand break through homologous recombination involving the enzymes XRCC2 and XRCC3 (Silva et al., 2000) and then the DNA strand is religated.

1.3.2. Metabolism of cyclophosphamide

Cyclophosphamide was initially developed to be specific for cancer cells possessing high levels of phosphamidase activity, as it was predicted that these enzymes would cleave the bond between phosphorous and nitrogen in cyclophosphamide and release nitrogen mustard (Friedman & Seligman, 1954). However, it was subsequently observed that this was not the case and that cyclophosphamide underwent extensive and complicated metabolism in the human body.

After administration, cyclophosphamide undergoes hydroxylation by hepatic the cytochrome P450 (CYP) enzymes (Figure 1-4) to form 4-hydroxycyclophosphamide (4-OHCP). In addition, cyclophosphamide can also undergo *N*-dechloroethylation. This is catalysed by CYP3A4 and produces the inactive minor metabolite dechloroethylcyclophosphamide and the by-product chloroacetaldehyde (Kaijser et al., 1993). In contrast, many CYP can catalyse the 4-hydroxylation of cyclophosphamide and include CYP2B6 (Xie et al., 2003), as CYP2C9, CYP2C19 (T. K. Chang et al., 1997), CYP2A6 and CYP3A4 (S. Ren et al., 1997; Roy et al., 1999). However, CYP2B6 and CYP2C19 appear to be the two important enzymes involved in human liver (Helsby et al., 2010). In addition, cyclophosphamide has been demonstrated to auto-induce CYP2B6, increasing the CYP2B6-catalysed metabolism of cyclophosphamide to 4-OHCP.

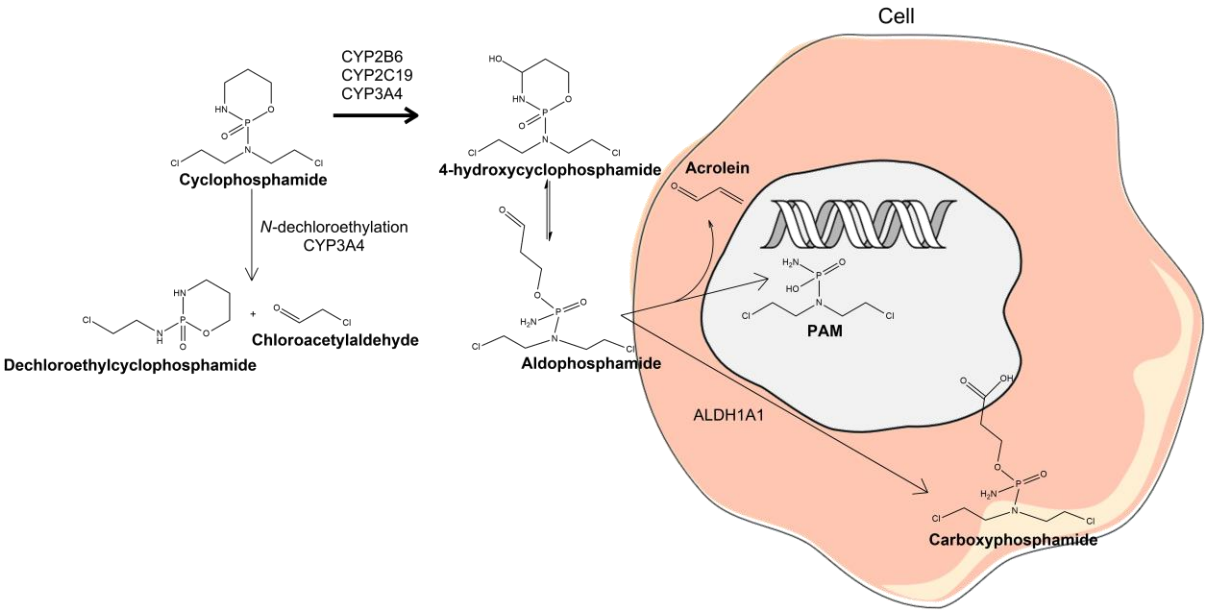

Figure 1-4. Metabolism pathways of cyclophosphamide. Cyclophosphamide is a prodrug and is activated by 4-hydroxylation, this is catalysed mainly by hepatic CYP2B6, CYP2C19 and CYP3A4. 4-hydroxycyclophosphamide exists in an equilibrium with its tautomer, aldophosphamide. This can then undergo hydrolysis (β-elimination) to release phosphoramide mustard (PAM), which alkylates DNA, and the by-product acrolein. Aldophosphamide can also be metabolised by ALDH1A1 into the inactive carboxyphosphamide. The other metabolic route of cyclophosphamide (N-dechloroethylation) also produces inactive metabolites.

The 4-OHCP metabolite is unstable and exists in an equilibrium with its open-ringed tautomer aldophosphamide (Valente et al., 1984). Aldophosphamide is assumed to then readily diffuse into target proliferating cells. Once in cells, such as lymphocytes, aldophosphamide then undergoes two different pathways.

The first pathway is one of detoxification, where aldehyde dehydrogenase 1A1 (ALDH1A1) converts aldophosphamide to the inactive carboxyphosphamide (Domeyer & Sladek, 1980; von Eitzen et al., 1994). The second pathway is via hydrolysis, where base catalysed β-elimination leads to the production of the DNA-alkylating PAM and the by-product acrolein. Subsequently, PAM may also undergo further chemical cleavage of the phosphoramide residue to form nornitrogen mustard (Struck et al., 1975); nornitrogen mustard can also form inter-strand and intra-strand DNA crosslinks (Hemminki, 1987), albeit less efficiently than PAM.

Formation of PAM from aldophosphamide has classically been considered to be non-enzymatic, however the involvement of phosphodiesterase enzymes in this final activation step has been postulated (Bielicki et al., 1983).

1.3.3. Basis of cell selectivity

The ability of cyclophosphamide to inhibit the proliferation of neoplastic and immune cells has contributed to its continued relevance despite the age of the drug. Thus, the basis of cell selectivity and toxicity should be considered.

A generally accepted factor in the selective cytotoxicity of cyclophosphamide is the level of ALDH1A1 activity of the cell. Higher ALDH1A1 activity allows the cell greater cyclophosphamide detoxification capacity and protects the cell from DNA damage. This was first demonstrated in cyclophosphamide-resistant leukaemic L1210 cell lines (Hilton, 1984).

This has also been observed in the immune context, where haematopoietic stem cells are protected by high endogenous ALDH1A1 activity (Levi et al., 2009; Magni et al., 1996) whereas mature immune cells are not. Furthermore, ALDH1A1-expressing regulatory T-cells (T_{regs}) recovered rapidly after posttransplant high-dose cyclophosphamide administration, unlike other T-cell populations with lower ALDH1A1 expression (Kanakry et al., 2013).

Alternative detoxification processes have also been suggested to contribute to cyclophosphamide cellular selectivity, notably, glutathione conjugation of cyclophosphamide metabolites such as PAM by glutathione S-transferase enzymes (Dirven et al., 1994). It has been suggested that since glutathione synthesis is an ATP-dependent process, high levels of ATP could allow more synthesis of glutathione and confer resistance to cyclophosphamide. This is one hypothesis to explain the effect of ultralow-dose (metronomic) cyclophosphamide administration on the selective depletion of T_{regs}, which have low ATP levels compared to other T-cells (Zhao et al., 2010).

Within the cell, the balance between the formation and the repair of the DNA crosslinks induced by PAM also determines the cytotoxicity of cyclophosphamide. If not repaired, the crosslinks will inhibit gene transcription and DNA replication by mechanically blocking the formation of enzyme complexes required for these processes. Thus, any proliferating cell is vulnerable to the cytotoxicity of cyclophosphamide as they are most dependent on these processes. Recently, an additional susceptibility of cells to cyclophosphamide-induced DNA damage has been suggested to lie in the impaired DNA damage repair capacity of tumour cells that occurs during cell cycle checkpoint adaptation. Thereby these neoplastic adaptations increase the susceptibility of tumour cells to cyclophosphamide-induced cell death (Swift & Golsteyn, 2014). Similarly, mass spectrometry analysis identified higher levels of G-nor-G DNA adducts (i.e. derived from interstrand cross-links) in PBMC from cyclophosphamide-treated patients with Fanconi anaemia (a known defective response to DNA damage) compared to patients without Fanconi anaemia (Johnson et al., 2012). This indicates either a greater capacity for adduct formation, reduced capacity to remove the adducts or a combination of both factors in these patients.

1.3.4. Toxicity

With the wide range of disease indications, various cyclophosphamide dosing regimens (differing in route of delivery, dosage and frequency) are used. For example, in myeloablative conditioning prior to haematopoietic stem cell transplantation, a very high dose of cyclophosphamide, typically above 5000 mg/m^2 of body surface area, is administered intravenously over 2 to 4 days. In contrast, the standard regimen for treatment of lupus nephritis is intravenous pulse cyclophosphamide, which consists of a single intravenous dose of 500 mg/m^2 cyclophosphamide once a month for 6 months (Valeri et al., 1994). More recently, the role of metronomic cyclophosphamide dosing (ultra-low continuous dosing) has highlighted the role of immunogenic cell death and stimulation of immune response in the treatment of

cancer (de Boo et al., 2017). This ultralow-dose cyclophosphamide regimen typically involves daily oral cyclophosphamide (100 mg). These different dosing regimens invariably result in different toxicity profiles. However, there are common toxicities that can be observed regardless of dose. These include ovarian toxicity, haemorrhagic cystitis, unwanted immunosuppression and alopecia. In SLE, ovarian toxicity is of particular concern as SLE patients are predominantly female and of childbearing age (Rees et al., 2017).

1.3.5. Pharmacokinetics of cyclophosphamide

There is considerable variation in the pharmacokinetics of cyclophosphamide and its metabolites when given at standard dosages. The clearance of cyclophosphamide varies between 1.0 to 12.6 L/h (de Jonge et al., 2005), and the AUC of cyclophosphamide and metabolites 4-OHCP and PAM were observed to vary up to 9-fold between patients (de Jonge et al., 2005). Alongside the variability in pharmacokinetic parameters, therapeutic response to and toxicity of cyclophosphamide is also variable between individuals. This inter-individual variation has been attributed largely to inherited germline variation.

1.3.6. Genetic polymorphisms

Polymorphisms present in the enzymes which metabolise cyclophosphamide are thought to be main genetic contributors to the variation in cyclophosphamide pharmacokinetics and clinical outcomes. The initial bioactivation of cyclophosphamide to 4-OHCP is catalysed mainly by CYP2B6 and CYP2C19. These isozymes are highly polymorphic due to the presence of single nucleotide polymorphisms (SNP) in the genes encoding them (Table 1-2), resulting in the highly variable expression and activity between individuals. Decreased or null function variants of these enzymes decrease the bioactivation of cyclophosphamide to 4-OHCP, resulting ultimately in decreased PAM formation and less cytotoxicity. Thus, understanding individual SNP profiles may be able to guide cyclophosphamide dosing and improve outcomes for patients.

Gene	SNP	Variant	Allele	Effect
CYP2B6	rs2279343	785A>G	*4	Increased function[1]
	rs3211371	1459C>T	*5	Unclear effect on expression[2]
	-	(516G>T and 785A>G)	*6	Decreased function[1]
	-	(516G>T, 785A>G and 1459C>T)	*7	Decreased function[1]
	rs3745274	516G>T	*9	Decreased function[1]
	rs4802101	-750T>C	*G	Altered HNF binding site[3]
CYP2C19	rs4244285	681G>A	*2	Null function[4]
	rs4986893	636G>A	*3	Null function[4]
	rs12248560	-806C>T	*17	Putative increased expression[4]

Table 1-2. Common polymorphisms of *CYP2B6* and *CYP2C19* and their effect on gene expression. [1]Desta et al. (2021) [2]Lang et al. (2001) [3]Nakajima et al. (2007) [4]Botton et al. (2021)

In *CYP2B6*, coding region SNP can impact the amount and activity of the enzyme. For example, the 516G>T SNP, located at a splice site, causes aberrant splicing and results in less functional enzyme. In contrast, non-coding region SNP such as -750T>C have been theorised to change transcription factor binding sites of the gene and alter the auto-inducibility of *CYP2B6*.

Pharmacogenomic studies of cyclophosphamide have mostly focussed on determining the association between the SNP in Table 1-2 and various parameters of cyclophosphamide exposure. An important parameter often used to measure exposure is the bioactivation ratio, which is the plasma AUC ratio of cyclophosphamide to 4-OHCP. This is an approximation of the extent of conversion from cyclophosphamide to the main metabolite 4-OHCP. Studies assessing the influence of the SNP on the bioactivation ratio have drawn conflicting conclusions, with several studies finding no association between SNP and the bioactivation ratio (Ekhart, et al., 2008; Kim et al., 2013; Raccor et al., 2012; Timm et al., 2005). However, the robustness of these conclusions is questionable. Many of these studies assessed a SNP individually without considering haplotype which accounts for different combinations of SNP, thus possibly overlooking synergistic effects a SNP may possess in a single individual (Nakajima et al., 2007; Raccor et al., 2012; Timm et al., 2005; Xie et al., 2006). Additionally, assessment of each of *CYP2B6* or *CYP2C19* genetic variation alone without consideration of the other gene may be unreliable (Helsby et al., 2010). These studies have been reviewed (Helsby et al., 2019) and whilst inconsistencies have been observed, there appears to be substantial evidence of a combined contribution of *CYP2B6* and *CYP2C19* genotype towards cyclophosphamide pharmacokinetics and response (Tables 1-3 and 1-4 respectively) in both cancer and autoimmune disease (Helsby et al., 2019).

Disease		Study size (n)	Population ancestry[a]	Variant allele assessed[b]			Significant Association	
				CYP2B6 SNP (Haplotypes assessed)	*CYP2C19*	Multivariate analysis	***CYP2B6***	***CYP2C19***
Cancer	[1]	51		516G>T, 785A>G, 1459C>T (*4, *5, *6)	ND	No	**-**	**ND**
	[2]	60		64C>T, 516G>T, 777C>A, 785A>G, 1459C>T (*2, *3, *4, *5, *6, *7)	*2	No	**-**	***2**
	[3]	49		516G>T, 785A>G, 1459C>T (*5, *6)	*2, *17	Yes	***5, *6**	**-**
	[4]	124		64C>T, 516G>T, 785A>G, 1459C>T	*2	Yes	**-**	**-**
	[5]	29		516G>T (*9)	*2	No	***9**	**-**
	[6]	68	Pakistan	516G>T, 785A>G, 1459C>T (*4, *5, *6)	*2	Yes	***4, *5, *6**	**-**
	[7]	103		-2320T>C, -750T>C, 136A>G, 296G>A, 419G>A, 415A>G, 516G>T, 785A>G, 1172T>A, 1459C>T, 15582C>T, 18492T>C (*G, *H, *4, *5, *6, *7, *8, *9, *11, *12, *14, *15)	*2, *3	No	***H**	**-**
	[8]	567	Chinese	64C>T, 516G>T, 785A>G, 1459C>T (*2, *4, *6, *9, *29, *30)	*2, *3	Yes	***2, *4, *6, *9, *29, *30**	***2**
Autoimmune disease	[9][c]	21		64C>T, 516G>T, 777C>A, 785A>G (*2, *3, *6)	*2	Yes	**-**	**-**
	[10]	16	Polynesian	516G>T, 785A>G, 1459C>T (*4, *5, *6, *7, *9)	*2, *3	Combined genotype	***5**	***2, *3**
	[11]	23	African-American	516G>T, 785A>G, 1459C>T (*4, *5, *9)	ND	No	***9**	**ND**
	[12]	18	Indian	ND	*2	No	**ND**	**-**
	[13]	189	Chinese	-2320T>C, -750T>C, 516G>T, 785A>G, 1459C>T, 15582C>T	*2, *3	Combined genotype	***G, *H, 15582C>T**	***2**

Table 1-3. Summary of studies (reference numbers in square brackets) assessing the relationship between *CYP2B6* and *CYP2C19* genetic polymorphisms and cyclophosphamide bioactivation plasma pharmacokinetics. Table was author's contribution to Helsby et al. (2019) and reproduced from the paper. [a]European ancestry was major ethnicity, unless indicated. [b]Alleles are as described in Table 1-2 with additional alleles (SNP or haplotypes) as follows: *CYP2B6**H (-750T>C & -2320T>C) = rs4802101 & rs7254579; *2 (64C>T) = rs8192709; *3 (777C>T) = rs45482602; *8 (415A>G) = rs12721655; *11 (136A>G) = rs35303484; *12 (296G>A) = rs36060847; *14 (419G>A) = rs35773040; *15 (1172T>A) = rs35979566; *29 &*30 are *CYP2B6-CYP2B7* hybrids (crossover in intron 4) (Martis et al., 2013); *CYP2B6* 15582C>T= rs4803419, 18492T>C = rs2279345; *CYP2C19**17 (-806C>T) = rs12248560. [c]This study did not fully disclose the *CYP2B6* and *CYP2C19* SNP assessed. **ND = Not Determined**

Disease		Study size (n)	Population ancestry[a]	Variant allele assessed[b]			**Significant Association**	
				CYP2B6 SNP (Haplotypes assessed)	*CYP2C19*	Multivariate analysis	***CYP2B6***	***CYP2C19***
Cancer	[8]	567	Chinese	64C>T, 516G>T, 785A>G, 1459C>T (*2, *4, *6, *9, *29, *30)	*2, *3	Yes	***4**	***2**
	[14]	44		516G>T, 785A>G (*6)	ND	No	-	**ND**
	[15]	26		516G>T, 785A>G, 1459C>T (*4, *5, *6, *9)	ND	No	***4**	**ND**
	[16]	119		516G>T, 785A>G (*6)	ND	No	***6**	**ND**
	[17]	93		516G>T, 785A>G, 1459C>T (*5, *6, *7)	*2	Yes	***5, *7**	-
	[18][c]	359		516G>T, 785A>G, 1459C>T (*4, *5, *6, *7)	*2, *3	No	***6**	***2,*3**
	[19][c]	38	Middle East	516G>T, 785A>G, 1459C>T (*4, *5, *6, *9)	ND	No	****5,*6,*9***	**ND**
	[20]	350		516G>T, 785A>G, 1459C>T (*4, *5, *6, *7, *9)	ND	Yes	-	**ND**
	[21]	230		64C>T, 415A>G, 516G>T, 777C>A, 785A>G, 1459C>T (*2, *3, *4, *5, *8, *9)	*2	No	***2, *4, *8, *9**	***2**
	[22]	111	Indian	516G>T (*9)	*2	Yes		
	[23]	250	Indian	GWAS (700,000 SNP)		-	-	***2**
Autoimmune disease	[12]	136	Indian	ND	*2	Yes	**ND**	***2**
	[13][d]	189	Chinese	-750T>C, -2320T>C, 785A>G, 1459C>T, 516G>T, 15582C>T	*2, *3	Combined genotype	***CYP2B6**H and *CYP2C19**2**	
	[24]	62		1459C>T (*5)	*2	No	***5**	***2**
	[25]	36		1459C>T (*5)	*2	Yes	-	-
	[26]	70		516G>T, 785A>G, 1459C>T (*5, *6)	*2, *3, *17	No	-	-
	[27]	93		1459C>T (*5)	*2	No	-	-
	[28]	109	Korean	GWAS (491,617 SNP)		-	-	-

Table 1-4. Summary of studies (reference numbers in square brackets) assessing the relationship between *CYP2B6* and *CYP2C19* genetic polymorphisms and therapeutic outcomes (overall and disease-free survival). Table was author's contribution to Helsby et al. (2019) and was reproduced from the paper. [a]European ancestry was major ethnicity, unless indicated. [b]Alleles are as described in Table 1-2 with the additional alleles (SNP or haplotypes) as follows: *CYP2B6**H (-750T>C & -2320T>C) = rs4802101 & rs7254579; *2 (64C>T) = rs8192709; *3 (777C>T) = rs45482602; *8 (415A>G) = rs12721655; *11 (136A>G) = rs35303484; *12 (296G>A) = rs36060847; *14 (419G>A) = rs35773040; *15 (1172T>A) = rs35979566; *29 &*30 are *CYP2B6-CYP2B7* hybrids (crossover in intron 4) (Martis et al., 2013); 15582C>T= rs4803419;

*CYP2C19**17 (-806C>T) = rs12248560. [c]These studies stratified patients by a putative metaboliser status based on various combinations of *CYP2B6* alleles assessed. [d]This study stratified patients by a putative metaboliser status based on combinations of both *CYP2B6* and *CYP2C19* alleles assessed. **ND = Not Determined**

Reference number	Paper	Reference number	Paper
1	Raccor et al., 2012	15	Jakobsen Falk et al., 2012
2	Timm et al., 2005	16	Johnson et al., 2013
3	Veal et al., 2016	17	Bachanova et al., 2015
4	Ekhart et al., 2008	18	Melanson et al., 2010
5	Xie et al., 2006	19	Haroun et al., 2015
6	Afsar et al., 2012	20	Gor et al., 2010
7	Nakajima et al., 2007	21	Bray et al., 2010
8	Shu et al., 2017	22	Tulsyan et al., 2014
9	Kim et al., 2013	23	Kalra et al., 2018
10	Helsby et al., 2010	24	Takada et al., 2004
11	Joy et al., 2012	25	Winoto et al., 2011
12	Kumaraswami et al., 2017	26	Audemard-Verger et al., 2016
13	Shu et al., 2016	27	Cartin-Ceba et al., 2017
14	Vukovic et al., 2019	28	Kim et al., 2016

Table 1-5. Reference numbers of papers assessed in Tables 1-3 and 1-4.

The commonly polymorphic enzyme ALDH1A1 should also be considered when assessing cyclophosphamide exposure. However, *ALDH1A1* variants are poorly characterised even though several have been observed to possess greatly diminished activity (Yoshida, 1992). In the same vein, not many clinical studies have been undertaken to assess the contribution of *ALDH1A1* variants to therapeutic response to cyclophosphamide. Those few which have done so have found associations of ALDH1A1 cellular levels with therapeutic response (Sládek et al., 2002) and certain SNP with toxicity (Yao et al., 2014). Increased ALDH1A1 cellular levels were found to associate with increased resistance to cyclophosphamide, whilst an *ALDH1A1* SNP was associated with increased toxicity.

Hence, determining an individual's profile of genetic polymorphisms is likely to be important when assessing cyclophosphamide activated metabolite exposure and eventually understanding variation in therapeutic response and toxicity.

1.3.7. DNA repair capacity

Another determinant of therapeutic response to cyclophosphamide is likely to be differences in DNA repair capacity between individuals. As described previously, several proteins are involved in the recognition and repair of the DNA crosslinks induced by activated cyclophosphamide. There is *in vitro* evidence that increased sensitivity to alkylating agents similar to cyclophosphamide is associated with deficiency in these processes. For example, sensitivity to alkylating agents and genomic instability was observed in *ERCC1* knockout mice (Weeda et al., 1997), whilst *XRCC2* and *XRCC3* mutant Chinese hamster ovary cell lines had increased sensitivity to nitrogen mustard (Silva et al., 2000). Furthermore, deficiency in other proteins involved in S phase homologous recombination repair such as FANC proteins and BRCA2 have been demonstrated to result in accumulation of DNA damage in the form of

double strand breaks, which are the repair intermediates of the inter-strand crosslinks (Sobeck et al., 2006).

Despite substantial evidence of impaired DNA damage-repair capacity increasing sensitivity to cyclophosphamide *in vitro*, few clinical studies have sought to elicit the link between DNA damage-repair capacity and response to cyclophosphamide. However, Fanconi anaemia patients with inherited FANC deficiencies, are known to require lower doses of cyclophosphamide, achieve similar amounts of G-nor-G DNA adducts as non-Fanconi anaemia patients receiving standard doses (Johnson et al., 2012). It has also been suggested that the DNA repair protein, O^6-methylguanine-DNA methyltransferase, may modulate cyclophosphamide toxicity by neutralising acrolein damage (Cai et al., 1999). However, beyond these studies, not much research has been conducted to determine if impaired DNA damage-repair capacity may contribute to the variation in response to and toxicity of cyclophosphamide.

1.4. MPA and Cyclophosphamide in treatment of lupus nephritis

The use of either MPA or cyclophosphamide in the treatment of lupus nephritis has had limited success. Traditional drug regimens in the initial 6-month induction phase of treatment usually consist of MPA or cyclophosphamide in combination with glucocorticoids and other immunosuppressive drugs such as tacrolimus or cyclosporin A. Maintenance therapy usually follows induction and has historically utilised pulsed (monthly) intravenous cyclophosphamide. However, over the past decades, MPA has gradually become the mainstay of maintenance therapy (Contreras et al., 2004) due to substantial germline toxicities observed with long-term cyclophosphamide use. In contrast, usage of MPA in induction therapy has relied on the patient's failure to respond to initial cyclophosphamide treatment, although more clinicians have started choosing MPA *in lieu* of cyclophosphamide. This is mainly due to the lack of clear evidence supporting superior efficacy of MPA over cyclophosphamide.

Several studies and a meta-analyses have demonstrated that MPA treatment achieves similar renal remission rates (50% to 70%) as cyclophosphamide when used in induction therapy (Appel et al., 2009; Mak et al., 2009; Ong et al., 2005; Sahay et al., 2018). However, other studies have concluded that MPA is superior to cyclophosphamide (Ginzler et al., 2005; W. Hu et al., 2002), in contrast, a recent meta-analysis has found cyclophosphamide in combination with glucocorticoids and tacrolimus to be superior even to regimens using MPA (J. Zhou et al., 2020).

Importantly, amidst the inconsistency among the studies, most agree that utilising MPA affords a more ideal profile of adverse reactions (Mak et al., 2009; J. Zhou et al., 2020), which may be the reason behind clinicians increasingly favouring MPA use in induction therapy. Whilst there is an increasing shift towards MPA as the standard in lupus nephritis treatment, cyclophosphamide may not be obsolete. The standard protocol for cyclophosphamide

induction therapy involves monthly intravenous cyclophosphamide at 500 to 1000 mg/m^2 for six months. A newer regimen calls for a lower fixed dose of cyclophosphamide (500 mg) to be administered fortnightly six times (Houssiau et al., 2002) and was observed in a meta-analysis to achieve similar remission rates as the standard dose cyclophosphamide regimen, whilst decreasing notable adverse reactions such as risk of infection and menstrual disorder (Tian et al., 2017). This may mean that cyclophosphamide can achieve a similar response and adverse reaction incidence as MPA if administered optimally.

1.5. Aims

The choice between MPA and cyclophosphamide in SLE treatment has to date been insufficiently informed and usually made empirically as a consequence of non-response to either drug. Certain aspects of an individual patient's response to these drugs remain unclear despite extensive research. Understanding these overlooked aspects may improve outcomes for SLE patients and guide future treatment.

Intracellular concentrations of MPA within peripheral blood leucocytes have been demonstrated to be better predictors of therapeutic response than plasma concentrations (Dom et al., 2018). This suggests that transport of MPA into lymphocytes may be important. Thus far, only uptake transport of the MPAG metabolite into hepatocytes has been well-characterised. Furthermore, pharmacodynamic assessment of IMPDH activity as well as *IMPDH* expression has not been well researched. Thus, this thesis aims to examine the kinetics of MPA uptake in a lymphoid-derived cell line using radiolabelled drug, and to characterise changes in IMPDH activity in response to drug treatment with an optimised and validated high performance liquid chromatography (HPLC) assay. Additionally, this thesis aims to examine *IMPDH1* and *IMPDH2* expression in relevant immune tissues to identify any potential inter-individual differences that could contribute to response to MPA through an iterative analysis of available online databases with aggregated datasets.

Despite the long use of cyclophosphamide, the understanding of its complicated metabolism and mechanism of action is still insufficient. Little is known about the complex dynamic interaction between 4-OHCP, aldophosphamide and PAM formation in immune cells and inter-individual differences in repair of the resulting DNA adducts. An assay to characterise inter-individual differences PAM-induced DNA damage-repair capacity in peripheral blood mononuclear cells (PBMC from LN patients and healthy individuals will be developed. Finally,

this thesis also aims to determine whether the final step of bioactivation from 4-OHCP to PAM is an enzyme-catalysed process in peripheral blood leucocytes and to identify whether phosphodiesterase enzymes are involved as was previously hypothesised (Bielicki et al., 1983).

These results may then provide a better understanding of treatment of autoimmune diseases such as SLE, using MPA and cyclophosphamide and serve as a basis for biomarker-guided regimen choice.

Chapter 2: Methods

2.1. Cyclophosphamide

2.1.1. Preparation of 4-OHCP and PAM solutions

4-hydroperoxycyclophosphamide (Niomech-IIT GmbH, Germany) was stored as 5 or 12.5 mg/mL (200 µL aliquots) in storage buffer (0.5 M Tris-HCl, pH 5) at -20 °C. Sodium thiosulphate solution (25 mM sodium thiosulphate, 10 mM Tris-HCl, pH 8.5) was freshly prepared and 800 µL of this solution was added to each 4-hydroperoxycyclophosphamide aliquot. The 1 mL solutions were then briefly vortexed and incubated for 2 hours at 37 °C to convert 4-hydroperoxycyclophosphamide into 4-OHCP (1 or 2.5 mg/mL), as previously described (Zon et al., 1984).

Phosphoramide mustard (PAM), purchased from Niomech-IIT GmbH (Germany) was stored as 1.7 mg aliquots at -20 °C. These aliquots were dissolved in 1.36 mL of phosphate-buffered saline (PBS) to produce 1.25 mg/mL stock solutions immediately prior to use.

2.1.2. Preparation of genomic DNA

Whole blood was collected from consented donors (ethics approval 18/NTB/170) in PAXgene Blood DNA tubes (Qiagen, Germany). Genomic DNA (gDNA) was then extracted from the blood using the PAXgene Blood DNA kit (Qiagen, Germany). The concentration and purity of DNA was assessed using a NanoDrop 2000 UV-Vis spectrophotometer (Thermo Fisher Scientific Inc., USA). The isolated gDNA was then pooled (n=3 donors), aliquoted and stored at -20 °C.

2.1.3. Preparation of peripheral blood mononuclear cells (PBMC)

Whole blood (24 mL) was drawn from consented donors (ethics approval 18/NTB/170) in BD Vacutainer® CPT™ sodium citrate tubes (Becton, Dickinson and Company, USA). PBMC

were isolated from the buffy coat layer by centrifugation at 1800 *g* for 30 minutes. The plasma layer was also collected and stored at -20 °C. Isolated PBMC were transferred to another tube and pelleted by centrifugation at 400 *g* for 40 minutes. The supernatant was discarded, and the pellet was resuspended in PBS to a target concentration of 37 x 10^6 cells/mL. The PBMC cell count and viability were assessed using trypan blue exclusion in a haematocytometer (Neubauer, Germany).

2.1.4. Pre-incubation of 4-OHCP with candidate enzymes

Solutions (500 µL) of freshly prepared 4-OHCP (3.6 mM) were pre-incubated with various candidate enzymes and human plasma. Briefly, the 4-OHCP solution was incubated with 1-2 units of phage T4 DNA Polymerase (Life Technologies, Australia), 0.1-0.2 units (10-20 mg) phosphodiesterase (PDE) I type IV from *Crotalus atrox* (snake venom PDE-I; Sigma-Aldrich, Germany), 0.64 µg purified human recombinant PDE 3B, 4B2, 8A1 and 11A4 (Sigma-Aldrich, Germany), or 125 µL human plasma for 1 hour at 37 °C. Subsequently, the solution was transferred into an Amicon Ultra-0.5 30 kDa Centrifugal filter unit (Merck, Germany) and centrifuged at 14,000 *g* for 15 minutes to separate the enzyme-protein from the hydrolysed 4-OHCP solution. Genomic DNA was then exposed to known volumes of the ultrafiltrate as described below.

2.1.5. Experimental incubations

2.1.5.1. Incubations with purified gDNA

Aliquots of gDNA (33.3 µg/mL) were exposed to 4-OHCP (0 – 3 mM) or PAM (0 – 23 µM) in ultrafiltrate solution, or ultrafiltrate solution in a final volume of 200 µL PBS, for 1 hour at 37 °C (n = 4 replicates), prior to analysis by PCR.

2.1.5.2. Incubations with PBMC

The viability of PBMC were first calculated through the trypan blue exclusion assay. PBMC (5 x 10^6 cells/mL) were then exposed to 4-OHCP solution (0 – 0.9 mM) or PAM solution (0 – 4.5 mM) in PBS in a final volume of 200 µL for 1 hour at 37 °C (n = 4 replicates for 4-OHCP activation, or n = 1 – 4 replicates for REPAIR). After the exposure to 4-OHCP or PAM the PBMC were pelleted by centrifugation (1600 *g*, 5 minutes), the supernatant was discarded, and the cell pellets were stored at -20 °C prior to analysis.

2.1.5.3. Incubation with cell lines

The Jurkat (T-cell leukaemia) cell line was purchased from Sigma-Aldrich (Germany) and cultured in RPMI1640 medium (Life Technologies, New Zealand) with 10% foetal bovine serum at 37 °C and 5% CO_2. Cells (30 – 50 x 10^6 cells) suspended in media were transferred to a 50 mL Falcon tube and pelleted (1600 *g*, 5 minutes). The supernatant was discarded and the cells resuspended to a target concentration of 37 x 10^6 cells/mL. Jurkat cells were then exposed in a final concentration of 5 x 10^6 cells/mL to 4-OHCP (0 – 3 mM) in PBS in a final volume of 200 µL for 1 hour at 37 °C (n = 4 replicates). After the exposure to 4-OHCP, the cells were pelleted by centrifugation (1600 *g*, 5 minutes), the supernatant was discarded, and the cell pellets were stored at -20 °C before analysis.

The Caco-2 (colorectal adenocarcinoma) cell line (Lot number 13J022) was purchased from Sigma-Aldrich (Germany) and cultured in MEMα medium (Life Technologies, New Zealand) with 10% foetal bovine serum at 37 °C and 5% CO_2. Prior to exposure to drugs, the cells were treated with 1X trypsin-EDTA solution (Sigma-Aldrich, Germany) to detach cells from the culture flasks. Cell pellets were then resuspended in their respective media and aliquoted into 96-well tissue culture plates at a cell density of 10,000 cells in 100 µL of media per well. The plates were incubated at 37 °C and 5% CO_2 overnight before the experiment. The wells were

visually inspected through the microscope before the experiment to ensure that the cells had formed a monolayer at the bottom of the well and were attached to the surface. The media was then aspirated from the wells and the cells were exposed to 4-OHCP solution (0 – 3.6 mM) in a final volume of 200 µL for an hour (n = 4 replicates). Subsequently, the drug solution was aspirated from the cells. Cells were detached from wells and then stored at -20 °C before analysis. Both cell lines were tested for mycoplasma every month.

2.1.6. Inhibitory effect of Rolipram

For the experiments assessing PDE4B2 inhibition by rolipram (Abcam PLC, UK), a 10 mM stock solution was prepared in ethanol. PBMC were then exposed to 80 µM rolipram in PBS (0.8 % ethanol) or control solution (PBS, 0.8% ethanol) for 1 hour at 37 °C, then pelleted (1600 *g*, 5 minutes), the supernatant discarded and the PBMC re-suspended in PBS containing vehicle (0.8% ethanol) prior to exposure to 4-OHCP (325 µM; 1 hour at 37 °C). For co-incubation experiments, PBMC were pre-incubated in the vehicle solution (PBS, 0.8% ethanol) for 1 hour at 37 °C, pelleted and resuspended in solutions containing 80 µM rolipram in 0.8% ethanol with 4-OHCP (325 µM) or control solutions (PBS, 0.8% ethanol) and incubated for 1 hour at 37 °C. For incubations involving purified human recombinant phosphodiesterase 4B2, the enzyme was incubated with 500 µL of 4-OHCP solution (3.6 mM) in the presence of 80 µM rolipram or control solution (PBS, 0.8% ethanol) prior to ultra-filtration.

2.1.7. REPAIR study

The recruitment of lupus nephritis (LN) patients (20/NTB/182) and healthy donors (18/NTB/170) was carried out with the approval of the Northern B Health and Disability Ethics Committee. LN patients were recruited at renal clinics conducted by the Auckland and Waitematā District Health Boards at Auckland City Hospital, Greenlane Clinical Centre and North Shore Hospital. Healthy donors were recruited at the University of Auckland, Grafton

Campus. The inclusion criteria for LN patients were that they had to be greater than 18 years old, able to give informed consent, had a diagnosis of either active or quiescent lupus nephritis and were not currently on cyclophosphamide or other alkylating agents. Exclusion criteria for LN patients were not being able to give a blood sample and currently taking cyclophosphamide or other alkylating agents. For healthy donors, the only inclusion criteria was that they had to be greater than 18 years old and the only exclusion criteria were that they were pregnant or currently breast feeding, or were on any medications besides oral contraceptives, or had current illness at the time of sampling.

Blood samples were drawn from LN patients by trained nurses at their next visit to the renal clinics after admission into the study. For healthy donors, trained phlebotomists drew blood samples at the University of Auckland Clinical Research Centre after admission into the study. Approximately 24 mL of blood was drawn into 3 8 mL BD Vacutainer® CPT™ sodium citrate tubes (Becton, Dickinson and Company, USA) and mixed thoroughly. The tubes were then centrifuged at 1800 *g* for 30 minutes at 24 °C for separation of PBMC from plasma and red blood cells. The PBMC in the buffy coat were pooled from the 3 tubes and the plasma stored at -80 °C. The pooled PBMC were mixed thoroughly and an aliquot was taken out to count the number of cells. The PBMC were then centrifuged again at 400 *g* for 40 minutes to isolate the PBMC pellet. The PBMC pellet was then resuspended in PBS in an appropriate volume to dilute the cells to 37 x 10^6 cells/mL. The PBMC suspension was aliquoted and the tubes were exposed to a range of PAM concentrations (0 – 1000 µM) for 1 hour at 37 °C. PBMC were then isolated from the PAM solution at the end of the hour by centrifugation at 1600 *g* for 5 minutes and stored as dry cell pellets.

2.1.8. QPCR-block assay

Stored cell pellets (previously exposed to treatments) were prepared for QPCR using Arcturus® PicoPure® DNA Extraction Kit (Life Technologies, Australia), as per the manufacturer's instructions. Briefly, PBMC Pellets were resuspended in 150 µL of DNA reconstitution buffer containing proteinase K and vortexed gently, then incubated (65 °C, 3 hours) followed by inactivation of proteinase K (95 °C, 10 minutes). The lysate solution containing DNA was then stored at -20 °C prior to QPCR.

The conditions used for the QPCR-block assay were as described (van Kan et al., 2019). The region amplified was a 1.6 kb region in the *TP53* gene. The primer sequences used were forward primer: 5′-TTCCTCTTCCTACAGTACTCC-3′ and reverse primer: 5′-CCTGCTTGCTTACCTCGCT-3′ (Invitrogen, Thermo Scientific, New Zealand). The PCR reactions (50 µL) consisted of 25 µL Taq PCR Master Mix (Qiagen, Germany), 0.2 µM of each primer, 50 ng of DNA (or 1.5 µL of DNA-PBMC cell lysate), and PCR-grade H_2O. Cycling conditions were: initial denaturation at 94 °C for 3 minutes; 35 cycles at 94 °C for 30 seconds, 53 °C for 30 seconds, 72 °C for 1 minute; and final extension at 72 °C for 10 minutes. The PCR amplicon was quantified using the Quant-iT PicoGreen dsDNA Assay Kit (Life Technologies, Australia) according to the manufacturer's instructions. Each PCR reaction was quantified in duplicate and the average value reported. Briefly, 20 µL of the PCR product, 80 µL of Tris-EDTA buffer and 100 µL of PicoGreen reagent was incubated at room temperature for 5 minutes. The resulting fluorescent product was measured at 485/20 nm excitation and 528/20 nm emission (BioTek Synergy 2 microplate reader). The average background fluorescence (determined from wells containing no PCR product) was subtracted and the dsDNA concentration of each well was calculated using a λDNA standard curve (30 – 1000 ng/mL, n = 3 technical replicates).

2.1.8.1. Data analysis

dsDNA concentration data were calculated in Excel (Microsoft, USA). All other analyses were conducted in GraphPad Prism 9.0.2 (GraphPad Prism Software Inc., USA). IC_{50} values for QPCR-block were calculated using least squares regressions ([Inhibitor] vs. response three parameter, four parameter or linear regression models, as appropriate), taking into account the N and scatter of the replicates (constraints: $IC_{50} > 0$, Bottom > 0 for nonlinear regression models). Three-parameter, four-parameter or linear regression models were selected based on a comparison of fits test conducted in Prism. In each experiment, replicate concentrations (n = 3 – 4) were also determined in replicate PCR amplifications (n = 4). Each PCR amplification was also quantified in duplicate. Independent repeat experiments (N = 2 – 3) were undertaken unless otherwise stated. Data are presented as mean ± SD. Where stated, data was assessed for likelihood of normality or lognormality of distribution using Akaike Information Criterion in GraphPad Prism 9.0.2. Subsequently, adherence to normality or lognormality was tested using the Shapiro-Wilk test. Correlation was tested using Pearson's product-moment correlations (parametric data) or Spearman's rank correlations (non-parametric data). Differences between groups were assessed using student's t-tests or one-way ANOVA if parametric. When the data was found to not be parametric, Mann-Whitney and Kruskal-Wallis rank sum tests were used instead. Differences between proportions were tested using either chi-square tests or Fisher's exact tests where stated. All *p*-values reported are two sided and were corrected for multiple testing using Šídák's multiple comparisons test if multiple comparisons were made. Adjusted *p*-values < 0.05 were considered statistically significant.

2.2. Mycophenolic acid

2.2.1. Preparation of MPA solutions

MPA was purchased from AK Scientific (USA) and stored in 10.267 mg/mL, 6.72 mg/mL and 0.672 mg/mL aliquots dissolved in 100% ethanol at -20˚C. Radiolabelled [carboxyl-^{14}C] MPA was purchased from ViTrax (USA) and stored as 100 µCi/mL (0.672 mg/mL) dissolved in 100% ethanol at -20˚C.

For the time-course assays, both radiolabelled MPA solutions were prepared using [^{14}C] MPA and non-radiolabelled MPA. The solutions were diluted to the concentrations 31.2 and 312 µM using complete uptake buffer (140 mM NaCl, 5 mM KCl, 0.4 mM KH_2PO_4, 0.8 mM $MgSO_4$, 1 mM $CaCl_2$, 25 mM glucose, 10 mM HEPES, pH 7.4) to give a final radioactivity concentration of 0.55 µCi/mL. In the incubations, 50 µL of the solutions were incubated with 50 µL of cell solution to give final concentrations of 15.6 and 156 µM MPA. MPA solutions used in all time-course assays had a final ethanol concentration of 1.5% (v/v). Vehicle controls in the time-course assays were made up using complete uptake buffer and ethanol (1.5% v/v)

For the determination of Michaelis-Menten curves, all radiolabelled MPA solutions (the final concentrations that cells were incubated with were 0 µg/mL, 2.5 µg/mL, 5 µg/mL, 10 µg/mL, 25 µg/mL, 50 µg/mL, 75 µg/mL, 100 µg/mL, and 250 µg/mL) were made up with radiolabelled [^{14}C] MPA and non-radiolabelled MPA, as well as complete uptake buffer for a final radioactivity concentration of 0.55 µCi/mL. All radiolabelled MPA solutions had a final ethanol concentration of 9.68% (v/v). Vehicle controls in these experiments were made up using complete uptake buffer and ethanol (9.68% v/v).

For the determination of IMPDH activity response to varying MPA concentrations, all non-radiolabelled MPA solutions (the final concentrations cells were incubated with were 0 µg/mL,

0.005 µg/mL, 0.05 µg/mL, 0.5 µg/mL, 1 µg/mL, 5 µg/mL, 20 µg/mL, 50 µg/mL, 100 µg/mL and 250 µg/mL) prepared in complete uptake buffer. All MPA solutions had a final ethanol concentration of 9.68% (v/v). Vehicle controls in these experiments were prepared using complete uptake buffer and ethanol (9.68% v/v).

In experiments determining the nature of MPA uptake, 156 µM (50 µg/mL) and 624 µM (200 µg/mL) radiolabelled MPA solutions were prepared in sodium-free complete uptake buffer (140 mM choline chloride, 5 mM KCl, 0.4 mM KH_2PO_4, 0.8 mM $MgSO_4$, 1 mM $CaCl_2$, 25 mM glucose, 10 mM HEPES, pH 7.4). In the incubations, 50 µL of the solutions were incubated with 50 µL of cell solution to give final concentrations of 78 and 312 µM MPA (4.84% ethanol v/v). Vehicle controls in these experiments were made up using sodium-free uptake buffer and ethanol (4.84% v/v).

2.2.2. Incubation of [^{14}C]MPA with Jurkat cell line

The Jurkat cell line was cultured as detailed previously (Section 2.1.5.3). There was no decrease in viability of Jurkat cells (viability at all time points was above 95%, range 97.2% to 99.3%) when incubated up to 4 hours with 5% ethanol (v/v). Cultured cells were counted with the trypan blue assay (>95% viability), harvested (30 – 50 x 10^6 cells) and pelleted by centrifugation (1600 *g*, 5 minutes). The pellet was then resuspended in complete uptake buffer at a concentration of 20 x 10^6 cells/mL. Then 50 µL of the cell solution (1.0 x 10^6 cells) was then aliquoted into Eppendorf tubes at 37°C.

The time-course assays included 0 s, 20 s, 40 s, 1 min, 3 min, 6 min, 20 min, 1 hour, 2 hour, 3 hour and 4 hour time points and the Michaelis-Menten curves included 5 min and 1 hour time points. Inhibitor experiments were conducted at a 5 min time point based on the initial uptake time first observed in time-course assays.

The start of the incubation time for each replicate was marked by the pipetting of 50 µL of radiolabelled MPA solution into the tube. The radiolabelled MPA solution was then mixed with the cell solution by pipetting up and down 3 times. The end of the incubation time for each replicate was then marked by the pipetting of 900 µL ice-cold complete uptake buffer and the transfer of the tube from the 37°C dry bath to an ice bath. Subsequently, the tubes were centrifuged (1600 *g*, 5 min) and the supernatant removed. The cell pellets were washed with 500 µL of ice-cold complete uptake buffer and centrifuged (discarding the supernatant each time) twice more. After the wash cycles, the cells were lysed with lysis buffer (1% SDS (v/v), 0.1 M NaOH). The solution was then transferred to a 6 mL scintillation tube and 5 mL of scintillation cocktail fluid Emulsifier-Safe^{TM} (PerkinElmer, USA) was added. The tube was inverted 3 times to mix and radioactivity was then measured using the Tri Carb® 4910TR liquid scintillation analyser (PerkinElmer, USA). The intracellular [^{14}C] MPA concentrations were measured in disintegrations per minute (DPM). DPM measurements were then analysed as follows.

Measured DPM was first converted to mCi (Equation 2-1).

$$DPM = \frac{1}{2.2\ x\ 10^{9}}\ x\ 1\ mCi$$

Equation 2-1. Conversion of measured DPM to mCi.

The intracellular concentration of MPA per million cells was then obtained by converting the previously obtained mCi (measured in 1 million cells) to pmol/10^6 cells using the specific activity of [^{14}C]MPA specified by the manufacturer (Equation 2-2).

$$Intracellular\ MPA\ concentration = \frac{mCi}{specific\ activity\ (mCi/mmol)}\ x\ 10^{12}\ pmol\ per\ 10^{6}\ cells$$

Equation 2-2. Conversion of obtained mCi to intracellular MPA concentration (pmol/10^6 cells).

Further conversion of the intracellular MPA concentration into molarity was undertaken for comparison to literature values (Equation 2-3).

$$Intracellular\ MPA\ concentration\ (\mu M) = \frac{Intracellular\ MPA\ concentration\ (pmol/10^{6}cells)}{volume\ of\ lysate\ (\mu L)}$$

Equation 2-3. Conversion of intracellular MPA concentration (pmol/10^6 cells) to molarity (µM).

2.2.3. IMPDH activity determination

To observe IMPDH activity changes in response to intracellular accumulation of MPA, time-course and MPA inhibitor concentration assays were undertaken. Identical to the radioactivity assays, the time-course assays included 0 s, 20 s, 40 s, 1 min, 3 min, 6 min, 20 min, 1 hour, 2 hour, 3 hour and 4 hour time points at two MPA concentrations (15.6 µM and 156 µM). The IMPDH activity relative to MPA concentration (0-780 µM) assays were undertaken at 5 minutes, 20 minutes and 4 hour time points.

2.2.3.1. HPLC determination of IMPDH activity

Incubation of non-radiolabelled MPA solutions with Jurkat cells was carried out as described in the Section 2.2.2. In summary, after incubation of 1.0 x 10^6 cells with the MPA solution in 100 µL, uptake of MPA was stopped by the addition of 900 µL of ice-cold complete uptake buffer and washed twice more before the cell pellet was isolated and stored in 83.3 µL of MilliQ

water at -80°C overnight before IMPDH activity determination through HPLC analysis. The trypan blue assay was then used to count cells with the Countess cell counter (Thermo-Fisher, USA) to ensure that the Jurkat cells were lysed (<2% viability).

Briefly, IMPDH activity of the treated cells was determined through the incubation of cell lysate with IMP to measure the conversion of IMP to XMP, which was then quantified by a validated HPLC assay.

The stored cell solutions were removed from -80°C and brought up to room temperature rapidly. Once warmed, the solution was vortexed vigorously for 30 seconds. The solution was then centrifuged at 16,000 *g* for 10 minutes, after which 50 µL of the supernatant (lysate) was incubated with 180 µL of the reaction mixture (1 mM IMP, 0.5 mM NAD^+, 40mM NaH_2PO_4, 100 mM KCl, pH 7.4) for 2.5 hours.

The incubation was terminated with the addition of 460 µL of ice-cold methanol. The mixture was then vortexed briefly and stored at -20 °C for at least 30 minutes. The solution was vortexed again and centrifuged at 16,000 *g* for 5 minutes. 650 µL of the supernatant was then transferred to a new Eppendorf tube and dried under nitrogen at 40°C for 30 to 45 minutes. The pellet was then resuspended in 100 µL of mobile phase (98% 0.1% formic acid in MilliQ, 2% methanol) and vortexed thoroughly before transferring into HPLC injection vials and injection onto column. 80 µL of the solution was injected onto column.

The HPLC method used for the determination of IMPDH activity was adapted from the method developed by Glander et al. (2009). Chromatographic separation was achieved using a Gemini reversed-phase C18 column (150 mm length x 4.6 mm inner diameter, 5 µm particle size), (Phenomenex, USA). The mobile phase used for elution consisted of 0.1% formic acid in MilliQ water (aqueous) and 100% methanol (organic). Gradient elution (as detailed in Table

2-1) was utilised to separate the compounds of interest, AMP and XMP, along with IMP and NAD^+. At a flow rate of 0.6 mL/min, the cycle time for the gradient elution was 22 minutes.

Time (min)	% organic
0-5	2
5-15	2-15
15-16	15-80
16-17	80
17-18	80-2
18-22	2

Table 2-1. Gradient elution for the quantification of AMP and XMP in the determination of IMPDH activity.

HPLC chromatography resulted in retention times for AMP and XMP of 7.9 minutes and 17.5 minutes (Figure 2-1).

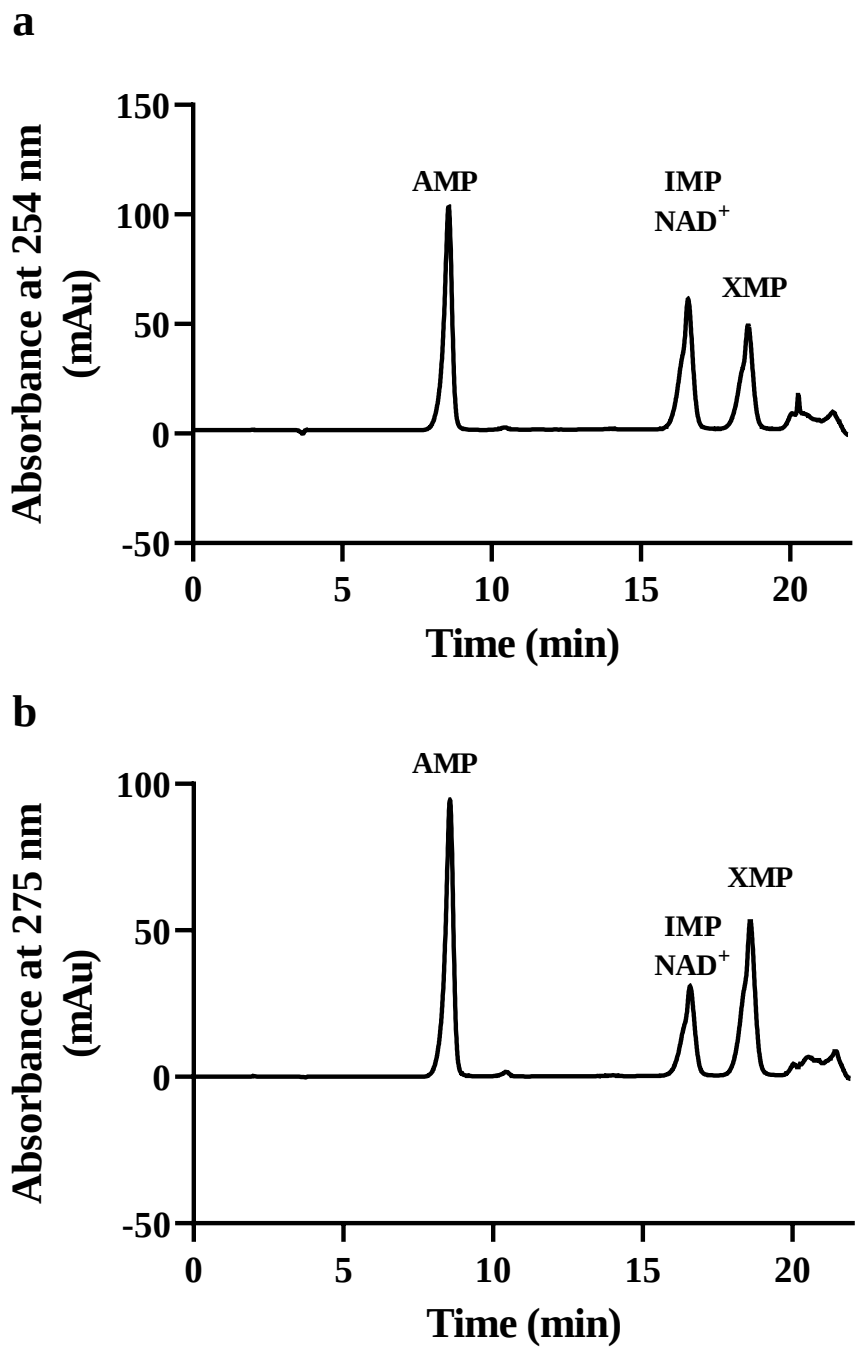

Figure 2-1. Representative HPLC chromatograms of AMP and XMP with IMP and NAD^+ spiked in blank Jurkat cells at a) 254 nm and b) 275 nm. HPLC chromatograms show the elution of the compounds of interest, AMP (7.9 minutes) and XMP (17.5 minutes) along with IMP and NAD^+ (16.2 minutes). The standards were spiked in blank Jurkat cells and extracted before elution. 254 nm is the wavelength used to quantify AMP whilst 275 nm is used to quantify XMP.

The range of concentrations used for the calibration curve of AMP was 10 to 50 µM, whilst the range of concentrations used for the calibration curve of XMP was 5 to 150 µM. Example calibration curves are shown in Figure 2-2. Initial runs to determine the lower limits of quantification assessed AMP and XMP concentrations (n = 6) down to 0.5 µM. The lowest concentrations of AMP and XMP where at least 75% of calibrators fell within ±20% of nominal concentrations were determined as the lower limits of quantification. The lower limits of quantification for AMP and XMP were 5 µM. Concentrations of AMP and XMP that were determined to fall below the lower limit of quantification were assigned a value of 0 and plotted as 0 on the graphs. Inter-run accuracy and precision were determined from 3 runs. 4 QCs (10, 18, 35 and 45 µM for AMP and 5, 10, 75 and 140 µM for XMP) were used (n = 5) in 3 separate runs to determine accuracy and precision. Accuracy and precision for AMP ranged from 96.1% to 108.1% and 103.2% to 107.4% respectively, whereas that for XMP ranged from 91.3% to 107.1% and 101.9% to 112.2% respectively.

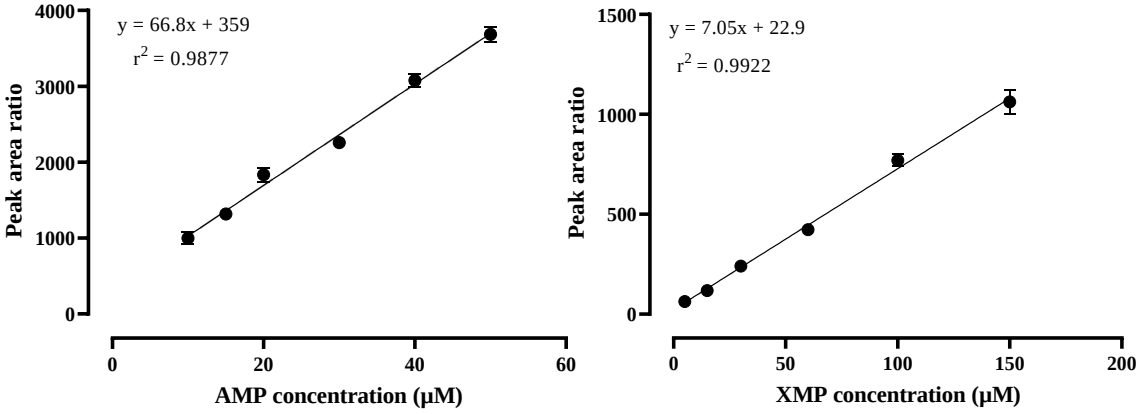

Figure 2-2. Typical calibration curves of AMP and XMP in Jurkat cells. Samples were analysed in triplicate and error bars represent SD.

After the determination of AMP and XMP concentrations, IMPDH activity was calculated (Equation 2-4). In the baseline normalisation of IMPDH activity, IMPDH activity was

determined in Jurkat cells incubated with 0 µg/mL MPA and the mean value of IMPDH activity was used as 100%.

$$IMPDH\ activity = \frac{\frac{Concentration\ of\ XMP\ measured\ (\mu M)}{Concentration\ of\ AMP\ measured\ (\mu M)}}{x\ Incubation\ time\ (seconds)}\ \mu M\ XMP\ formed\ per\ \mu M\ AMP\ s^{-1}$$

Equation 2-4. Calculation of IMPDH activity normalised to amount of AMP (µM XMP formed per µM AMP s^{-1}.

2.2.4. IMPDH database analysis

In the database analysis of factors affecting *IMPDH1* and *IMPDH2* gene expression, three databases were chosen and analysed iteratively to generate results. These three databases are the Genotype-Tissue Expression (GTEx), All RNA-seq and ChIP-seq sample and signature search (ARCHS[4]), (Lachmann et al., 2018) and the Human Protein Atlas (HPA) databases (Pontén et al., 2008; Uhlen et al., 2019). The general characteristics and data extracted from the databases are shown in Table 2-2.

		Databases		
		GTEx	**ARCHS[4]**	**HPA**
Data stratified based on	**Sex**	Yes	No	No
	Polymorphisms	Yes	No	No
	Immune cell/tissue types	Yes, but immune cell types unavailable	Yes, immune cell types available	Yes, immune cell types available
Dataset used		GTEx	GEO	HPA

Table 2-2. The general characteristics of the three databases used for the determination of factors affecting *IMPDH1* and *IMPDH2* expression. GEO = Gene Expression Omnibus.

IMPDH1 and *IMPDH2* gene expression data (mRNA transcription quantification data) was first extracted from GTEx, and expression differences in the data were analysed based on sex,

polymorphisms and immune tissue type. The gene expression data was then extracted from ARCHS[4] and expression differences between immune cell and tissue types were analysed. This data was then compared to GTEx. Lastly, protein-coding mRNA expression data was extracted from HPA and analysed based on immune cell and tissue type. This was then compared to both GTEx and ARCHS[4] data and results.

2.2.4.1. GTEx

The data from the GTEx portal was first extracted using the GTEx API (v1), which was accessed through the website: https://www.gtexportal.org/home/api-docs/#. First, normalised transcription data was extracted. This was accessed with the following parameters: datasetId (gtex_v8), gencodeId (ENSG00000106348.16 for *IMPDH1* and ENSG00000178035.11 for *IMPDH2*), tissueSiteDetailId (Whole_Blood, Spleen and Cells_EBV-transformed_lymphocytes), attributeSubset (sex for data stratified by sex) and format (tsv). The .tsv format file was then downloaded and data extracted in Excel. The data was subsequently transferred to GraphPad Prism 9.0.2 and analysed. Next, expression quantitative trait loci (eQTL) and splicing quantitative trait loci (sQTL) were analysed for the three most commonly assessed SNP rs2278293, rs2278294 and rs11706052, as well as the genes *IMPDH1* and *IMPDH2*. These were queried individually on the GTEx portal (website: https://gtexportal.org/home/) by either the SNP ID or the gene ID. The data was then downloaded in a .csv format and extracted (9th June 2023) and analysed in Excel.

Differences in *IMPDH1* and *IMPDH2* expression between the sexes in different tissues, as well as differences between *IMPDH1* and *IMPDH2* expression were analysed using 2-tailed Mann-Whitney tests in GraphPad Prism 9.0.2.

2.2.4.2. ARCHS[4]

The *IMPDH1* and *IMPDH2* expression data from ARCHS[4] was extracted with R scripts. First, the master file (ARCHS4 version 2.2 Ensembl 107, human_transcript_v2.2.h5) was downloaded (website: https://maayanlab.cloud/archs4/download.html). Individual R scripts for each immune cell/tissue type as well as each cell line were downloaded (website: https://maayanlab.cloud/archs4/data.html). The sample code for each R script is provided (Figure 2-3). Each R script was then run in RStudio 2022.12.0 Build 153 (RStudio Team, USA) with R 4.2.2. The output of the code was then saved as a .tsv tab separated file and data for *IMPDH1* and *IMPDH2* gene expression was extracted (16th June 2023) using Excel. The data was then transferred to GraphPad Prism 9.0.2 and graphed.

```
# R script to download selected samples
# Copy code and run on a local machine to initiate download
# Check for dependencies and install if missing
library("rhdf5")    # can be installed using Bioconductor

destination_file = "human_matrix_v9.h5"
extracted_expression_file = "GSM2679484_expression_matrix.tsv"
url = "https://s3.amazonaws.com/mssm-seq-matrix/human_matrix_v9.h5"

# Check if gene expression file was already downloaded, if not in current direct
ory download file form repository
if(!file.exists(destination_file)){
    print("Downloading compressed gene expression matrix.")
    download.file(url, destination_file, quiet = FALSE, mode = 'wb')
}

# Selected samples to be extracted
samp = c("GSM2679452","GSM2679453","GSM2679454","GSM2679455","GSM2679456","GSM26
79457","GSM2679458","GSM2679459","GSM2679460","GSM2679461","GSM2679462","GSM2679
463","GSM2679464","GSM2679465","GSM2679466","GSM2679467","GSM2679468","GSM267946
9","GSM2679470","GSM2679471","GSM2679472","GSM2679473","GSM2679474","GSM2679475"
,"GSM2679476","GSM2679477","GSM2679478","GSM2679479","GSM2679480","GSM2679481","
GSM2679482",
"GSM2679483","GSM2679484","GSM2679485","GSM2679486","GSM2679487","GSM2679488","G
SM2679489","GSM2679490","GSM2679491","GSM2679492","GSM2679493","GSM2679494","GSM
2679495","GSM2679496","GSM2679497","GSM2679498","GSM2679499","GSM2679500","GSM26
79501","GSM2679502","GSM2679503","GSM2679504","GSM2679505","GSM2679506","GSM2679
507","GSM2679508","GSM2679509","GSM2679510","GSM2679511","")

# Retrieve information from compressed data
samples = h5read(destination_file, "meta/samples/geo_accession")
genes = h5read(destination_file, "meta/genes/genes")

# Identify columns to be extracted
sample_locations = which(samples %in% samp)

# extract gene expression from compressed data
expression = t(h5read(destination_file, "data/expression", index=list(sample_loc
ations, 1:length(genes))))
H5close()
rownames(expression) = genes
colnames(expression) = samples[sample_locations]

# Print file
write.table(expression, file=extracted_expression_file, sep="\t", quote=FALSE, c
ol.names=NA)
print(paste0("Expression file was created at ", getwd(), "/", extracted_expressi
on_file))
```

Figure 2-3. Sample R script for the extraction of data for each immune cell/tissue type and cell line. The R scripts were provided by ARCHS[4], and the sample script was taken from ARCHS[4] documentation for parsing the H5 file.

2.2.4.3. HPA

Data for *IMPDH1* and *IMPDH2* expression was then extracted and analysed from HPA. The full dataset (18th dataset, RNA HPA immune cell gene data) was downloaded from the HPA data page (website: https://www.proteinatlas.org/about/download) in .tsv format. Data was then extracted (9th June 2023) from the file in Excel and transferred to GraphPad Prism 9.0.2 for visualisation and analysis.

Chapter 3: Intracellular activation of 4-hydroxycyclophosphamide into a DNA-alkylating agent in human leukocytes

3.1. Introduction

3.1.1. Cyclophosphamide use

Despite its age and the advent of many alternative treatments, cyclophosphamide has continued to be an important and relevant therapeutic agent in its treatment of cancers and autoimmune diseases. This is due in part to its efficient killing of neoplastic lymphoid cells, as well as its immunomodulatory properties. Cyclophosphamide has selectivity for mature immunocytes (e.g. T- and B-lymphocytes) but spares the early haematopoietic progenitors and stem cells at doses between 500-1000 mg/m^2, making it useful for control of some autoimmune diseases. It can also induce peripheral immune tolerance by preventing the clonal proliferation of reactive T-lymphocytes, which has led to the use of a short-pulse of post-transplant cyclophosphamide (PTCy) to prevent graft-versus host disease (Kato et al., 2020). This short-pulse (1-2 day, low dose ~1000 mg/m^2) PTCy approach is now established for allogeneic-haematopoietic stem cell transplant (HSCT) and is also under investigation for kidney transplantation. Cyclophosphamide is also used for conditioning (lymphodepletion) prior to chimeric antigen receptor-T cell (CAR-T) immunotherapy of haematological malignancies (Hirayama et al., 2019).

3.1.2. Cyclophosphamide metabolism

Cyclophosphamide is a prodrug and requires enzymatic bioactivation (reviewed in Emadi et al. 2009; Helsby et al. 2019). This occurs via hydroxylation to 4-hydroxycyclophosphamide (4-OHCP), which is catalysed primarily by the hepatic cytochrome P450 enzymes CYP2B6, CYP2C19, and to a lesser extent CYP3A4, as was discussed in chapter 1. Importantly, 4-OHCP exists in an equilibrium with aldophosphamide, its open-ringed tautomer (Figure 3-1). Aldophosphamide can then either (a) be detoxified by aldehyde dehydrogenase 1A1 (ALDH1A1) to form the inactive metabolite carboxyphosphamide, or (b) undergo conversion into the DNA alkylating agent phosphoramide mustard (PAM) with formation of the by-product acrolein.

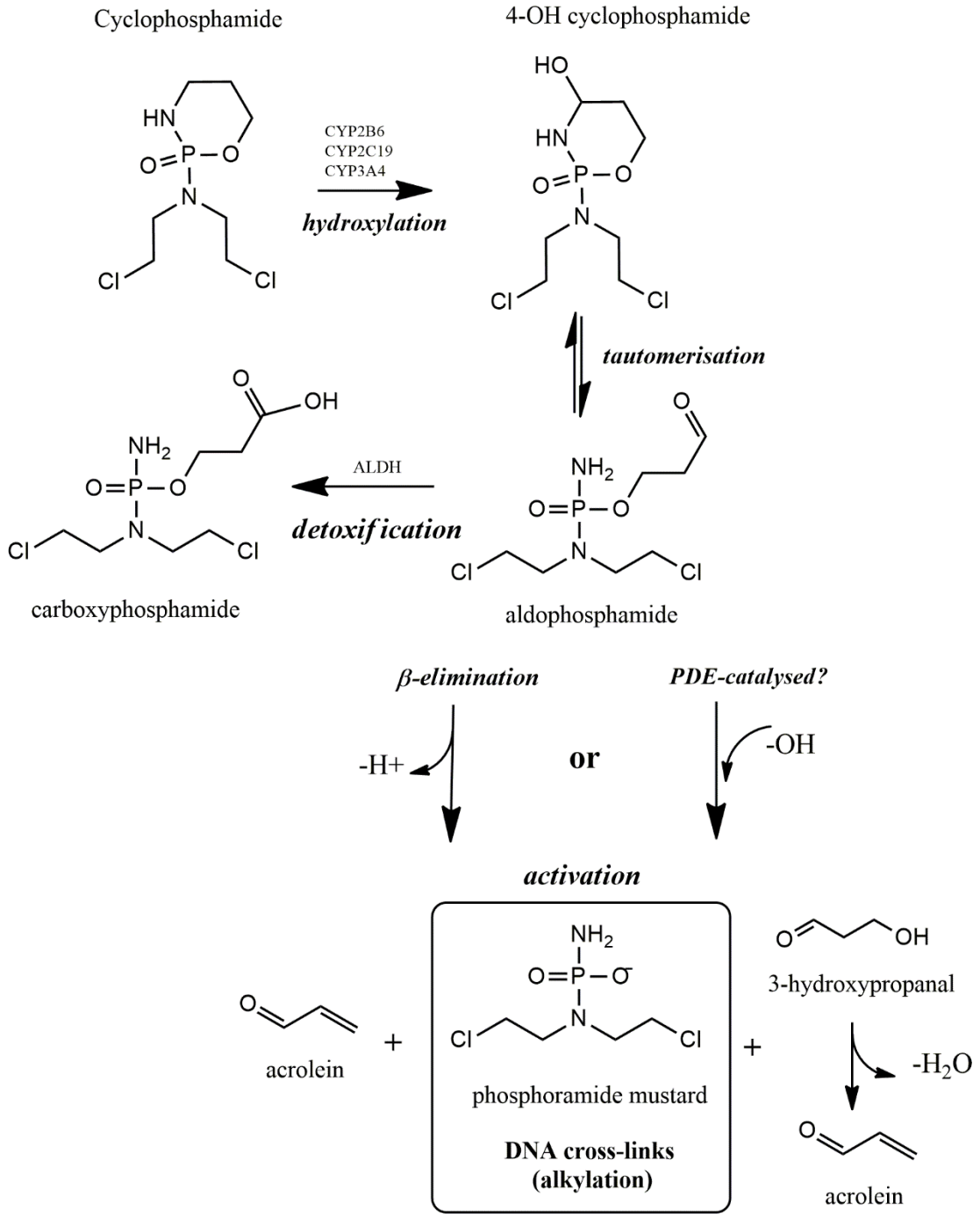

Figure 3-1. Activation of the prodrug cyclophosphamide into phosphoramide mustard, a DNA crosslinking agent.

The cytotoxic mechanism of action of cyclophosphamide is via alkylation of DNA (Cushnir et al., 1990) to form inter-strand crosslinks, which then inhibit DNA replication and lead to cell death (as discussed in Chapter 1, Section 1.3.1). This DNA alkylating activity has been attributed to PAM, since 4-OHCP/aldophosphamide tautomer and carboxyphosphamide are poor alkylating compounds (Colvin et al., 1976; Jardine et al., 1978; Struck et al., 1975).

3.1.3. Formation of PAM

Conversion of aldophosphamide into PAM (Figure 3-1) has classically been considered to be a non-enzymatic decomposition process (β-elimination) that directly results in the formation of the by-product acrolein (Borch & Millard, 1987). More recently it has been suggested that the by-product in mammalian tissue is 3-hydroxypropanal (Voelcker, 2017), which can then readily dehydrate to form acrolein (Engels et al., 2016). A number of studies suggest a possible role for enzyme catalysed hydrolysis of the phospho-ester bond in 4 -OHCP/aldophosphamide. Decomposition of 4-OHCP is faster following incubation in human plasma than in phosphate buffer (k_{cat} = 285 vs 0.013 M^{-1} min^{-1}), with this reaction observed only in the macromolecular fraction (>10 kDa) (Kwon et al. 1987); these data suggest that 4-OHCP decomposition is catalysed by a protein in human plasma. Both rat and human serum can also catalyse this reaction (Bielicki et al., 1983; Voelcker et al., 1981; Voelcker, 2017). Additionally, the release of acrolein (as a biomarker of PAM formation) following incubation of 4-OHCP with enzymes that have ribonucleotide phosphohydrolase activity has been reported (Bielicki et al., 1983). Enzymes with 3'-5' exonuclease activity could catalyse the release of acrolein from 4-OHCP (or 4-peroxyCP), with the highest activity observed with rabbit DNA polymerase δ (summarised in Table 3-1). In contrast, 5'-3' exonuclease could not catalyse this reaction.

Source	Enzyme name	Activity	Rate of acrolein formation (nmol/min/mg protein)
Rabbit (bone marrow) EC 2.7.7.7	DNA polymerase δ	3'-5' exonuclease	97.0
Escherichia coli EC 2.7.7.7	DNA polymerase I	3'-5' exonuclease	31.3 and 37.8
Penicillium citrium EC 3.1.4	Nuclease P1[#]	3-5' exonuclease	2.3
Crotalus adamanteus (Snake venom) EC 3.1.4.1	Phosphodiesterase I	3'-5' cAMP phosphodiesterase /3-5' exonuclease	4.2
Bovine (heart) EC 3.1.4.53	Phosphodiesterase (PDE3)	3'-5' cAMP/cGMP phosphodiesterase	0.7
Calf (spleen) EC 3.1.16.1	Phosphodiesterase II	5'-3' exonuclease	0

Table 3-1. Summary of the rate of acrolein formation from 4-hydroxycyclophosphamide catalysed by various enzyme candidates, as previously described in Bielicki et al. (1983). #has activity for both DNA and RNA. The activity in human lymphocytes (n= 5 donors) was reported to range between range 22-67 nmol/min/mg.

The rate of acrolein formation following incubation of 4-OHCP with a range of rat tissues has been assessed (Bielicki et al., 1983). Acrolein formation was detected only in lymphocyte-rich tissues (spleen and thymus) of the rat. Notably, when 4-OHCP was incubated with human lymphocytes (n = 5 donors), formation of acrolein was observed at a range >44-fold higher than in human plasma (22-67 nmol/min/mg vs 0.56 nmol/min/mg). This *indirectly* suggests that formation of PAM is an enzymatic process associated with lymphocytes.

From these studies Bielicki et al. (1983) hypothesised that 4-OHCP was selectively activated by 3'-5'exonucleases *within* the nucleus. In human cells these exonucleases are DNA polymerases α, δ and ε (EC 2.7.7.7), known as "proofreading" DNA polymerases (Brieba, 2008), as well as TREX1 (three prime exonuclease-1; EC 3.1.11.2), which is considered to be the major cellular 3'-5' DNA exonuclease in humans (Mazur & Perrino, 1999). Tissue specific expression of these DNA exonucleases (i.e. in lymphocytes) is unlikely and hence other enzymes with the ability to activate 4-OHCP/aldophosphamide tautomer may account for the relative tissue specificity of hydrolysis of 4-OHCP observed by Bielicki et al. (1983).

Notably, snake venom phosphodiesterase-I (PDE-I) could also efficiently catalyse formation of acrolein from 4-OHCP (Table 3-1). This protein has both exonuclease and cAMP phosphodiesterase activity (Uzair et al., 2018). Mammalian class I PDE enzymes consist of eleven families, each with different substrate specificity (cAMP and/or cGMP) and have different kinetic properties for these substrates (Omori & Kotera, 2007). The non-selective (cAMP/cGMP) PDE3 isoform had negligible ability to hydrolyse 4-OHCP (Table 3-1), which was in agreement with the lack of formation of acrolein in rat heart, a tissue which selectively expresses PDE3 (Bielicki et al. 1983). The possibility that 4-OHCP activation could be catalysed by isoforms of cAMP-phosphodiesterase (EC 3.1.4.53) that are selectively expressed in human lymphocytes, i.e. PDE4B, PDE4D, PDE7A, PDE8A and PDE10A (Azevedo et al. 2014; Wang et al. 1999), has not been assessed.

In summary there is preliminary evidence that 4-OHCP/aldophosphamide may undergo enzyme catalysed hydrolysis and that this potentially occurs in lymphocytes. However, these previous studies did not directly demonstrate formation of the key alkylating metabolite, PAM.

3.1.4. Study design

An assay to quantify DNA-adduct formation in human peripheral blood mononuclear cells (PBMC) when exposed *ex vivo* to alkylating agents was recently developed (van Kan et al., 2019). This Quantitative PCR-block (QPCR-block) assay is a well-validated approach based on the ability of a DNA lesion to block DNA polymerase and stall amplification. Increasing numbers of adducts in the DNA template proportionally decrease the amplification of a target sequence.

The aim of this study was to use this QPCR-block assay to quantify the formation of the DNA-alkylating product (i.e. PAM) following incubation of 4-OHCP with human PBMC, and to assess the ability of various cAMP/cGMP-PDE isoforms, known to be expressed in lymphocytes, to activate 4-OHCP into a DNA-alkylating agent. To do so, optimal concentration ranges of 4-OHCP and PAM for incubation with DNA and PBMC were first obtained. Since 4-OHCP is an unstable metabolite, PAM was freshly made up immediately prior to each experiment; 4-hydroperoxycyclophosphamide (4-OOHCP) was first converted to 4-OHCP by base reduction, before incubation with genomic DNA (gDNA) or PBMC for 1 hour. Subsequently, 4-OHCP was also incubated with immortalised cells (Jurkat, Caco-2) to compare their sensitivity to 4-OHCP with that of healthy PBMC. 4-OHCP was also pre-incubated with various enzyme candidates such as recombinant catalytically active human PDE before treating with gDNA to assess the effect on its alkylating ability. Treated gDNA, or DNA extracted from cells (detailed in Chapter 2 Section 2.1.8) that were treated with 4-OHCP or PAM were then amplified in the QPCR-block assay.

Briefly, 50 ng of gDNA or 1.5 µL of cell lysate were mixed with 25 µL Taq PCR Master Mix, 0.2 µM of reverse and forward primer and PCR-grade H_2O before amplification in the QPCR-block assay. The amplification conditions were an initial denaturation at 94 °C for 3 minutes; 35 cycles at 94 °C for 30 seconds, 53 °C for 30 seconds, 72 °C for 1 minute; and final extension at 72 °C for 10 minutes. Amplified DNA was then kept at -20 °C or used for quantification immediately. The amplification product was assessed in duplicate and 20 µL of the product was mixed with 80 µL of Tris-EDTA buffer and 100 µL of PicoGreen reagent for 5 minutes at room temperature. The mixture was excited at 485/20 nm and emission was measured at 528/20 nm. The calculation of double-stranded DNA concentration from the fluorescence values is covered in detail in Chapter 2 Section 2.1.8. Results were graphed in GraphPad Prism 9.0.2 and differences between groups were analysed using either student's t-tests or one-way ANOVA. All *p*-values reported are two sided and were corrected for multiple testing using Šídák's multiple comparisons test.

3.2. Results

3.2.1. DNA alkylation in gDNA incubated with 4-OHCP and PAM

To compare the intrinsic DNA-alkylating reactivity of 4-OHCP and PAM, purified pooled genomic DNA (gDNA) was exposed to increasing concentrations of these compounds *in vitro* (Figure 3-2). No appreciable inhibition of the PCR amplicon was observed for 4-OHCP concentrations below 1000 µM, suggesting little or no alkylation of purified gDNA (calculated IC_{50} = 6343 µM, 95% CI = 114.8 to 17091 µM). In contrast, PAM exposure inhibited PCR amplification at low drug concentrations, with an IC_{50} of 2.27 µM (95% CI = 0.636 to 5.08 µM). The maximum QPCR-block (mean PCR amplification) calculated for PAM was 29.0% (95% CI 19.7 to 36.0%) of untreated control amplification. The comparable data for 4-OHCP could not be determined, as concentrations greater than the calculated IC_{50} were not tested.

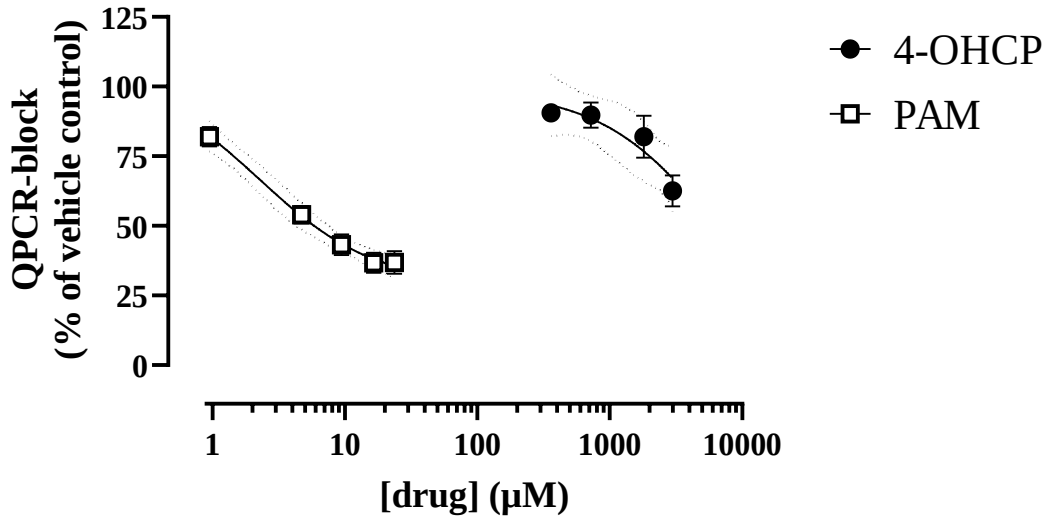

Figure 3-2. The effect of known concentrations of 4-OHCP or PAM on alkylation of purified gDNA. Data points represent the mean ± SD of two independent experiments (n = 4 technical replicates per experiment). Least squares regressions (solid lines) were calculated taking into account the N and scatter of the replicates using an [Inhibitor] vs. response three parameter model in GraphPad Prism 9.0.2 (constraints: IC_{50} > 0, Bottom > 0); 95% confidence intervals of the curve are indicated by the dotted lines.

3.2.2. DNA alkylation in PBMC incubated with 4-OHCP and PAM

The ability of 4-OHCP and PAM (Figure 3-3) to alkylate DNA in intact, viable cells was then assessed. In all experiments, PBMC viability was more than 98%. The 4-OHCP concentration that resulted in 50% QPCR-block (IC_{50}) in freshly collected donor PBMC ranged from 123.9 µM (donor 2) to 350.5 µM (donor 3). This was >18-fold more sensitive than the IC_{50} observed following exposure of purified gDNA to 4-OHCP. In contrast, the intact PBMC were >227-fold less sensitive to PAM than was observed for the purified gDNA, with IC_{50} ranging from 514.8 µM (donor 1) to 1157 µM (donor 3). Notably, 4-OHCP had slightly increased potency relative to PAM in each of the three PBMC donors (IC_{50} ratio 0.51, 0.17 and 0.30 respectively) compared to the very low alkylating potency relative to PAM in purified gDNA (IC_{50} ratio 2794). This suggests that activation of 4-OHCP occurs within PBMC.

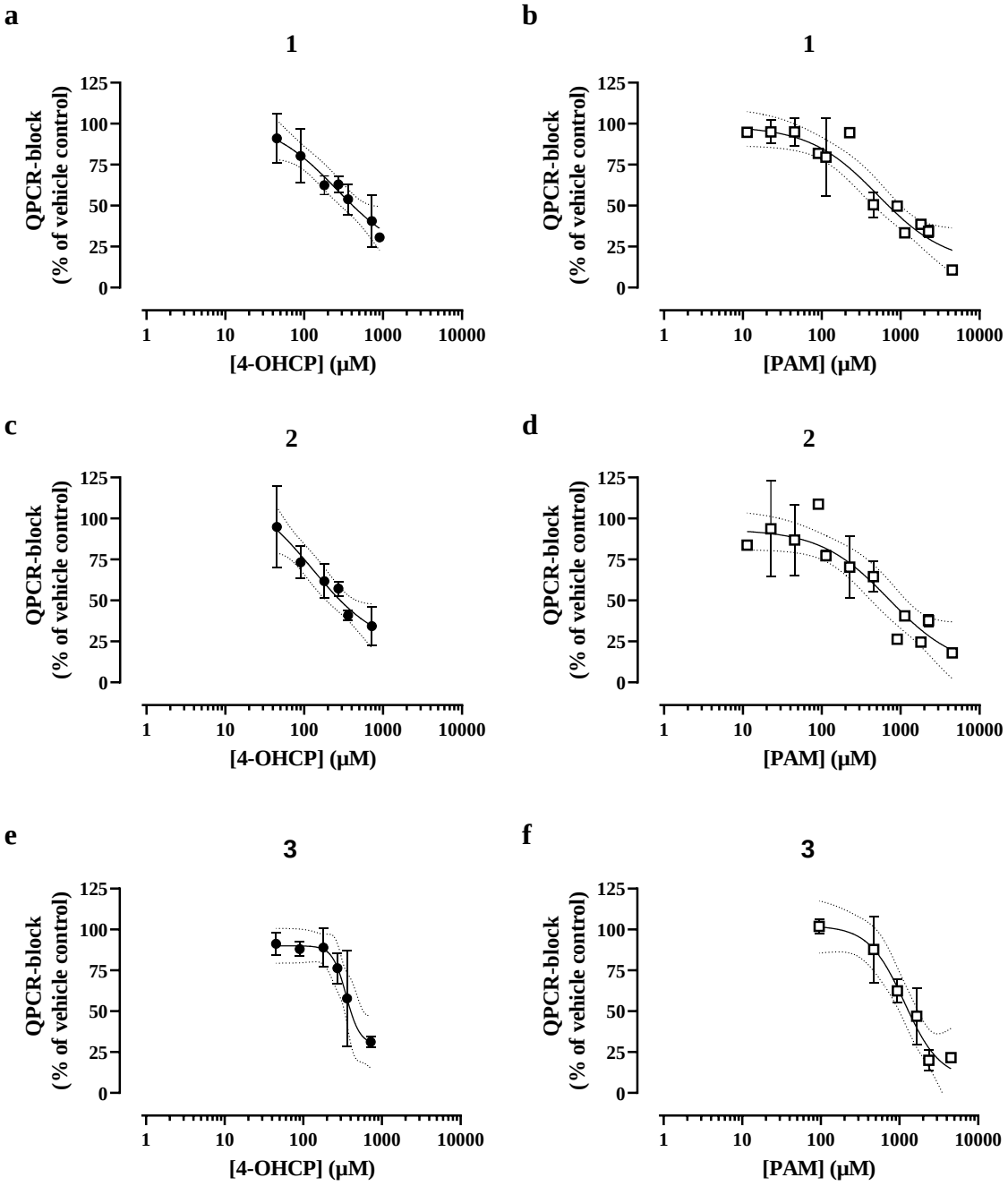

Figure 3-3. The ability of 4-OHCP (a, c, e) and PAM (b, d, f) to alkylate DNA in intact PBMC from three individual donors. Data are mean ± SD from N = 3 repeat experiments, undertaken using either triplicate or quadruplicate technical replicates, as cell numbers permitted. Least squares regressions (solid lines) were calculated taking into account the N and scatter of the replicates using either an [Inhibitor] vs. response three parameter model or an [Inhibitor] vs. response variable slope four parameter model, as appropriate, in GraphPad Prism 9.0.2 (constraints: $IC_{50} > 0$, Bottom > 0); 95% confidence intervals of the curve are indicated by the dotted lines.

3.2.3. DNA alkylation in cell lines incubated with 4-OHCP

To investigate whether this 4-OHCP activation was specific to lymphoid-derived cells, the ability of Jurkat cells (immortalised T-cells) to convert 4-OHCP into a DNA alkylating agent were compared with intestinal epithelial Caco-2 cells (derived from colon adenocarcinoma). While there was no evidence of QPCR-block following incubation of Caco-2 cells with up to 3609 µM 4-OHCP, significant inhibition of PCR amplification was observed in the Jurkat cells over this concentration range (Figure 3-4). These immortalised cells were 1.6 – 4.5-fold less sensitive than individual donor PBMC to 4-OHCP (Jurkat IC_{50} = 553.4 µM, 95% CI = 179.0 to 2092 µM).

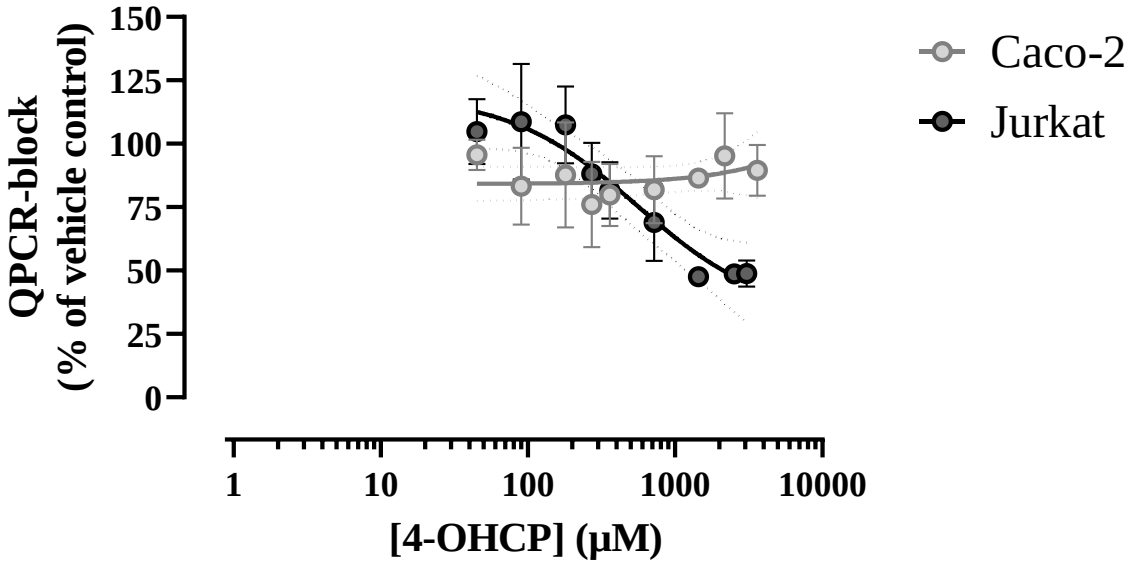

Figure 3-4. Activation of 4-OHCP into a DNA alkylating agent in immortalised T-cells (Jurkat) compared to epithelial cells (Caco-2). Data points represent the mean ± SD of N = 3 independent repeat experiments, each undertaken using n = 4 technical replicates.

3.2.4. Pre-incubation of 4-OHCP with candidate enzymes

In an attempt to identify the enzyme(s) capable of this activation 4-OHCP was pre-incubated with T4 phage DNA polymerase, which has both 3'-5' and 5'-3' exonuclease activity. Following ultrafiltration of the solution to remove the enzyme and 1 h exposure of gDNA there was no change in PCR-block compared to the effect of 4-OHCP in the absence of this enzyme (Figure 3-5a). Human plasma was similarly ineffective for 4-OHCP activation into a gDNA-alkylating product (Figure 3-5b). In contrast, pre-incubation of 4-OHCP with snake venom PDE-I significantly increased QPCR-block (Figure 3-5c). Since snake venom PDE-I has both DNA-exonuclease and cAMP phosphodiesterase activity, an initial assessment of the major cAMP-phosphodiesterase isoform found in lymphocytes, PDE4B, was then undertaken (Figure 3-5d). Following pre-incubation of 4-OHCP with purified human recombinant PDE4B, a significant (p = 0.0011) increase in QPCR-block was observed compared to zero enzyme control (40.7 ± 11.5% vs 74.0 ± 0.3% of vehicle control, respectively). Unpaired t-tests and one-way ANOVA were used to assess the differences in QPCR-block.

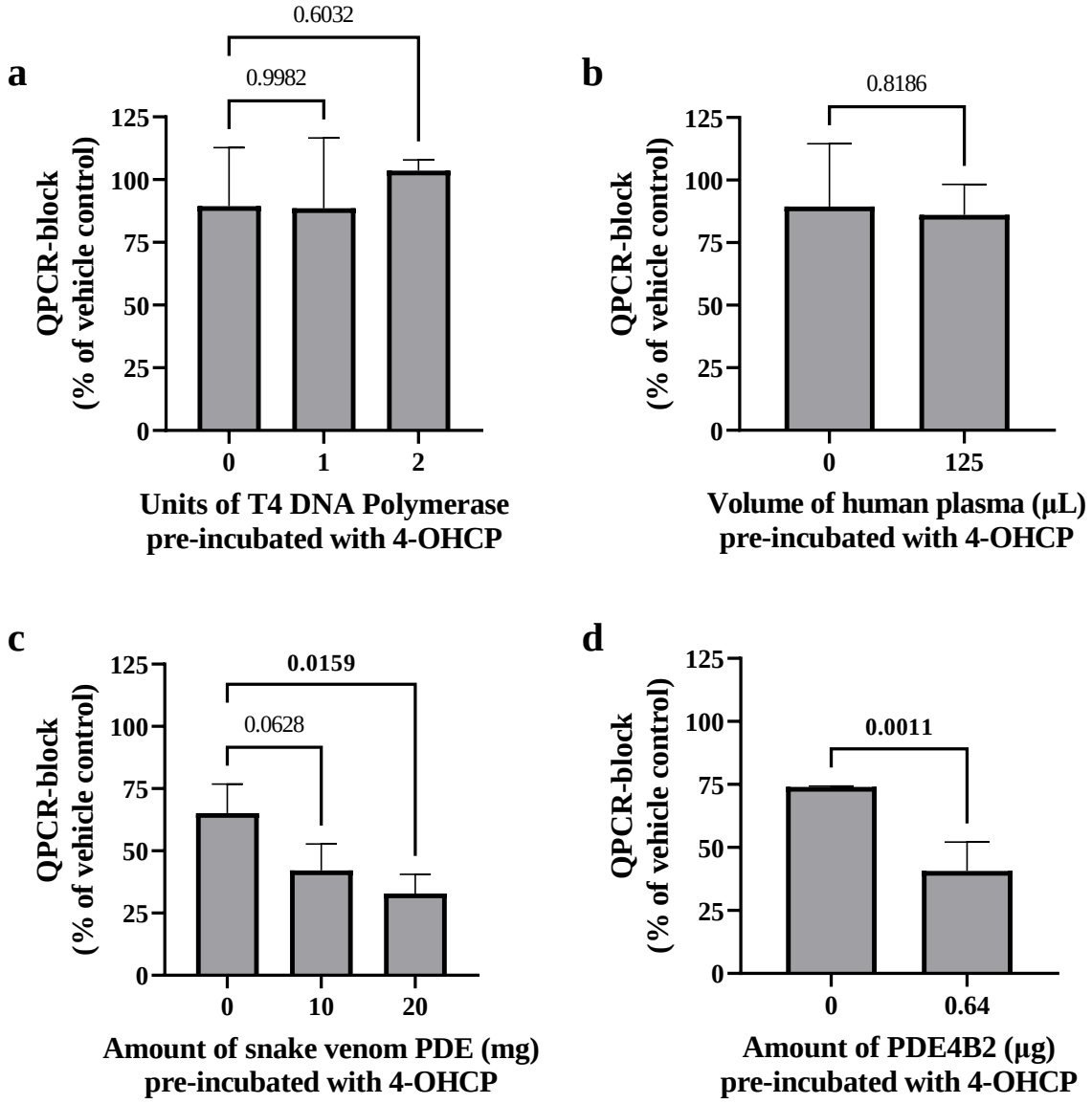

Figure 3-5. The effect of pre-incubation of 4-OHCP with a) phage T4 DNA Polymerase, b) human plasma, c) snake venom phosphodiesterase-I type IV, and d) recombinant human PDE4B2 on activation to a DNA alkylating agent. Data are mean ± SD of either N = 3 (A, B, C) or N = 1 (D) independent repeat experiments, each undertaken using n = 4 technical replicates. Adjusted *p*-values are indicated for pairwise comparisons.

3.2.5. Pre-incubation of 4-OHCP with PDE

A range of other commercially available PDE isoforms known to be expressed in lymphocytes were then assessed for ability to activate 4-OHCP into a DNA alkylating agent (Figure 3-6). Pre-incubation of 4-OHCP with purified human recombinant PDE3B, PDE8A1 and PDE11A4 did not significantly alter QPCR-block compared to zero enzyme control. This confirmed the previously reported lack of formation of the by-product acrolein following incubation of 4-OHCP with bovine heart PDE3. This isoform (PDE3B), well as PDE11A4, is a non-specific cAMP/cGMP PDE. Pre-incubation with PDE4B2 again confirmed that this cAMP-specific isoform could activate 4-OHCP, although this increase in QPCR-block did not reach the threshold for significance following correction for multiple testing (p= 0.017, unadjusted; p = 0.0822, adjusted). Snake venom PDE-I was also included as a positive control and significantly activated 4-OHCP compared with zero enzyme control (p = 0.0406 adjusted).

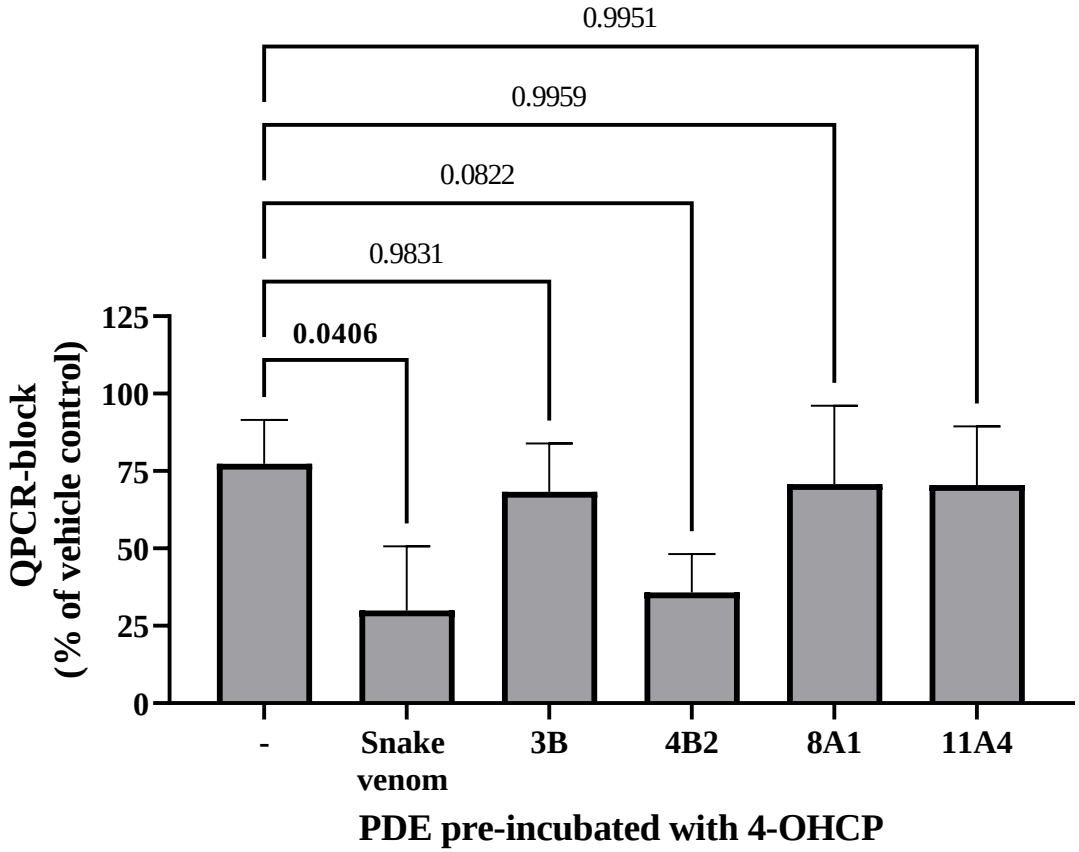

Figure 3-6. The effect of pre-incubation with PDE isoforms (0.64 µg) found in lymphocytes on the activation of 4-OHCP to a DNA alkylating agent. Data are mean ± SD of N = 3 independent repeat experiments, each undertaken using n = 4 technical replicates. Adjusted *p* values for pairwise comparisons are indicated. Snake venom PDE-I (0.2 units, 20 mg) was included as a positive control.

Hence, of the enzymes assessed, only snake venom phosphodiesterase (PDE-I) and the cAMP specific PDE4B2 could activate 4-OHCP into a DNA-alkylating agent. However, snake venom PDE-I had low specific activity for 4-OHCP (1.53 nmol/min/mg) [calculated from data in Bielicki et al. (1983)] compared with PDE4B2 (47.0 nmol/min/mg).

3.2.6. Rolipram treatment of PDE and effect on 4-OHCP activation

To determine whether the activation of 4-OHCP in PBMC is primarily catalysed by PDE4B the effect of rolipram, a selective inhibitor of PDE4, was assessed. Firstly, it was confirmed that rolipram could inhibit the activation of 4-OHCP into a DNA alkylating agent by purified PDE4B2 (Figure 3-7a). Then PBMC were exposed to 4-OHCP following either a 1 h pre-incubation or co-incubation with rolipram. Unexpectedly co-incubation of rolipram with 4-OHCP in PMBC resulted in a significant (p = 0.0387) *increase* in QPCR-block relative to the 4-OHCP-only control (Figure 3-7b). Pre-incubation with rolipram for an hour prior to the addition of 4-OHCP did not have this stimulatory effect and resulted in QPCR-block that was not significantly different from 4-OHCP-only control. Rolipram had no direct effect on the QPCR-block assay in the absence of 4-OHCP.

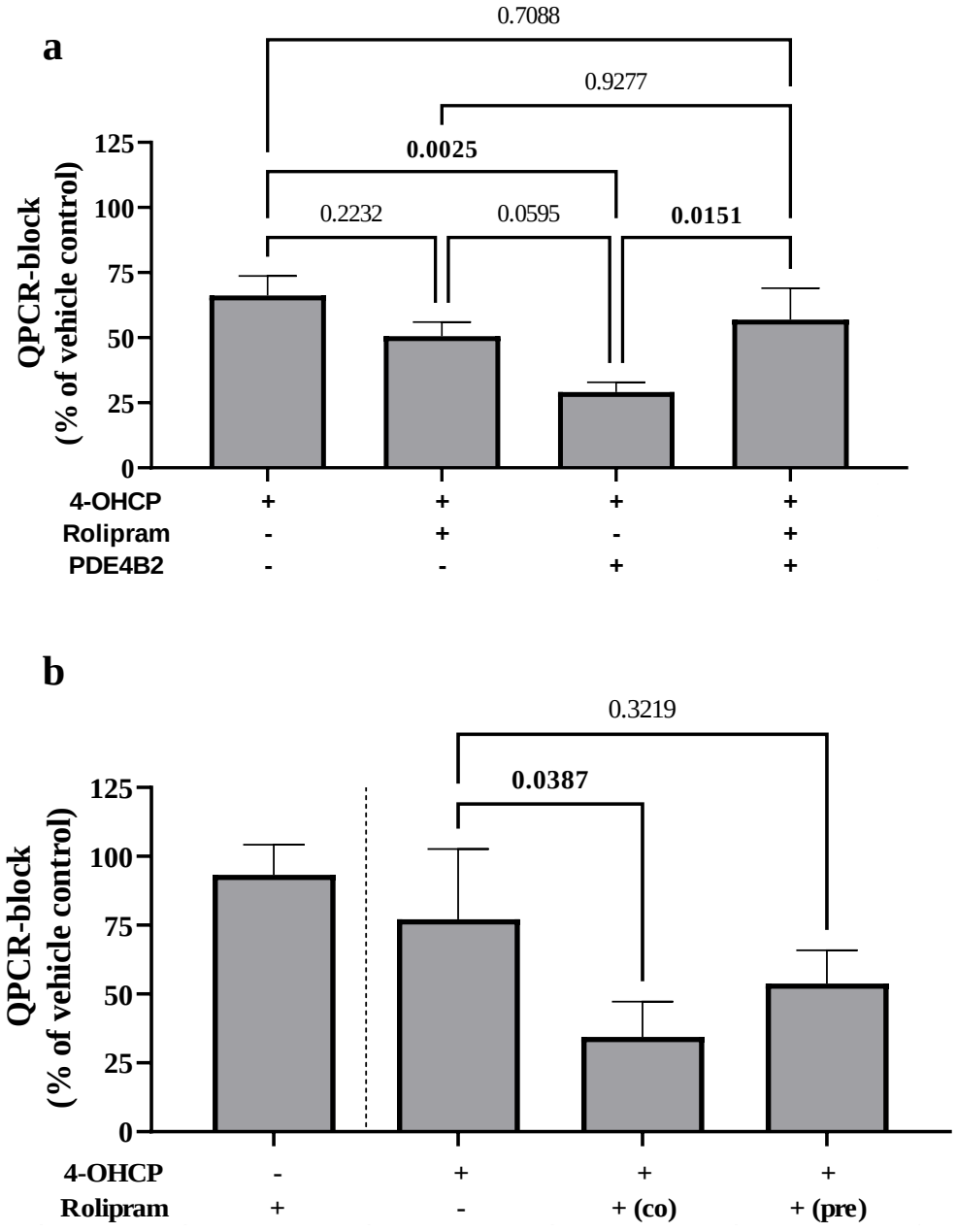

Figure 3-7. The effect of rolipram on the activation of 4-OHCP to an alkylating agent A) by human recombinant PDE4B2 (0.64 µg) or B) in PBMC (1 x 10^6 cells). Data are mean ± SD of N = 3 independent repeat experiments, each undertaken using n = 4 technical replicates. Adjusted *p* values for pairwise comparisons are indicated.

3.3. Discussion

It has previously been assumed that the major process involved in the conversion of aldophosphamide (the tautomer of 4-OHCP) into PAM is chemical hydrolysis of the phospho-ester bond via β-elimination. Whilst it has been suggested previously that this reaction could be enzyme-catalysed (Bielicki et al., 1983), there was only indirect evidence for this (i.e. formation of the by-product acrolein). Using an assay to detect formation of DNA-alkylating adducts which block PCR amplification, the work detailed in this chapter has demonstrated that 4-OHCP had only a very weak ability to alkylate purified gDNA, unlike the potent effect of its hydrolytic product PAM. This data not only confirms previous data of poor alkylating reactivity of 4-OHCP/aldophosphamide (Struck et al., 1975), but also suggests that over the 1 hour incubation period at physiological pH there was little spontaneous hydrolysis of 4-OHCP aldophosphamide tautomer into PAM.

There was an increased potency of DNA-alkylation in PBMC exposed to 4-OHCP relative to exogenous PAM for all three donors tested. Indeed, the DNA-alkylating potency of 4-OHCP in cells increased >18-fold compared to the intrinsic reactivity of 4-OHCP for purified gDNA. This contrasts with the >190-fold *decrease* in potency of PAM in PBMC relative to purified gDNA. This could be related to the ability of PAM to alkylate cysteine-rich proteins (Wei et al., 1999) and other intracellular proteins (Groehler et al., 2016). Such reactions with membrane and cytosolic proteins will sequester PAM as it enters cells and decrease the amount able to reach the nuclear compartment. In contrast, intra-cellular conversion, as opposed to extra-cellular conversion, of 4-OHCP into PAM would be expected to increase the relative amount of PAM reaching the nucleus. This would result in an apparently higher alkylating potency of 4-OHCP compared to exogenous PAM. However, the possible additional effect of DNA adduct formation by the by-product hydroxypropanal/acrolein cannot be discounted. This by-product,

formed from hydrolysis of the phospho-ester bond of aldophosphamide, can cause DNA single strand breaks (Crook et al., 1986; Fleer & Brendel, 1982; McDiarmid et al., 1991; M. Tang et al., 2011) and apoptosis (Engels et al., 2016; Voelcker, 2017). The effect of acrolein on the QPCR-block assay could not be assessed since it was not commercially available in New Zealand. However, PAM, rather than acrolein, is considered to be the major contributor to DNA-alkylation.

Previous reports suggested that only lymphocyte-rich tissues, (i.e. spleen and thymus of the rat) could substantially produce acrolein from 4-OHCP (Bielicki et al., 1983). Notably, activation of 4-OHCP into a DNA alkylating product was observed in immortalised T-cells (Jurkat) but not in neoplastic colorectal enterocytes (Caco-2). Moreover, this intracellular activation of 4-OHCP by PBMC and Jurkat cells is also consistent with previous reports that substantial DNA inter-strand cross-links were formed in K562 cells (myeloid leukaemia) following exposure of 4-OHCP, whereas exposure to equimolar amounts of PAM resulted in minor formation of these adducts in the DNA extracted from these cells (Crook et al., 1986; McGown & Fox, 1986). Assessment of activation of 4-OHCP by isolated myeloid and lymphoid subsets from normal blood cells or neoplastic cell lines should be considered in future studies.

Previous reports demonstrated that 3'-5'-exonucleases (such as DNA polymerase δ and *E. coli* DNA polymerase I) could catalyse the formation of the by-product acrolein from 4-OHCP with high specific activity, and it was speculated that activation may occur within the nuclei of cells (Bielicki et al., 1983). However, activation of 4-OHCP by T4 phage DNA polymerase, a 3'-5'-exonuclease with highly conserved amino-acid residues and a comparable catalytic site to *E. coli* DNA polymerase I (Frey et al., 1993; Reha-Krantz & Nonay, 1993) was not observed. It is possible that this enzyme can catalyse formation of PAM, but that PAM then alkylates the enzyme and is trapped as a protein adduct and not released into the buffer. Indeed, this type of

inactivation (suicide inhibition) of a 3'-5'exonuclease enzyme following pre-incubation with 4-OHCP or PAM (10 mM) has been previously demonstrated with *E coli* DNA polymerase I (Bielicki et al., 1984). Future studies should assess the ability of mammalian 3'-5'-exonucleases, such as polymerases α, δ and ε, or the cytosolic TREX1 (three prime exonuclease-1) to activate 4-OHCP into PAM. If 4-OHCP is activated into PAM by these 3'-5' exonucleases this could selectively target rapidly proliferating rather than quiescent cells.

The possibility of leucocyte-selective activation of 4-OHCP was intriguing, and hence subsequent experiments assessed enzymes with ribonucleotide phosphohydrolase activity, namely the cyclic-nucleotide phosphodiesterases (PDE). Snake venom PDE-I was observed to catalyse the formation of a DNA-alkylating product from 4-OHCP, confirming the previous observation that this enzyme could produce the by-product acrolein when incubated with 4-OHCP (Bielicki et al., 1983). The specific activity of snake venom PDE-I for activation of 4-OHCP was remarkably similar to that previously reported (1.53 nmol/min/mg vs 4.2 nmol/min/mg; Bielicki et al. 1983).

Since snake venom PDE-I has both 3'-5'-exonuclease and 3'5-cAMP phosphodiesterase activity (Uzair et al., 2018), the ability of those human cyclic-nucleotide PDE isoforms known to be expressed in human lymphocytes to catalyse the hydrolysis 4-OHCP into a DNA alkylating product was then investigated. Of the eleven members of the superfamily identified to date, isoforms PDE4, PDE7 and PDE8 are specific for catalysis of cAMP, PDE5, PDE6 and PDE9 are specific for cGMP, whilst PDE1, PDE2, PDE3, PDE10 and PDE11 hydrolyse both of these cyclic nucleotides (Omori & Kotera, 2007). Of the isoforms assessed, only the cAMP-specific phosphodiesterase PDE4B2 could activate 4-OHCP. The specific activity for activation of 4-OHCP into a DNA alkylating product was 30-fold greater than snake venom PDE-I. This specific activity of PDE4B (47 nmol/min/mg) was at least as high as that

previously observed for 3'-5'-exonuclease DNA polymerases (Belicki et al. 1983, Table 1 p. 28)

This is the first time that a human cAMP-PDE has been indirectly shown to catalyse the hydrolysis of 4-OHCP/aldophosphamide. The possible role of a PDE isoform selective for cAMP is further corroborated by the previous observation of 4-hydroperoxycyclophosphamide inhibition of cAMP-specific phosphodiesterase activity in a rat tumour cell line (Tisdale, 1977). This study demonstrated that 4-hydroperoxycyclophosphamide, but not its other metabolites, could competitively inhibit cAMP phosphodiesterase activity with a K_i of 0.19 mM. Moreover, these authors described the molecular similarity (bond length and angle) of the phospho-ester (P-O-C) bonds in cAMP and 4-OHCP, as well as the chair conformation of both cAMP and 4-OHCP. They hypothesised that some of the therapeutic effects of cyclophosphamide were mediated through the elevation of cAMP. While this may be a possible mechanism for some of the pharmacological effects of cyclophosphamide, the catalysis of 4-OHCP to a DNA alkylating product by PDE4B2 demonstrated in our *in vitro* experiments provides a direct link to the classical DNA-alkylation mechanism of cyclophosphamide cytotoxicity.

It is well established that cyclophosphamide spares haematopoietic stem cells and early lymphoid-myeloid progenitor cells whilst targeting mature B- and T-lymphocytes. Indeed, both cyclophosphamide (in patients) and 4-OHCP (*in vitro*) have selective effects on $CD4^+CD25^+$ (Berd & Mastrangelo, 1988; Lutsiak et al., 2005; Zhao et al., 2010) and the $CD8^+$ regulatory T-cell (T_{regs}) subset of cytotoxic T-cells (Traverso et al., 2012). Furthermore, T_{reg} cells have increased numbers of inter-strand crosslinks (a biomarker of PAM formation) in comparison to T-helper ($CD4^+$) or cytotoxic T-cells ($CD8^+$) after exposure to the 4-OHCP precursor mafosfamide (Heylmann et al., 2013). The selectivity of cyclophosphamide for mature lymphocytes is generally attributed to high levels of aldehyde dehydrogenase, which detoxifies aldophosphamide (Figure 1-1), in the stem/progenitor cells. However, there are also reports of

increased expression of PDE4 and PDE7 in activated (compared to quiescent) T-cells (Glavas et al., 2001; Szczypka, 2020). Moreover, PDE4 is upregulated in cyclophosphamide-sensitive illnesses such as rheumatoid arthritis (Wu et al., 2012) and chronic B-cell lymphocytic leukaemia (Kim & Lerner, 1998). The intracellular conversion of 4-OHCP/aldophosphamide tautomer into PAM by PDE4 could further explain the selective immunomodulatory effects of cyclophosphamide on the subsets of mature immune cells that express this isoform.

There was a somewhat paradoxical behaviour of the PDE4-inhibitor, rolipram, on the activation of 4-OHCP in PBMC; co-incubation of rolipram with 4-OHCP in PBMC appeared to enhance, rather than inhibit, the latter's activation into a DNA alkylating compound. There could be a number of reasons for this. Firstly, PDE4B2 is a short form of PDE4 with a truncated N-terminal region called URC2. The URC2-region interacts with the catalytic region and can alter enzyme dimerisation. The ability of rolipram to bind to the catalytic site of PDE4 can alter substantially depending on enzyme conformation (Omori & Kotera, 2007). The apparent increase (rather than inhibition) of activation of 4-OHCP by rolipram in PBMC could be due to this type of allosteric effect on this splice variant of PDE4, which may have a different enzyme conformation from wild-type PDE4. However, pre-incubation of rolipram with PBMC prior to addition of 4-OHCP did not stimulate the activation into a DNA alkylating agent. It has previously been noted that agents which elevate cAMP can cause a transient stimulation of PDE activity, which is thought to be due to negative feedback regulation via cAMP-dependent protein kinase phosphorylation of PDE4 (Madelian & Vigne, 1996). It may be that this transient increase in activity has declined when cells were pre-incubated with rolipram, prior to exposure to 4-OHCP.

Whilst purified PDE4B has been demonstrated to have the ability to activate 4-OHCP, the lack of inhibition of this activation in PBMC by rolipram could also be due to the involvement of another PDE isoform. The other major PDE in lymphocytes is PDE7, which is a rolipram-

insensitive cAMP-specific PDE. Unfortunately, isolated PDE7A was not commercially available for assessment in these studies. Further investigation will be needed to determine whether PDE7A is able to activate 4-OHCP and if this an important isoform for this activation in PBMC.

Intracellular activation of 4-OHCP to PAM by PDE4 may also explain some of the toxicities associated with cyclophosphamide chemotherapy. Of note, rolipram has been shown to prevent cyclophosphamide-induced cystitis in rats (Büyüknacar et al., 2008; Sakura et al., 2009). Urotoxic injury is generally considered to be a consequence of high exposure of the bladder epithelium to excreted acrolein, and the anti-inflammatory effects of rolipram may therefore account for this effect. However, activation of 4-OHCP by PDE4, which is expressed at high levels in bladder, could be an alternative explanation for this tissue-selective toxicity. High dose tadalafil (a selective PDE5/PDE11A inhibitor) has also been shown to inhibit cyclophosphamide-induced haemorrhagic cystitis in rats (Bischoff, 2004) and to ameliorate the cyclophosphamide-induced apoptosis of spermatogonia (Yigitaslan et al., 2014). Rolipram and pentoxifylline (a non-specific PDE inhibitor) have also been shown to attenuate cyclophosphamide-induced type 1 diabetes in NOD mice (Liang et al., 1998).

When cyclophosphamide is used in the treatment of auto-immune diseases the major toxicity of concern is premature ovarian failure. 4-OHCP has been shown to have a direct cytotoxic effect on granulosa cells of the ovarian follicle *in vitro* (Tsai-Turton et al. 2007). However, granulosa cells cannot convert cyclophosphamide into 4-OHCP (Ataya et al. 1990). Granulosa cells do however, express very high levels of PDE4, PDE7 and PDE8, since the tight control of cAMP levels by these enzymes is important for appropriate timing of oocyte meiosis and maturation (Vigone et al., 2018). If 4-OHCP is a substrate for PDE4 and/or PDE7 this could also explain this tissue specific toxicity.

In conclusion, the experiments conducted have demonstrated that hydrolysis of the phospho-ester bond of 4-OHCP/aldophosphamide to form the DNA alkylating agent PAM appears to be an enzyme catalysed reaction. This activation is observed to occur in leucocytes and cyclic-nucleotide PDE, such as PDE4, are promising candidates for this process. This should be investigated further as a possible additional mechanism for the tissue-specific immunomodulatory effects of cyclophosphamide.

Chapter 4: Differences in DNA repair capacity in lupus nephritis patients: The REPAIR study

4.1. Introduction

The inter-individual variability of therapeutic response to cyclophosphamide treatment has mainly been attributed to differences in cyclophosphamide metabolism, particularly the conversion of the prodrug cyclophosphamide to the intermediate metabolite 4-hydroxycyclophosphamide (4-OHCP) by cytochrome P450 (CYP) enzymes. However, inter-individual variability in the degree of DNA alkylation caused by the ultimate cyclophosphamide product, phosphoramide mustard (PAM) may also contribute to differences in therapeutic response. This chapter focuses on determining whether SLE patients exhibit higher sensitivity to DNA alkylation by PAM than healthy individuals.

As was outlined in Chapter 1 (Section 1.3.1), the generally accepted mechanism of action of cyclophosphamide cytotoxicity is through the formation of inter- and intra-strand crosslinks in DNA. These bulky crosslinks act as physical barriers to DNA replication and eventually result in cell cycle arrest. In the context of SLE treatment this leads to the suppression of immune expansion particularly in T- and B- lymphocytes.

The variability in the degree of DNA alkylation following cyclophosphamide therapy can thus arise from numerous factors, such as transport of 4-OHCP/aldophosphamide tautomer or PAM into the cell, inactivation of aldophosphamide by aldoketoreductase enzymes (such as aldehyde dehydrogenase), differences in the intracellular formation of PAM (via PDE enzymes) alkylation of intracellular proteins and ultimately differences in the capacity of the cell to repair the DNA damage.

4.1.1. Transport of 4-OHCP/aldophosphamide tautomer or PAM into cells

The consensus in the literature is that the 4-OHCP/aldophosphamide tautomer passively diffuses into the cell and is ultimately converted to PAM intracellularly (Zhang et al., 2005). This is assumed to be the mechanism since PAM is a charged molecule at physiological pH and unlikely to passively diffuse across the membrane. Both PAM and 4-OHCP/aldophosphamide tautomer are detectable in the plasma of patients and there is evidence that PAM, as well as 4-OHCP/aldophosphamide tautomer, can be actively transported into cells (Erickson et al., 1980). Although the transporters have not been identified, it is feasible that transporter expression and/or function may influence the amount of 4-OHCP/aldophosphamide tautomer and PAM transported into the cell and ultimately the extent of DNA alkylation caused by PAM.

4.1.2. Inactivation of 4-OHCP/aldophosphamide tautomer

Once inside the cell the 4-OHCP/aldophosphamide tautomer can be inactivated through numerous pathways. Aldophosphamide is primarily inactivated by the conversion to carboxyphosphamide, and this is catalysed by the enzyme aldehyde dehydrogenase 1A1 (ALDH1A1). Increased ALDH1A1 expression has been associated with worse overall survival in breast cancer patients receiving cyclophosphamide therapy (Khoury et al., 2012). Similarly, *ALDH1A1* genetic polymorphisms (rs3764435 and rs8187996) have been associated with haematological toxicity in breast cancer patients treated with cyclophosphamide in combination with doxorubicin (Yao et al., 2014). Interestingly, in a separate study, the *ALDH1A1* variant rs8187996 was found to associate with a lower risk of toxicity in cancer patients treated with cyclophosphamide (Hwang et al., 2022). However, there has been little headway made in understanding the relationship between these genetic polymorphisms and their impact on ALDH1A1 activity. Inter-individual differences in ALDH1A1 activity arising

from genetic polymorphisms could result in differences in the inactivation of aldophosphamide/4-OHCP, ultimately influencing the total amount of the cytotoxic metabolite PAM formed within a cell.

4.1.3. Intracellular formation of PAM (via PDE enzymes)

As demonstrated in the previous chapter (Chapter 3), there is evidence that 4-OHCP/aldophosphamide tautomer can be activated into the DNA-alkylating molecule (PAM) by cellular enzymes. The preliminary data suggests that this may be catalysed by phosphodiesterase enzymes including PDE4B. Hence differences in the enzymatic formation of PAM could also influence extent of DNA alkylation and therapeutic response.

4.1.4. Protein alkylation

In addition to factors which influence the amount of PAM formed from the 4-OHCP/aldophosphamide tautomer, the final concentration of PAM within the nucleus, and therefore the amount of DNA damage, is dependent on the extent of PAM alkylation of other biomolecules. PAM is a highly reactive electrophilic molecule and will alkylate glutathione and proteins within the cell as well as DNA.

Whilst PAM can directly alkylate the cysteine moiety of glutathione, it has been suggested that a glutathione S-transferase (GSTA1) enzyme catalyses the formation of a glutathione-conjugated form of PAM, monochloro-monoglutathionylphosphoramide mustard (Dirven et al., 1994). This is an inactive form of PAM and can no longer alkylate other biomolecules such as DNA or proteins. Decreased expression of *GSTA1* was associated with decreased risk of death (increased survival) in the first 5 years after diagnosis in breast cancer patients treated with cyclophosphamide (Sweeney et al., 2003). This suggests that decreased detoxification via glutathione conjugation of PAM led to more favourable therapeutic outcome.

Many intracellular proteins alkylated by PAM have been identified and these include the metallothionein protein family. These are cysteine- and thiol-rich, low molecular weight family of proteins which are localised to the Golgi apparatus. *In vitro*, PAM has been found to alkylate metallothioneins, forming covalent links at cysteine residues of the proteins (Wei et al., 1999). Importantly, a study has shown that upregulation of metallothioneins is associated with worse outcomes in cancer patients treated with cyclophosphamide (Poulsen et al., 2006). This suggests that increased metallothionein expression decreases the therapeutic effectiveness of cyclophosphamide, possibly through the increased detoxification of PAM.

In addition, other proteins can be alkylated by PAM and within the nuclear compartment many of these have been identified as DNA-protein complexes. Importantly these PAM adducts on DNA-proteins are involved in transcriptional regulation, translation, RNA processing and also the DNA damage response (Groehler et al., 2016). Hence alkylation of DNA-proteins by PAM could be an additional way in which this molecule damages DNA and leads to cell death.

4.1.5. DNA damage repair capacity

The DNA repair capacity of the cells will also influence the eventual cytotoxicity of the PAM product of cyclophosphamide. As was previously mentioned in Chapter 1 (Section 1.3.1), the monoadducts and inter-strand cross links formed by PAM at the 3'-GnC-5' sequences in DNA form bulky lesions that block DNA replication and transcription. This initiates DNA repair pathways, in particular, nucleotide excision repair and double strand break repair.

Inherited variants in many DNA repair pathways are well characterised to predispose to carcinogenesis due to poor repair of endogenous damage, induced by factors such as random replication-induced errors, as well as hormonal and environmental carcinogens. However, there is also increasing evidence that impaired function in both nucleotide excision repair and double strand break repair pathways is observed in patients with SLE (Davies et al., 2012;

Jahantigh et al., 2015; Manolakou et al., 2022; Namas et al., 2016; Souliotis et al., 2016). Indeed, there is some suggestion that differences in repair of UV- or ROS- damaged DNA could predispose to autoantigen generation in this immune-mediated disease (Lo, 2016; Lo & Tsokos, 2018; Meas et al., 2017; Noble et al., 2016).

The formation of PAM-induced DNA monoadducts mainly triggers the nucleotide excision repair pathway. DNA damage that leads to this pathway can be sensed by two different mechanisms, global genome repair and transcription-coupled repair. Global genome repair targets localised lesions in the genome whereas transcription-coupled repair detects damage in active genes during transcription. Subsequently, the DNA double helix is unwound by helicase activity and the lesion is removed, followed by re-ligation of this area of DNA. In SLE patients, deficiencies in various steps of this pathway have been observed (Lee et al., 2011; Souliotis et al., 2016).

On the other hand, inter-strand crosslinks caused by PAM induce the double strand break repair response. The double strand break repair response is mediated through different mechanisms including, non-homologous end joining and homologous recombination. Both utilise different sets of proteins with different mechanisms to repair double strand breaks. SLE patients generally exhibit impaired capacity to repair these double strand breaks (Davies et al., 2012; Souliotis et al., 2016).

There are numerous proteins involved in each of these repair pathways, each of which may be differentially expressed in individuals. Due to the complex overlapping nature of the numerous proteins involved in DNA damage repair, a single protein (and its coding variant) within a pathway is unlikely to be individually causative of the impaired capacity previously reported in SLE patients. Therefore, a functional endpoint-based assay such as southern blotting, single

cell gel electrophoresis assay (COMET) or the QPCR-based assay (described in Chapter 2 Section 2.1.8) is required.

The studies to date have assessed the repair capacity in lupus patients compared to healthy controls following damage due to alkylating agents, such as melphalan (Souliotis et al., 2016), UV or oxidants (Davies et al., 2012; Harris et al., 1982; McCurdy et al., 1997). Remarkably, despite this evidence of impaired DNA-damage repair capacity in patients with SLE, there has been little consideration as to the therapeutic consequences with respect to differences in repair of PAM-induced DNA damage.

Individuals with impaired repair could thus be more sensitive to cyclophosphamide (PAM)-induced DNA damage and would be expected to have an earlier or more robust response to cyclophosphamide treatment.

To further investigate the putative differences in the functional-capacity to repair DNA damage in SLE patients the QPCR-based assay was used quantify differences in PAM-induced DNA damage in *ex vivo* exposed PBMC from healthy controls and patients with lupus nephritis (LN).

4.1.6. Study design

The study was approved by the Northern B Health and Disability Ethics Committee (18/NTB/170 for healthy donors, 20/NTB/182 for lupus nephritis (LN) patients). Following informed consent, patients above 18 years old diagnosed with either active or quiescent lupus nephritis and not currently being treated with cyclophosphamide or any other alkylating agent were recruited into the study. Donors above 18 years old and were healthy were recruited into the study. Patients who were not able to provide a blood sample or donors who were pregnant or breast feeding, on any medication other than oral contraception or had current illness were excluded from the study.

Following informed consent, lupus nephritis patients were recruited at renal clinics conducted at Auckland District Health Board and Waitematā District Health Board and healthy donors were recruited at the University of Auckland. In a previous study (Souliotis et al., 2016), 6 participants per group (active and quiescent lupus nephritis) and 6 healthy donors were enough to detect differences in DNA damage repair capacity following treatment with a different DNA alkylating agent (melphalan). Assuming an effect size of 30%, and a population standard deviation of 0.3, the study aimed to recruit 17 patients and 17 healthy donors, which would provide 80% power to detect a difference in mean QPCR-block IC_{50} between lupus nephritis patients and healthy donors using the Mann-Whitney test.

Following recruitment into the study, a blood sample was taken from the patients at their next renal clinic visit. Blood samples were drawn by a trained phlebotomist from healthy donors following informed consent after recruitment at the University of Auckland. The blood sample (24 mL) was collected in 3 x 8 mL BD Vacutainer® CPT™ sodium citrate tubes (Becton, Dickinson and Company, USA). The tubes were then centrifuged (1800 *g*, 30 min, 24 °C) within half an hour of collection and the plasma removed and stored at –80 °C. The remaining buffy coat (containing PBMC) was pooled from the 3 tubes and an aliquot of the cells were counted (as described in Chapter 2 Section 2.1.3). The pooled PBMC were centrifuged (400 *g*, 40 min) and the pellet was gently resuspended in an appropriate volume of PBS to provide 37 x 10^6 cells/mL. Subsequently, PBMC in PBS were exposed to a range of PAM concentrations (0 – 1000 µM) for 1 hour at 37°C. The PBMC were then removed from the PAM solution by centrifugation (1600 *g*, 5 min). The DNA was then extracted from the PBMC through lysis (detailed in Chapter 2 Section 2.1.8). The extracted DNA was then amplified in the QPCR assay (detailed in Chapter 2 Section 2.1.8).

The amount of PAM-induced DNA adduct was quantified as the amplification of a treated sample relative to untreated control (% QPCR block) and the concentration of PAM which

resulted in 50% of untreated control was calculated and reported as IC_{50}. For comparison of the differences between patients and donors in PAM-induced DNA damage repair, the data are reported as the IC_{50} values (mean of four technical replicates) for each individual donor.

The statistical analyses were conducted in GraphPad Prism 9.0.2 (Graphpad Software Inc., USA). All *p*-values calculated were two-sided and considered significant below 0.05. To determine the likelihood of continuous data being sampled from a normal or lognormal distribution, the Akaike Information Criterion was used in Prism. Thereafter, the Shapiro-Wilk normality test was used to determine normality or lognormality of the data, depending on the result above. Correlation between continuous variables was calculated using Pearson's product-moment correlations if parametric or using Spearman's rank correlations if non-parametric. Differences between parametric data sets were calculated using unpaired t-tests (with Welch's correction) and 1-way ANOVA, whereas differences between non-parametric data sets were calculated using Mann-Whitney rank sum tests and Kruskal-Wallis rank sum tests.

4.2. Results

4.2.1. Study demographics

The demographics of the patient and healthy volunteer populations in the study are summarised in Table 4-1. Of the 17 patients recruited for the study, blood samples could be obtained from 16, of which 75% were female. Multiple ethnicities were reported for both study populations. The average age of lupus nephritis (LN) patients included in the study was 38.7 ± 12.9 years, with 37.5% identifying as New Zealand European or European, 37.5% Asian, 25% Pasifika. A similar proportion of the 13 healthy volunteers recruited for the study were female (77%). The average age of healthy volunteers recruited for the study was 35.4 ± 13.1 years, with 61.5% identifying as New Zealand European or European and 23.1% Asian. There was no significant difference in the ages ($p = 0.409$), or the female to male proportion in the two study populations (chi-square test, $p = 0.904$). Fisher's exact tests were used to test differences in ethnicity proportions between the two populations. In both study populations, there was no statistically significant difference between the proportion of New Zealand European/European ($p = 0.175$), Māori ($p = 0.417$), Pasifika ($p = 0.125$), Asian ($p = 0.705$) and Middle Eastern/Latin American/African ($p > 0.999$) ethnicities.

	Healthy donors (n = 13)	LN patients (n = 16)
Age		
(years)	35.4 ± 13.1	38.7 ± 12.9
Sex		
Female (%)	77	75
Male (%)	23	25
Ethnicity[1]		
New Zealand European/European (%)	61.5	37.5
Māori (%)	7.69	0
Pasifika (%)	0	25.0
Asian (%)	23.1	37.5
Middle Eastern/Latin American/African (%)	15.4	6.25
Others (%)	0	0

Table 4-1. Demographics of lupus nephritis (LN) patients and healthy donors recruited for the study. Multiple ethnicities were reported. [1]Categories of self-identified ethnicity as described in the NZ census (2021).

In the patient group, 50% of the patients included in the study had active lupus nephritis and 50% had quiescent disease. All patients with quiescent or active disease were concomitantly treated with prednisone at varying dosages (2.5 – 80 mg/day). Several of these patients were also treated with other drugs, such as hydroxychloroquine and mycophenolate for control of lupus as well as calcineurin inhibitors, such as tacrolimus and cyclosporin (listed in Table 4-2).

ID	Medications given	ID	Medications given	ID	Medications given
01	Hydroxychloroquine Mycophenolate Prednisone Cotrimoxazole Colchicine Cholecalciferol Amlodipine Ferrous fumarate	07	Cyclosporine Prednisone Candesartan Allopurinol Omeprazole Ezetimibe Carvedilol Frusemide Cotrimoxazole Erythropoietin Nortriptyline	13	Prednisone Folic Acid Methotrexate Sulphasalazine Cholecalciferol Cetirizine
02	Mycophenolate Prednisone Cholecalciferol Tenofovir Omeprazole	08	Prednisone Hydroxychloroquine	14	Prednisone Mycophenolate Hydroxychloroquine
03	Hydroxychloroquine Mycophenolate Prednisone Cilazapril Cholecalciferol	09	Prednisone Azathioprine Hydroxychloroquine	15	Hydroxychloroquine Mycophenolate Aspirin Omeprazole Cilazapril Risedronate Cholecalciferol Prednisone Sertraline
04	Mycophenolate Hydroxychloroquine Prednisone Amlodipine Cotrimoxazole Cholecalciferol Oxynorm	10	Hydroxychloroquine Prednisone Mycophenolate	16	Prednisone Hydroxychloroquine Omeprazole
05	Hydroxychloroquine Prednisone Frusemide Cilazapril Sodium bicarbonate Cholecalciferol Erythropoietin	11	Amlodipine Cotrimoxazole Aspirin Metoprolol Candesartan Omeprazole GTN Prednisone Mycophenolate Hydroxychloroquine Atorvastatin		
06	Mycophenolate Prednisone Hydroxychloroquine Tacrolimus	12	Prednisone Mycophenolate		

Table 4-2. Concomitant medications of recruited lupus nephritis patients at the time of blood sampling.

4.2.2. Quantification of PAM-induced DNA damage repair

Sensitivity of PBMC to PAM was quantified by the QPCR-block assay after exposure to a range of PAM concentrations, and the IC_{50} value for each PBMC donor was calculated. Example IC_{50} curves are shown for two donors with widely differing sensitivity to PAM-induced DNA damage (Figure 4-1).

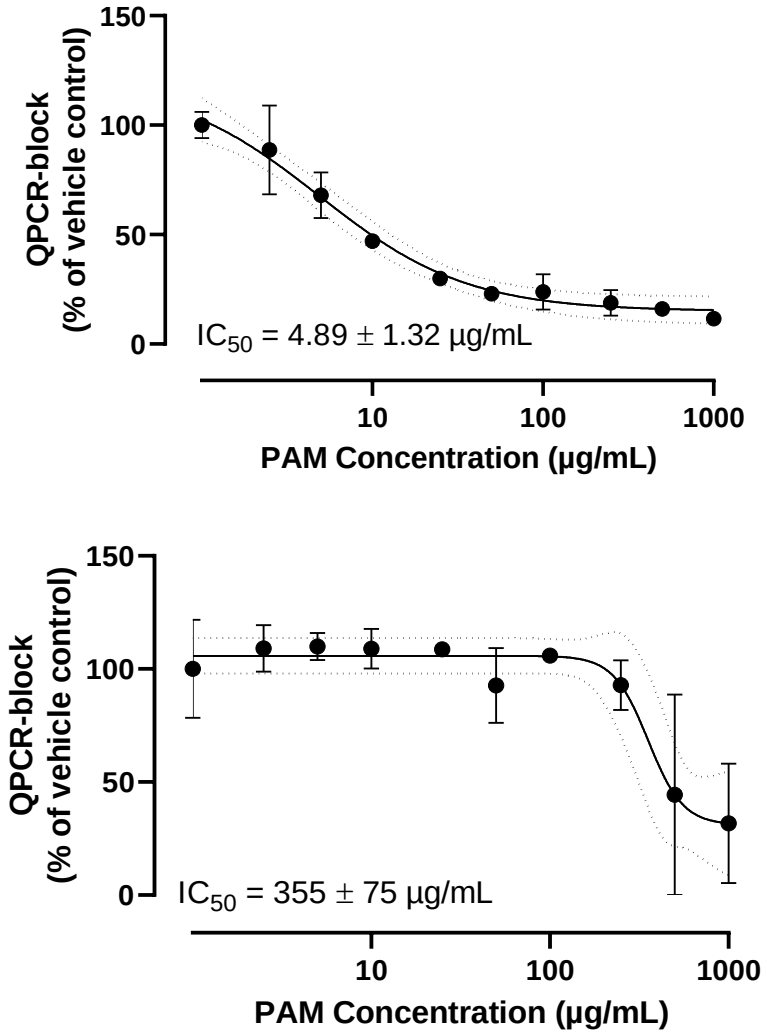

Figure 4-1. Example IC_{50} curves of two individual lupus nephritis patients with differing sensitivity to PAM. Individual datapoints are the mean QPCR-block of experimental (n = 1 – 4) and technical replicates (n = 4) as determined by the concentrations of double-stranded DNA after PCR. Error bars around datapoints represent the standard deviation of the mean and the dotted lines around the curve represent the 95% confidence intervals of the fit of the curve. IC_{50} values and standard deviations were determined by the curve fit in GraphPad Prism 9.0.2.

There was a wide range of sensitivity to PAM observed in the healthy donors, the IC_{50} ranged 8-fold from 100 µg/mL to 815 µg/mL. In lupus nephritis (LN) patients, a wider range of sensitivity to PAM was observed, with IC_{50} values ranging more than 300-fold from 2.23 µg/mL to 733 µg/mL (Figure 4-2). The median (IQR) of IC_{50} values were 260 (100-587) and 161 (13.74-733) µg/mL for healthy donors versus LN patients respectively. There was a significant difference ($p = 0.0319$, Mann-Whitney test) in the sensitivity to PAM-induced DNA damage between the healthy donors and the lupus nephritis patients (Figure 4-2).

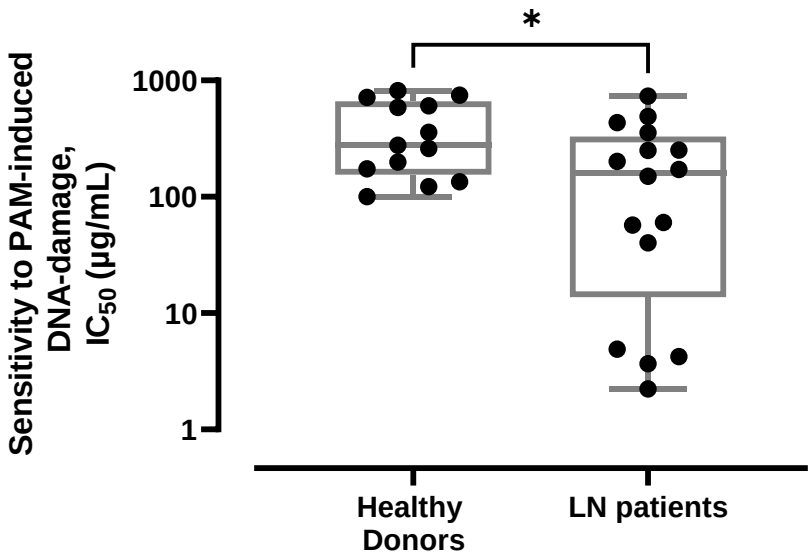

Figure 4-2. Lupus nephritis (LN) patients (n = 16) have higher sensitivity to PAM-induced DNA damage than healthy donors (n = 13). Individual datapoints are IC_{50} values determined in each donor by the QPCR-block assay. Box and whisker plots represent the median, 25-75 % IQR (boxes) and the minimum and maximum of each population. A significant (* $p < 0.05$) difference between the two groups was observed, (Mann-Whitney test).

The data for the LN patients was highly skewed (1.209) with a positive kurtosis (1.144), suggesting a non-Gaussian distribution. The spread of the IC_{50} values obtained in the study populations were therefore assessed for conformity to a normal (Gaussian) distribution and for lognormal distribution. Initial comparison of likelihoods suggested that both populations followed a lognormal distribution. Both the healthy donors (AIC_c P(lognormal) = 0.852) and LN patients (AIC_c P(lognormal) = 0.999) were found more likely to follow a lognormal distribution. In healthy donors, sensitivity to PAM conformed to a lognormal distribution. However, in LN patients, sensitivity to PAM did not conform to either a normal or lognormal distribution in more than one test. Significant deviation from lognormality was: p = 0.0245, Shapiro-Wilks test; p = 0.0184, Andersen-Darling test. The quantile-quantile (QQ) lognormality plots are shown (Figure 4-3). This suggests that that the distribution of the data in the LN patients is not lognormal.

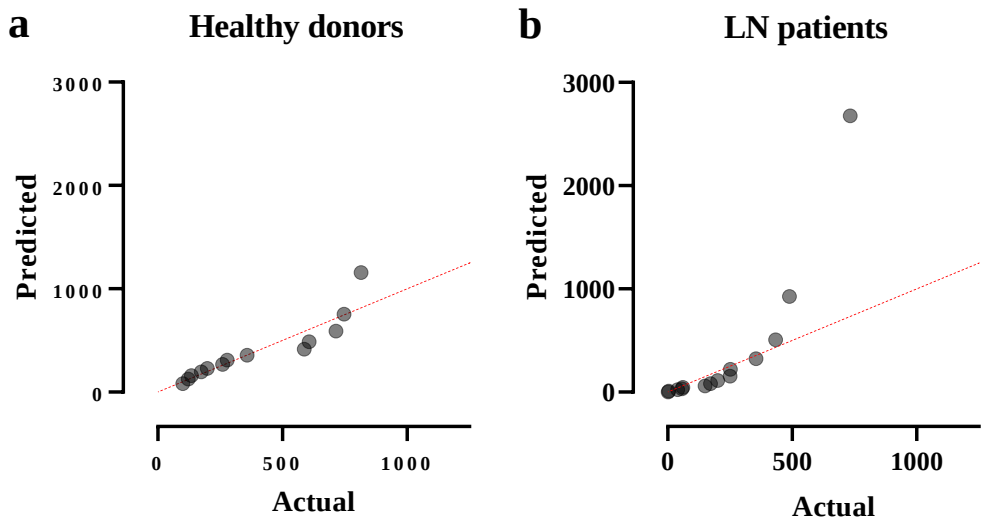

Figure 4-3. The quantile-quantile (QQ) probability plots for lognormality in sensitivity to PAM-induced DNA damage in a) healthy donors (n = 13) and b) LN patients (n = 16). Individual datapoints are IC_{50} values determined in each donor by the QPCR-block assay. LN patients substantially deviate from the null hypothesis (dotted line) by two lognormality tests (p = 0.0245, Shapiro-Wilks test; p = 0.0184 Andersen-Darling test).

To visualise the distribution of IC_{50} values for both the healthy donor and LN patient populations, the values were log-transformed (as both populations were found to more likely follow a lognormal distribution) and graphed in histograms (Figure 4-4). In healthy donors, the log-transformed IC_{50} values followed a unimodal shape whereas 2 peaks were present in LN patients. Additionally, an extra sum-of-squares F test was conducted for both populations to compare a Gaussian distribution model against a sum of 2 Gaussian distributions model. In healthy donors, the single Gaussian distribution model was considered the better fit ($p = 0.996$), whereas the sum of 2 Gaussian distributions model was a better fit in LN patients ($p = 0.0258$). This suggests a bimodal population distribution in LN patients.

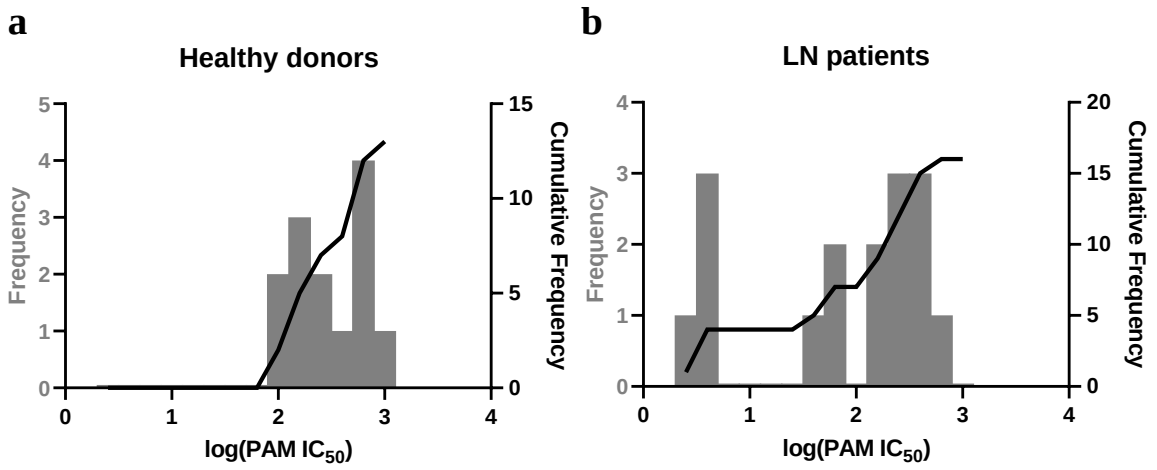

Figure 4-4. The histograms of log-transformed IC_{50} values in a) healthy donors (n = 13) and b) LN patients (n = 16). The frequencies of bin buckets are plotted on the left axis, whilst cumulative frequency is represented by the solid black line and is plotted on the right axis. IC_{50} values for PAM sensitivity in LN patients fit a bimodal population model (sum of 2 Gaussians preferred over single Gaussian model, $p = 0.0258$) whereas healthy donors fit a unimodal Gaussian model (sum of 2 Gaussians not preferred over single Gaussian model, $p = 0.996$).

4.2.3. Comparison of active versus quiescent disease

The sensitivity to PAM-induced DNA damage data was then sub-categorised into patients with active versus quiescent disease as determined by clinicians. In patients with active LN (n = 8), the sensitivity to PAM-induced DNA damage (IC_{50}) ranged from 3.67 µg/mL to 433 µg/mL (median: 59, IQR 4.4-188 µg/mL), whilst in patients with quiescent LN (n = 8), the range of IC_{50} values was greater at 2.23 µg/mL to 733 µg/mL (median: 251, IQR 73-456 µg/mL), (Figure 4-5).

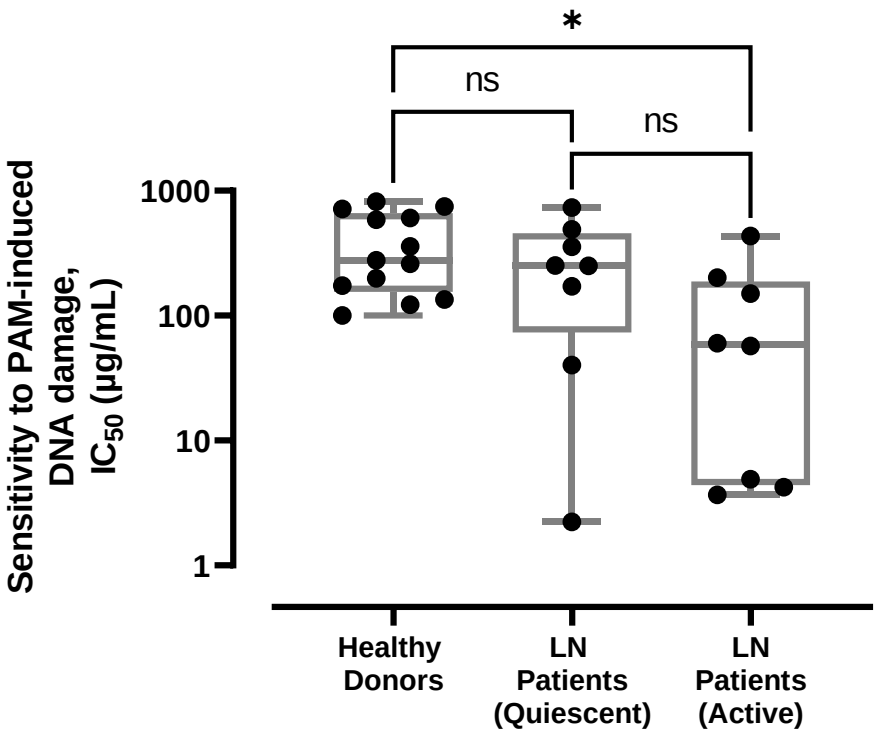

Figure 4-5. Active LN patients (n = 8) appear to have higher sensitivity to PAM-induced DNA damage than healthy donors (n = 13). Individual datapoints are IC_{50} values determined in each donor by the QPCR-block assay. Box and whisker plots represent the median, 25-75% IQR (boxes) and minimum and maximum of each population. Kruskal-Wallis multiple comparisons tests were conducted to determine *p*-values. * $p < 0.05$.

There was no significant difference (p = 0.682) in PAM sensitivity (IC_{50} values) between healthy donors and quiescent LN patients (median 278 µg/mL versus 251 µg/mL, respectively). Despite the substantial difference between the median value for active LN patients and quiescent LN patients (58.7 µg/mL vs 251 µg/mL), this was not statistically significant (p = 0.269). This is likely due to the small population size as well as the skew (0.8) of data in the quiescent group.

In contrast, a significant difference was observed between healthy donors and active LN patients (p = 0.0177), (Figure 4-2). Overall, 4 LN patients (3 with active and 1 with quiescent disease) had very high sensitivity to PAM-induced DNA damage with IC_{50} values below 10 µg/mL.

4.2.4. Comparison of male-female and age-related differences in PAM sensitivity

No significant difference in sensitivity to PAM was observed between male and female LN patients in the study (p = 0.599). However, there was a significant difference in sensitivity to PAM between male and female healthy donors (p = 0.0020), (Figure 4-6). This may be influenced by the relatively small sample size, and a larger study is needed to confirm this finding.

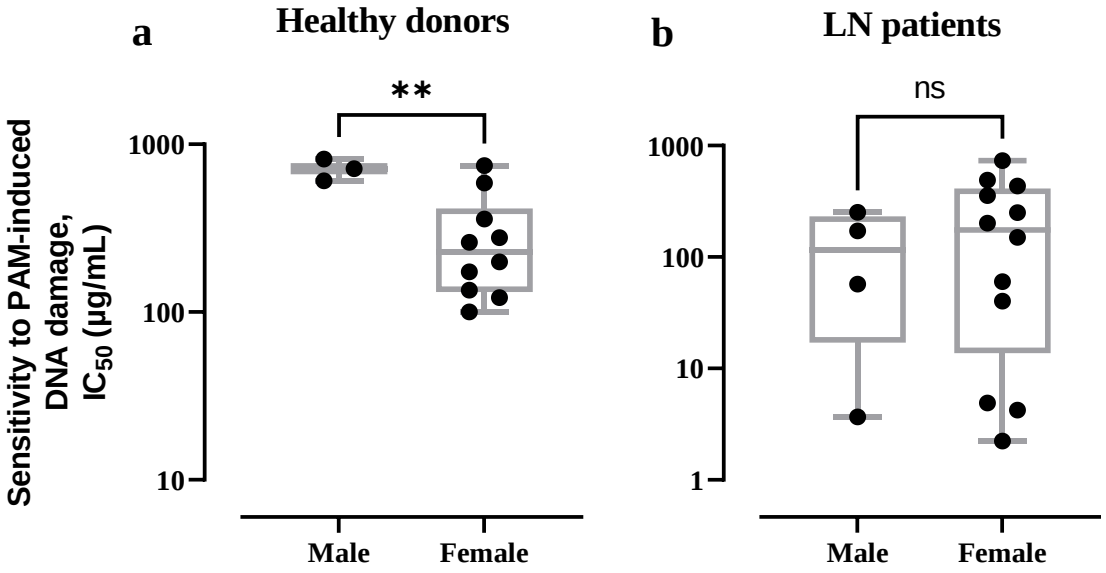

Figure 4-6. a) Male healthy donors (n = 3) had lower sensitivity to PAM-induced DNA damage than female healthy donors (n = 10). (b) No difference in sensitivity to PAM was observed between male (n = 4) and female (n = 12) LN patients. Box and whisker plots represent the median, 25-75% IQR (boxes) and minimum and maximum of each population. An unpaired t-test was conducted to statistical significance in a). A Mann-Whitney rank sums test was conducted in b), due to the non-normal distribution of the data. ** p <0.01

There was no significant correlation between age and sensitivity to PAM in either the LN patient group (Spearman's R = -0.236 (95% CI -0.664 to 0.309), p = 0.376) or the healthy donor group (Pearson's R = -0.157 (95% CI -0.652 to 0.431), p = 0.609). Finally, there was no significant correlation between daily prednisone dosage and PAM sensitivity in LN patients (Spearman's R = -0.390 (95% CI -0.750 – 0.146), p = 0.136).

4.3. Discussion

The observation that lupus patients appear to have increased sensitivity to DNA damage (i.e., decreased DNA repair capacity) than healthy individuals in the current work is supported by previous studies. These studies however used various methods of DNA damage detection and different DNA damaging agents. Of note are the studies conducted by Souliotis et al. (2016), who demonstrated this difference through Southern blotting and immunohistochemistry, as well as the finding that SLE patients had higher endogenous mitochondrial DNA damage than healthy individuals (López-López et al., 2014) detected by a QPCR assay.

Notably, Souliotis et al. (2016) assessed DNA damage-repair activity in PBMC from SLE patients and healthy volunteers treated *ex vivo* with a different alkylating agent (melphalan). This report observed significant differences in DNA damage between the healthy donors and SLE patients similar to our observations. However, in contrast to the findings in this chapter, Souliotis et al. (2016) observed a significant increase in DNA damage between the quiescent SLE patients and those with active proliferative lupus nephritis. It is also important to note that the present study was only powered to detect differences between healthy individuals and lupus nephritis patients. This lack of power could be the reason why there was no difference detected between quiescent and active lupus nephritis patients.

However, these authors (Souliotis et al., 2016) used a different technique to assess DNA-damage repair. They measured melphalan-induced DNA damage in a nucleotide sequence from a selected region of the *N-ras* gene using the semi-quantitative Southern blotting method. Melphalan has very similar DNA-alkylating behaviour to PAM. The Southern blotting assay involves converting the melphalan DNA-adducts into strand breaks using alkaline hydrolysis and heat denaturation. These strand breaks decrease the size of the nucleotide sequence. Following addition of ^{32}P nucleotide probes detection of the full-length nucleotide sequence in

treated versus untreated samples is assessed by autoradiography (Episkopou et al., 2009). The assumption is that the melphalan monoadducts are repaired by nucleotide excision repair and that an increased number of adducts (decreased full length nucleotide sequence) indicates lower repair. However, this autoradiography method is semi-quantitative unlike the QPCR block assay described in this thesis. In addition, this Southern blotting technique is an indirect measure of the adducts produced by melphalan, since it only measures strand breaks.

Levels of endogenous damage using DSB repair were also assessed in these patients. For quantification of double strand break repair capacity in SLE patients' PBMC, the authors (Souliotis et al., 2016) used immunocytochemistry. Detection of the DNA double strand break damage sensor (γH2Ax) and Rad51 (a homologous recombination repair protein) was used, with the number of immunoreactive foci counted per nucleus. Manual counts of foci in this method of detection are prone to inter- and intra-user variability. Furthermore, these measures do not encompass all aspects of double strand break repair capacity. Whilst the phosphorylation of γH2Ax is a damage sensor that is important in both non-homologous end joining and homologous recombination processes (Feng et al., 2017; Podhorecka et al., 2010), Rad51 is only involved in homologous recombination repair.

Hence, the Southern blotting technique is limited to detection of strand breaks and immunocytochemistry approaches assume that non-homologous end joining and homologous recombination processes have been activated. It is of note that there is a plethora of other DNA-damage repair processes that may be important for alkylating agents such as PAM, these include base-excision repair and direct-repair. It is also important to note that the QPCR-block assay described in this thesis will detect any adduct or DNA damage that prevents amplification of the nucleotide sequence, this includes DNA-proteins that have been alkylated by PAM and it is therefore a more holistic approach and does not make assumptions as to which type of DNA-repair process is impaired.

The PBMC from healthy donors and lupus patients used in the REPAIR study described in this thesis chapter were isolated and immediately exposed to PAM for 1 hour prior to determination of the DNA-repair capacity. In contrast, the study by Souliotis et al. (2016) used phytohaemagglutinin-stimulated PBMC. These cells were allowed to proliferate for 48 h before assessment of DNA-repair capacity following exposure to melphalan. This difference may be important since PMBC typically consist of resting T-lymphocytes. Some of the processes of repair of PAM-induced DNA damage are pathways only available during S-phase of mitosis (during DNA synthesis). Indeed, when stimulated T-cells are exposed to a double strand break-inducing drug (zeocin), they can repair via homologous repair and non-homologous end joining pathways. In contrast, resting T-cells with zeocin-induced double strand breaks undergo apoptosis as these specific pathways are not available (Hu et al., 2018). Hence the use of non-proliferating (unstimulated) cells in this study may have biased this assay towards repair of PAM monoadducts by processes such as nucleotide-excision repair rather than processes which repair double-strand DNA breaks.

The DNA adducts induced by PAM rapidly convert from a monoadduct into an inter-strand crosslink (in less than 30 minutes). In contrast, this conversion is much slower (>6 hours) for melphalan (Bauer & Povirk, 1997). However, on a molar basis, PAM is 25-fold less efficient than melphalan at forming an inter-strand crosslink. This could be another reason for a lower sensitivity in detection of differences between quiescent and active lupus patients in the REPAIR study compared with the earlier report by Souliotis et al. (2016).

The study by Souliotis et al. (2016) is not the first to have demonstrated DNA repair deficiencies in lupus patients. It has been suggested that defective DNA repair capacity in SLE/LN patients contributes to the cycle of autoimmunity and predisposes these individuals to the development of SLE. An early study observed that human lymphocytes from SLE patients possessed lower amounts of endonuclease required for DNA repair after exposure to UV light

(Beighlie & Teplitz, 1975). Cleaver (1968) also suggested that individuals with the hereditary disease xeroderma pigmentosum (caused by a mutation in a DNA repair gene family *XP*) were susceptible to greater amounts of UV damage and this could be a first step in the development of SLE. Other studies have also shown various aspects of defective DNA repair, such as inhibited repair of double strand breaks in paediatric SLE patients through the COMET assay (Davies et al., 2012), delayed repair response to ionising radiation (McCurdy et al., 1997) and difficulty in repairing methylated bases as evidenced by delayed cell growth (Harris et al., 1982).

The results of the REPAIR study reported in this chapter therefore confirm many previous reports that lupus nephritis patients appear to have a significantly impaired DNA damage repair capacity compared to healthy individuals. Many of these previous reports have focussed on the possible role of impaired-DNA damage repair as a factor which increases immunogenic DNA and pre-disposes individuals to risk of SLE.

In contrast to these previous reports, this assay directly measures sensitivity to PAM, the ultimate cytotoxic metabolite of cyclophosphamide. The use of PAM as the damaging agent in the assay, avoids the complexity of the differences in the rate of formation or detoxification of the intermediate metabolites of cyclophosphamide and hence reports directly on the differences in sensitivity as an endpoint. This is the first time that differences in DNA repair sensitivity to cyclophosphamide (a treatment for active lupus nephritis) have been considered in lupus patients.

Following treatment with cyclophosphamide, patients with Fanconi anaemia (a very severe DNA repair deficiency) have 15-fold higher DNA adduct formation than in patients with haematological malignancies (L. A. Johnson et al., 2012b). In contrast, the difference in median DNA-damage sensitivity (following in vitro exposure to PAM) in the LN patients compared to

healthy controls observed in the REPAIR study was only ~1.6-fold. This suggests that the aberrant DNA-damage repair processes may be relatively mild in the lupus patients. However, this could still have consequences for individual patient sensitivity to cyclophosphamide treatment.

Although it was a relatively small sample size, the PAM induced DNA damage in the lupus patients did not follow a normal distribution in contrast to the distribution in healthy individuals. There was also a larger inter-individual variability within lupus nephritis patients than in healthy individuals. In particular, four patients appeared to be very sensitive to PAM exposure with IC_{50} <10 µg/mL.

This suggests that these four patients may have the potential to be particularly responsive to cyclophosphamide therapy. Conversely, this could also indicate that these patients may be more vulnerable to adverse excessive immunosuppression outcomes, such as severe infections. With further validation, this assay could potentially be utilised in a clinical setting to screen patients before deciding use of either mycophenolic acid or cyclophosphamide for induction therapy.

Notably, three of these patients with extreme sensitivity to PAM-induced DNA damage were older females and one was a younger male. SLE has a well-characterised female predominance (McDonald et al., 2015; Ramírez Sepúlveda et al., 2019; Tan et al., 2012; Thomas & Jawad, 2022) and this was evident in the present study, with the majority of LN patients recruited being female. Importantly, the distribution of sex and age was similar in the healthy donor group and the patients recruited into this study.

Some studies in the literature have found sex differences in DNA damage repair, particularly during aging. In one study it was observed that the percentage of double strand breaks that were repaired and re-joined was consistently lower in women than in men irrespective of age (Mayer

et al., 1991). In another study conducted in cultured peripheral blood lymphocytes, Rall-Scharpf et al. (2021) found that non-homologous end joining was impaired in elderly females above 60 years old compared to younger females below 60 years old, whereas this was increased in males above 60 years old compared to younger males. Additionally, genes such as *KU70*, *ATM* and *BLM*, which encode for key proteins involved in the repair of the inter-strand crosslinks formed by PAM, were found to be downregulated only in older females, not in older males. In the present study, although the sample size was small (with a low proportion of male participants), there was a significantly increased sensitivity to PAM-induced DNA damage in healthy females compared to males. However, there was no difference observed in the sensitivity of PBMC to PAM-induced DNA damage between males and females in the LN patients. It is also likely that sex or age differences in DNA-repair are only a few of the potential factors that determine the sensitivity to PAM.

The use of concomitant therapies is prevalent in the treatment of LN and has proven to be useful in managing various SLE symptoms. In particular, glucocorticoids are a staple of LN treatment and are effective at managing acute flare ups because of their anti-inflammatory properties. Prednisone is the most used glucocorticoid in SLE treatment (Johns Hopkins Lupus Center, 2024), and this is also evident in the present study wherein all patients were prescribed prednisone.

Whilst prednisone is effective in modulating inflammation in LN, the main concern arising from long-term usage stems from irreversible organ damage frequently associated with glucocorticoid use. Hence, the schedule for prednisone use in LN treatment has been suggested by the European Alliance of Associations for Rheumatology to not exceed 7.5 mg/day and be withdrawn completely if possible (Fanouriakis et al., 2019). Thus, common practice for the prescription of prednisone usually involves a variable starting dose that tapers quickly to a low, maintenance dose of 2.5 to 5 mg/day (Ruiz-Irastorza, 2021). The starting dosage of prednisone

depends largely on the patient and the severity of symptoms, with high doses of prednisone (>20 mg/day) being used only in the most severe cases. This explains the range of dosage reported for the patients in this study (2.5 – 80 mg/day).

Glucocorticoids were first suggested to impair DNA damage repair in 1974 (Gaudin et al., 1974), but this is still poorly understood, with a recent study finding that prednisone increased endogenous DNA damage in mouse bone marrow cells (de Oliveira et al., 2021). The effect of prior treatment with prednisone on the activity of DNA repair pathways in the LN patients could explain the difference in sensitivity to PAM-induced DNA damage between the healthy donors and the patients. However, there was no correlation between prednisone dose and the PAM-induced DNA damage (IC_{50} values) obtained (data not shown), suggesting that prednisone use does not further sensitise patients to PAM.

Hydroxychloroquine (used by 14 of 16 patients in the study) was also recently observed to induce oxidative DNA damage in mouse embryonic fibroblasts (Besaratinia et al., 2021). Further experiments could determine the potential for prednisone or hydroxychloroquine to modulate DNA damage or DNA damage repair processes through co-incubation of prednisone and/or hydroxychloroquine, with PAM and PBMC *ex vivo*.

There are various limitations in this preliminary study that should be addressed. First, the further sub-categorisation of LN patients into quiescent and active was not initially considered in the study design and this is likely to have resulted in insufficient power to discern any statistical differences between these two patient groups and the healthy donors. Future work should consider a larger sample size to independently verify if differences in sensitivity to PAM due to disease status can be observed. Furthermore, whilst the ethnicities of the patient and donor populations were not statistically different, the number of different ethnicities and small sample size could mean that ethnicity contributed in part to the differences observed. This is

particularly relevant considering the large disparity in SLE susceptibility as well as health outcomes between Māori, Pasifika, Asian and European NZ ethnicities. Māori and Pasifika, in particular, display increased SLE and LN prevalence as well as worse health outcomes due to systemic social and health inequities. Differing sensitivity to cyclophosphamide treatment could then aid in improving health outcomes for Māori and Pasifika.

Chapter 5: Assessment of Mycophenolic acid intracellular uptake and effect on IMPDH activity

5.1. Introduction

The immunosuppressive properties of mycophenolic acid (MPA) have established the drug as an important therapy in several indications, primarily solid organ transplantations and autoimmune diseases, such as lupus nephritis. As discussed in Chapter 1 (Section 1.2.1), mycophenolic acid immunosuppression is mediated through IMPDH inhibition which leads to selective inhibition of lymphocyte proliferation.

5.1.1. IMPDH structure and activity

IMPDH is the rate-limiting enzyme in the *de novo* biosynthesis of guanine nucleotides (Figure 5.1). In the *de novo* pathway of purine synthesis, inosine monophosphate (IMP) is the common precursor of adenosine monophosphate (AMP) and guanosine monophosphate (GMP). Following the synthesis of IMP from ribose-5-phosphate, the conversion of IMP to xanthosine monophosphate (XMP), catalysed by IMPDH, represents the first committed step in guanine nucleotide synthesis. This contrasts with the conversion of IMP to succinyl-AMP, catalysed by adenylosuccinate synthase, which is the first committed step in adenine nucleotide synthesis.

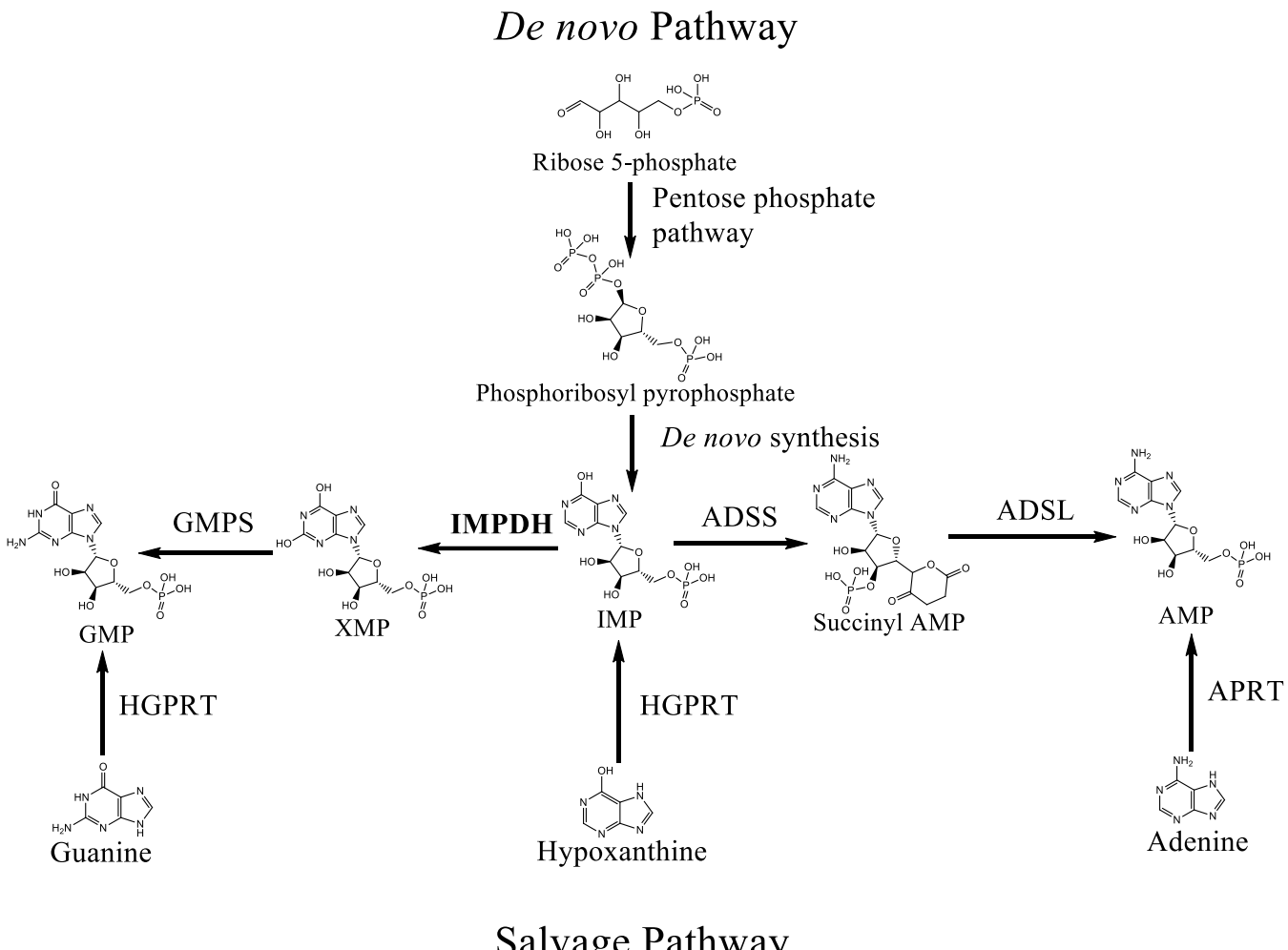

Figure 5-1. The *de novo* and salvage pathway of synthesising guanosine and adenosine. IMPDH is bolded to show the rate-limiting and committed step to guanine nucleotide synthesis.

IMPDH has two isoforms, IMPDH1 and IMPDH2, which both contain 514 amino-acid residues and are 84% identical. Regardless of the isoform, the IMPDH protein monomer consists of two main domains, a catalytic domain comprised of both α- and β-barrels, as well as a regulatory Bateman domain. The enzyme (IMPDH1/2) exists within cells as a stable tetramer, which is ordered in square planar geometry, with the Bateman domains located at the corners of the tetramer and the sides of the α/β barrels located between the IMPDH monomers. The active site is located in the catalytic domain at the C-terminal loops of the β-barrels and can be covered, depending on enzyme conformation, by a large 50-residue polypeptide segment acting as a flap (Hedstrom, 2009).

Using purified recombinant protein the enzyme has been shown to be a *bi-bi* reaction with product inhibition (Carr et al., 1993) and that the two isoforms have similar *kcat* (1.5 and 1.3 sec^{-1}). The active site consists of various residues critical to the catalysis of IMP to XMP. This conversion is a biphasic process: a dehydrogenase reaction followed by a hydrolysis reaction. The dehydrogenase reaction produces an enzyme-bound thioimidate intermediate, E-XMP* through the transfer of a hydride from IMP to the cofactor NAD^+. The active site cysteine residue (Cys331 in human IMPDH2) forms the covalent bond with IMP, thus trapping the substrate, whilst the cofactor NAD^+ is held in place through hydrogen bonds to various residues such as aspartate (Asp274) and serine (Ser276), (Futer et al., 2002). During the dehydrogenase reaction, the enzyme is in an open conformation, with the polypeptide flap oriented away from the active site. Having produced the thioimidate intermediate, the by-product NADH dissociates from IMPDH, inducing a conformational change in the enzyme. The enzyme shifts to a closed conformation, with the flap moving to cover the NAD^+-binding site. The flap contains an arginine residue (Arg429) which, along with the adjacent tyrosine residue (Tyr430), acts as a proton acceptor for water, generating a hydroxyl ion (Hedstrom, 2009). The

hydroxyl ion undertakes nucleophilic attack on C_2 of the E-XMP* intermediate, breaking the bond between Cys331 and XMP. This releases the final product XMP.

The IMPDH enzyme can also be allosterically regulated by both adenine and guanine nucleotides. The Bateman domain contains three nucleotide binding sites (Fernández-Justel, et al., 2019): ATP/ADP and GTP/GDP bind competitively to the second site, whilst ATP/ADP and GTP/GDP bind exclusively to the first and third site respectively. The binding of GDP and GTP to the second and third sites of Bateman domains of IMPDH enzymes induces a tight and compressed octamer conformation. This octamer is made up of two tetramers stacked against each other at their Bateman domains and induces a 'bowed' conformation of the IMPDH enzyme such that the active site cannot adopt the position necessary for catalysis, thus decreasing catalytic activity (Buey et al., 2015, 2017). In contrast, the binding of ATP to the Bateman domains of IMPDH results in the formation of a looser octamer conformation ('flat') with unaltered catalytic activity (Fernández-Justel, Núñez, et al., 2019; Thomas et al., 2012).

5.1.2. Mechanism of IMPDH inhibition by mycophenolate (MPA)

Mycophenolate (MPA) binds IMPDH at the NAD^+-binding portion of the active site. When bound to the active site, the 6,5-ring of MPA is oriented similarly to the nicotinamide ring of NAD^+, forming hydrogen bonds with many of the residues that bind NAD^+ (Colby et al., 1999). Notably, MPA occupies this site only after the hydride transfer from IMP to NAD^+ has occurred (and NADH has been released), this results in MPA trapping the intermediate E-XMP*. It is also important to note that MPA has high selectivity for E-XMP* in human IMPDH in contrast to bacterial IMPDH where MPA does not display such affinity (Hedstrom, 2009). The occupation of the NAD^+-binding site thus prevents the enzyme from assuming the closed conformation necessary for the hydrolysis reaction to take place. Hence, MPA is a non-

competitive inhibitor as it does not compete with NAD^+ for the binding site. This also means that MPA inhibition increases as substrate concentration increases.

MPA is a very potent non-competitive inhibitor and the enzyme inhibitor constant (k_i) of MPA is reported to be 37 nM and 9.5 nM for IMPDH1 and IMPDH2 respectively, using purified recombinant protein (Carr et al., 1993), and 11 nM and 6 nM when using purified human protein preparations (Hager et al., 1995).

5.1.3. Cellular responses to MPA inhibition of IMPDH

The inhibition of IMPDH by MPA is especially relevant in cells that rely on *de novo* guanine nucleotide synthesis. This is important as MPA immunosuppression in the treatment of autoimmune diseases and post-transplant regimens primarily targets stimulated/proliferating lymphocytes. Resting lymphocytes, like most other tissues, generally utilise the salvage pathway for any purine and pyrimidine nucleotide requirements. However, when expansion and proliferation are required, the turnover of nucleotides from the salvage pathway is no longer sufficient and *de novo* nucleotide biosynthesis becomes crucial (Fairbanks et al., 1995).

Several feedback mechanisms maintain the balance of the purine nucleotide pools within the cell. Both branches of purine synthesis contain steps utilising the other nucleotide (i.e. the conversion of IMP to succinyl-AMP is driven by GTP hydrolysis whilst XMP to GMP conversion is driven by ATP hydrolysis) and can be inhibited by their end products. Notably, 5-phosphoribosyl-1-pyrophosphate amidotransferase, which catalyses the rate-limiting step in the conversion of ribose-5-phosphate to IMP, can also be inhibited by purine nucleotides (Camici et al., 2018). Thus, the inhibition of IMPDH by MPA and subsequent guanine nucleotide deprivation has further downstream effects on the *de novo* purine biosynthesis pathway. In fact, the interlinkage and intricacies of both salvage and *de novo* purine and pyrimidine pathways mean that MPA-mediated guanine nucleotide deprivation results in

overall nucleotide deprivation (Qiu et al., 2000). This nucleotide deprivation leads to G_1/S phase cell cycle arrest since DNA cannot be replicated, thus inhibiting proliferation of the cell. Besides this cytostatic effect, MPA has also been shown to possess cytotoxic effect, although its cytotoxicity does not appear to be primarily mediated through apoptosis following cell cycle arrest. Rather, cell death from MPA treatment occurs via a caspase-independent necrotic signal (Chaigne-Delalande et al., 2008).

5.1.4. Quantification of IMPDH activity

The methods for the quantification of IMPDH activity have mostly utilised three techniques: measurement of radiolabelled compounds, spectrophotometry and high-performance liquid chromatography (HPLC). These methods have been devised with the core principle of measuring either the loss of substrate/cofactor (IMP/NAD^+) or the formation of product (XMP).

5.1.4.1. Radiolabelled IMP assays

Initial attempts to assay IMPDH activity used radiolabelled [^{14}C]-IMP and thin layer chromatography (TLC) to separate the substrate and product (Ikegami et al., 1985; Proffitt et al., 1983; Saccoccia & Miech, 1969) followed by measurement of radioactivity from the different spots. The commercial availability of [^{3}H]-IMP led to the development of an alternative assay measuring enzyme activity based on ^{3}H-release over time (Langman et al., 1996). This has become the standard radiolabelled isotope for assay of IMPDH activity.

5.1.4.2. Spectrophotometric assays

Spectrophotometric assays have not been as popular as radioactivity assays or HPLC assays due to lower sensitivity, but this approach has been used due to the high throughput and relatively quick run time. Carr et al. (1993) first used spectrophotometry to monitor the

formation of NADH during IMPDH catalysed metabolism of IMP, by monitoring changes in absorbance of NADH at 340 nm. Subsequent assays have utilised the same conditions (Gollapalli et al., 2010; Pua et al., 2017) or with modified detection methods. For example, measuring emission at 440 nm (Anthony et al., 2017) or coupling NADH release with the reduction of iodonitrotetrazolium (INT) to INT-formazan to increase assay sensitivity (Keppeke et al., 2018). Several commercial IMPDH activity assays also rely on this method.

5.1.4.3. HPLC assays

The inconvenience of the radioactivity assays resulted in the use of HPLC methods to separate the product XMP from the substrate IMP and cofactor NAD^+. The first published HPLC method used reversed-phase liquid chromatography and an ion-pairing reagent, tetrabutylammonium hydrogen sulphate (TBAS), and monitored the chromatographically separated compounds at 254 nm and 280 nm to determine IMPDH activity in erythrocytes (Montero et al., 1995). Further optimisation of the HPLC assay eventually led to the development of conditions for IMPDH activity determination in PBMC (Glander et al., 2009). This assay used a PBMC lysate in a 2.5-hour incubation with IMP and NAD^+ followed by termination of the reaction and protein precipitation using 4 M perchloric acid. The supernatant was then neutralised with 5 M potassium carbonate before injection onto the column. The products were then chromatographically separated using either an isocratic or gradient elution with methanol and an aqueous phase (50 mM KH_2PO_4 containing 7 mM TBAS). The authors also established a procedure to standardise the amount of XMP produced relative to the amount of AMP present in the lysate, rather than the more widely used normalisation to the number of cells used or amount of protein in the cell lysate. This assay has since become the standard HPLC assay for the determination of IMPDH activity in PBMC (Chariyavilaskul et al., 2022; Dom et al., 2018; Tang et al., 2017). A liquid chromatography-mass spectrometry (LCMS)

method has been reported with improved sensitivity, and this assay can also quantify numerous purine bases simultaneously (Vethe et al., 2014).

5.1.5. Pharmacokinetic-guided personalised dosing of MPA

The current standard of personalised dosing is through monitoring the plasma pharmacokinetics of MPA, although it is also important to note that a fixed dosing strategy is still more commonly used clinically in transplantation and autoimmune disease, especially SLE, than personalised dosing with target concentration intervention (TCI) or therapeutic drug monitoring (TDM). The routinely used plasma pharmacokinetic parameters for MPA are concentrations immediately prior to next dose (C_{trough}) and the area under the plasma concentration-time curve ($AUC_{0\text{-}12h}$). The use of an $AUC_{0\text{-}12h}$ rather than C_{trough} has gained more traction, especially with new techniques such as maximum *a posteriori* Bayesian estimation and limited sampling strategies. As noted previously, MPA dose adjustment (using either TCI or TDM using these parameters has substantially decreased acute rejection incidence compared to fixed dose MPA dosing regimens (Metz et al., 2019). Despite this, a substantial percentage of patients (7.7 to 11.5%) who had achieved optimal MPA plasma pharmacokinetic exposure, following dose adjustment still experienced acute rejection (Le Meur et al., 2007; van Gelder et al., 1999). This could be attributed to several factors including inadequate intracellular MPA concentrations in the target cells or inter-individual variability in IMPDH inhibition.

5.1.6. Pharmacodynamics: Clinical measurement of IMPDH activity

Using assays to detect IMPDH activity in PBMC, high inter-individual variability in baseline IMPDH activity (0.8 – 35 nmol h^{-1} mg^{-1}) in untreated subjects has been observed (Chiarelli et al., 2010; Schaier et al., 2015). In addition, some researchers have tried to correlate therapeutic response with inter-individual differences in IMPDH activity following MPA dosing. These

studies have been undertaken in patients receiving MPA for immunosuppression following organ transplant and to date there is little information regarding IMPDH activity following MPA treatment in SLE patients.

Pre-dose (trough) IMPDH activity, prior to subsequent MPA doses, rather than treatment naïve baseline IMPDH activity, is typically assessed as this can be undertaken during collection of blood for TDM. However, some studies have also assessed enzyme activity at baseline (treatment-naïve), as well as at selected times during the dosing interval to investigate whether inter-individual variability may account for differences in clinical outcome.

5.1.7. Pharmacodynamic assessment of IMPDH activity

5.1.7.1. Baseline (treatment-naïve) IMPDH differences

An early study measuring baseline IMPDH activity observed that relatively high IMPDH activity significantly correlated with the occurrence of acute rejection (< 6 months) in renal transplant patients (Glander et al., 2004). In addition, relatively low pre-transplant (baseline) IMPDH activity in recipients of nonmyeloablative haematopoietic stem cell transplant was unexpectedly associated with higher incidence of acute graft versus host disease (Bemer et al., 2014).

5.1.7.2. Associations between MPA plasma concentration and IMPDH inhibition

Using an E_{max} model, the pharmacodynamic effect has been determined to have a direct relationship with MPA plasma concentrations (Fukuda et al., 2011; Li et al., 2014; Tang et al., 2017; Vethe et al., 2008). Using this approach, Fukuda et al. (2011) observed that the predicted EC_{50} value of 1.0 mg/L MPA was close to the C_{trough} concentrations typically observed during therapeutic drug monitoring (1.0 mg/L to 3.5 mg/L) of patients receiving mycophenolate

mofetil (MMF) for transplantation. Glander et al. (2010) also determined the E_{max} (78.7 µmol/s/mol ATP) and an EC_{50} of 1.24 mg/L MPA. This suggests that IMPDH should be more than 50% inhibited during the whole of the dosing interval. Notably this EC_{50} value in patient samples is equivalent to 3.1 µM and this is ~80-fold greater than the K_i for the purified enzyme (<37 nM).

A number of studies that have obtained matched pharmacodynamic (IMPDH activity) and plasma pharmacokinetic MPA profiles broadly confirm this >50% enzyme inhibition during the dosing interval. The 12-hour pharmacodynamic profile in patients dosed with MMF twice daily displays a maximal inhibition of IMPDH activity that corresponds to the plasma MPA C_{max}, which occurs about 1 to 2 hours after the drug dose. Subsequently, IMPDH activity recovers slowly to pre-dose levels by 12 hours. Another study conducted in liver transplant patients (already on MMF treatment for at least 3 months) observed that IMPDH activity inversely correlated with plasma MPA levels both at 30 minutes and 2 hours post-dose (Neuberger et al., 2020). In children with nephrotic syndrome treated with MPA, Sobiak et al. (2020) observed that the mean IMPDH activity was lowest when the mean plasma MPA concentration was highest (at 1 hour post-dose). Mean IMPDH activity then increased as mean plasma MPA decreased (1 to 4 hours post-dose). The authors also noted that the highest variability in IMPDH activity was observed at 1 hour post-dose when IMPDH activity was lowest, suggesting inter-individual variability in the inhibitory capacity of IMPDH.

In contrast to the above, (Molinaro et al., 2013) observed that following multiple-doses of the drug, there was no correlation between IMPDH activity pre-dose (a C_{trough} sample) or at 2 hours post-dose with the corresponding total or free plasma MPA concentrations. Furthermore, detailed assessment of both MPA plasma pharmacokinetics (AUC) and IMPDH enzyme activity-time curve (AEC) during the 12-hour post dose interval in 65 renal transplant patients

after 3 days of dosing (Glander et al., 2010) demonstrated that whilst there was an inverse relationship, this relationship was very weak ($r^2 = 0.24$).

5.1.7.3. IMPDH activity during a dosing interval and associations with outcome

IMPDH activity assessment at timepoints during the 12-hour MPA dosing interval is less well studied. However, some studies have assessed limited timepoints during the dosing interval and these suggest a lack of relationship between extent of IMPDH inhibition, during the early part of the dosing interval, and therapeutic outcome.

One study, conducted in renal transplant patients, found no difference in IMPDH activity at 2 hours post-dose between patients who suffered acute rejection and patients who did not (Molinaro et al., 2013). Another study also observed that there was no difference in the 1.5 h post-dose IMPDH activity between renal transplant patients who suffered acute rejection and those who did not (Klaasen et al., 2020).

Using assessment of the enzyme activity-time curve from multiple samples across a dosing interval, associations with therapeutic outcomes have been inconsistent (Glander et al., 2010; Li et al., 2014; Schaier et al., 2015; Sommerer et al., 2010; Tang et al., 2017). In renal transplant patients, Sommerer et al. (2010) found that there was no difference in IMPDH (area under the time-effect curve, $AUEC_{0-12}$) assessed at week 12, between patients who experienced biopsy proven acute rejection and patients who did not. However, there was a significant difference in $AUEC_{0-12}$ was detected between patients who experienced gastrointestinal side effects and those who did not, suggestive of greater immunosuppression in these individuals.

In MMF-treated haematopoietic stem cell transplant recipients, a higher IMPDH $AUEC_{0-6}$ (greater IMPDH inhibition) assessed at day 21 was significantly associated with better therapeutic outcomes (observed as lower cytomegaly virus reactivation, as well as decreased

non-relapse and overall mortality), (Li et al., 2014). Notably, a higher median 2-month IMPDH $AUEC_{0-12}$ was also significantly associated with relapse occurrence in MMF-treated patients with the autoimmune disease ANCA-associated vasculitis.

5.1.7.4. IMPDH activity following multiple doses

Interestingly chronic changes in IMPDH activity following multiple doses of MPA have been observed. Notably a study conducted in heart transplant patients observed that, despite stable plasma MPA trough levels across a 12-month period, the IMPDH activity substantially altered during this chronic dosing period. In the initial three months of MPA treatment the pre-dose IMPDH activity (at C_{trough} sampling) decreased by almost 50%. After six months of treatment activity was almost completely inhibited, whilst at twelve months there was a small increase in this pre-dose IMPDH activity (Devyatko et al., 2008). Interestingly, this study also observed positive correlations between lymphocyte activation markers and IMPDH activity, indicating that high IMPDH activity was associated with weaker immunosuppression. In contrast, Dom et al. (2018) found no correlation between the incidence of renal transplant rejection and the pre-dose IMPDH activity (at C_{trough} sampling) when activity was assessed between 5-22 days post-transplantation.

Chronic changes in pharmacodynamic effects of MPA have also been reported following detailed assessment of IMPDH activity during the dosing interval. Glander et al. (2010) assessed IMPDH activity (0-12 h) on four occasions (day 3, 10, 21 and 56) in 75 renal transplant patients receiving MPA. The average IMPDH activity (A_{avg}) during the 0-12 h post dose period was highest at day 10 and at later timepoints declined to values similar to those observed at day 3.

Moreover, the authors also noted that of four patients with biopsy-proven acute rejection, two patients had relatively weak inhibition of IMPDH at day 0 (IMPDH activity values in the upper

quartile of the population (n = 75). One patient had strong inhibition of IMPDH in a day-3 sample but had very high IMPDH activity (value in the upper quartile of the population) at day 56 prior to experiencing biopsy-proven acute rejection.

Whether the observed variability in IMPDH inhibition following chronic dosing accounts for the inconsistent associations of pre-dose IMPDH activity (measured in a C_{trough} sample) and outcomes, noted above, is unclear.

5.1.7.5. Relationship between intracellular mycophenolate and IMPDH inhibition in clinical samples

Few studies have assessed the intracellular MPA concentrations achieved clinically in target cells. The assumption in the majority of studies which have assessed IMPDH activity was that plasma MPA is an accurate reflection of intracellular MPA. Of note, the clinically observed EC_{50} (1 mg/L) is ~80-fold higher than the k_i of MPA for the purified enzyme, suggesting that assessment of free (unbound) MPA rather than total plasma concentrations may be important.

To date, only three studies have explored the intracellular pharmacokinetic-pharmacodynamic relationship. Intracellular concentrations of MPA at C_{trough} in lymphocytes from treated patients are between 0.1 to 3.9 ng 10^{-7} cells (median = 0.68 ng 10^{-7} cells), n = 48 patients (Dom et al., 2018). A similar range was observed in a separate study, 0.69 to 3.39 ng/10^7 cells, n= 40 patients (Nguyen Thi et al., 2013), with similar results also reported in an additional study by these authors, (mean: 1.42 ng/10^7 cells; range: 0.12–8.23, n = 40 patients), (Nguyen Thi et al., 2015).

Both studies (Dom et al., 2018; Nguyen Thi et al., 2013) have independently reported that there was a poor relationship between plasma MPA concentrations and these intracellular concentrations. Although the second study by Nguyen Thi et al. (2015) suggested that a significant association was observed, this remained a weak linear correlation. Dom et al.

(2018) also measured the free (unbound) plasma concentration of MPA and noted that there was a statistically significant association between the free MPA plasma concentrations and the resulting intracellular concentrations, however the Spearman's coefficient was $r_s = 0.418$.

Importantly, all three studies (Dom et al., 2018; Nguyen Thi et al., 2013, 2015) reported a lack of a correlation between intracellular concentrations and IMPDH activity. This includes a further report of lack of association when using limited sampling (0. 1.5 and 3.5 h post dose) to determine an $AUEC_{0\text{-}3.5h}$ (Nguyen Thi et al., 2015). This is particularly intriguing since the intracellular concentrations (assessed in C_{trough} sample) was a predictor of transplant rejection risk (Dom et al., 2018). However, it remains unclear as to why IMPDH activity did not associate with rejection risk.

It is not known how MPA is taken up into these target cells, or if it is actively effluxed from the cells. Whilst MPA is effluxed from hepatocytes into the bile by MRP-2 (encoded by *ABCC2)*, no relationship between the mRNA expression of this efflux pump in the PBMC and the intracellular levels of MPA was observed (Dom et al., 2018).

5.1.8. Conclusion and aims

In summary, whilst plasma MPA concentrations are obtained for dose adjustment in transplant recipients, the clinical assessment of inhibition of IMPDH activity is not routinely undertaken in any therapeutic context. The research studies to date suggest that there is substantial inter-subject variability in treatment-naïve (baseline) IMPDH. There is reported to be a general inverse relationship between MPA plasma concentrations and inhibition of IMPDH, although the concentration-dependent effect correlation is weak. Notably, intracellular concentrations in target cells do not appear to correlate with plasma concentrations. Data from three studies also suggest a lack of association between intracellular concentrations and IMPDH activity in patient samples. The relationship between extent of IMPDH inhibition and therapeutic

outcomes, particularly in autoimmune diseases such as SLE, is remarkably scant and inconsistent. This may relate to the timepoint of data collection within a dosing interval and/or chronic changes that effect on IMPDH activity over time.

Thus, the aims of the following experiments were to investigate the relationship between intracellular uptake of mycophenolic acid and IMPDH activity using an *in vitro* model of human lymphocytes. As this is an exploratory study, the experiments in this chapter were designed to establish baseline behaviour of MPA transport and interactions with its target IMPDH in a well-characterised cell line before taking into account potential external factors such as inter-individual variability in buffy coat cells.

5.1.9. Study design

To assess the effects of MPA on IMPDH activity, Jurkat cells (immortalised T-lymphocytes were used). The activity of IMPDH was determined using a HPLC assay for detection of the reaction product XMP. This assay was modified from previously published methods and was validated as accurate and reproducible with an LLOQ of 5 µM (detailed in Chapter 2 section 2.2.3.1). The uptake kinetics (intracellular accumulation) of MPA was determined using radiolabelled $^{[14C]}$MPA with liquid scintillation counting (detailed in Chapter 2 Section 2.2.2).

Initial studies were undertaken at two concentrations of MPA, these were chosen to be representative of MPA plasma concentrations that PBMC would be exposed to *in vivo*. A low concentration (15.6 µM, equivalent to 5 µg/mL) was chosen as an approximate total plasma 'C_{trough}', similar to that observed in a large cohort of lupus nephritis patients (Pourafshar et al., 2019). A high concentration (156 µM, equivalent to 50 µg/mL) was chosen to approximate to total plasma 'C_{max}' values. Large inter-individual variability in plasma C_{max} MPA concentrations are observed in lupus nephritis patients (Lertdumrongluk et al., 2010) and this value is within the upper range of those values.

To observe the intracellular uptake kinetics of MPA, Jurkat cells (10 x 10^6 cells/mL) were incubated in suspension with radiolabelled $^{[14C]}$MPA in complete uptake buffer for up to 4 hours. At chosen timepoints, the cells were isolated from the incubation by centrifugation and then washed, lysed and the intracellular radioactivity measured by scintillation counting (detailed in Chapter 2 Section 2.2.2). The scintillation counts (DPM) were converted to mCi and molarity determined using the specific activity of the compound (Section 2.2.2). Data are reported as pmol.10^6 cells^{-1}.

Identical experiments were undertaken in parallel with non-radiolabelled MPA to determine the effect of MPA on IMPDH activity relative to the observed intracellular $^{[14C]}$MPA concentrations. Following incubation, the Jurkat cells were centrifuged, the cell pellet was washed and re-pelleted and then resuspended in MilliQ water and stored at -80°C overnight. The cell solution was then thawed, and the lysate centrifuged to remove debris. The resulting supernatant was then incubated with IMP and NAD^+ for 2.5 hours, the analytes were then extracted using methanol and the XMP and AMP concentrations determined by HPLC (detailed in Chapter 2 Section 2.2.3.1). IMPDH activity following incubation with MPA is expressed as percentage of IMPDH activity of Jurkat cells incubated with vehicle for 240 minutes.

To determine the concentration-time effect of MPA on IMPDH inhibition, Jurkat cells were incubated with a range of concentrations of MPA (0 – 780 μM) for 5, 20 and 240 minutes.

Characterisation of the nature of MPA uptake into Jurkat cells included experiments to establish the effect of MPA concentration on uptake under both first order (5 minutes) or zero order (1 hour) conditions. The Michaelis-Menten kinetics of this data were then derived. To assess whether this uptake was a sodium-dependent process, uptake at was evaluated in Na^+

free buffer (NaCl replaced with equimolar choline chloride) using two concentrations of MPA (78 µM and 312 µM) under first order rate conditions (5-minute incubation).

All incubations were undertaken in triplicate and independent experiments (n = 3) undertaken to confirm the results. Graphical analyses were undertaken in GraphPad Prism 9.0.2 (GraphPad Prism Software Inc., USA). Differences between groups were assessed using unpaired t-tests. MPA uptake rate, IMPDH activity response curves as well as the Eadie-Hofstee analysis were fitted using the Akaike Information Criterion.

5.2. Results

5.2.1. Time-course of MPA accumulation and corresponding IMPDH activity change in Jurkat cells

Assessment of the intracellular concentrations of MPA in Jurkat cells following incubation with either 15.6 µM or 156 µM MPA for up to 4 hours indicated that there was rapid uptake into cells. When Jurkat cells were incubated with 156 µM MPA (Figure 5-2a) intracellular concentrations after 6 minutes were 12640 ± 3880 pmol.10^6 cells^{-1} (mean ± SD), and after incubation with a 10-fold lower MPA concentration (15.6 µM) the mean ± SD uptake was 3206 ± 809 pmol.10^6 cells^{-1} (Figure 5-3a). The uptake curve was hyperbolic over the first 60 minutes at the high MPA concentration (156 µM), with a relatively small increase over the next 2 hours to a plateau at 26350 ± 4160 pmol.10^6 cells^{-1} (Figure 5-2a). In contrast, at the low MPA concentration (15.6 µM) the initial period of uptake (0-6 minutes) appeared to follow linear kinetics, followed by a substantial but not statistically significant (p = 0.126) decrease in the intracellular concentrations at 20 minutes (33% decrease). Intracellular concentrations then remained relatively constant over the next 220 minutes at 2145 ± 503 pmol.10^6 cells^{-1} (Figure 5-3a).

Baseline (untreated) IMPDH activity was determined in Jurkat cells from n = 6 independent experimental repeats. Formation of XMP was 8.53 ± 3.16 nmol.s^{-1}.10^6 cells^{-1}. The formation of XMP normalised to AMP was 3530 ± 1560 µmol.s^{-1}.mol AMP^{-1}.

The time-dependent effect of MPA on inhibition of IMPDH activity was then assessed and the data are reported as % change compared to untreated control. After exposure to 156 µM MPA IMPDH was rapidly inhibited, with activity decreased to below the LLOQ within 60 seconds. IMPDH remained maximally inhibited up to 6 minutes (Figure 5-2b). Notably, after 180

minutes of incubation and despite the MPA intracellular concentration remaining high (26350 ± 4160 pmol.10^6 cells^{-1}), IMPDH activity rebounded to 116% of the baseline (untreated) activity in these cells.

At the lower MPA concentration (15.6 µM), IMPDH activity was also maximally inhibited (9.63% of baseline untreated activity) within the first 6 minutes of incubation (Figure 5-3b). At 20 minutes the activity increased to 75.6% of untreated activity and this corresponded with the apparent small decrease in intracellular MPA observed at this timepoint. This rebound in activity was not sustained and IMPDH activity was minimal at 60 minutes (5.36% of baseline), despite evidence that the intracellular concentrations were not significantly different to that observed at the 20-minute timepoint (1640 vs 2150 pmol.10^6 cells^{-1}, p = 0.321). IMPDH activity then increased in a linear manner at 120, 180 and 240 minutes to 120% of baseline. The intracellular concentrations of MPA were not significantly different between the 60-minute timepoint and the 180-minute timepoint (1640 vs 2190 pmol.10^6 cells^{-1}, p = 0.529).

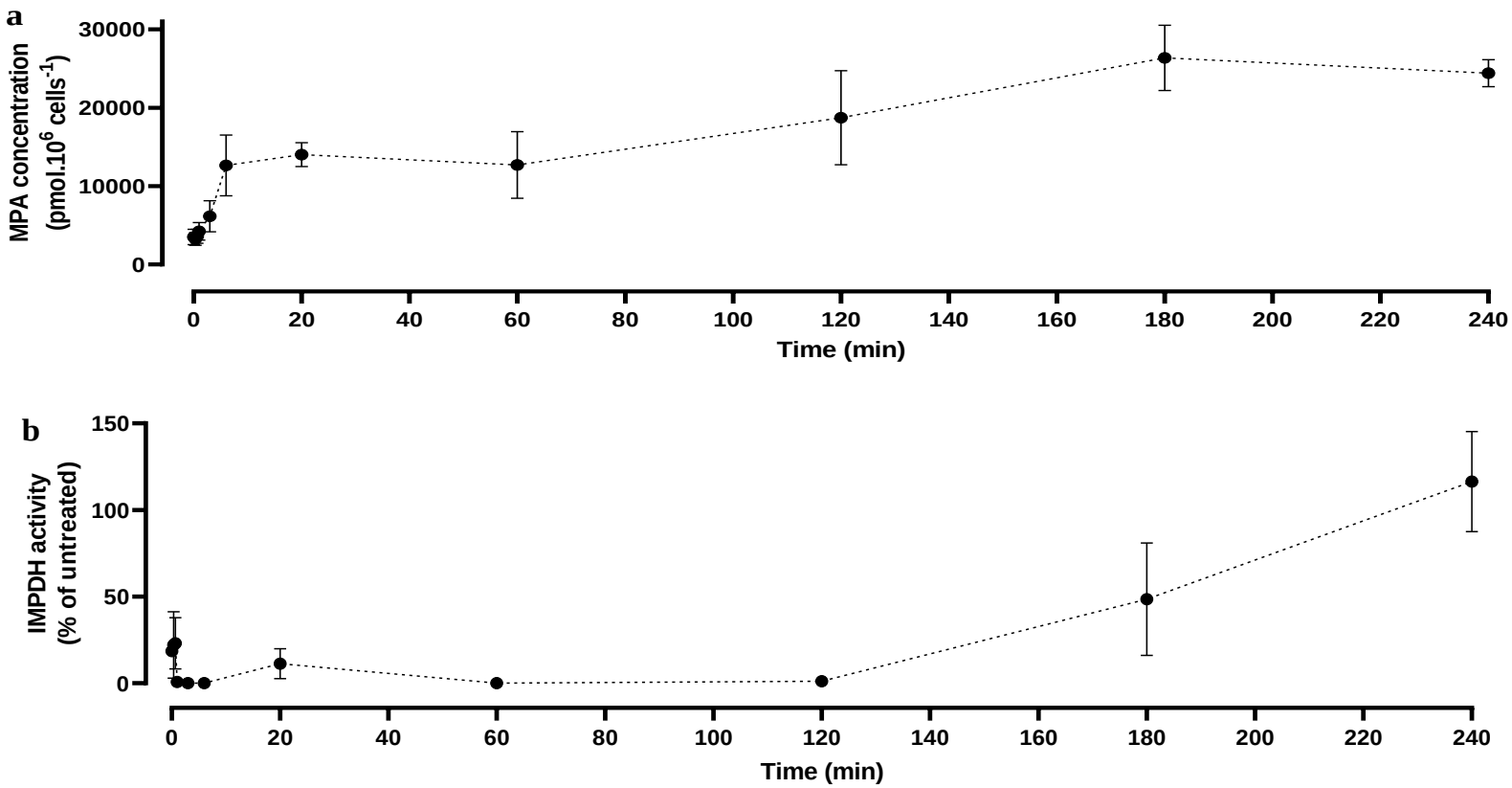

Figure 5-2. a) The intracellular accumulation of MPA within Jurkat cells incubated with 156 µM MPA over 4 hours. b) The IMPDH activity of Jurkat cells incubated with 156 µM MPA over 4 hours. Data points represent the mean ± SD of three independent experiments (n = 3 technical replicates per experiment). IMPDH activity is expressed as percentage of IMPDH activity in cells incubated with vehicle-only (untreated) for 4 hours (n = 3).

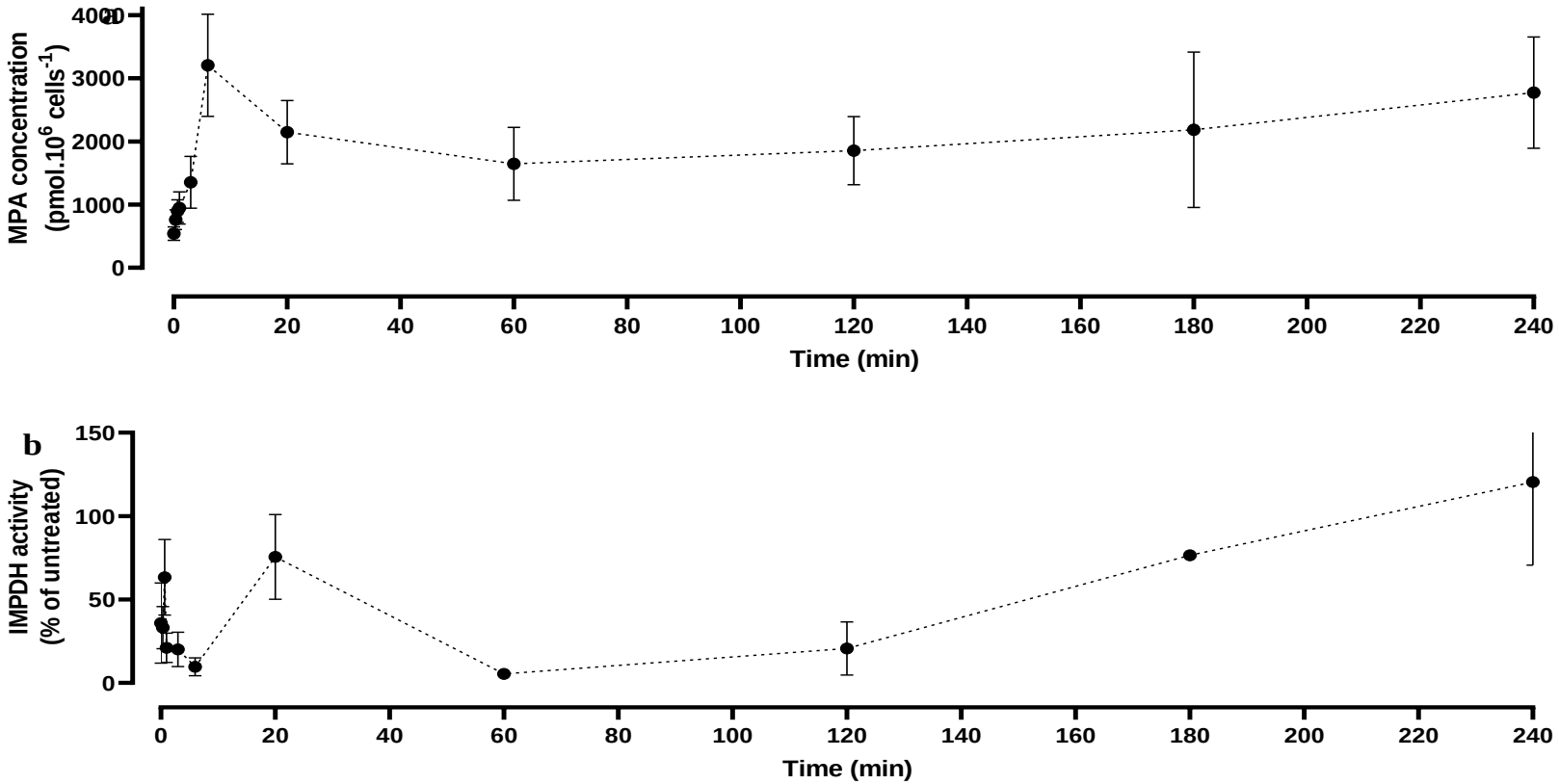

Figure 5-3. a) The intracellular accumulation of MPA within Jurkat cells incubated with 15.6 µM MPA over 4 hours. b) The IMPDH activity of Jurkat cells incubated with 15.6 µM MPA over 4 hours. Data points represent the mean ± SD of three independent experiments (n = 3 technical replicates per experiment). IMPDH activity is expressed as percentage of IMPDH activity in cells incubated with vehicle-only (untreated) for 4 hours (n = 3).

Since a small rebound (11.3 %) in IMPDH activity after 20 minutes was also apparent in the incubations with 156 µM MPA, a more detailed determination of this apparent rebound in IMPDH activity was conducted over a 60-minute time course in three independent experiments (Figure 5-4).

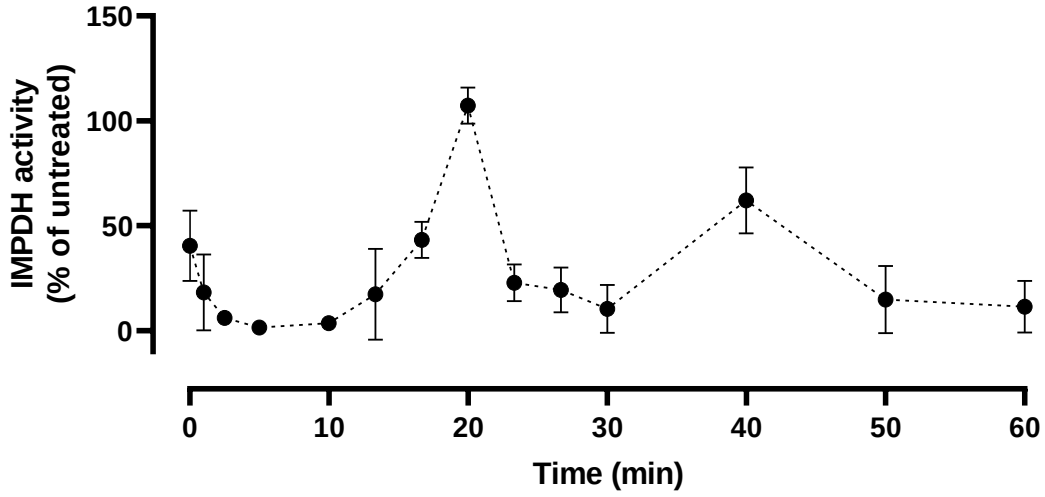

Figure 5-4. Profile of the IMPDH activity response in Jurkat cells over 1 hour following exposure to 15.6 µM MPA. Data represent mean of three independent experiments (n = 3 technical replicates per experiment) and error bars represent SD.

Following incubation with 15.6 µM MPA, a gradual loss of inhibitory effect of MPA on IMPDH activity was observed as early as 13.3 minutes of incubation. There was clear rebound in IMPDH activity to baseline levels observed after 20 minutes of incubation (107.29 ± 8.66 % of untreated activity). This independently confirmed the earlier observations (Figure 5-3). The rebound peak in activity at 20 minutes was not significantly different from untreated control ($p = 0.762$), indicating complete loss of MPA inhibition of enzyme activity. In addition, there also appears to be a second rebound in activity (62.1 ± 15.7 % of untreated activity) at 40 minutes. At this timepoint the IMPDH activity was significantly higher ($p = 0.0007$) than that

observed at either adjacent timepoint (30 or 50 minutes) following incubation with 15.6 µM MPA.

5.2.2. MPA concentration-dependent effect on IMPDH activity

To ascertain the concentration-time dependence of MPA on IMPDH activity a range of MPA concentrations (0 – 780 µM) were incubated with Jurkat cells for 5, 20 and 240 minutes (Figure 5-5). The logarithmic concentration-effect curves were generated using non-linear regression and the concentration which resulted in 50% of maximal inhibitory response (EC_{50}) was determined.

After 5 minutes of incubation of Jurkat cells with MPA, the EC_{50} of IMPDH activity inhibition was 0.266 ± 0.135 µM. After 20 minutes of incubation the EC_{50} increased by more than 40-fold to 42.4 ± 9.5 µM. After 240 minutes of incubation there was no observable inhibition of IMPDH even at the highest MPA concentration tested (780 µM) and the EC_{50} could not be determined. This decreased sensitivity to MPA after 20 and 240 minutes incubation is consistent with that observed (Figures 5-2 and 5-3) for 15.6 and 156 µM MPA incubations.

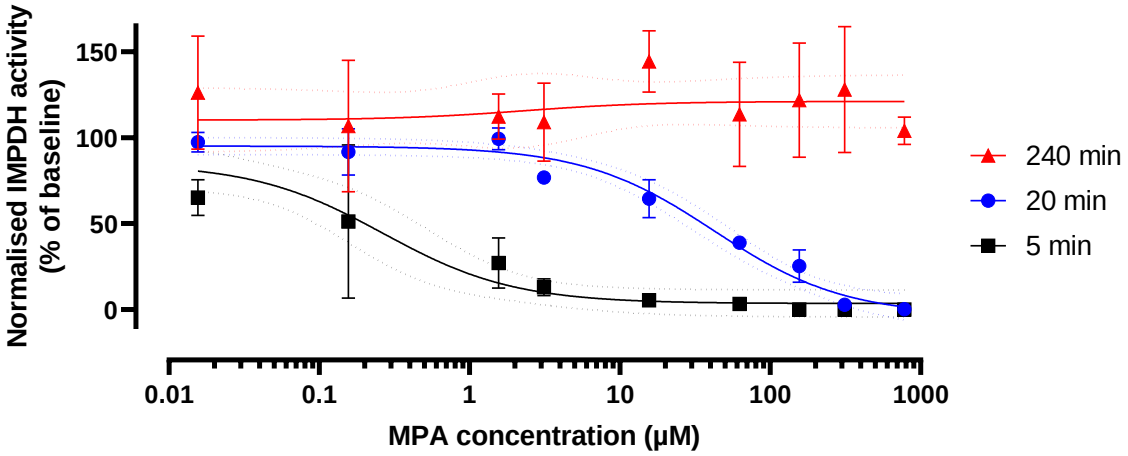

Figure 5-5. Time dependent decrease in IMPDH inhibition sensitivity across MPA concentrations. Incubations were assessed at 5 minutes (black squares), 20 minutes (blue circles) and 240 minutes (red triangles). Data points represent the mean ± SD of three independent experiments (n = 3 technical replicates per experiment). MPA concentration is plotted on a logarithmic axis. The logarithmic concentration-effect curves were generated using non-linear regression in Prism and the EC_{50} determined. The dotted plots represent the 95% confidence interval of the curve fit.

The HPLC assay for IMPDH catalysed formation of XMP also quantified the amount of AMP in the cell lysate (Chapter 2 Section 2.2.3) and the XMP formation data are normalised to the molar amount of ATP in the lysate (IMPDH activity = µmol.s.mol AMP^{-1}). IMPDH activity is known to be positively regulated in an allosteric manner by intracellular AMP. To ascertain whether the apparent time-dependent changes in sensitivity of IMPDH to MPA observed above (Figure 5-5) was due to changes in AMP concentration leading to an apparent change in normalised IMPDH activity, the AMP and XMP concentrations determined at all MPA concentrations at each timepoint are shown (Figure 5-6).

There was a time-dependent decrease in AMP concentration, which were significantly lower (4.6 ± 0.73 µM, adjusted $p < 0.001$) in the 240-minute incubation samples compared to the 5- and 20-minute incubation samples (9.1 ± 1.0 µM and 7.8 ± 1.2 µM, respectively), (Figure 5-6). There was no change in AMP concentration with respect to MPA concentration at any of these incubation times (Tukey's multiple comparisons test), except for a statistically significant lower AMP concentration observed in Jurkat cells incubated with 780 µM than with 312 µM for 20 minutes.

The pattern of XMP formation in response to MPA remained broadly similar to the AMP-normalised IMPDH activity (Figure 5-5). The EC_{50} of XMP formation are summarised in Table 5-1.

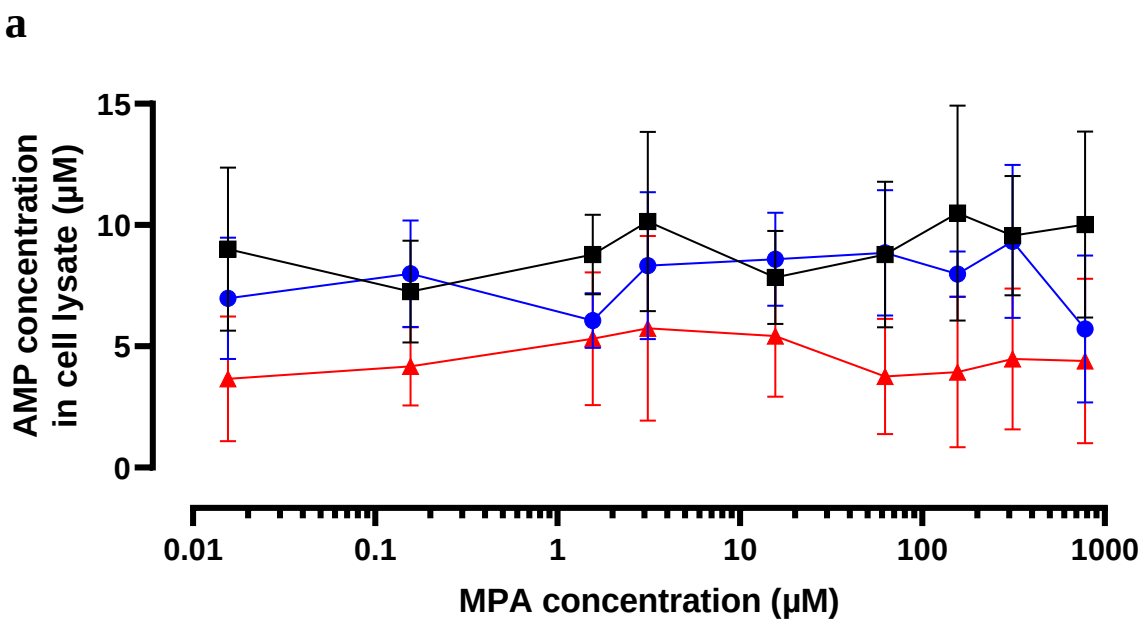

Figure 5-6. a) AMP and b) XMP concentrations determined in lysates of Jurkat cells incubated with a range of MPA concentrations at different incubation timepoints. Incubations were assessed at 5 minutes (black squares), 20 minutes (blue circles) and 240 minutes (red triangles). Data points represent the mean ± SD of three independent experiments (n = 3 technical replicates per experiment). MPA concentration is plotted on a logarithmic axis. The logarithmic concentration-effect curves were generated using non-linear regression in Prism and the EC_{50} determined. The dotted plots represent the 95% confidence interval of the curve fit.

	MPA EC_{50} (µM)	
	AMP-normalised XMP formation	**XMP formation**
5-minute MPA incubation	0.266 ± 0.135	0.045 ± 0.326
20-minute MPA incubation	42.4 ± 9.5	57.5 ± 40
240-minute MPA incubation	>780	>780

Table 5-1. EC_{50} values of AMP-normalised XMP formation and XMP formation in 5-, 20-, and 240-minute incubations with MPA.

5.2.3. Characterisation of MPA transport into cells

The uptake kinetics of MPA into Jurkat cells were then determined at 5 minutes and 1 hour. Based on the initial time course data (Figures 5-2a and 5-3a), these time points will detect first order and zero order uptake kinetics respectively.

The first order concentration dependent MPA uptake in Jurkat cells was saturable with hyperbolic behaviour (Figure 5-7a). This suggests a transport-mediated process rather than simple diffusion. A Michaelis-Menten non-linear regression model was a good fit ($r^2 = 0.933$) for this data. The maximal velocity (V_{max}) for uptake was 8540 ± 1180 $pmol.min^{-1}.10^6$ $cells^{-1}$ (95% CI = 6540 – 11800 $pmol.min^{-1}.10^6$ $cells^{-1}$). The K_m for MPA uptake under these first order conditions was 478 ± 116 µM (95% CI = 290 – 821 µM). Hence the "clearance" (V_{max}/K_m) of extracellular MPA into cells by this transporter-mediated process was 17.9 $\mu L.min^{-1}.10^6$ $cells^{-1}$.

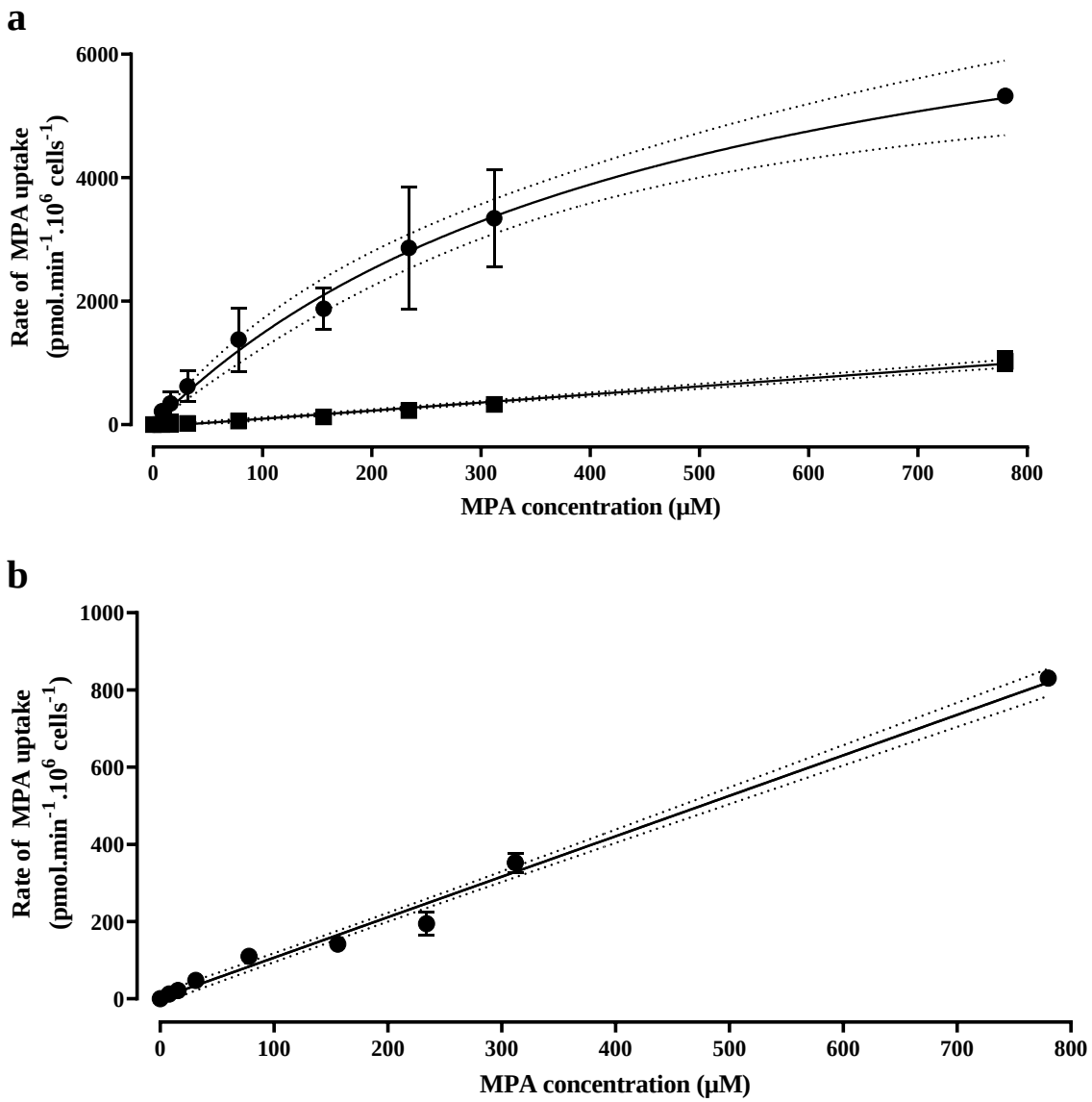

Figure 5-7. The rate of MPA uptake into Jurkat cells as a function of MPA concentrations. a) First order and zero order uptake kinetics (5 -minute incubation) at 37°C (circles) and 0°C (squares) respectively and b) Zero order uptake kinetics (1- hour incubation). Note the different Y-axis scale. Data points represent the mean ± SD of three independent experiments (n = 3 technical replicates per experiment. The first-order uptake curve was fitted using the Michaelis-Menten regression model and the zero-order uptake curve was fitted using a simple linear regression model in Prism.). Dotted plots represent the 95% confidence interval of the curve fit.

MPA uptake at 1 hour was linear ($r^2 = 0.985$), (Figure 5-7b). The slope was not zero, suggesting that some passive diffusion of MPA occurs over a 60-minute incubation time. At the highest

MPA concentration tested (780 µM) this passive diffusion rate was 830.61 ± 2.07 pmol.min^{-1}.10^{6} cells^{-1} and this was 85% lower than that observed via active transport at this concentration. The slope of this linear regression indicates that the passive diffusion 'clearance' of extracellular MPA into cells was 1.05 µL.min^{-1}.10^{6} cells^{-1}. This is 17-fold lower than the transporter-mediated 'clearance' process.

To further characterise the nature of the transporter-mediated process an Eadie-Hofstee analysis (velocity of transport vs velocity relative to substrate concentration) was undertaken (Figure 5-8). The lack of linearity of the transformed data (comparison of linear and non-linear likelihoods AICc P(non-linear) = 0.997) is suggestive of more than one transporter-mediated process under these first order conditions. However, additional datapoints at higher MPA concentrations are required to confirm this.

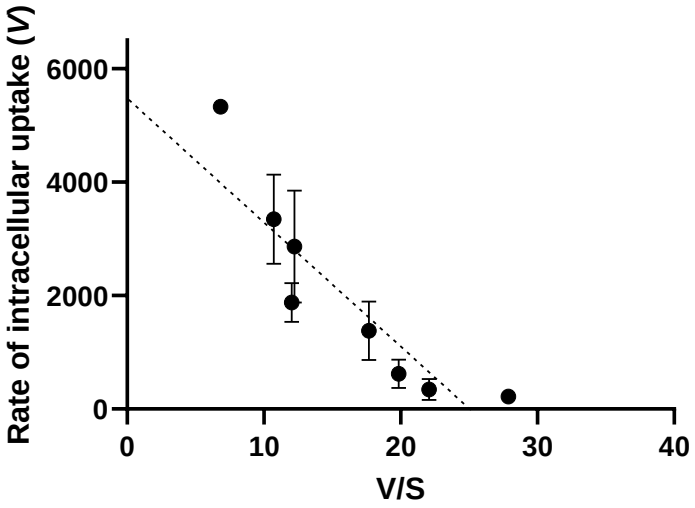

Figure 5-8. Eadie-Hofstee plot of rate of MPA uptake at 5 minutes. Data points represent the mean ± SD of three independent experiments (n = 3 technical replicates per experiment). The data was fitted using a simple linear regression model in Prism, to demonstrate the lack of a simple linear effect, which would be indicative of a single transporter.

Several proteins involved in the transport of drug molecules across cell membranes rely on co-transport of sodium ions. Preliminary experiments were then undertaken to assess the effect of sodium ions on transport of MPA in Jurkat cells. Two concentrations of MPA were chosen (78

μM and 312 μM MPA) which are below the K_m of uptake reported above. MPA intracellular accumulation under first order conditions (5 minute incubation time) was determined in sodium-free uptake buffer (NaCl replaced with choline chloride) and the data compared to incubations in complete uptake buffer (Figure 5-9).

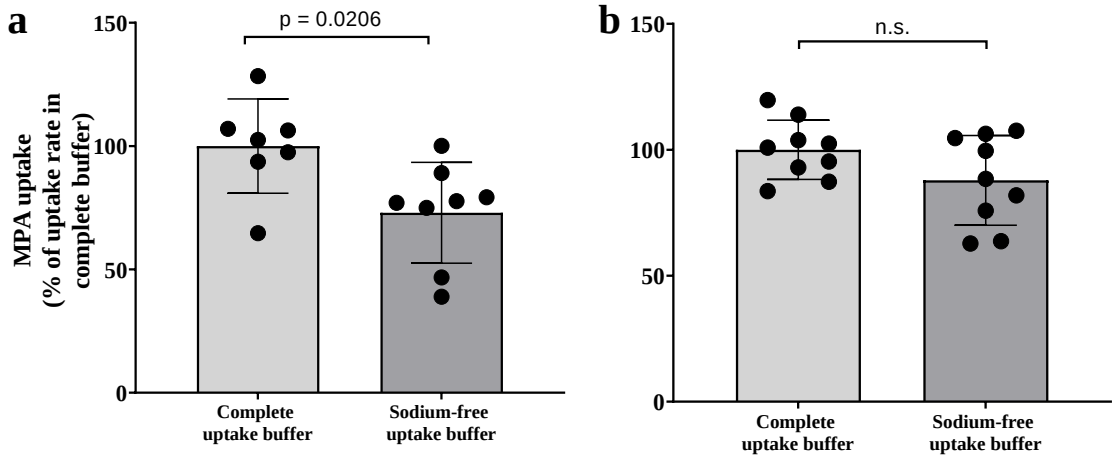

Figure 5-9. MPA uptake in sodium-free buffer compared to complete buffer when Jurkat cells were incubated for 5 minutes with (a) 78 μM and (b) 312 μM MPA. Data represent mean of three independent experiments (n = 3 technical replicates per experiment) and error bars represent SD. Student's t-tests were conducted in Prism to compare the uptake of MPA in both buffers at the two MPA concentrations tested.

In the absence of sodium ions the rate of MPA uptake significantly (p = 0.0206) decreased by 27.0 ± 10.3% at 78 μM MPA. When incubated with 312 μM MPA in sodium-free buffer, a small but non-significant (p = 0.107) change in MPA uptake was also observed. This suggests that the major component of MPA transport into cells is likely to be mediated by a transporter protein which is not dependent on the co-transport of sodium ions. Further preliminary experiments to assess the effect of chemical inhibitors selective for transporters such as the organic anion transporter and organic anion transporter polypeptide families including probenecid (50 – 750 μM) and cyclosporin (400 μM) did not result in significant inhibition of MPA uptake into cells (data not shown).

5.3. Discussion

5.3.1. Intracellular MPA accumulation

The hyperbolic kinetics of intracellular accumulation of MPA indicates that there was active uptake of MPA into Jurkat cells. The rapid initial uptake of MPA and consistent accumulation of MPA intracellularly further indicates that efflux processes over the 4-hour period were minimal. The concentration-dependent uptake kinetics at first order (initial rate) and zero order were determined and the values (V_{max} and K_M) indicate that active transport is the major process by which MPA accumulates in Jurkat cells, since the passive diffusion was 17-fold lower than the transporter-mediated 'clearance' process. This is the first report of the mechanism of uptake of MPA into cells.

Since the K_M (concentration which results in half-maximal uptake) was 478 ± 116 µM and the lowest plasma concentration (C_{trough}) during a dosing interval is ~ 3.12 µM (Staatz & Tett, 2007), this suggests that active uptake into cells is unlikely to be a limiting factor in the therapeutic response to MPA. However, whilst Jurkat cells were used as an *in vitro* model of lymphocytes, these findings need to be confirmed in primary human lymphocytes.

The lack of a linear Eadie-Hofstee transformation of the uptake kinetics suggests that multiple transporter proteins are involved in this uptake. At least one of these transporters appears to be sodium-dependent, but this is unlikely to be the major uptake transporter of MPA in Jurkat cells. The transport of MPA into cells is poorly characterised. It has been observed that MPA is able to inhibit the uptake of *p*-aminohippurate and estrone sulphate by SLC22A6 and SLC22A8 (Uwai et al., 2007; Wolff et al., 2007). Co-incubation of MPA and probenecid, a well characterised probe for organic anion transporters, with Jurkat cells had no effect on MPA uptake. This likely discounts a role for SLC22A6, SLC 22A28 and SLC22A12. Cyclosporin A, a known inhibitor of organic anion transporter polypeptides and the putative MPA efflux-

transporter candidates P-gp and MRP-2 (Wang et al., 2008), was also tested but had no effect on MPA uptake. Additionally, cyclosporin A is a common immunosuppressant prescribed concomitantly with mycophenolic acid in lupus patients as well as solid organ transplant recipients. Cyclosporin A has been observed to decrease MPA plasma concentrations in patients (Grinyó et al., 2009; Gregoor et al., 1999; van Hest et al., 2005). However, the inhibition of the biliary efflux transporter MRP-2 – and therefore the enterohepatic recirculation of MPA – by cyclosporin A is thought to be the primary mechanism. However, the lack of inhibition of MPA active uptake into Jurkat cells by cyclosporin A suggests that in patients taking both MPA and cyclosporin A, MPA exposure at the site of action would not be further decreased.

Whilst MRP2 has been suggested as an efflux transporter, as it is involved in MPA hepatic efflux, it is also expressed on PBMC cell membranes (Giraud et al., 2010). It has been previously shown that MPA is a substrate of the multidrug resistance protein 1 (MDR1) transporter in mice (J. Wang, Figurski, et al., 2008) and in a *MDR1*-expressing cell line MDCK (Sawamoto et al., 2001). Importantly, this MDR-1 transporter is also expressed on PBMC cell membranes (Giraud et al., 2010) and may also be involved in efflux of MPA from PBMC. However, efflux of MPA is unlikely to be a major determinant of intracellular MPA concentration, as there was no significant decrease of intracellular MPA concentrations observed in the time-course assays of Jurkat cells' incubation with MPA. Even when exposed to trough concentrations of MPA, intracellular MPA concentrations (1.08 µM to 6.41 µM) remained well above the k_i of recombinant IMPDH1 and IMPDH2 (37 nM). However, whilst Jurkat cells were used as an *in vitro* model of lymphocytes, these findings need to be confirmed in primary human lymphocytes.

5.3.2. IMPDH activity response

Unlike the gold standard IMPDH assay established by Glander et al. (2009) or other adaptations based on this method, the modified HPLC-UV assay used in these experiments did not require the use of ion-pairing reagents or phosphate buffers. This ensured the adaptability of the assay to LCMS/MS if required in the future. However, there were a few noteworthy drawbacks, namely a slightly lower sensitivity and longer chromatographic run-time. Despite this, the modified HPLC assay was accurate and sensitive enough for the quantification of changes in IMPDH activity in Jurkat cells in response to MPA exposure.

Most studies exploring pharmacokinetic-pharmacodynamic relationships have noted that the peak of IMPDH activity inhibition coincided with the peak of plasma MPA concentrations. This was also observed in the current work; the peak of IMPDH activity inhibition (i.e. low IMPDH activity) also coincided with the peak in intracellular MPA concentrations at 5 minutes when incubated with either 15.6 µM or 156 µM MPA. However, at 20 minutes, the observed rebound in IMPDH activity was disproportionate to the small decrease in intracellular MPA concentrations in both the 15.6 µM and 156 µM MPA incubations. Surprisingly even though intracellular MPA concentrations remained well above the reported k_i the IMPDH activity did not remain inhibited and instead increased. Similarly, even though MPA continued to accumulate within Jurkat cells at concentrations well above k_i, the IMPDH activity continued to increase after 20 minutes of exposure.

The changes in the intracellular pharmacokinetic-pharmacodynamic relationship demonstrated in these experiments have thus far not been explicitly reported in most studies assessing such relationships in patient samples. However, there is some evidence that some patients may exhibit this *in vivo*. Sanquer et al. (1999) observed varying IMPDH pharmacodynamic profiles in kidney transplant patients who had been treated with MPA and identified three subgroups

of profiles. The first group of profiles exhibited typical features of previously characterised pharmacodynamics, with IMPDH activity inhibited and slowly returning to pre-dose activity levels as plasma MPA decreased. Conversely, in the second group of profiles, following maximal inhibition, a sharp increase in IMPDH activity was observed. IMPDH activity subsequently increased to 300% of pre-dose activity levels as MPA plasma concentration decreased. In the third group of profiles, IMPDH activity seemed to be relatively uninhibited and eventually increased to almost 7-fold of pre-dose activity levels. Thus, there seems to be complex IMPDH activity response to MPA exposure than simply predicted from the simple enzyme-inhibitor relationship.

Characterisation of the IMPDH activity response (EC_{50}) following *in vitro* MPA exposure over time indicated that at initial exposure (5-minute incubation) the extracellular MPA to achieve EC_{50} was almost 10-fold higher (0.27 µM) than the reported k_i of recombinant IMPDH inhibition by MPA (37 nM). This was apparent in the time-course assays as the intracellular MPA concentrations were only a fraction (15.1 – 21.3%) of the extracellular MPA concentrations. At 20 minutes, the EC_{50} increased to 42.4 µM, whereas at 4 hours, IMPDH was insensitive to MPA and could not be inhibited.

Notably, the reported EC_{50} for MPA inhibition of cell proliferation was 2.5 µM (Sugiyama et al., 2008). This was also similar to the EC_{50} for IMPDH activity inhibition (3.03 µM MPA) obtained through plasma pharmacokinetic-pharmacodynamic modelling in MPA-treated patients (Fukuda et al., 2011). However, these studies used values obtained at either 96 hours of incubation (Sugiyama et al., 2008) or a range of timepoints (0 – 9 hours), (Fukuda et al., 2011). These time-dependent changes in EC_{50} suggest that the sensitivity of IMPDH activity in response to MPA exposure may decrease over time within a single dosing period. This could be the result of several different mechanisms, such as an increase in *IMPDH1* or *IMPDH2* gene transcription or allosteric regulation of IMPDH via the formation of IMPDH filaments.

An increase in gene transcription and/or protein translation would result in the increase in IMPDH protein levels, increasing IMPDH activity. The expression of *IMPDH1/2* after MPA administration has not been widely studied. *IMPDH1* is generally regarded as the constitutively expressed gene, with expression remaining constant even with increased need for guanine biosynthesis. In contrast, *IMPDH2* expression is thought to increase rapidly in response to increased cellular requirements for guanine biosynthesis. Indeed that has been observed in male volunteers after the administration of MPA (Kim et al., 2014). In the 10 hours following MPA administration to 6 MPA-naïve volunteers, *IMPDH1* mRNA expression did not fluctuate markedly from baseline, except in 1 volunteer where *IMPDH1* gene expression increased from 1 hour and plateaued at 3 hours. In contrast, *IMPDH2* gene expression showed substantial upregulation. Peak *IMPDH2* mRNA expression could be seen as early as 1 hour after MPA administration. In addition, there was also considerable inter-individual variability in *IMPDH2* mRNA, with some individuals displaying multiple peaks of transcription whereas others had little to no change in expression. Conversely, another study, in $CD4^+$ cells and whole blood, observed significantly decreased *IMPDH1* expression following MMF administration whereas *IMPDH2* expression was not changed (Bremer et al., 2009). The large inter-individual variability of *IMPDH1/2* expression patterns in response to MPA could thus contribute to different extent of IMPDH inhibition in patients. However, changes in gene expression and the resulting increased protein production are unlikely to have occurred within the timeframe (20-240 min) of the changes in IMPDH activity observed in the experiments described in this chapter.

An important recent discovery has demonstrated that IMPDH may also be regulated at the oligomeric level in response to MPA treatment. The study observed the formation of extended filaments of clustered IMPDH enzymes when various cell types, cancer cell lines and healthy lymphocytes, were treated with MPA (Ji et al., 2006). These IMPDH filaments took on the

appearance of long linear arrays (rods) as well as circular arrays (rings) and are made up of stacked IMPDH octamers. Addition of GTP led to the disassembly of these filaments, as did ATP to a lesser extent. Further research has elucidated the physiological aspects of these IMPDH filaments. Calise et al. (2018) observed rapid formation of IMPDH filaments in rapidly proliferating splenic B- and T-lymphocytes in mice and observed that filament formation correlated with the proliferation marker Ki-67 in *ex vivo* stimulated human T-lymphocytes. Another study utilised mutant IMPDH with a non-functional Bateman domain along with *IMPDH2* gene knockdown to show that filament formation was required to maintain proliferation of HeLa cells (Keppeke et al., 2018). The same study also showed that increasing IMP levels in cells (either through allopurinol or an increase in GMP reductase expression) led to a substantial increase in IMPDH filament formation. These findings indicate that IMPDH filament formation is an essential cellular response to the increased guanine nucleotide requirements that arise from cell proliferation. In the context of MPA inhibition, the trapping of IMPDH in the E-XMP* complex leads to a decrease in guanine nucleotide production and an increased need for guanine nucleotide production and could thereby induce IMPDH filament formation.

Once formed, these IMPDH filaments have been reported to be insensitive to further inhibition either by MPA or other endogenous substrates (Johnson & Kollman, 2020). This could explain the time-dependent insensitivity of IMPDH inhibition by MPA observed in this thesis. However, to date, studies have not established patterns of filament formation in response to MPA administration to patients. Instead, most studies have only noted the presence of fully formed IMPDH filaments, or the proportion of cells in which the filaments are present, using various cell lines and tissues following between 30 minutes to 24 hours of *in vitro* MPA treatment (Calise & Chan, 2020). The mechanisms that contribute to the time-dependent

decrease in sensitivity of IMPDH to MPA inhibition are thus unclear and should be explored further in future studies.

A limitation in the studies detailed in this chapter is the use of only one immortalised cell line.

In conclusion, characterisation of the uptake kinetics and intracellular MPA accumulation within cells has suggested that MPA uptake may not be a limiting factor in the inhibition of IMPDH and thus therapeutic effectiveness. Instead, the extent to which IMPDH remains inhibited over time may be more pertinent and should be explored further in future studies.

Chapter 6: Differential expression of *IMPDH1* and *IMPDH2*

6.1. Introduction

The previous chapter demonstrated that following *in vitro* incubation with Jurkat cells (immortalised neoplastic T-cells) the relationship between intracellular MPA concentration and its effect on inhibition of IMPDH activity displays temporal changes. However, the immune response, either disordered (as in the autoimmunity of SLE) or activated (as in the graft vs host disease after transplantation), is complex and comprised of many different immune cell types. Each immune cell-type may exhibit different IMPDH behaviour in the presence of MPA and this could be an additional reason for the heterogenous MPA therapeutic responses between individuals. However, other factors could influence *IMPDH* expression in immune cells, such as genetic polymorphisms and even sex-related differences.

6.1.1. *IMPDH1* and *IMPDH*2 genetic polymorphisms

Various studies have tried to assess the impact of *IMPDH1* and *IMPDH2* genetic polymorphisms on therapeutic outcomes in SLE/LN or transplant patients receiving MPA therapy. Other studies have assessed *IMPDH1* and *IMPDH2* single nucleotide polymorphisms (SNP) in the inherited predisposition to SLE/LN. However, there is conflicting evidence and hence no clear consensus on the impacts of such genetic variants. *IMPDH1* genetic SNP have been assessed more frequently than those of *IMPDH2*, this may be due to greater conservation of *IMPDH2* than *IMPDH1* (Wang et al., 2007).

The *IMPDH1* SNP rs2278293 and rs2278294 are the most frequently assessed *IMPDH1* variants. Both are SNP in intron 7 of the *IMPDH1* gene. In a comprehensive study of prevalence of SNP in this gene, these variants (rs2278293 and rs2278294) were the most common with minor allele frequencies of 42.7% and 40.6% respectively. Moreover, these *IMPDH1* SNP associated with the increased incidence of biopsy-proven acute rejection of renal transplant within 12 months in patients receiving MPA (Wang et al., 2008). However,

subsequent assessment of these two SNP has yielded conflicting results depending on the clinical outcome reported. A lower risk of biopsy-proven acute rejection and greater immunosuppression resulting in higher leukopenia post-renal transplantation has been reported with rs2278294 (Gensburger et al., 2010). This rs2278294 SNP has been found to significantly associate with increased risk of adverse events related to excessive immunosuppression (leukopenia) in Chinese autoimmune patients receiving MPA (Shu et al., 2021). It is also associated with increased GI intolerance in paediatric heart transplant patients (Ohmann et al., 2010). There have also been other studies that have found no association between this SNP and MPA therapeutic outcomes in LN patients (Schwartz et al., 2012), or between this SNP and risk of acute rejection in renal transplant patients (Kagaya et al., 2010).

The other SNP (rs2278293) also has contradictory associations, with a lower incidence of chronic graft vs host disease in nonmyeloablative haematopoietic stem cell transplant recipients (McCune et al., 2018) and also with an increased risk of acute rejection in renal transplant patients (Zhou et al., 2018). However, rs2278293 (in contrast to rs2278294) did not associate with GI intolerance in paediatric heart transplant patients (Ohmann et al., 2010) or any clinical outcome post-renal transplant in a large clinical study (Gensburger et al., 2010).

Conversely, *IMPDH2* SNP are less well characterised. The most assessed variant, rs11706052 is a polymorphism in intron 7, with a minor allele frequency of 19% (Winnicki et al., 2010). This SNP has been found to associate with decreased graft rejection in renal transplant patients (Cilião et al., 2018) although several other studies have not observed such an association with clinical outcomes (McCune et al., 2018; Scalzotto et al., 2017; Schwartz et al., 2012).

In summary, although these SNP have been extensively studied, there has been no consistent association with MPA therapeutic response. Importantly, no study thus far has questioned the effect these SNP have on *IMPDH* expression.

6.1.2. Roles of immune cells in SLE/LN

While the main effectors of the dysfunctional immune response in SLE/LN are T- and B- cells, other immune cells such as macrophages, neutrophils and dendritic cells have also been implicated in SLE/LN pathogenesis. As was detailed in Chapter 1 Section 1.1, the autoimmunity observed in SLE/LN is a self-propagating cycle that broadly consists of two stages: immune complex formation, and then tissue damage due to immune complex deposition. The lupus self-antigens produced are presented by dendritic cells to autoreactive $CD4^+$ T-cells, which aid the maturation of autoreactive B-cells, leading to the formation of autoantibodies. These autoantibodies then bind to the self-antigens, forming immune complexes which are then deposited in tissues. After the deposition of immune complexes in tissues, inflammatory cytokine cascades trigger the involvement of innate immune cells, such as macrophages and neutrophils, leading to inflammation and tissue damage. This in turn results in the further production and release of self-antigens. Hence, these multiple different immune cell types mediate unique pathways in SLE/LN pathogenesis and may have different responses to MPA therapy.

6.1.2.1. T-cells

Different subsets of T-cells play different roles in the autoimmunity of SLE/LN. A major subpopulation of T-cells, the $CD4^+$ helper T-cells, aid in the production of autoantibodies and tissue inflammation. $CD4^+$ helper T-cells primarily assist in the maturation of autoantibody-producing B-cells and do so through differentiation from naïve $CD4^+$ T-cells to various subtypes, such as T-helper cells, T-follicular helper cells and regulatory T-cells. T-helper cells mainly produce cytokines which aid in the proliferation and differentiation of B-cells. T-helper type 1 cells produce IFN-γ, a cytokine that promotes IgG class switch recombination as well as autoantibody formation in B-cells (Peng et al., 2002). T-helper type 2 cells produce

cytokines including IL-4 and IL-13, which can promote differentiation of B-cells into autoantibody-producing plasma cells (Raphael et al., 2015). T-follicular helper cells localise to B-cell follicles and the geminal centres within these follicles (Craft, 2012), where they secrete cytokines such as IL-21 and ICOS that promote B-cell maturation and somatic class switching. Additionally, T-follicular helper cells highly expresses the receptor PD-1, which ensure the survival of B-cells and the differentiation into high-affinity plasma cells, via signalling through the surface ligands PD-L1 and PD-L2 on geminal centre B-cells (Good-Jacobson et al., 2010).

In SLE/LN, abnormal circulating T- follicular helper cells have been observed to form geminal centres and lymphoid-like structures within organs such as the kidney, contributing to the autoimmune response (Chang et al., 2011). On the other hand, whilst regulatory T-cells inhibit the expansion and differentiation of T-cells and dampen autoimmunity, there is conflicting evidence on their role in SLE/LN. Some reports suggest decreased capacity for T-cell suppression (Bonelli et al., 2008; Miyara et al., 2005) while others have observed expansion of regulatory T-cell populations and increased suppression (Alexander et al., 2013; Yan et al., 2008).

Other notable T-cell subpopulations include the cytotoxic $CD8^+$ T-cells, γδT-cells and mucosal-associated invariant T (MAIT) cells. Naïve $CD8^+$ cytotoxic T-cells recognise and process antigens presented by MHC I cells which, along with other cytokines and extracellular signals, trigger various pathways that result in the clonal expansion of antigen-specific $CD8^+$ T-cells and differentiation into effector cells. These effector cells then release perforin and granzymes to kill cells with the antigen they are specific for (Zhang & Bevan, 2011). $CD8^+$ T-cells in SLE patients have been found to have impaired cytotoxic capacity with decreased perforin and granzyme production (Comte et al., 2017).

In contrast, γδT-cells are double negative T-cells and make up a small proportion of circulating lymphocytes. These γδT-cells can take on other T-cell phenotypes and secrete various cytokines that aid in immune response activation, such as IFN-γ and IL-17 (Paul et al., 2014). These cells also aid in B-cell class switching and plasma cell longevity (Huang et al., 2016) and can also function as antigen-presenting cells to aid T-cell maturation and differentiation (Brandes et al., 2005). There is emerging evidence that γδT-cells could play important roles in the pathogenesis of SLE autoimmunity, such as the promotion of B-cell hyperactivity through increased expression of CD40L and IL-21 (Yin et al., 2015).

The mucosal-associated invariant T-cells (MAIT) are an abundant T-cell subpopulation that possess innate-like characteristics. These MAIT cells are uniquely specific to a microbial metabolite, 5-amino-6-D-ribitylaminouracil (Corbett et al., 2014). When activated, MAIT cells produce cytokines such as IFN-γ that promote B-cell maturation and antibody production (Dusseaux et al., 2011) and can also act as cytotoxic effector cells (Kurioka et al., 2015; Le Bourhis et al., 2013). In SLE patients, MAIT cell numbers have been found to be decreased but a higher proportion are in the activated state compared to healthy individuals (Chiba et al., 2017).

6.1.2.2. B-cells

The role of B-cells in the adaptive immune system is complex and encompasses antibody production, presentation of antigens and cytokine secretion. After initial production to form a mature but naïve B-cell in the bone marrow, the cells become activated through contact with antigens in peripheral lymphoid tissues. These antigens can be soluble foreign molecules or smaller peptides presented on the surfaces of antigen-presenting cells, such as dendritic cells. Once activated by its specific antigen, B-cells then internalise the antigen via endocytosis and present the antigen on MHC class II molecules on their surfaces. These antigens are recognised

by T-cells, which further activate B-cells through cytokine secretion and signal cascades. The activated B-cells can then proliferate and differentiate into antibody-producing plasma cells (Merlo & Mandik-Nayak, 2013).

The involvement of B-cells in SLE autoimmunity is well characterised. A central role is the production of autoantibodies, which target self-antigens such as double-stranded DNA, ribonucleoproteins and histones. These autoantibodies form immune complexes with self-antigens which result in tissue inflammation. The presence of B-cell abnormalities promotes dysfunctional B-cell activity, such as increased proportion of memory B- cells, allowing lower activation requirement, or evasion of central tolerance by the autoreactive B-cells (Karrar & Cunninghame Graham, 2018).

6.1.2.3. Dendritic cells

Dendritic cells are innate immune cells which make up most of the antigen-presenting cells, which are crucial for the engagement of adaptive immunity, i.e. T- and B-cell activation. These cells have two distinct subpopulations from two lineages, conventional myeloid dendritic cells and plasmacytoid dendritic cells. Myeloid dendritic cells mainly assist in $CD4^+$ and $CD8^+$ T-cell activation through phagocytosis and subsequent presentation of antigens through expressed MHC I and II proteins. Conversely, plasmacytoid dendritic cells have low expression of MHC proteins and have been theorised to promote regulatory T-cell proliferation (Swiecki & Colonna, 2010) whilst suppressing other T-cell expansion (Jahrsdörfer et al., 2010).

In SLE, plasmacytoid dendritic cells are thought to play a critical role in autoimmunity. Several studies have found that increased production of type 1 IFN by these cells in SLE leads to their own increased activation in an autocrine manner, resulting in a further increase in IFN production and the increased expression of stimulatory surface markers such as CD80 and MHC class II (Chan et al., 2012; Elkon & Wiedeman, 2012). This leads to enhanced capability

to activate T-cells by plasmacytoid dendritic cells, as well as direct simulation of B-cell proliferation and antibody production. Phenotypic changes in myeloid dendritic cells have also been implicated in SLE pathogenesis. Increased pro-inflammatory cytokine (CD80 and CD86) expression has been observed in myeloid dendritic cells which may lead to increased activation of T-cells and enhanced differentiation (Carreño et al., 2009).

6.1.2.4. Macrophages

Macrophages are an important component of innate immunity. They are derived from haematopoietic stem cells and are differentiated from monocytes. Macrophages are mostly situated in tissues, where their specific environment define their phenotypes. Their main role is the ingestion and clearance of debris, including dead cells and foreign material such as bacteria. Macrophages also serve as antigen-presenting cells, and present digested peptides on MHC II molecules. Importantly, macrophages present antigens in tissues, and do not take part in the activation and differentiation of naïve $CD4^+$ T-cells. Instead, they activate differentiated helper T-cells in tissues.

Macrophages also contribute to the pathogenesis of SLE. In particular, the defective clearance of apoptotic cells by macrophages has been observed in SLE, leading to an increased release of self-antigens. This then results in the accumulation of self-antigens and, together with sustained production of autoantibodies, the formation of immune complexes. Macrophages with digested cellular fragments were found to be markedly decreased in SLE patients. Furthermore, anti-inflammatory signalling by macrophages when clearing apoptotic cells was found to be decreased, leading to greater tissue inflammation and damage (Herrmann et al., 1998). Autoantibodies in the macrophage environment have also been observed to downregulate phagocytosis and increase pro-inflammatory cytokine production, leading to

impaired clearance of apoptotic cells and increased tissue inflammation by macrophages (Thanei & Trendelenburg, 2016).

6.1.2.5. Neutrophils

Neutrophils are the most abundant cell type in blood and have important roles in the innate immune system. They are important effector cells which mainly clear foreign microorganisms. They can do this through three methods: degranulation, phagocytosis, and formation of neutrophil extracellular traps (NET). In degranulation, neutrophils release the digestive content of their intracellular granules to the environment which degrades the microorganism. Neutrophils can also phagocytose the microorganism, engulfing it in a vacuole containing digestive enzymes and with a low pH. Lastly, neutrophils also form NET when the microorganism is too big to phagocytose. This is the release of granular proteins and DNA fibres, forming extensive net-like structures that trap the microorganism.

Neutrophils have also been implicated in the pathogenesis of SLE. As with macrophages, neutrophils appear to have impaired phagocytic capacity in SLE patients (Brandt & Hedberg, 1969). Furthermore, neutrophils in SLE have been observed to overexpress adhesion molecules, causing aggregation and inhibition of phagocytosis and release of lysosomal enzymes (Abramson et al., 1983). Neutropenia and increased apoptosis of neutrophils have also been observed in SLE, resulting in increased production of self-antigens (Y. Ren et al., 2003). Importantly, impaired NET degradation and increased NETosis also contribute to the release of self-antigens and promote autoimmunity (Hakkim et al., 2010; Villanueva et al., 2011).

6.1.3. Conclusion and aims

The immune disruption observed in SLE is complex and involves multiple immune cells. Hence the effect of MPA on overall therapeutic effectiveness may be related to the expression patterns of *IMPDH1* and/or *IMPDH2* in these various immune cell types. Importantly, it is not known whether there are any differences in *IMPDH* expression based on sex; given the sex bias of SLE/LN, this may be an important factor to consider for MPA effect. Lastly, the effect of genetic polymorphisms (rs2278293, rs2278294 and rs11706052) in *IMPDH1* and *IMPDH2* on the gene transcription is not known.

This chapter aims to investigate whether there are differences in *IMPDH1* and *IMPDH2* expression relative to sex, genetic polymorphisms and immune cell type using an iterative assessment of gene-expression data available in multiple public databases.

6.1.4. Study design

Three databases were chosen to extract and analyse the mRNA expression data of both *IMPDH1* and *IMPDH2*. These were the Genotype-Tissue Expression (GTEx), All RNA-seq and ChIP-seq sample and signature search (ARCHS^4) databases (Lachmann et al., 2018) and the Human Protein Atlas (HPA), (Pontén et al., 2008; Uhlen et al., 2019).

The GTEx database was chosen for the ability to segregate the mRNA expression data based on sex, as well as the capability to analyse expression quantitative trait loci (eQTL) and also splicing quantitative trait loci (sQTL). The ARCHS^4 database was chosen for its more detailed categorisation of mRNA expression in different immune cell types and importantly has an independent dataset from that available in GTEx. Lastly, the HPA was chosen for its inclusion of protein expression data. Whilst this database includes mRNA expression data from the Functional Annotation of Mammalian Genomes 5 (FANG5) dataset, it also includes the GTEx dataset; unless indicated, only the former data were used in this study. The full details of the

publicly available datasets, sequencing techniques used to derive these data as well as the information of the tissue, cell type and cell lines that have been included in these datasets are detailed in Table 6-1.

An iterative approach was taken to analyse the data from these datasets. In brief, data was first extracted from GTEx and analysed, followed by extraction and analysis of data from ARCHS[4], and then the analysis of the HPA data was undertaken. The comprehensive detail of the methods undertaken are described in Chapter 2 section 2.2.4.

Graphical analyses were undertaken in GraphPad Prism 9.0.2 (GraphPad Prism Software Inc., USA). Differences between groups were assessed using Mann-Whitney or Kruskal-Wallis tests.

	GTEx Genotype-Tissue Expression	**ARCHS[4]** All RNA-seq and ChIP-seq sample and signature search	**HPA** Human Protein Atlas
Human Tissues	Whole blood (n=670) Spleen (n=227)	**Granulocytic** Granulocyte (n=152) Neutrophil (n=1518) **Lymphoid** B lymphocyte (n=186) Plasma Cell (n=1294) Plasmacytoid Dendritic Cell (n=276) T lymphocyte (n=300) **Myeloid** Alveolar Macrophage (n=560) Dendritic Cell (n=2300) Kupffer Cell (n=16) Macrophage (n=5342) **Spleen** Spleen (Bulk Tissue), (n=880) **Thymus** Thymus (Bulk Tissue), (n=208) Thymocyte (n=18)	**Granulocytes** Basophil Eosinophil Neutrophil **Monocytes** Classical monocyte Non-classical monocyte Intermediate monocyte **T-cells** T-reg GdT-cell MAIT T-cell Memory CD4 T-cell Naïve CD4 T-cell Memory CD8 T-cell Naïve CD8 T-cell **B-cells** Memory B-cell Naïve B-cell **Dendritic cells** Plasmacytoid Dendritic Cell Myeloid Dendritic Cell **NK-cells** **Total PBMC** **Bone Marrow** **Spleen** **Thymus**

Cell Lines	EBV-transformed lymphocytes (n=147)	**Lymphoid** Jurkat (n=2492) MT4 (n=20) NALM6 (n=168) REH (n=230) RPMI-8226 (n=62) **Myeloid** THP-1 (n=1128) U-937 (n=352)	**Lymphoid** Jurkat U-698 HDLM-2 REH U-266/84 U-266/70 RPMI-8226 MOLT-4 Karpas-707 Daudi **Myeloid** HEL U-937 HMC-1 HL-60 THP-1 NB-4 K-562 HAP1
Datasets used	Genotype-Tissue Expression (GTEx)	Gene Expression Omnibus Sequence Read Archive (**Does not include GTEx**)	**Tissue Atlas** Human Protein Atlas (HPA) Genotype-Tissue Expression (GTEx) Functional Annotation of Mammalian Genomes 5 (FANTOM5) **Blood Atlas** Human Protein Atlas (HPA) Schmiedel Monaco

Sequencing techniques and platforms	Illumina TrueSeq RNA-seq Affymetrix Human Gene 1.1 ST Expression Array (V3, 837 samples)	Illumina HiSeq 2000 Illumina HiSeq 2500 Illumina NextSeq 500	**Tissue Atlas** Illumina HiSeq 2000 (HPA) Illumina HiSeq 2500 (HPA) Illumina TrueSeq (GTEx) Cap Analysis of Gene Expression and Illumina Sequencing (FANTOM5) **Blood Atlas** Illumina HiSeq 2000 (HPA) Illumina HiSeq 2500 (HPA) Illumina HiSeq 2500 (Schmiedel) Illumina HiSeq 2000 (Monaco)

Table 6-1. A summary of the datasets, sequencing techniques, and platforms as well as immune human tissues and cell lines assessed in the publicly available databases: GTEx, ARCHS[4] and Human protein atlas.

6.2. Results

6.2.1. *IMPDH1* and *IMPDH2* expression in GTEx

The GTex database contains only two tissues of relevance, whole blood and spleen. The mRNA expression (transcripts per million, TPM) of *IMPDH1* and *IMPDH2* in these two tissues are shown in Figure 6-1. Expression of *IMPDH1* ranged from 6.08 to 906 TPM in whole blood (median and IQR: 173 TPM, 68.4 – 416 TPM). This data was not normally distributed and significantly ($p < 0.0001$) deviated from a normal or lognormal distribution in all statistical tests of normality undertaken (Table 6-2). Expression of *IMPDH2* ranged from 2.65 to 205 TPM in whole blood (median and IQR: 36.8 TPM, 23.8 – 53.8 TPM). This data was also not normally distributed and also significantly deviated from a normal or lognormal distribution in numerous statistical tests of normality (Table 6-2).

Test name	Significant deviation from normality (p-value)	
	IMPDH1	***IMPDH2***
Anderson-Darling	< 0.0001	< 0.0001
D'Agostino & Pearson	< 0.0001	< 0.0001
Shapiro-Wilk	< 0.0001	< 0.0001
Kolmogorov-Smirnov	< 0.0001	0.0002

Table 6-2. Normality and lognormality tests of whole blood *IMPDH1* expression data in GTEx dataset.

In the spleen the expression of *IMDPH1* was lower than in whole blood ranging from 43.9 to 200 TPM (median and IQR: 95.6 TPM, 73.8 – 115 TPM). The expression of *IMPDH2* was median and IQR: 122 TPM, 102 – 146 TPM. The distribution of expression of both *IMPDH1* and *IMPDH2* did not significantly deviate from lognormal (Gaussian distribution) in spleen ($p > 0.100$ in all 4 lognormality tests for both *IMPDH1* and *IMPDH2*). The expression of *IMPDH2* was significantly lower than *IMPDH1* in whole blood ($p < 0.0001$) and in contrast was significantly higher than *IMPDH1* ($p < 0.0001$) in spleen (Figure 6-1).

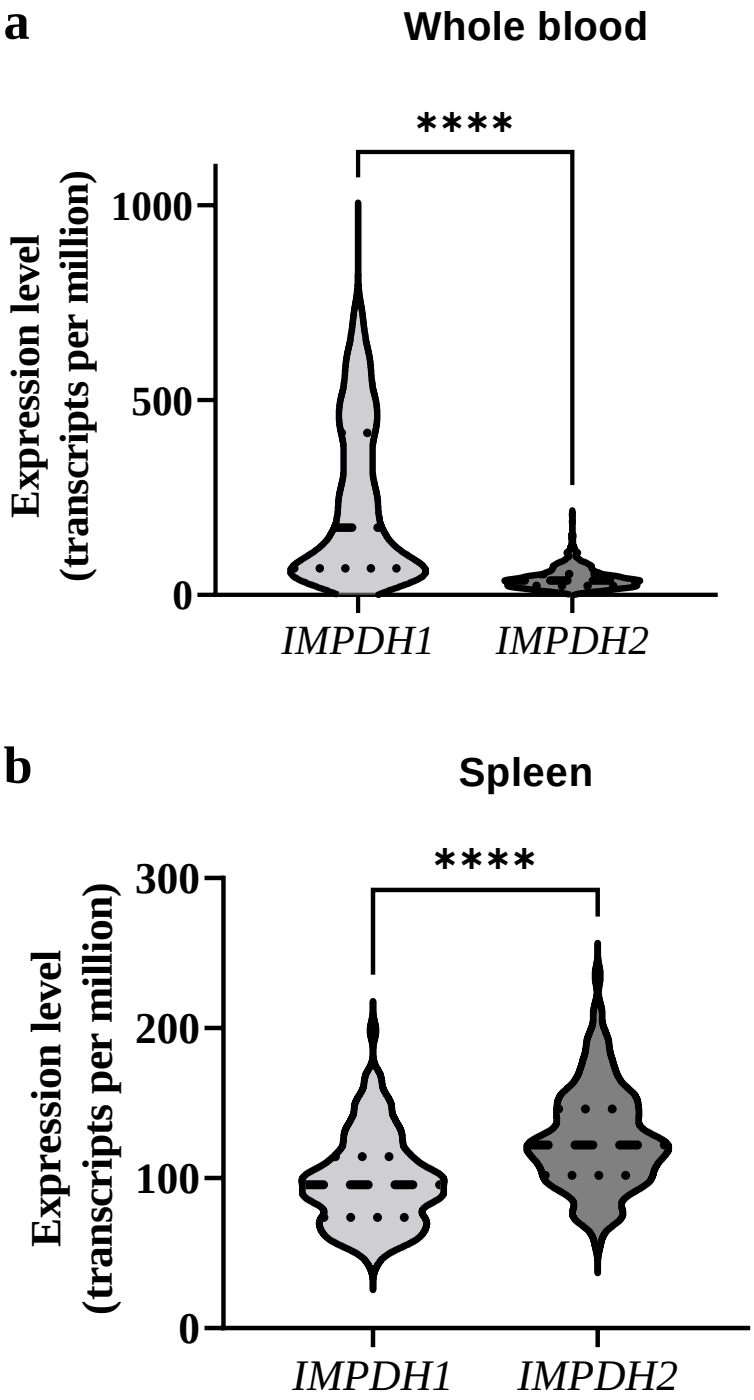

Figure 6-1. *IMPDH1* mRNA expression was significantly higher than *IMPDH2* expression in (a) whole blood (n = 755) but *IMPDH2* expression was significantly higher than *IMPDH1* expression in (b) spleen (n = 241). Data was extracted from GTEx database. The hatched line (- - -) in each violin plot represents the median of the population. The 25th and 75th quartile as shown as dotted lines (· · ·). Two-tailed Mann-Whitney tests were conducted separately for each tissue in Prism. Note y-axes for a) and b) are on different scales. **** $p < 0.0001$

In whole blood (Figure 6-2), males had a significantly lower *IMPDH1* expression (median = 148 TPM) than females (median = 228 TPM, $p = 0.0038$, 95% CI of difference = 9.50 – 51.8 TPM). However, in spleen tissue, *IMPDH1* expression was significantly higher (median = 99.8 TPM) in males than females (median = 88.3 TPM, $p = 0.0093$, 95% CI of difference = 2.52 – 17.6 TPM).

In contrast *IMPDH2* expression did not differ between sexes in either of these tissues (Figure 6-3). In whole blood, males had similar expression levels as females (median = 36.8 vs 37.1 TPM respectively, $p = 0.736$). Similarly, in spleen tissue, males had similar expression levels of *IMPDH2* as females (median = 122 TPM vs 118 TPM respectively, $p = 0.632$).

Both ARCHS[4] and HPA did not have expression data stratified by sex, so no expression data stratified by sex was extracted from these two databases.

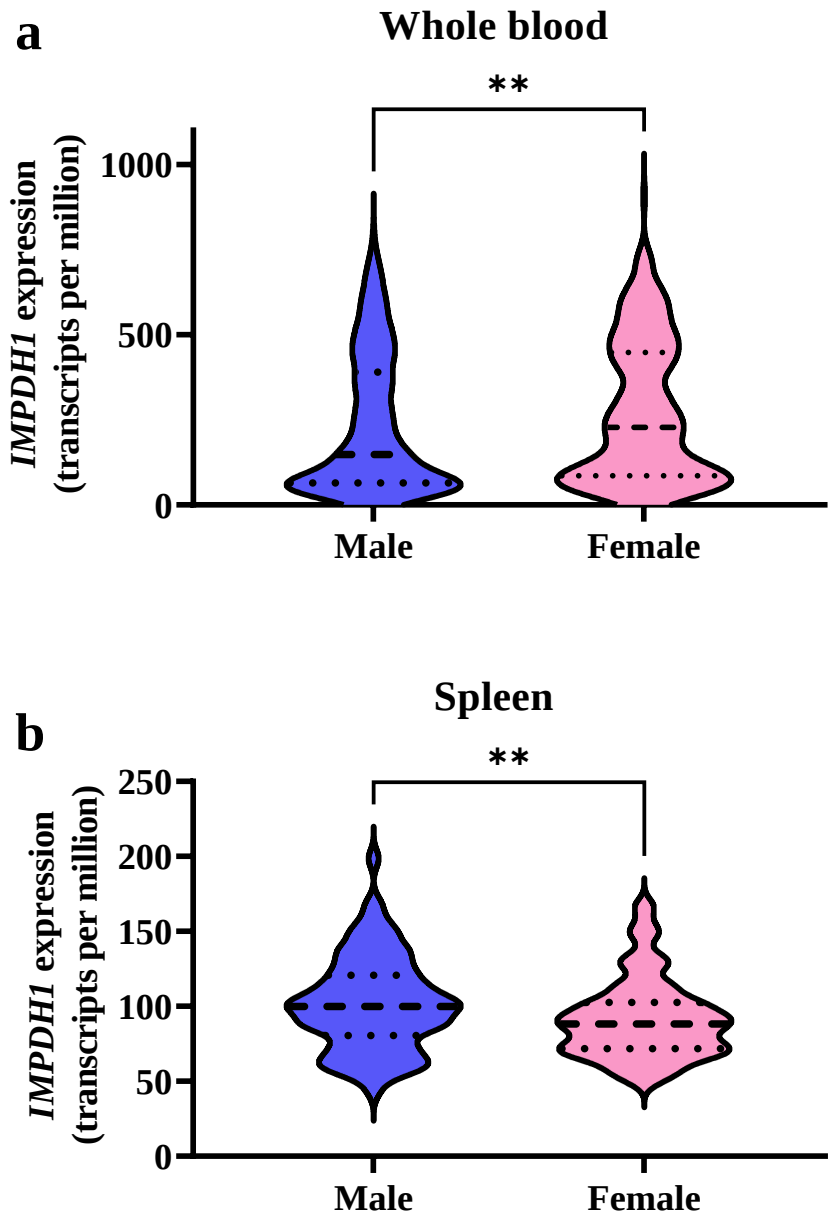

Figure 6-2. *IMPDH1* expression in (a) whole blood is higher in females compared to males, in contrast in (b) spleen, *IMPDH1* expression is lower in females compared to males. Data was extracted from GTEx database (whole blood male n = 501, female n = 254; spleen male n = 154, female n = 87). The hatched line (- - -) in each violin plot represents the median of the population. The 25th and 75th quartile as shown as dotted lines (· · ·). Two-tailed Mann-Whitney tests were conducted separately for each tissue in Prism. Note y-axes for a) and b) are on different scales. ** $p < 0.001$

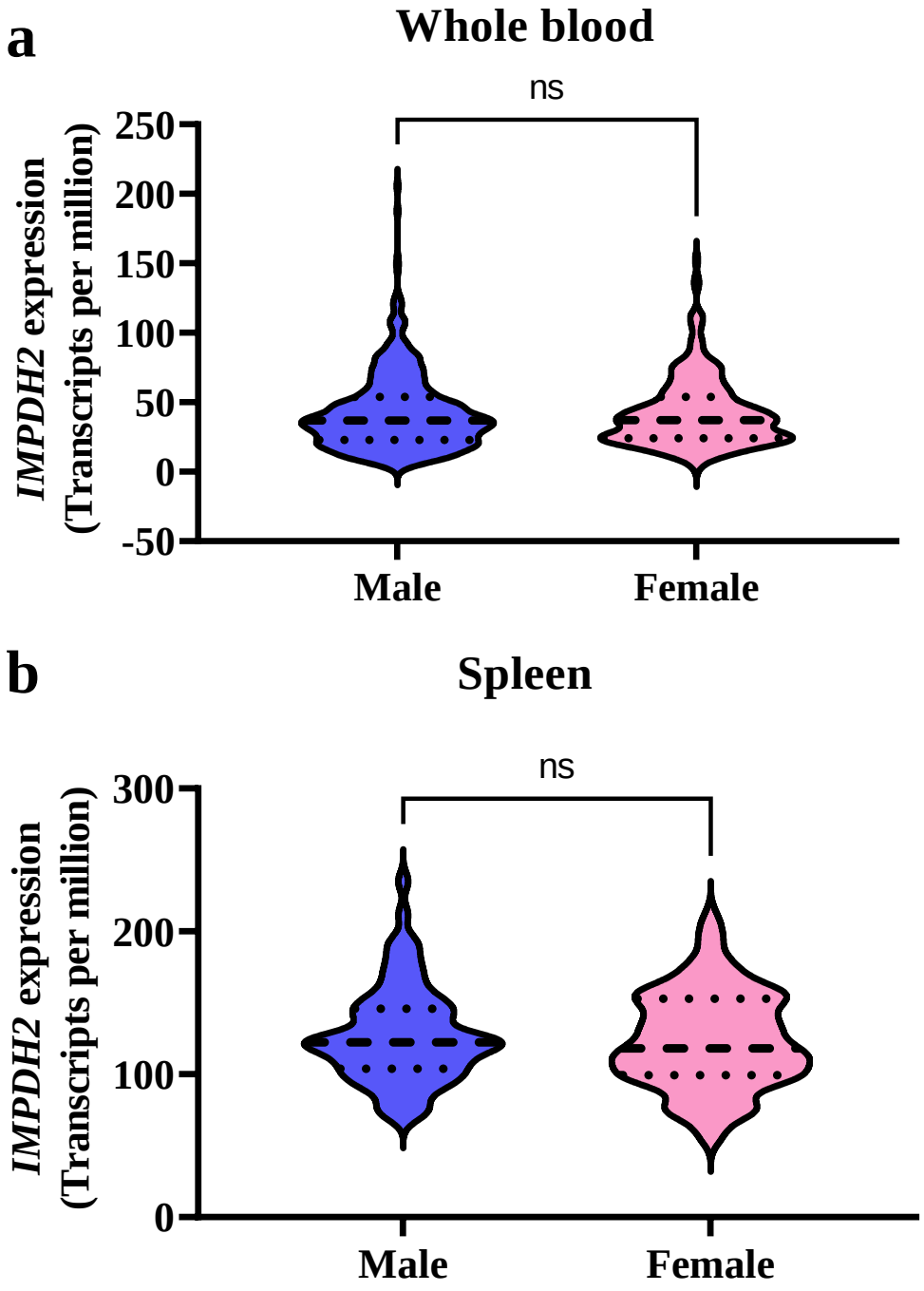

Figure 6-3. No difference in *IMPDH2* expression between males and females in (a) whole blood and (b) spleen. Data was extracted from GTEx database (whole blood male n = 501, female n = 254; spleen male n = 154, female n = 87). The hatched line (- - -) in each violin plot represents the median of the population. The 25th and 75th quartile as shown as dotted lines (···). Two-tailed Mann-Whitney tests were conducted separately for each tissue in Prism. Note y-axes for a) and b) are on different scales. ns = not significant

6.2.2. Gene transcript expression relative to *IMPDH* SNP

The eQTL and sQTL for the *IMPDH1* SNP (rs2278293 and rs2278294) and the *IMPDH2* SNP (rs11706052) were then queried in the GTEx web interface for all tissues.

There was no association for these three SNP and the expression of either *IMPDH1* or *IMPDH2* in whole blood, spleen or EBV-transformed lymphocytes in this database. However, there were significant associations of the *IMPDH1* SNP rs2278293 and rs2278294 with *IMPDH1* expression differences in a number of other tissues which are not directly related to the immune system (Tables 6-3 and 6-4).

Tissue	*p*-value	Normalised Effect Size (NES)
Adipose - Subcutaneous	1.70E-20	-0.22
Adipose - Visceral (Omentum)	2.50E-08	-0.14
Esophagus - Mucosa	2.00E-09	0.18
Skin - Not Sun Exposed (Suprapubic)	8.10E-14	0.17
Skin - Sun Exposed (Lower leg)	1.90E-08	0.14

Table 6-3. Significant eQTL observed for rs2278293 with *IMPDH1* expression in different tissues.

Tissue	*p*-value	Normalised Effect Size (NES)
Adipose - Subcutaneous	4.50E-32	-0.3
Adipose - Visceral (Omentum)	2.80E-18	-0.22
Breast - Mammary Tissue	2.80E-08	-0.12
Skin - Not Sun Exposed (Suprapubic)	0.0000037	0.11
Testis	0.0000045	0.14

Table 6-4. Significant eQTL observed for rs2278294 with *IMPDH1* expression in different tissues.

Both of these SNP (rs2278293 and rs2278294) were associated with decreased expression in adipose tissue and with increased expression in the skin (not sun-exposed). Of note, rs2278293 was significantly associated with an increase in *IMPDH1* expression ($p = 2.00 \times 10^{-9}$, NES = 0.18) in the mucosa of the oesophagus.

However, these three SNP in *IMPDH1* and *IMPDH2* have been found to associate with expression changes in different genes in whole blood, spleen and EBV-transformed lymphocytes. The rs2278293 SNP associated with the expression (eQTL) of the *RP11-274B21.x* pseudogenes and the *CICP14* gene in both whole blood and spleen. A significant eQTL was also observed between this SNP and *RP11-274B21.x*. in EBV-transformed lymphocytes. These eQTL are summarised in Table 6-5.

For rs2278294, significant eQTL were also observed for these same genomic regions, *RP11-274B21.x* and *CICP14* in whole blood. In the spleen, however a significant eQTL was only observed between rs2278294 and the pseudogenes, *RP11-274B21.x*. (table 6-6).

For the SNP (rs11706052) in *IMPDH2* there were significant eQTL observed for the following genomic regions: *WDR6, RBM6, CCDC71, RP11-3B7.1, NCKIPSD*, and *CCDC36* in spleen ($p < 0.001$, NES = -0.57). In whole blood, significant eQTL were observed between the SNP and *WDR6, NCKIPSD, RBM6* and *UBA7* (table 6-7).

Tissue	Gene	*p*-value	Normalised Effect Size (NES)
Whole Blood	*RP11-274B21.4*	7.40E-29	0.23
	RP11-274B21.12	3.30E-22	0.22
	RP11-274B21.3	1.30E-18	0.17
	RP11-274B21.2	1.60E-11	0.13
	CICP14	3.20E-10	0.14
	RP11-274B21.1	0.0000016	0.094
	RP11-274B21.13	0.000002	0.12
	RP11-212P7.2	0.0000022	-0.11
Spleen	*RP11-274B21.3*	8.90E-08	0.33
	RP11-274B21.12	4.80E-07	0.36
	RP11-274B21.4	7.60E-07	0.37
	CICP14	0.0000023	0.27
	RP11-212P7.2	0.0000058	-0.33
	RP11-274B21.2	0.0000083	0.26
EBV-transformed lymphocytes	*RP11-274B21.3*	4.10E-08	0.47
	RP11-274B21.4	9.30E-08	0.44
	RP11-274B21.12	1.00E-07	0.49
	RP11-274B21.2	6.00E-07	0.32
	RP11-274B21.13	0.0000054	0.3
	RP11-274B21.1	0.000022	0.26

Table 6-5. Significant eQTL observed for *IMPDH1* SNP (rs2278293) in whole blood, spleen, and EBV-transformed lymphocytes.

Tissue	Gene	*p*-value	Normalised Effect Size (NES)
Whole Blood	*RP11-274B21.4*	3.40E-19	0.2
	RP11-274B21.12	6.00E-12	0.17
	RP11-274B21.3	1.30E-10	0.13
	CICP14	1.90E-09	0.14
	RP11-274B21.2	2.70E-08	0.11
	RP11-274B21.13	0.00009	0.1
Spleen	*RP11-274B21.12*	0.000016	0.31
	RP11-274B21.3	0.000073	0.25

Table 6-6. Significant eQTL observed for *IMPDH1* SNP (rs2278294) in whole blood and spleen.

Tissue	Gene	*p*-value	Normalised Effect Size NES
Whole Blood	*WDR6*	2.10E-28	0.44
	NCKIPSD	0.0000015	-0.19
	RBM6	0.000018	0.23
	UBA7	0.000038	0.13
Spleen	*WDR6*	1.60E-07	0.44
	RBM6	0.0000089	0.41
	CCDC71	0.000017	0.33
	RP11-3B7.1	0.000019	-0.64
	NCKIPSD	0.0001	-0.41
	CCDC36	0.00011	-0.57

Table 6-7. Significant eQTL observed for *IMPDH2* SNP (rs11706052) in whole blood and spleen.

No significant eQTL for the expression of either *IMPDH1* or *IMPDH2* in whole blood, spleen and EBV-transformed lymphocytes was observed for any SNP loci in other genomic regions in the database.

Associations of the three SNP with splice variant expression (sQTL) were assessed. This included assessment of *IMPDH1* and *IMPDH2* splice variants as well as other loci.

The rs2278293 SNP in *IMPDH1* displayed associations with mRNA expression of splice variants (sQTL) in the *FAM71F2* gene in whole blood (p = 0.000037, NES = -0.21). Significant sQTL were observed between rs2278294 and *METTL2B* in EBV-transformed lymphocytes (p = 0.000003, NES = 0.57) and *RP11-274B21.1* in whole blood ($p = 1.00 \times 10^{-7}$, NES = -0.33). The SNP (rs11706052) in *IMPDH2* displayed significant sQTL with splice variants of *MST1* in spleen (p = 0.0000011, NES = -0.93), *SLC26A6* in whole blood ($p = 7.30 \times 10^{-7}$, NES = 0.48) and also *ARIH2* in whole blood (p = 0.0000015, NES = 0.46). In whole blood there was a number of significant sQTL associations between various SNP in the *IMPDH1* gene and the expression of a splice variant (intron ID: 128405865:128409756:clu27651) of the *IMPDH1* gene (Table 6-8). There were however, no associations with the rs2278293 or rs2278294 SNP and this *IMPDH1* splice variant. In contrast, no significant sQTL were observed with any *IMPDH2* SNP and expression of *IMPDH2* splice variants.

IMPDH1 SNP ID	*p*-value	NES	*IMPDH1* SNP ID	*p*-value	NES
rs10228542	1.20E-09	0.32	rs17152065	1.70E-10	0.34
rs10239919	3.70E-09	0.31	rs184013121	9.20E-09	0.31
rs10247945	1.20E-10	0.34	rs201811442	9.20E-09	0.31
rs10264312	5.10E-07	0.21	rs202102209	1.30E-08	0.31
rs10273872	2.70E-10	0.34	rs28391244	2.30E-10	0.34
rs1053124	8.90E-07	-0.22	rs28429588	2.30E-10	0.34
rs111671542	1.30E-08	0.31	rs28580600	5.90E-10	0.33
rs112711903	1.30E-08	0.31	rs3213981	9.20E-09	0.31
rs112715555	1.30E-08	0.31	rs373300541	7.80E-09	0.31
rs112948804	9.20E-09	0.31	rs375057895	5.80E-09	0.31
rs113275480	1.30E-08	0.31	rs3802003	3.20E-07	0.25
rs114191334	1.30E-08	0.31	rs3993558	9.20E-09	0.31
rs11562031	3.70E-09	0.31	rs4731449	1.20E-10	0.34
rs115939256	9.20E-09	0.31	rs4731452	1.20E-10	0.3
rs117260885	1.30E-08	0.31	rs531807355	5.80E-07	0.21
rs117639833	1.30E-08	0.31	rs532701505	2.80E-07	0.22
rs12111997	2.90E-09	0.31	rs549906784	5.80E-07	0.21
rs12113115	3.50E-09	0.32	rs57075087	2.30E-08	0.3
rs12113427	8.80E-09	0.31	rs571143742	5.50E-11	0.35
rs1327355829	5.80E-07	0.21	rs571296380	5.80E-07	0.21
rs138294558	5.40E-09	0.31	rs61266907	4.40E-07	0.24
rs138727180	1.30E-08	0.31	rs6944392	6.70E-09	0.31
rs138876806	5.40E-09	0.31	rs6978246	5.70E-10	0.32
rs1397373054	5.80E-07	0.21	rs714510	5.50E-10	0.3
rs140544495	6.50E-07	0.24	rs714511	2.80E-10	0.33
rs141071648	9.20E-09	0.31	rs72624928	5.50E-11	0.35
rs141499142	2.40E-08	0.3	rs74343948	1.30E-08	0.31
rs142590003	5.10E-07	0.25	rs74986205	3.70E-09	0.31
rs142719374	9.20E-09	0.31	rs75746814	1.30E-08	0.31
rs143866678	1.30E-08	0.31	rs76672854	9.90E-11	0.34
rs144684667	5.30E-09	0.35	rs76951139	4.20E-08	0.32
rs145488283	9.20E-09	0.31	rs77699733	1.30E-08	0.31
rs146312386	1.00E-07	0.28	rs7779455	5.40E-09	0.31
rs146461766	1.30E-08	0.31	rs7779818	2.30E-10	0.34
rs146695703	1.30E-08	0.31	rs7779945	3.70E-09	0.31
rs147009057	1.30E-08	0.31	rs7781310	4.20E-10	0.33
rs147597701	1.30E-08	0.31	rs7783540	3.70E-09	0.31
rs147749075	1.30E-08	0.31	rs7784120	2.30E-10	0.34
rs148028705	3.50E-09	0.36	rs77906067	1.20E-09	0.33
rs1560215	5.80E-09	0.31	rs7806193	5.80E-09	0.31
			rs78763502	2.70E-10	0.34

Table 6-8. The sQTL associations between SNP within *IMPDH1* and the expression of the splice variant (intron ID: 128405865:128409756:clu27651) of *IMPDH1*.

IMPDH1 has 18 exons (gene model is shown in Figure 6-4) and this splice variant (intron ID: 128405865:128409756:clu27651) results in expression of a transcript that excludes exon 17. However, the splice variant transcript also includes expression of the intron between exons 1 and 4, this encompasses transcription of both exons 2 and 3 (Figure 6-4). It is of note that the predominant exons expressed in whole blood do not include exon 17 (GTEx exon expression data).

The SNP (Table 6-8) which associate with this splice variant (sQTL) are interspersed across all of the noncoding and coding regions of the *IMPDH1* gene and also upstream of the transcription start site, TSS, of this gene (Figure 6-5).

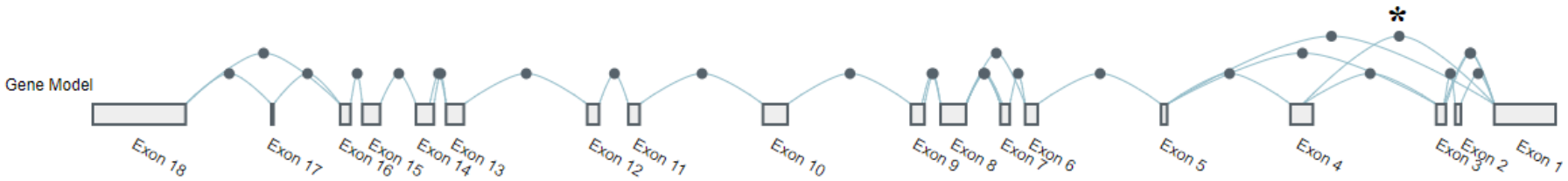

Figure 6-4. The gene model of *IMPDH1* exons and introns. This image was modified from GTEx. Curves with closed circles in the middle connecting exons represent possible introns identified by LeafCutter software (Y. I. Li et al., 2018). * is the intron included in the *IMPDH1* splice variant associated in sQTL analysis with numerous *IMPDH1* SNP.

Figure 6-5. The distribution of SNP in relation to the *IMPDH1* gene. This image was modified from GTEx. SNP which had a normalised effect size (NES) greater than 0.3 were included. SNP annotated in pink have a positive NES on splice variant expression, whereas SNP annotated in blue have a negative NES on splice variant expression. TES and TSS represent the transcription end site and transcription start site of the *IMPDH1* gene respectively. The exon model of *IMPDH1* (in red bars) show the position of the coding region of the gene with respect to the SNP.

6.2.3. Immune tissue expression of *IMPDH1 and IMPDH2* in ARCHS[4]

As noted earlier (Figure 6-1), the data extracted from the GTEx database indicated that *IMPDH1* was expressed at almost a 5-fold higher level than *IMPDH2* in whole blood, whereas in spleen, *IMPDH1* was expressed at a lower level than *IMPDH2*. Moreover, *IMPDH1* expression was almost 2-fold higher in whole blood than in spleen, whereas *IMPDH2* expression was almost 4-fold lower in whole blood than in spleen. To investigate this further data extracted from the ARCHS[4] database to assess the expression of *IMPDH1* and *IMPDH2* in numerous individual immune cell types, immune related tissues, as well as in lymphoid and myeloid cell lines (Figure 6-6 and 6-7).

IMPDH1 was most highly expressed in granulocytes (median = 2566 TPM), followed by B-lymphocytes (median = 2454 TPM). Macrophages expressed approximately 50% *IMPDH1* lower than these two cell types (median = 1373 TPM), whereas T-lymphocytes expressed even less (median = 887 TPM). Plasmacytoid dendritic cells (median = 512.5) had almost 4-fold higher *IMPDH1* expression than myeloid dendritic cells (median = 155 TPM). Interestingly, little or no expression of *IMPDH1* (median = 0 TPM) was observed in plasma cells or the spleen.

Of all the cell lines, Jurkat displayed the lowest expression of *IMPDH1* (median and IQR: 40 TPM, 0 – 737 TPM) and the highest variability in expression of *IMPDH1* (range: 0 – 16900 TPM).

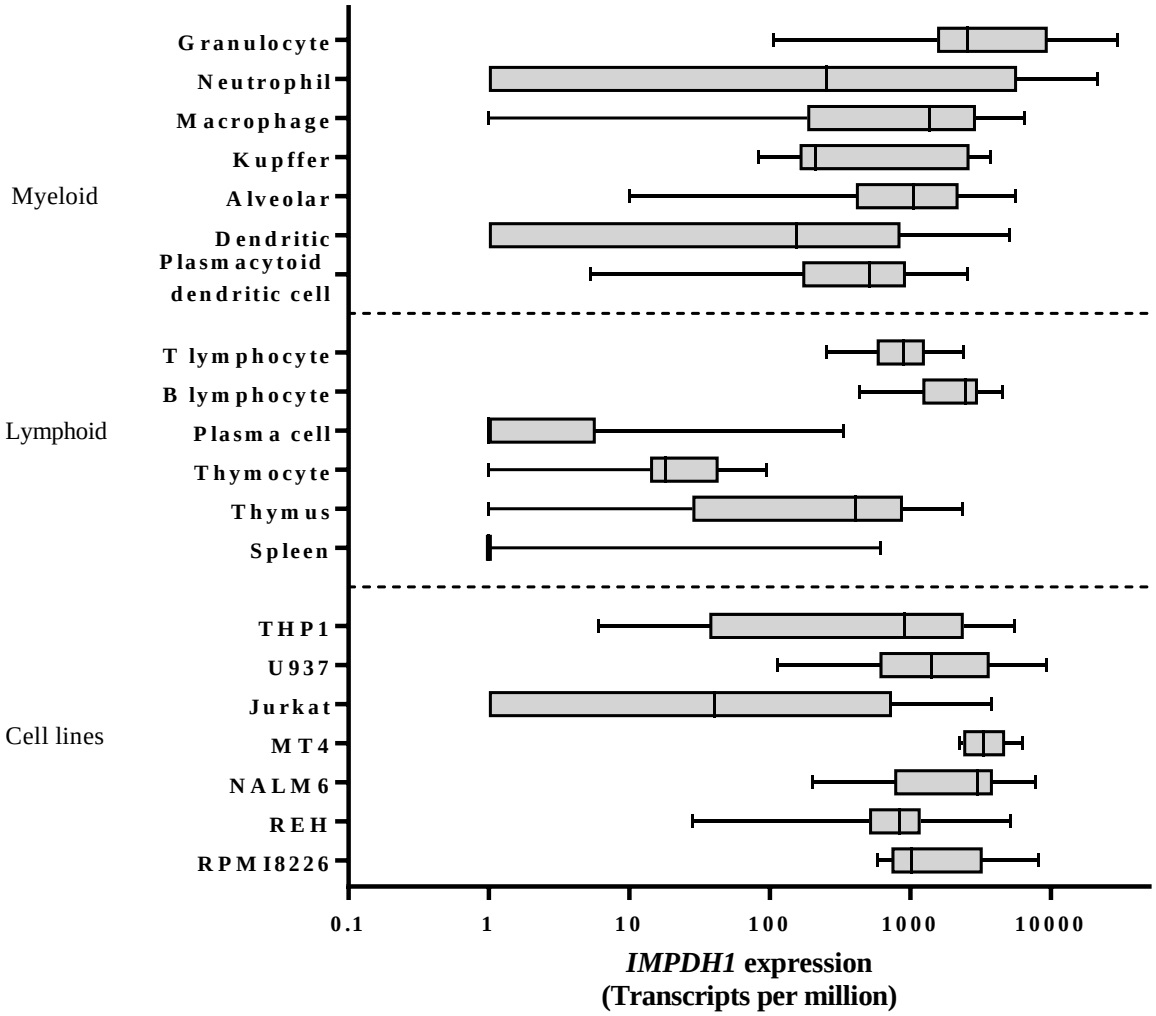

Figure 6-6. The expression of *IMPDH1* in various immune cell types and tissues, as well as myeloid and lymphoid cell lines. Data was extracted from ARCHS[4] and error bars around the box represent the 10th to 90th percentile TPM measured in individual experiments. The line in the box represents the median value measured.

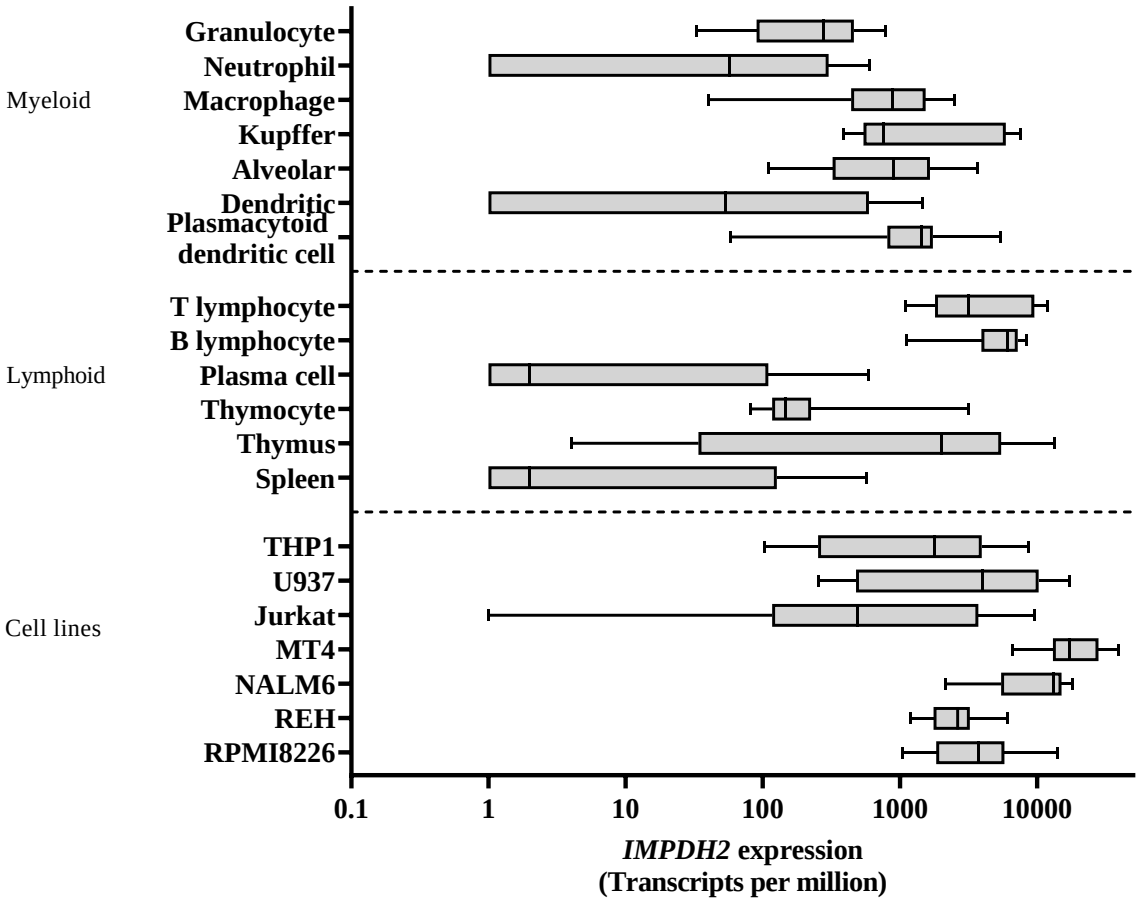

Figure 6-7. The expression of *IMPDH2* in various immune cell types and tissues, as well as myeloid and lymphoid cell lines. Data was extracted from ARCHS[4] and error bars around the box represent the 10th to 90th percentile TPM measured in individual experiments. The line in the box represents the median value measured.

In contrast, *IMPDH2* was most highly expressed in B-lymphocytes (median = 6103 TPM), at more than twice the expression of *IMPDH1*. Conversely, granulocytes expressed almost 10-fold lower *IMPDH2* (median = 278 TPM) than *IMPDH1*. T-lymphocytes had lower *IMPDH2* than granulocytes (median = 3175 TPM) however IMPDH*2* was 3-fold higher compared to *IMPDH1 i*n these T-cells. Plasmacytoid dendritic cells also had high levels of *IMPDH2* (median = 1439 TPM) expression compared to *IMPDH1*, whereas myeloid dendritic cells had lower expression of *IMPDH2* (median = 53 TPM) relative to *IMPDH1*. Macrophages also had lower expression of *IMPDH2* (median = 884 TPM) relative to *IMPDH1*. Both plasma cells and the spleen had very low expression of *IMPDH2* (median values of 2 TPM).

In cell lines, Jurkat again had the lowest *IMPDH2* expression (median and IQR: 492 TPM, 117 – 3730 TPM).

The expression of *IMPDH1* relative to *IMPDH2* are summarised in Table 6-9. In contrast to the data extracted from GTEx, (figure 6-1) the ARCHS[4] data indicates that the spleen expresses minimal *IMPDH1* and *IMPDH2*. However, the high expression of *IMPDH1* relative to *IMPDH2* in whole blood and the higher overall expression of *IMPDH1* in whole blood relative to the spleen in the data extracted from GTEx is also observed in the ARCHS[4] data.

Immune cell types/tissue		**Median *IMPDH1* expression (TPM)**	**Median *IMPDH2* expression (TPM)**	**Ratio of *IMPDH1*:*IMPDH2* expression**
Myeloid	Granulocyte	2566	278	9.23
	Neutrophil	251	57	4.40
	Macrophage	1373	884	1.55
	Kupffer	209	757	0.276
	Alveolar	1048	905.5	1.16
	Dendritic	155	53	2.93
	Plasmacytoid dendritic cell	512.5	1439	0.356
Lymphoid	T lymphocyte	886.5	3175	0.279
	B lymphocyte	2454	6103	0.402
	Plasma cell	0	2	0.00
	Thymocyte	18	147	0.122
Tissue	Thymus	403	2003	0.201
	Spleen	0	2	0.00
Cell lines	THP1	904.5	1795	0.504
	U937	1408	4032	0.349
	Jurkat	40	491.5	0.081
	MT4	3290	17145	0.192
	NALM6	2982	13180	0.226
	REH	841	2636	0.319
	RPMI8226	1018	3707	0.275

Table 6-9. Median *IMPDH1* and *IMPDH2* expression levels (TPM) and ratio of *IMPDH1*:*IMPDH2* expression of immune cell types, tissues and cell lines assessed in ARCHS[4].

6.2.4. Immune tissue expression of *IMPDH1* and *IMPDH2* in HPA

Data were then extracted from the HPA database. This focussed on the mRNA expression data that results in a protein coding transcript. In brief, transcript per million reads were normalised to protein-coding transcripts only. The median values of expression of *IMPDH1* in the immune cells was determined and is shown in Table 6-10.

Neutrophils have the highest *IMPDH1* expression (median = 161 pTPM), followed by the non-classical monocyte (131.8 pTPM), intermediate monocyte (102.8 pTPM), eosinophil (87.2 pTPM) and classical monocyte (82.1 pTPM).

The myeloid dendritic cells have high *IMPDH1* expression (62.3 pTPM) compared to the plasmacytoid dendritic cells (6.8 pTPM). Memory B-cells (13.5 pTPM) and naïve B-cells (8.8 pTPM) have lower *IMPDH1* expression than T-cells. The *IMPDH1* expression levels of T-cells is around 20-30 pTPM, except for naïve $CD4^+$ and $CD8^+$ T-cells, which express lower levels of *IMPDH1* (11.2 and 14.7 pTPM respectively). Total PBMC have a relatively low *IMPDH1* expression (26.1 pTPM).

In contrast, *IMPDH2* expression levels (Table 6-10) are highest in MAIT T-cells (96.1 pTPM), followed by naïve $CD4^+$ T-cells (91.6 pTPM) and natural killer (NK) cells (79.5 pTPM). Interestingly, memory T-cells (65.4 and 58 pTPM) have lower *IMPDH2* expression than naïve T-cells (91.6 and 81 pTPM) whereas naïve B-cells (72 pTPM) have similar *IMPDH2* expression to memory B-cells. Myeloid dendritic cells had similar *IMPDH2* expression (53.3 pTPM) as observed for *IMPDH1*, although plasmacytoid dendritic cells had increased *IMPDH2* expression (42.2 pTPM) compared to *IMPDH1*. Neutrophils (8.9 pTPM) had much lower *IMPDH2* expression than *IMPDH1* (almost 20-fold lower), whilst total PBMC exhibited low levels of *IMPDH2* expression similar to the low *IMPDH1* expression.

Immune cell types/tissues		Protein-coding *IMPDH1* expression (pTPM)	Protein-coding *IMPDH2* expression (pTPM)	Ratio *IMPDH1*:*IMPDH2* expression
	Total PBMC	26.1	23.8	1.10
	Basophil	10.3	17	0.606
	Eosinophil	87.2	10.9	8.00
	NK cell	15.7	79.5	0.197
	Neutrophil	161	8.9	18.1
Myeloid	Classical monocyte	82.1	26.3	3.12
	Non-classical monocyte	131.8	39.6	3.33
	Intermediate monocyte	102.8	45.4	2.26
	Myeloid DC	62.3	53.3	1.17
	Plasmacytoid DC	6.8	42.9	0.159
	Naive $CD4^+$ T-cell	11.2	91.6	0.122
	Naive $CD8^+$ T-cell	14.7	81	0.181
	Memory $CD4^+$ T-cell	20	65.4	0.306
	Memory $CD8^+$ T-cell	24.4	58	0.421
Lymphoid	γδT-cell	29.4	56.3	0.522
	MAIT T-cell	29.1	96.1	0.303
	T_{reg}	22.9	42.9	0.534
	Naive B-cell	8.8	72	0.122
	Memory B-cell	13.5	65.5	0.206
Tissue	Thymus	13.9	159	0.0874
	Spleen	42.8	76.5	0.559

Table 6-10. Protein-coding transcript levels of *IMPDH1* and *IMPDH2* and ratio of protein-coding transcript levels of *IMPDH1:IMPDH2* in individual immune cell types assessed from the HPA database. pTPM = transcripts per million of protein-coding mRNA.

Data from the HPA database indicate that in PBMC, *IMPDH1* is expressed slightly higher at the protein-coding transcript level than *IMPDH2* with a ratio of 1.10. This is consistent with the expression of *IMPDH1* versus *IMPDH2* in whole blood in the GTEx data (ratio of 4.69), but the relative difference in *IMPDH1* and *IMPDH2* expression is larger in GTEx.

The data from the ARCHS[4] and the HPA databases independently indicate several consistent trends but also highlight various differences. Firstly, *IMPDH2* was consistently expressed at lower levels than *IMPDH1* in neutrophils. Secondly, dendritic cells (myeloid and plasmacytoid) displayed similar *IMPDH1:IMPDH2* expression ratios in both HPA (1.17 and

0.159 respectively, ratio 7.36) and ARCHS[4] (2.93 and 0.356 respectively, ratio 8.23). However, contradictory to ARCHS[4], myeloid dendritic cells were observed to have higher *IMPDH1* and *IMPDH2* protein transcript levels than plasmacytoid dendritic cells.

Similar to the data from ARCHS[4], in the HPA dataset, B- and T-cells had higher *IMPDH2* expression than *IMPDH1* expression. However, B-lymphocytes were shown to have a larger ratio of *IMPDH1:IMPDH2* ratio than T-lymphocytes in ARCHS[4], whereas in HPA, T-cells generally had greater *IMPDH1:IMPDH2* expression ratios than B-cells. Interestingly, T-cells were found to have higher protein-coding expression of *IMPDH2* than B-cells in HPA, whereas in ARCHS[4], B-cells expressed twice as much *IMPDH2* mRNA. In both HPA and ARCHS[4], *IMPDH2* was expressed at a higher level than *IMPDH1* in thymus. The protein-coding transcript levels in spleen observed in HPA followed the same trend as in GTEx, with an *IMPDH1:IMPDH2* ratio of 0.559 compared to 0.783 in GTEx.

6.3. Discussion

This exploratory assessment of differential *IMPDH* expression has shown that baseline (MPA-naïve) *IMPDH* expression can vary substantially inter-individually and between tissues. These expression differences could potentially contribute to the variability in response to MPA therapy observed in patients.

The consensus in the literature is that the primary target of MPA therapy is the two isoforms of IMPDH in proliferative lymphocytes. PBMC are predominantly lymphocytes, and these cells are also at high density in the spleen or the thymus (Rowland-Jones & McMichael, 2000). Most studies have used PBMC as a way of measuring IMPDH activity, either as a baseline marker or response parameter, based on the convenience and ease of access to blood sampling.

In GTEx, *IMPDH1* expression in whole blood appears to have substantial variability, with a 150-fold difference across the range of samples (n = 755), compared to a 25-fold difference in *IMPDH2*. This has not been previously reported in the literature, although this finding is consistent with the variability in baseline IMPDH activity observed in patients. Several studies have observed a high interpatient variability in baseline IMPDH activity (40-fold difference) when measured prior to the start of MPA therapy (Kuypers et al., 2008; Schaier et al., 2015; Schütz et al., 1998), which would be due in part to such high variability in *IMPDH1* and *IMPDH2* mRNA expression.

A novel result from the analysis of the GTEx database is the finding of sex-based differences in *IMPDH1* in both whole blood and spleen. This could have important implications for MPA therapy in SLE/LN patients due to the female predominance of the disease (Stojan & Petri, 2018). A previous study demonstrated that female rats were more susceptible to MPA-induced GI toxicity than male rats (Stern et al., 2007), although this was thought to be due to decreased glucuronidation of MPA in the GI tract. Importantly, in whole blood, females express 54%

more *IMPDH1* than males. Whereas in the spleen, *IMPDH1* expression in males was slightly (13%) higher than in females. A higher *IMPDH* mRNA expression in females' whole blood may imply that IMPDH activity in females may be higher. However, IMPDH activity has not been found to significantly differ in PBMC between males and females in children 4 to 16 years old (Sobiak et al., 2022), although no information is available for adults.

Higher baseline IMPDH activity prior to MPA treatment could associate with worse therapeutic outcomes (Glander et al., 2004), since subsequent MPA inhibition of IMPDH may not be sufficient to cause cell cycle arrest. Females who possess higher baseline *IMPDH* expression may also have higher baseline IMPDH activity, potentially predisposing female patients to worse therapeutic outcomes. Higher baseline *IMPDH* expression in females could also imply that *IMPDH1* transcription is greater in females than in males while translation into IMPDH protein could remain similar. Considering the temporal changes in MPA-IMPDH inhibition relationship observed in the previous chapter, this could have further implications. Higher *IMPDH1* gene expression and a higher number of mRNA transcripts could allow a more rapid response to MPA inhibition and faster restoration of IMPDH activity in response to MPA. This may then result in worse therapeutic outcomes for females receiving MPA treatment.

Another key finding was that the most common *IMPDH1* and *IMPDH2* SNP did not associate with their respective gene or splice variant expression in immune tissues. Interestingly, both *IMPDH1* SNP (rs2278293 and rs2278294) were associated with changes in *IMPDH1* expression in tissues of little concern in MPA therapy such as adipose, skin and testis. Of maybe more relevance, due to the known GI toxicity of MPA, is the association of rs2278293 with a slight (13%) increase in *IMPDH1* expression in the mucosa of the oesophagus. However, as was noted above, rs2278293 did not associate with GI toxicity parameters in paediatric heart transplant patients (Ohmann et al., 2010) or any clinical outcome in another study (Gensburger

et al., 2010). Importantly, GI cells do not rely on *de novo* synthesis of purines through IMPDH1 or IMPDH2 (LeLeiko et al., 1983) as they are exposed to purines through diet, implying that the associated increase of *IMPDH1* expression may not influence GI toxicity. Furthermore, GI toxicity from MPA exposure has been suggested to occur either via local exposure to a toxic metabolite of MPA, acyl-MPA-glucuronide or through the release of N-2-hydroxyethyl-morpholine after de-esterification of mycophenolate mofetil, the ester formulation of MPA (Arns, 2007).

Since there was no relevant association of *IMPDH1* and *IMPDH2* mRNA expression changes with the three most common SNP (rs2278293, rs2278294 and rs11706052) in these genes, this suggests that any of the reported associations these SNP may have with therapeutic outcomes is likely to be due to other reasons. This could be catalytic changes to the IMPDH enzyme, changes in efficiency of protein translation or protein stability.

Whilst the functional effects of most SNP in *IMPDH1* and *IMPDH2* have not been characterised, some SNP have been shown to result in lower catalytic activity (Wang et al., 2007; Wu et al., 2010). Although only one SNP (rs2278293) thus far appears to alter catalytic activity through changes in enzymatic structure, other SNP may have effects on post-transcriptional pathways such as altering mRNA stability, protein quantity, or protein degradation. Since the SNP assessed were intronic SNP, it was theorised that they could alter the splicing of the mRNA. However, the lack of associations of the assessed SNP with different splice variants of *IMPDH1* and *IMPDH2* also indicates that these SNP are unlikely to influence splicing of both *IMPDH1* and *IMPDH2* mRNA, further implying that there would be no differences in the translated enzyme from mRNA with these SNP. Thus, it is unlikely that these SNP alter catalytic activity of the enzymes.

These SNP in *IMPDH1* and *IMPDH2* do appear to associate with changes in the expression of other genes which may influence therapeutic outcomes. Interestingly, the SNP in *IMPDH2* was associated with changes in expression of a number of different genes and the proteins these genes encode could have clinically relevant effects. This includes *WDR6*, a protein-coding gene that is involved in cell cycle arrest which has also been found to be differentially expressed in SLE patients (Lyons et al., 2010). An increase in *WDR6* expression could result in an increase in vulnerability to cell cycle arrest and possibly improve therapeutic outcomes. Other genes include, *NCKIPSD*, a gene involved in stress fibre formation but has not been implicated in SLE to date, *RBM6*, which codes for an alternative spliced RNA processing protein and has been found to be decreased in expression in SLE monocytes (Patel, 2008), *UBA7*, which codes for the UBE1L ubiquitin modifier protein, *CCDC36*, which codes for a protein involved with gamete generation, and *CCDC37*, which codes for a protein involved with ciliary movement. These genes have no interaction with SLE or MPA as far as it is known.

In contrast, the two SNP in *IMPDH1* are associated with altered expression of *CICP14* and the *RP11-247B21.x* gene family. These are pseudogenes and are not implicated in any regulatory processes or pathways relevant to MPA therapy or SLE/LN pathogenesis as far as it is known. However, some *RP11-247B21.x* genes are located in close proximity to *IMPDH1* (Figure 6-8), which could explain the effect these SNP have on the expression of this family of genes.

Associations of these *IMPDH1, IMPDH2* SNP (rs2278293, rs2278294 and rs11706052) with increased expression of alternatively spliced variants of other genes may also impact susceptibility to MPA treatment. Importantly, this includes changes to *FAM71F2* and *METTL2B*. These genes are in close proximity to *IMPDH1* as well (Figure 6-8), which could explain the SNP associations with differential expression of splice variants of these genes. Of particular note is the association of the *IMPDH2* SNP with expression of a splice variant of *SLC26A6*. Although there has not been much characterisation of SLC26A6, it is an anion

transporter and could be involved in MPA pharmacokinetic pathways of absorption, distribution, and excretion.

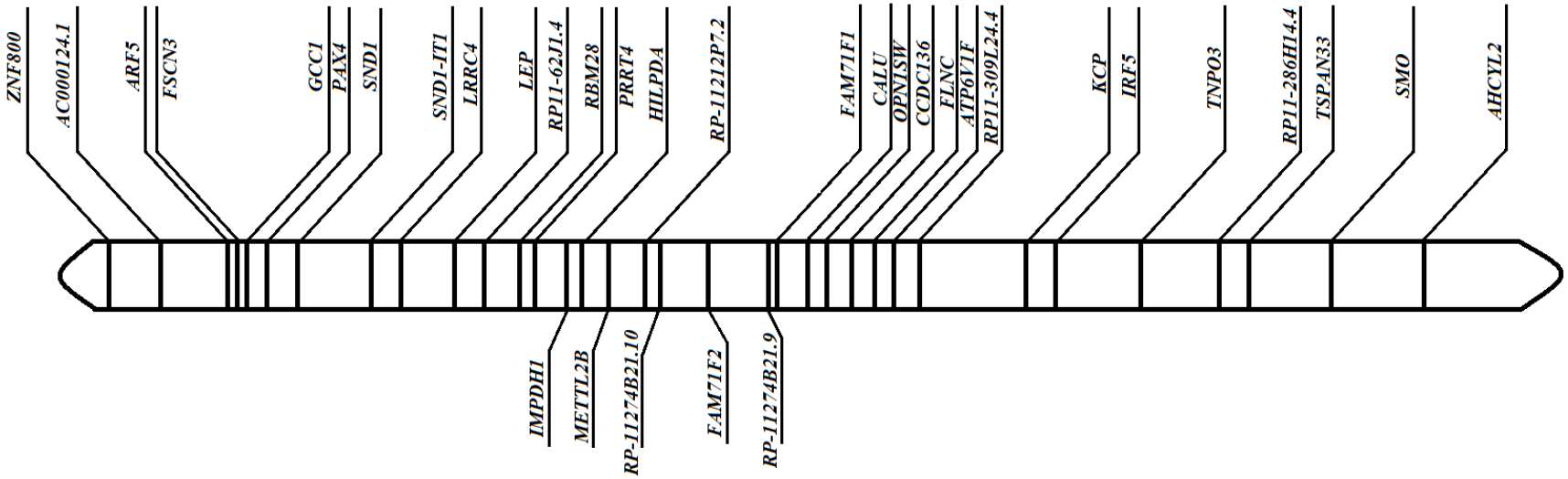

Figure 6-8. The gene map of *IMPDH1* and adjacent genes. The genes of interest are branched downwards, and includes *IMPDH1*, *METTL2B*, *RP-11274B21.10*, *FAM71F2* and *RP-11274B21.9*.

Interestingly, no eQTL were observed with respect to these SNP and the expression of *IMPDH1* and *IMPDH2* in immune tissues. This suggests that at the transcription level, gene expression of *IMPDH* is unaffected by SNP, although no inferences can be made about the functional effects and translational effects of other SNP besides the three assessed. The association of the *IMPDH1* splice variant with several SNP spread throughout the *IMPDH1* gene (and beyond) could also imply a functional or translational change from wild-type IMPDH1, however, more research has to be conducted into this splice variant (intron ID: 128405865:128409756:clu27651) and how it potentially affects catalytic activity and/or translation of IMPDH1.

The three different databases have shown that there are subtle differences in the expression of *IMPDH1* and *IMPDH2* in different immune cell subsets. A common observation that was particularly highlighted in GTEx and ARCHS[4] is the large variability in *IMPDH1* and *IMPDH2* expression, especially in the circulating blood. Whilst it is widely accepted in the literature that IMPDH1 and IMPDH2 have similar enzyme inhibition kinetics with MPA, there is evidence that there may be differences in the response to MPA. It was noted that IMPDH2 had a 4-fold lower k_i than IMPDH1 (Carr et al., 1993), and it was also suggested that IMPDH1 and IMPDH2 may undergo different regulatory processes when assembling macrostructures due to different nucleotide-binding properties (Thomas et al., 2012). Thus, understanding how *IMPDH1* and *IMPDH2* are differentially expressed individually in immune cell subsets may aid in understanding the response to MPA therapy.

Importantly, the data from GTEx and HPA have shown that in whole blood *IMPDH1* is expressed at a higher level than *IMPDH2*, which is consistent with the general assumption in the literature that IMPDH1 is the constitutively expressed housekeeping protein whereas IMPDH2 is induced only when proliferative need for *de novo* purine synthesis arises. In the thymus, there was also consensus from ARCHS[4] and HPA that *IMPDH2* was more highly

expressed than *IMPDH1*. This is consistent with the function of the thymus in the immune system as the regulator of T-cell selection and maturation, along with expansion of T-cell subsets (Thapa & Farber, 2019). This would thus require higher IMPDH activity and hence higher expression driven by *IMPDH2*. Data from both GTEx and HPA also displayed similar ratios of *IMPDH1* to *IMPDH2* expression in the spleen, indicating higher levels of *IMPDH2* than *IMPDH1* expression. The spleen is a secondary lymphoid organ which can also be a site of lymphocyte proliferation (Bronte & Pittet, 2013), which would be again consistent with the higher expression of *IMPDH2* than *IMPDH1*.

In the immune cell subsets, broad trends that persist across both ARCHS[4] and HPA include the consistently high *IMPDH1* expression of granulocytes, including neutrophils and eosinophils. Granulocytes represent the bulk of circulating white blood cells and are terminally differentiated cells. A high *IMPDH1* expression level as opposed to *IMPDH2* could represent the lower requirements for purine synthesis. The dendritic cell subsets, myeloid and plasmacytoid, have also displayed similar *IMPDH1:IMPDH2* ratios across the databases. Interestingly, myeloid dendritic cells expressed higher *IMPDH1* than *IMPDH2* whereas plasmacytoid dendritic cells had the opposite characteristic. It has been noted that MPA can have differential effects on these subsets of dendritic cells, such as the inhibition of STAT4 signalling in myeloid dendritic cells but not in plasmacytoid, and the disruption of type I IFN production in plasmacytoid dendritic cells (Shigesaka et al., 2020). This could be due to different expression profiles of IMPDH isoforms in these subsets.

In comparison to the myeloid lineage, cells of the lymphoid lineage had substantially higher levels of *IMPDH2* relative to *IMPDH1* in both the databases (ARCHS4 and HPA), (mean *IMPDH1:IMPDH2* ratio for myeloid cells is 4.11 vs mean *IMPDH1:IMPDH2* ratio for lymphoid cells is 0.302). This indicates that lymphoid cells generally have a higher *IMPDH2* expression than *IMPDH1* regardless of proliferation status, whereas myeloid cells generally

have higher *IMPDH1* than *IMPDH2* expression. The general consensus within the literature is that IMPDH2 is more abundant in cell types which have high proliferative requirements, and the results observed here are consistent with this.

However, there were also several inconsistencies amongst the databases. First, the spleen was observed to have minimal *IMPDH1* and *IMPDH2* expression in ARCHS[4], in contrast to the data obtained from HPA and GTEx. This could be due to the differences in the datasets used by the databases. Whilst both HPA and GTEx use specifically curated datasets, ARCHS[4] pulls in a large number of user-submitted experiments in the publicly available GEO dataset, which could result in less consistent data. Also, data from HPA did not always corroborate ARCHS[4] data in the hierarchy of *IMPDH* expression amongst the various immune subsets. This could also be due to the use of protein-coding transcript levels in HPA in contrast to total mRNA transcript in ARCHS[4]. Hence the data from HPA may be more robust and more relevant.

There are several limitations in this database assessment of associations with *IMPDH* expression differences. Firstly, the key pharmacodynamic parameter, IMPDH activity, cannot be inferred directly *IMPDH* expression. Further research should be conducted to elucidate the impact differential *IMPDH* expression has on IMPDH activity. Additionally, the assessment of sex-based differences could not be further investigated in different immune cell subsets in GTEx and the other databases do not include sex as a parameter to investigate. Hence this finding requires further independent verification. Whilst there is detailed categorisation of immune cell subpopulations and subsets in ARCHS[4] and HPA, these two datasets do not always corroborate each other (for reasons noted above). Hence in the context of SLE/LN, studies characterising *IMPDH* expression relative to biological sex in all the immune cell subpopulations important for this disease may be useful in the future.

In conclusion, possible sex-based differences in *IMPDH* expression and heterogeneity in immune cell *IMPDH* expression appear to exist. It is not known if this contributes to differences in the response to MPA therapy. Further studies are required to determine if these mRNA expression differences affect IMPDH protein levels and/or IMDPH activity and whether these will in turn affect therapeutic outcomes.

Chapter 7: General Discussion

7.1. Preamble

Immunosuppressive drugs are key for the treatment of the autoimmune disease SLE/LN. The two drugs assessed in this thesis, cyclophosphamide and mycophenolic acid (MPA), are both excellent at suppressing the immune system but do so via different pathways. The novel findings detailed in this thesis demonstrate that there is additional complexity to the mechanisms of action of these drugs at their targets (IMPDH for mycophenolate, and formation of PAM and its interaction with DNA for cyclophosphamide).

In this chapter, the findings from this thesis are discussed in the broader context of the disease and how they could aid in optimising treatment on an individualised basis for better therapeutic outcomes.

7.2. Cyclophosphamide

The observation that lymphocytes and phosphodiesterase enzymes, in particular PDE4B2, can activate 4-OHCP/aldophosphamide into the DNA reactive PAM is an important finding that could further explain the selectivity of cyclophosphamide for this cell type in autoimmune disease. Whilst lymphocyte depletion has been generally accepted as main immunosuppressive mechanism of action of cyclophosphamide (Hurd & Giuliano, 1975), it is currently thought that this is mainly due to the low levels of ALDH in these mature cells compared to the progenitor cells. However, it is becoming increasingly apparent that cyclophosphamide has differential effects on lymphocyte subsets. For example, numerous studies have shown that cyclophosphamide selectively depletes T_{reg} cells when administered in low doses (Lutsiak et al., 2005; Motoyoshi et al., 2006; Noordam et al., 2018; Zhao et al., 2010). Cyclophosphamide is selective for B-cell apoptosis (Hemendinger & Bloom, 1996) when both T- and B-cells were exposed to cyclophosphamide. Such differential effects on the lymphocyte subsets could be due to not only differences in ALDH expression but also differences in the expression/regulation of PDE4B2 and the intracellular formation of PAM.

PDE4B2 is constitutively associated with the CD3ε chain of the T-cell receptor, and upon activation of T-cell receptor signalling, PDE4B is phosphorylated when the CD3ε chain is ligated (Baroja et al., 1999). The release of phosphorylated PDE4B2 is accompanied by a transient increase of cAMP followed by a subsequent decline in cAMP levels. Whilst the authors were not able to determine the functional significance of the phosphorylation of PDE4B2, they hypothesised that tyrosine phosphorylation of PDE4B2 could induce a conformational change in the enzyme, thereby increasing its stability, leading to an effective increase in phosphodiesterase activity and degradation of cAMP. This may suggest that there is an additional mechanism of selectivity of cyclophosphamide for activated T-cells. Following

activation of T-cells via T-cell receptor signalling, the increase in PDE4B2 activity would increase the conversion of 4-OHCP to PAM and hence result in increased cytotoxicity in activated T-cells. cAMP is also a key regulator of T_{reg} function (Klein et al., 2012) and whilst it is unclear whether this subtype of lymphocytes over-express PDE4B, competitive inhibition of this enzyme by 4-OHCP/aldophosphamide could decrease cAMP degradation and hence be an additional mechanism by which cyclophosphamide has immunosuppressive effects in autoimmune disease.

Inter-individual variability in response to cyclophosphamide could also arise from differences in PDE4B2 expression. Genetic polymorphisms in PDE-encoding genes have not been investigated thoroughly, but in recent years, there has been emerging research on the associations of SNP with various diseases or therapeutic response (M. E. Gurney, 2019; Yee et al., 2019). Interestingly, in patients with diffuse large B-cell lymphoma treated with cyclophosphamide, increased expression of *PDE4B* in the tumours was associated with poorer therapeutic outcomes (Shipp et al., 2002). The work in this thesis would suggest that this higher expression should lead to a more selective and increased activation of 4-OHCP/aldophosphamide in these tumour cells and a better therapeutic response. However, the authors hypothesised that higher expression of *PDE4B* could lead to decreased cAMP levels, limiting protein kinase A signalling and increasing proliferation, cytokine release and chemotaxis. The elevated proliferation rate in these neoplastic cells could outweigh the increased selective activation in the cells.

The increased susceptibility to the DNA damage following exposure to PAM observed in LN patients from the REPAIR study is also another attribute that should be considered in the context of inter-individual differences in response to cyclophosphamide in SLE/LN patients. DNA-adduct formation is the mechanism of action of cyclophosphamide and the pharmacodynamic measurement of therapeutic response to cyclophosphamide using this

measure has not been thoroughly investigated. Some studies have reported surrogate measures for DNA-alkylation and cytotoxicity such as the relationship between cyclophosphamide exposure (AUC of plasma concentration curves) and neutropenic toxicity (neutrophil counts), (Ahmed et al., 2020; Joerger et al., 2007). These studies found associations between the two measures and concluded that cyclophosphamide plasma concentration could be a useful parameter to include in models to predict effectiveness and/or toxicity of cyclophosphamide therapy. However, using cyclophosphamide exposure as a surrogate measure of effect does not take into account a) the conversion of the prodrug via hepatic CYP enzymes into 4-OHCP/aldophopshamide, b) the catalytic conversion of aldophosphamide into PAM by phosphodiesterases and c) the differences in the repair of the DNA adducts of PAM. The data from the REPAIR study suggests that there was a non-normal distribution of formation of PAM-induced DNA adducts in the LN patients compared to the normal distribution observed in the healthy individuals. This suggests that there may be individuals who are extremely sensitive to cyclophosphamide. This thesis has not investigated the role of differences in specific DNA-adduct repair processes in this extreme sensitivity. These studies were undertaken in unstimulated PBMC which contains mostly lymphocytes and some monocytes. Hence the differences in DNA-adduct formation (measured by PCR-block) are not likely to be due to DNA repair that occurs during mitosis (such as double strand break repair/homologous recombination) and is more likely to be due to differences in transcription-coupled nucleotide excision repair or possibly base-excision repair processes. Germline variants in nucleotide excision repair proteins, such as ERRC2 and ERRC3, are relatively common and these could be assessed in future studies to further interrogate which patients are very sensitive to cyclophosphamide. However, a simple method, which is agnostic to the cause of slower DNA-repair in each individual, such as the PCR block assay could be used to pre-screen patients and

to prioritise use of cyclophosphamide rather than mycophenolate in those that are most sensitive to the drug.

A notable difference between the healthy individuals and LN patients was the higher Pasifika (25%) and Asian (37.5%) demographic in the LN patient population. The higher incidence of SLE and LN in Pasifika (almost 3-fold higher), Māori and Asian (1.5 fold higher) as compared to those of European descent is well established (Lao et al., 2023). Importantly, Māori and Pasifika have worse health outcomes than other ethnicities in New Zealand (Disney et al., 2017) and early prediction/screening of susceptibility to cyclophosphamide could aid close monitoring of therapeutic response and/or excessive toxicity particularly in these populations, improving health outcomes.

7.3. MPA

This thesis has found a novel observation in that, following prolonged MPA exposure, there was a time-dependent decline in the ability of MPA to inhibit IMPDH activity in Jurkat cells. The mechanism for this has not been investigated in this thesis, but this could be an important way in which proliferating immune cells can resist MPA-induced depletion of purines and cell death. due to. One possible mechanism for this upregulation of IMPDH activity, even in the presence of high concentrations of MPA, is the allosteric effect of formation of IMPDH filaments.

IMPDH enzyme is a tetramer and IMPDH filaments are helical polymers formed from stacked octamers of IMPDH. These filaments are formed through dimerization of the Bateman domains of IMPDH tetramers (Fernández-Justel, et al., 2019). The formation of IMPDH filaments stabilises the 'flat' conformation of the octamers (which is seen when ATP/ADP binds to the Bateman domains) but does not inhibit the 'bowed' (when GTP/GDP binds) conformation (Anthony et al., 2017; Johnson & Kollman, 2020). Some studies suggest that IMPDH filaments possess similar catalytic activity to unassembled IMPDH enzymes (Anthony et al., 2017; Fernández-Justel et al., 2019). However, others suggest that IMPDH filaments consist of both catalytically active and inactive enzymes (Anthony et al., 2017) suggesting that these filaments could serve to quickly modulate IMPDH function by facilitating transitions between active and inactive conformations throughout the filaments.

Another function that IMPDH filament formation seems to serve is to decrease the sensitivity to allosteric inhibition by guanine nucleotides (Johnson & Kollman, 2020). The differences in the "flat" versus "bowed" form, alters the affinity for guanine nucleotides hence increasing the enzyme activity. Future studies should investigate whether filament formation and conformational changes also effect the ability of MPA to inhibit this enzyme.

Whilst there is consensus in the literature that IMPDH filament assembly acts as a general sensor of the increased need for guanine nucleotides, the mechanism by which the filaments form is not well-researched. To date, only one study has been conducted to elucidate the signalling mechanisms for filament formation. Duong-Ly et al. (2018) hypothesised that filament assembly would be triggered by early biochemical changes in T-cell activation, specifically through the mTOR pathway and the STIM1 pathway. The mTOR pathway plays a central role in T-cell activation and integrates immune signals to effect various metabolic changes necessary for expansion (Chi, 2012). The STIM1 pathway is upstream of the mTOR pathway and in response to Ca^{2+} release from the endoplasmic reticulum mediates the expression of crucial genes such as nuclear factor of activated T-cells (*NFAT*) and also cytokines (Desvignes et al., 2015). The knockout of *STIM1* was found to decrease IMPDH filament formation in mouse splenic T-cells, disproportionate to the decrease in IMPDH expression observed. Furthermore, treatment of splenic T-cells with mTOR inhibitors such as rapamycin resulted in disassembly of IMPDH filaments. These observations suggest that the STIM1 and mTOR pathways that are essential in T-cell activation may be part of the mechanism through which IMPDH filaments form. This suggests that the effect of MPA on changes in IMPDH filament formation in activated immune cells could be an important focus of further research in lupus therapy.

Thus, the time-dependent decrease in sensitivity of IMPDH to MPA inhibition within cells relative to the formation of filaments should be investigated. However, filament formation has not been extensively researched *in vivo*, and it is not known whether the effect of MPA on IMPDH activity displays the same properties in PBMC as in Jurkat cells. This future work could help determine if there is a role of IMPDH filament formation in MPA resistance in some SLE/LN patients.

Interestingly, database analysis of IMPDH expression suggested that females intrinsically express higher levels of *IMPDH1* compared to males in whole blood but lower levels than males in spleen. Along with the unclear therapeutic implications of higher *IMPDH1* expression and/or IMPDH activity, these findings also pose further questions in the context of IMPDH filaments formation, namely whether higher *IMPDH1* expression affect IMPDH1 filament formation, structure and conformation. Recent research has shown that IMPDH1 forms filaments with similar properties to IMPDH2, albeit with a few notable differences (Burrell et al., 2022). When bound with GTP, the IMPDH1 filament was demonstrated to have different points of contact between monomers compared to IMPDH2. These different points of contact allow a more bent tetramer structure, in turn increasing the inhibitory capacity of GTP on IMPDH1. Furthermore, N-terminal extension of IMPDH1 stabilised the active, compressed form of the filament whilst a C-terminal extension had the opposite effect. Whether these conformational differences affect MPA-inhibition in IMPDH1 filaments is unknown.

Interestingly, the association of various SNP in *IMPDH1* with altered expression of an IMPDH1 splice variant could have implications for IMPDH1 filament formation. This splice variant has an intron not normally included at the 5' end of the mRNA, which may cause an extension in the N-terminal of the polypeptide chain. Thus, higher expression of this splice variant may then stabilise the active form of the IMPDH1 filament, increasing IMPDH1 activity. An individual with these SNP could theoretically have increased IMPDH1 activity, whether this would influence the therapeutic effect of MPA is not known.

The finding that there is substantial variation in *IMPDH1* and *IMPDH2* expression in different immune cell types could have therapeutic implications in MPA treatment. Whilst MPA has been thought to target mainly lymphocytes, effects on other immune cells have also been observed. For example, in dendritic cell subsets, MPA was shown to interfere with the nuclear translocation of interferon regulatory factor 7, a transcription factor that is crucial to type 1 IFN

production, decreasing IFN production by plasmacytoid dendritic cells (Shigesaka et al., 2020). The decrease in IL-17 produced by T-cells as a result of inhibition of T-cell proliferation is also hypothesised to decrease granulopoiesis and cause neutropenia (von Vietinghoff et al., 2010). However, not much research has been conducted on whether the effects of MPA treatment on the different immune cell types are mediated through IMPDH inhibition. Although it is important to note that different immune cells may have different dependencies on the *de novo* purine synthesis pathway, which may further influence the effect of MPA on these cells. Thus, more research needs to be conducted on the impact of varying *IMPDH* expression in different immune cell types and the effect of MPA on these cells.

7.4. Conclusion

In summary, it is not currently known which patients will most benefit from cyclophosphamide or MPA, and biomarkers which could help stratify patients for each therapy would be clinically useful in SLE/LN.

In cyclophosphamide therapy, in addition to the well characterised inherited differences in the initial CYP catalysed hepatic bioactivation of this prodrug, the activation of 4-OHCP into the cytotoxic metabolite PAM via phosphodiesterases, such as PDE4B2, could vary between individuals and in different subsets of immune cells. Once PAM is formed, differences in the amount of DNA-adduct produced and repaired may further influence which patients are most susceptible to the therapeutic effects of cyclophosphamide. These factors should be further assessed *in vivo* to examine the impact this may have on response to cyclophosphamide.

In the context of MPA therapy, inter-patient differences in the uptake of MPA into immune cells is unlikely to be the limiting factor in terms of therapeutic outcomes, since uptake transport was rapid and concentrations achieved within cells were well above the concentrations which inhibit the enzyme. However, the time-dependent loss of IMPDH inhibition suggests that additional regulatory changes occur. Investigation of whether in this time-dependent rebound in IMPDH activity in the presence of MPA occurs in patients is required, since inter-individual differences in this process could account for the poor therapeutic response in some SLE/LN patients.

References

Abramson, S. B., Given, W. P., Edelson, H. S., & Weissmann, G. (1983). Neutrophil aggregation induced by sera from patients with active systemic lupus erythematosus. *Arthritis and Rheumatism*, *26*(5), 630–636. https://doi.org/10.1002/art.1780260509

Afsar, N. A., Ufer, M., Haenisch, S., Remmler, C., Mateen, A., Usman, A., Ahmed, K. Z., Ahmad, H. R., & Cascorbi, I. (2012). Relationship of drug metabolizing enzyme genotype to plasma levels as well as myelotoxicity of cyclophosphamide in breast cancer patients. *European Journal of Clinical Pharmacology*, *68*(4), 389–395. https://doi.org/10.1007/s00228-011-1134-0

Ahmed, J. H., Makonnen, E., Bisaso, R. K., Mukonzo, J. K., Fotoohi, A., Aseffa, A., Howe, R., Hassan, M., & Aklillu, E. (2020). Population Pharmacokinetic, Pharmacogenetic, and Pharmacodynamic Analysis of Cyclophosphamide in Ethiopian Breast Cancer Patients. *Frontiers in Pharmacology*, *11*. https://www.frontiersin.org/articles/10.3389/fphar.2020.00406

Al-Awadhi, A. M., Haider, M. Z., Sukumaran, J., & Balakrishnan, S. (2018). High prevalence of protein tyrosine phosphatase non-receptor N22 gene functional variant R620W in systemic lupus erythematosus patients from Kuwait: Implications for disease susceptibility. *BMC Rheumatology*, *2*(1), 7. https://doi.org/10.1186/s41927-018-0015-x

Alexander, T., Sattler, A., Templin, L., Kohler, S., Groß, C., Meisel, A., Sawitzki, B., Burmester, G.-R., Arnold, R., Radbruch, A., Thiel, A., & Hiepe, F. (2013). Foxp3+ Helios+ regulatory T cells are expanded in active systemic lupus erythematosus. *Annals of the Rheumatic Diseases*, *72*(9), 1549–1558. https://doi.org/10.1136/annrheumdis-2012-202216

Allison, A. C., & Eugui, E. M. (1993). The design and development of an immunosuppressive drug, mycophenolate mofetil. *Springer Seminars in Immunopathology*, *14*(4), 353–380. https://doi.org/10.1007/BF00192309

Allison, A. C., Hovi, T., Watts, R. W., & Webster, A. D. (1977). The role of de novo purine synthesis in lymphocyte transformation. *Ciba Foundation Symposium*, *48*, 207–224. https://doi.org/10.1002/9780470720301.ch13

Anthony, S. A., Burrell, A. L., Johnson, M. C., Duong-Ly, K. C., Kuo, Y.-M., Simonet, J. C., Michener, P., Andrews, A., Kollman, J. M., & Peterson, J. R. (2017). Reconstituted IMPDH polymers accommodate both catalytically active and inactive conformations. *Molecular Biology of the Cell*, *28*(20), 2600–2608. https://doi.org/10.1091/mbc.e17-04-0263

Anthony, S., Peterson, J. R., & Ji, Y. (2017). Use of Inosine Monophosphate Dehydrogenase Activity Assay to Determine the Specificity of PARP-1 Inhibitors. *Methods in Molecular Biology (Clifton, N.J.)*, *1608*, 337–342. https://doi.org/10.1007/978-1-4939-6993-7_22

ANZDATA Registry, 42nd Report, Chapter 7: Transplantation. (2019). Australia and New Zealand Dialysis and Transplant Registry, Adelaide, Australia. http://www.anzdata.org.au

Appel, G. B., Contreras, G., Dooley, M. A., Ginzler, E. M., Isenberg, D., Jayne, D., Li, L.-S., Mysler, E., Sánchez-Guerrero, J., Solomons, N., & Wofsy, D. (2009). Mycophenolate Mofetil versus Cyclophosphamide for Induction Treatment of Lupus Nephritis. *Journal of the*

American Society of Nephrology, *20*(5), 1103–1112. https://doi.org/10.1681/ASN.2008101028

Arns, W. (2007). Noninfectious Gastrointestinal (GI) Complications of Mycophenolic Acid Therapy: A Consequence of Local GI Toxicity? *Transplantation Proceedings*, *39*(1), 88–93. https://doi.org/10.1016/j.transproceed.2006.10.189

Ataya, K. M., Pydyn, E. F., & Ramahi-Ataya, A. J. (1990). The effect of "activated" cyclophosphamide on human and rat ovarian granulosa cells in vitro. *Reproductive Toxicology*, *4*(2), 121–125. https://doi.org/10.1016/0890-6238(90)90006-H

Audemard-Verger, A., Martin Silva, N., Verstuyft, C., Costedoat-Chalumeau, N., Hummel, A., Le Guern, V., Sacré, K., Meyer, O., Daugas, E., Goujard, C., Sultan, A., Lobbedez, T., Galicier, L., Pourrat, J., Le Hello, C., Godin, M., Morello, R., Lambert, M., Hachulla, E., … Bienvenu, B. (2016). Glutathione S Transferases Polymorphisms Are Independent Prognostic Factors in Lupus Nephritis Treated with Cyclophosphamide. *PLoS ONE*, *11*(3). https://doi.org/10.1371/journal.pone.0151696

Azevedo, M. F., Faucz, F. R., Bimpaki, E., Horvath, A., Levy, I., de Alexandre, R. B., Ahmad, F., Manganiello, V., & Stratakis, C. A. (2014). Clinical and molecular genetics of the phosphodiesterases (PDEs). *Endocrine Reviews*, *35*(2), 195–233. https://doi.org/10.1210/er.2013-1053

Bachanova, V., Shanley, R., Malik, F., Chauhan, L., Lamba, V., Weisdorf, D. J., Burns, L. J., & Lamba, J. K. (2015). Cytochrome P450 2B6*5 Increases Relapse after Cyclophosphamide-containing Conditioning and Autologous Transplantation for Lymphoma. *Biology of Blood and Marrow Transplantation : Journal of the American Society for Blood and Marrow Transplantation*, *21*(5), 944–948. https://doi.org/10.1016/j.bbmt.2015.02.001

Baroja, M. L., Cieslinski, L. B., Torphy, T. J., Wange, R. L., & Madrenas, J. (1999). Specific CD3ε Association of a Phosphodiesterase 4B Isoform Determines Its Selective Tyrosine Phosphorylation After CD3 Ligation1. *The Journal of Immunology*, *162*(4), 2016–2023. https://doi.org/10.4049/jimmunol.162.4.2016

Bastian, H. M., Roseman, J. M., McGwin, G., Alarcón, G. S., Friedman, A. W., Fessler, B. J., Baethge, B. A., Reveille, J. D., & LUMINA Study Group. LUpus in MInority populations: NAture vs nurture. (2002). Systemic lupus erythematosus in three ethnic groups. XII. Risk factors for lupus nephritis after diagnosis. *Lupus*, *11*(3), 152–160. https://doi.org/10.1191/0961203302lu158oa

Bauer, G. B., & Povirk, L. F. (1997). Specificity and kinetics of interstrand and intrastrand bifunctional alkylation by nitrogen mustards at a G-G-C sequence. *Nucleic Acids Research*, *25*(6), 1211–1218.

Beighlie, D. J., & Teplitz, R. L. (1975). Repair of UV damaged DNA in systemic lupus erythematosus. *The Journal of Rheumatology*, *2*(2), 149–160.

Bemer, M. J., Risler, L. J., Phillips, B. R., Wang, J., Storer, B. E., Sandmaier, B. M., Duan, H., Raccor, B. S., Boeckh, M. J., & McCune, J. S. (2014). Recipient pretransplant inosine monophosphate dehydrogenase activity in nonmyeloablative hematopoietic cell transplantation. *Biology of Blood and Marrow Transplantation: Journal of the American*

Society for Blood and Marrow Transplantation, *20*(10), 1544–1552. https://doi.org/10.1016/j.bbmt.2014.05.032

Berd, D., & Mastrangelo, M. J. (1988). Effect of Low Dose Cyclophosphamide on the Immune System of Cancer Patients: Depletion of CD4+, 2H4+ Suppressor-inducer T-Cells. *Cancer Research*, *48*(6), 1671–1675.

Bernard, O., & Guillemette, C. (2004). The Main Role of Ugt1a9 in the Hepatic Metabolism of Mycophenolic Acid and the Effects of Naturally Occurring Variants. *Drug Metabolism and Disposition*, *32*(8), 775–778. https://doi.org/10.1124/dmd.32.8.775

Besaratinia, A., Caliri, A. W., & Tommasi, S. (2021). Hydroxychloroquine induces oxidative DNA damage and mutation in mammalian cells. *DNA Repair*, *106*, 103180. https://doi.org/10.1016/j.dnarep.2021.103180

Bielicki, L., Voelcker, G., & Hohorst, H. J. (1983). Enzymatic toxicogenation of "activated" cyclophosphamide by 3'-5' exonucleases. *Journal of Cancer Research and Clinical Oncology*, *105*(1), 27–29.

Bielicki, L., Voelcker, G., & Hohorst, H. J. (1984). Activated cyclophosphamide: An enzyme-mechanism-based suicide inactivator of DNA polymerase/3′–5′ exonuclease. *Journal of Cancer Research and Clinical Oncology*, *107*(3), 195–198. https://doi.org/10.1007/BF01032606

Bijl, M., Horst, G., Limburg, P. C., & Kallenberg, C. G. M. (2001). Anti-CD3-induced and anti-Fas-induced apoptosis in systemic lupus erythematosus (SLE). *Clinical and Experimental Immunology*, *123*(1), 127–132. https://doi.org/10.1046/j.1365-2249.2001.01418.x

Bischoff, E. (2004). Potency, selectivity, and consequences of nonselectivity of PDE inhibition. *International Journal of Impotence Research*, *16 Suppl 1*, S11-14. https://doi.org/10.1038/sj.ijir.3901208

Bonelli, M., Savitskaya, A., von Dalwigk, K., Steiner, C. W., Aletaha, D., Smolen, J. S., & Scheinecker, C. (2008). Quantitative and qualitative deficiencies of regulatory T cells in patients with systemic lupus erythematosus (SLE). *International Immunology*, *20*(7), 861–868. https://doi.org/10.1093/intimm/dxn044

Borch, R. F., & Millard, J. A. (1987). The mechanism of activation of 4-hydroxycyclophosphamide. *Journal of Medicinal Chemistry*, *30*(2), 427–431. https://doi.org/10.1021/jm00385a029

Bottini, N., Vang, T., Cucca, F., & Mustelin, T. (2006). Role of PTPN22 in type 1 diabetes and other autoimmune diseases. *Seminars in Immunology*, *18*(4), 207–213. https://doi.org/10.1016/j.smim.2006.03.008

Botton, M. R., Whirl-Carrillo, M., Del Tredici, A. L., Sangkuhl, K., Cavallari, L. H., Agúndez, J. A. G., Duconge, J., Lee, M. T. M., Woodahl, E. L., Claudio-Campos, K., Daly, A. K., Klein, T. E., Pratt, V. M., Scott, S. A., & Gaedigk, A. (2021). PharmVar GeneFocus: CYP2C19. *Clinical Pharmacology and Therapeutics*, *109*(2), 352–366. https://doi.org/10.1002/cpt.1973

Brandes, M., Willimann, K., & Moser, B. (2005). Professional antigen-presentation function by human gammadelta T Cells. *Science (New York, N.Y.)*, *309*(5732), 264–268. https://doi.org/10.1126/science.1110267

Brandt, L., & Hedberg, H. (1969). Impaired phagocytosis by peripheral blood granulocytes in systemic lupus erythematosus. *Scandinavian Journal of Haematology*, *6*(5), 348–353. https://doi.org/10.1111/j.1600-0609.1969.tb02420.x

Bray, J., Sludden, J., Griffin, M. J., Cole, M., Verrill, M., Jamieson, D., & Boddy, A. V. (2010). Influence of pharmacogenetics on response and toxicity in breast cancer patients treated with doxorubicin and cyclophosphamide. *British Journal of Cancer*, *102*(6), 1003–1009. https://doi.org/10.1038/sj.bjc.6605587

Bremer, S., Vethe, N. T., Rootwelt, H., & Bergan, S. (2009). Expression of IMPDH1 is regulated in response to mycophenolate concentration. *International Immunopharmacology*, *9*(2), 173–180. https://doi.org/10.1016/j.intimp.2008.10.017

Brieba, L. G. (2008). Template dependent human DNA polymerases. *Current Topics in Medicinal Chemistry*, *8*(15), 1312–1326. https://doi.org/10.2174/156802608786141098

Brinkmann, V., Reichard, U., Goosmann, C., Fauler, B., Uhlemann, Y., Weiss, D. S., Weinrauch, Y., & Zychlinsky, A. (2004). Neutrophil extracellular traps kill bacteria. *Science (New York, N.Y.)*, *303*(5663), 1532–1535. https://doi.org/10.1126/science.1092385

Brock, N., & Wilmanns, H. (1958). [Effect of a cyclic nitrogen mustard-phosphamidester on experimentally induced tumors in rats; chemotherapeutic effect and pharmacological properties of B 518 ASTA]. *Deutsche Medizinische Wochenschrift (1946)*, *83*(12), 453–458. https://doi.org/10.1055/s-0028-1114243

Bronte, V., & Pittet, M. J. (2013). The spleen in local and systemic regulation of immunity. *Immunity*, *39*(5), 806–818. https://doi.org/10.1016/j.immuni.2013.10.010

Buey, R. M., Fernández-Justel, D., Marcos-Alcalde, Í., Winter, G., Gómez-Puertas, P., de Pereda, J. M., & Luis Revuelta, J. (2017). A nucleotide-controlled conformational switch modulates the activity of eukaryotic IMP dehydrogenases. *Scientific Reports*, *7*(1), Article 1. https://doi.org/10.1038/s41598-017-02805-x

Buey, R. M., Ledesma-Amaro, R., Velázquez-Campoy, A., Balsera, M., Chagoyen, M., de Pereda, J. M., & Revuelta, J. L. (2015). Guanine nucleotide binding to the Bateman domain mediates the allosteric inhibition of eukaryotic IMP dehydrogenases. *Nature Communications*, *6*, 8923. https://doi.org/10.1038/ncomms9923

Bullingham, R. E. S., Nicholls, A. J., & Kamm, B. R. (1998). Clinical Pharmacokinetics of Mycophenolate Mofetil. *Clinical Pharmacokinetics*, *34*(6), 429–455. https://doi.org/10.2165/00003088-199834060-00002

Bullingham, R., Monroe, S., Nicholls, A., & Hale, M. (1996). Pharmacokinetics and bioavailability of mycophenolate mofetil in healthy subjects after single-dose oral and intravenous administration. *Journal of Clinical Pharmacology*, *36*(4), 315–324. https://doi.org/10.1002/j.1552-4604.1996.tb04207.x

Burrell, A. L., Nie, C., Said, M., Simonet, J. C., Fernández-Justel, D., Johnson, M. C., Quispe, J., Buey, R. M., Peterson, J. R., & Kollman, J. M. (2022). IMPDH1 retinal variants control filament architecture to tune allosteric regulation. *Nature Structural & Molecular Biology*, *29*(1), 47–58. https://doi.org/10.1038/s41594-021-00706-2

Buyon, J. P., Shadick, N., Berkman, R., Hopkins, P., Dalton, J., Weissmann, G., Winchester, R., & Abramson, S. B. (1988). Surface expression of gp165/95, the complement receptor CR3, as a marker of disease activity in systemic lupus erythematosus. *Clinical Immunology and Immunopathology*, *46*(1), 141–149. https://doi.org/10.1016/0090-1229(88)90014-1

Büyüknacar, H. S., Kumcu, E. K., Göçmen, C., & Onder, S. (2008). Effect of phosphodiesterase type 4 inhibitor rolipram on cyclophosphamide-induced cystitis in rats. *European Journal of Pharmacology*, *586*(1–3), 293–299. https://doi.org/10.1016/j.ejphar.2008.02.022

Cadet, J., Douki, T., Ravanat, J.-L., & Mascio, P. D. (2009). Sensitized formation of oxidatively generated damage to cellular DNA by UVA radiation. *Photochemical & Photobiological Sciences*, *8*(7), 903–911. https://doi.org/10.1039/B905343N

Cai, Y., Wu, M. H., Ludeman, S. M., Grdina, D. J., & Dolan, M. E. (1999). Role of O6-alkylguanine-DNA alkyltransferase in protecting against cyclophosphamide-induced toxicity and mutagenicity. *Cancer Research*, *59*(13), 3059–3063.

Calise, S. J., Abboud, G., Kasahara, H., Morel, L., & Chan, E. K. L. (2018). Immune Response-Dependent Assembly of IMP Dehydrogenase Filaments. *Frontiers in Immunology*, *9*, 2789. https://doi.org/10.3389/fimmu.2018.02789

Calise, S. J., & Chan, E. K. L. (2020). Anti-rods/rings autoantibody and IMPDH filaments: An update after fifteen years of discovery. *Autoimmunity Reviews*, *19*(10), 102643. https://doi.org/10.1016/j.autrev.2020.102643

Camici, M., Allegrini, S., & Tozzi, M. G. (2018). Interplay between adenylate metabolizing enzymes and AMP-activated protein kinase. *The FEBS Journal*, *285*(18), 3337–3352. https://doi.org/10.1111/febs.14508

Carr, S. F., Papp, E., Wu, J. C., & Natsumeda, Y. (1993). Characterization of human type I and type II IMP dehydrogenases. *The Journal of Biological Chemistry*, *268*(36), 27286–27290.

Carreño, L. J., Pacheco, R., Gutierrez, M. A., Jacobelli, S., & Kalergis, A. M. (2009). Disease activity in systemic lupus erythematosus is associated with an altered expression of low-affinity Fcγ receptors and costimulatory molecules on dendritic cells. *Immunology*, *128*(3), 334–341. https://doi.org/10.1111/j.1365-2567.2009.03138.x

Cartin-Ceba, R., Indrakanti, D., Specks, U., Stone, J. H., Hoffman, G. S., Kallenberg, C. G. M., Langford, C. A., Merkel, P. A., Spiera, R. F., Monach, P. A., St Clair, E. W., Seo, P., Tchao, N. K., Ytterberg, S. R., Brunetta, P. G., Song, H., Birmingham, D., Rovin, B. H., & RAVE-Immune Tolerance Network Research Group. (2017). The Pharmacogenomic Association of Fcγ Receptors and Cytochrome P450 Enzymes With Response to Rituximab or Cyclophosphamide Treatment in Antineutrophil Cytoplasmic Antibody-Associated

Vasculitis. *Arthritis & Rheumatology (Hoboken, N.J.)*, *69*(1), 169–175. https://doi.org/10.1002/art.39822

Cerboni, B., Morozzi, G., Galeazzi, M., Bellisai, F., Micheli, V., Pompucci, G., & Sestini, S. (2009). Poly(ADP-ribose) polymerase activity in systemic lupus erythematosus and systemic sclerosis. *Human Immunology*, *70*(7), 487–491. https://doi.org/10.1016/j.humimm.2009.04.021

Chaigne-Delalande, B., Guidicelli, G., Couzi, L., Merville, P., Mahfouf, W., Bouchet, S., Molimard, M., Pinson, B., Moreau, J.-F., & Legembre, P. (2008). The Immunosuppressor Mycophenolic Acid Kills Activated Lymphocytes by Inducing a Nonclassical Actin-Dependent Necrotic Signal. *The Journal of Immunology*, *181*(11), 7630–7638. https://doi.org/10.4049/jimmunol.181.11.7630

Chan, V. S.-F., Nie, Y.-J., Shen, N., Yan, S., Mok, M.-Y., & Lau, C.-S. (2012). Distinct roles of myeloid and plasmacytoid dendritic cells in systemic lupus erythematosus. *Autoimmunity Reviews*, *11*(12), 890–897. https://doi.org/10.1016/j.autrev.2012.03.004

Chang, A., Henderson, S. G., Brandt, D., Liu, N., Guttikonda, R., Hsieh, C., Kaverina, N., Utset, T. O., Meehan, S. M., Quigg, R. J., Meffre, E., & Clark, M. R. (2011). In situ B cell-mediated immune responses and tubulointerstitial inflammation in human lupus nephritis. *Journal of Immunology (Baltimore, Md. : 1950)*, *186*(3), 1849–1860. https://doi.org/10.4049/jimmunol.1001983

Chang, T. K., Yu, L., Goldstein, J. A., & Waxman, D. J. (1997). Identification of the polymorphically expressed CYP2C19 and the wild-type CYP2C9-ILE359 allele as low-Km catalysts of cyclophosphamide and ifosfamide activation. *Pharmacogenetics*, *7*(3), 211–221.

Chariyavilaskul, P., Phaisal, W., Kittanamongkolchai, W., Rukrung, C., Anutrakulchai, S., & Avihingsanon, Y. (2022). Pharmacokinetics and pharmacodynamics profiles of enteric-coated mycophenolate sodium in female patients with difficult-to-treat lupus nephritis. *Clinical and Translational Science*, *15*(7), 1776–1786. https://doi.org/10.1111/cts.13295

Chernoff, N., Rogers, J. M., Alles, A. J., Zucker, R. M., Elstein, K. H., Massaro, E. J., & Sulik, K. K. (1989). Cell cycle alterations and cell death in cyclophosphamide teratogenesis. *Teratogenesis, Carcinogenesis, and Mutagenesis*, *9*(4), 199–209. https://doi.org/10.1002/tcm.1770090403

Chi, H. (2012). Regulation and function of mTOR signalling in T cell fate decision. *Nature Reviews. Immunology*, *12*(5), 325–338. https://doi.org/10.1038/nri3198

Chiarelli, L. R., Molinaro, M., Libetta, C., Tinelli, C., Cosmai, L., Valentini, G., Canton, A. D., & Regazzi, M. (2010). Inosine monophosphate dehydrogenase variability in renal transplant patients on long-term mycophenolate mofetil therapy. *British Journal of Clinical Pharmacology*, *69*(1), 38–50. https://doi.org/10.1111/j.1365-2125.2009.03542.x

Chiba, A., Tamura, N., Yoshikiyo, K., Murayama, G., Kitagaichi, M., Yamaji, K., Takasaki, Y., & Miyake, S. (2017). Activation status of mucosal-associated invariant T cells reflects disease activity and pathology of systemic lupus erythematosus. *Arthritis Research & Therapy*, *19*(1), 58. https://doi.org/10.1186/s13075-017-1257-5

Choi, J., Kim, S. T., & Craft, J. (2012). The Pathogenesis of Systemic Lupus Erythematosus – An Update. *Current Opinion in Immunology*, *24*(6), 651–657. https://doi.org/10.1016/j.coi.2012.10.004

Chung, S. A., & Criswell, L. A. (2007). PTPN22: Its role in SLE and autoimmunity. *Autoimmunity*, *40*(8), 582–590. https://doi.org/10.1080/08916930701510848

Cilião, H. L., Camargo-Godoy, R. B. O., Souza, M. F. de, Zanuto, A., Delfino, V. D. A., & Cólus, I. M. de S. (2018). Polymorphisms in IMPDH2, UGT2B7, and CES2 genes influence the risk of graft rejection in kidney transplant recipients taking mycophenolate mofetil. *Mutation Research/Genetic Toxicology and Environmental Mutagenesis*, *836*, 97–102. https://doi.org/10.1016/j.mrgentox.2018.06.008

Cleaver, J. E. (1968). Defective Repair Replication of DNA in Xeroderma Pigmentosum. *Nature*, *218*(5142), Article 5142. https://doi.org/10.1038/218652a0

Colby, T. D., Vanderveen, K., Strickler, M. D., Markham, G. D., & Goldstein, B. M. (1999). Crystal structure of human type II inosine monophosphate dehydrogenase: Implications for ligand binding and drug design. *Proceedings of the National Academy of Sciences of the United States of America*, *96*(7), 3531–3536.

Colvin, M., Brundrett, R. B., Kan, M.-N. N., Jardine, I., & Fenselau, C. (1976). Alkylating Properties of Phosphoramide Mustard. *Cancer Research*, *36*(3), 1121–1126.

Comte, D., Karampetsou, M. P., Yoshida, N., Kis-Toth, K., Kyttaris, V. C., & Tsokos, G. C. (2017). SLAMF7 engagement restores defective effector CD8+ T cells activity in response to foreign antigens in systemic lupus erythematosus. *Arthritis & Rheumatology (Hoboken, N.J.)*, *69*(5), 1035–1044. https://doi.org/10.1002/art.40038

Contreras, G., Pardo, V., Leclercq, B., Lenz, O., Tozman, E., O'Nan, P., & Roth, D. (2004). Sequential Therapies for Proliferative Lupus Nephritis. *New England Journal of Medicine*, *350*(10), 971–980. https://doi.org/10.1056/NEJMoa031855

Corbett, A. J., Eckle, S. B. G., Birkinshaw, R. W., Liu, L., Patel, O., Mahony, J., Chen, Z., Reantragoon, R., Meehan, B., Cao, H., Williamson, N. A., Strugnell, R. A., Van Sinderen, D., Mak, J. Y. W., Fairlie, D. P., Kjer-Nielsen, L., Rossjohn, J., & McCluskey, J. (2014). T-cell activation by transitory neo-antigens derived from distinct microbial pathways. *Nature*, *509*(7500), Article 7500. https://doi.org/10.1038/nature13160

Craft, J. E. (2012). Follicular helper T cells in immunity and systemic autoimmunity. *Nature Reviews. Rheumatology*, *8*(6), 337–347. https://doi.org/10.1038/nrrheum.2012.58

Crook, T. R., Souhami, R. L., & McLean, A. E. M. (1986). Cytotoxicity, DNA Cross-Linking, and Single Strand Breaks Induced by Activated Cyclophosphamide and Acrolein in Human Leukemia Cells. *Cancer Research*, *46*(10), 5029–5034.

Cushnir, J. R., Naylor, S., Lamb, J. H., Farmer, P. B., Brown, N. A., & Mirkes, P. E. (1990). Identification of phosphoramide mustard/DNA adducts using tandem mass spectrometry. *Rapid Communications in Mass Spectrometry*, *4*(10), 410–414. https://doi.org/10.1002/rcm.1290041014

Davies, R. C., Pettijohn, K., Fike, F., Wang, J., Nahas, S. A., Tunuguntla, R., Hu, H., Gatti, R. A., & McCurdy, D. (2012). Defective DNA double-strand break repair in pediatric systemic lupus erythematosus. *Arthritis and Rheumatism*, *64*(2), 568–578. https://doi.org/10.1002/art.33334

de Boo, L. W., Vulink, A. J. E., & Bos, M. E. M. M. (2017). Metronomic cyclophosphamide-induced long-term remission after recurrent high-grade serous ovarian cancer: A case study. *Molecular and Clinical Oncology*, *7*(6), 1130–1134. https://doi.org/10.3892/mco.2017.1457

de Jonge, M. E., Huitema, A. D. R., Rodenhuis, S., & Beijnen, J. H. (2005). Clinical Pharmacokinetics of Cyclophosphamide. *Clinical Pharmacokinetics*, *44*(11), 1135–1164. https://doi.org/10.2165/00003088-200544110-00003

de Jonge, M. E., Huitema, A. D. R., van Dam, S. M., Rodenhuis, S., & Beijnen, J. H. (2005). Population Pharmacokinetics of Cyclophosphamide and Its Metabolites 4-Hydroxycyclophosphamide, 2-Dechloroethylcyclophosphamide, and Phosphoramide Mustard in a High-Dose Combination With Thiotepa and Carboplatin. *Therapeutic Drug Monitoring*, *27*(6), 756. https://doi.org/10.1097/01.ftd.0000177224.19294.92

de Oliveira, L. C., de Melo Bisneto, A. V., Puga, S. C., Fernandes, A. S., Véras, J. H., Cardoso, C. G., Ribeiro E Silva, C., Carneiro, C. C., & Chen-Chen, L. (2021). Prednisone is genotoxic in mice and Drosophila melanogaster. *Mutation Research. Genetic Toxicology and Environmental Mutagenesis*, *865*, 503334. https://doi.org/10.1016/j.mrgentox.2021.503334

Desta, Z., El-Boraie, A., Gong, L., Somogyi, A. A., Lauschke, V. M., Dandara, C., Klein, K., Miller, N. A., Klein, T. E., Tyndale, R. F., Whirl-Carrillo, M., & Gaedigk, A. (2021). PharmVar GeneFocus: CYP2B6. *Clinical Pharmacology and Therapeutics*, *110*(1), 82–97. https://doi.org/10.1002/cpt.2166

Desvignes, L., Weidinger, C., Shaw, P., Vaeth, M., Ribierre, T., Liu, M., Fergus, T., Kozhaya, L., McVoy, L., Unutmaz, D., Ernst, J. D., & Feske, S. (2015). STIM1 controls T cell–mediated immune regulation and inflammation in chronic infection. *The Journal of Clinical Investigation*, *125*(6), 2347–2362. https://doi.org/10.1172/JCI80273

Devyatko, E., Dunkler, D., Bohdjalian, A., Zuckermann, A., Grimm, M., Muehlbacher, F., & Weigel, G. (2008). Lymphocyte activation and correlation with IMPDH activity under therapy with mycophenolate mofetil. *Clinica Chimica Acta*, *394*(1), 67–71. https://doi.org/10.1016/j.cca.2008.04.006

Dirven, H. A. A. M., Ommen, B. van, & Bladeren, P. J. van. (1994). Involvement of Human Glutathione S-Transferase Isoenzymes in the Conjugation of Cyclophosphamide Metabolites with Glutathione. *Cancer Research*, *54*(23), 6215–6220.

Disney, G., Teng, A., Atkinson, J., Wilson, N., & Blakely, T. (2017). Changing ethnic inequalities in mortality in New Zealand over 30 years: Linked cohort studies with 68.9 million person-years of follow-up. *Population Health Metrics*, *15*(1), 15. https://doi.org/10.1186/s12963-017-0132-6

Dom, Z. I. M., Coller, J. K., Carroll, R. P., Tuke, J., McWhinney, B. C., Somogyi, A. A., & Sallustio, B. C. (2018). Mycophenolic acid concentrations in peripheral blood mononuclear

cells are associated with the incidence of rejection in renal transplant recipients. *British Journal of Clinical Pharmacology*, *84*(10), 2433–2442. https://doi.org/10.1111/bcp.13704

Domeyer, B. E., & Sladek, N. E. (1980). Metabolism of 4-hydroxycyclophosphamide/aldophosphamide in vitro. *Biochemical Pharmacology*, *29*(21), 2903–2912. https://doi.org/10.1016/0006-2952(80)90035-0

Duong-Ly, K. C., Kuo, Y.-M., Johnson, M. C., Cote, J. M., Kollman, J. M., Soboloff, J., Rall, G. F., Andrews, A. J., & Peterson, J. R. (2018). T cell activation triggers reversible inosine-5′-monophosphate dehydrogenase assembly. *Journal of Cell Science*, *131*(17), jcs223289. https://doi.org/10.1242/jcs.223289

Dusseaux, M., Martin, E., Serriari, N., Péguillet, I., Premel, V., Louis, D., Milder, M., Le Bourhis, L., Soudais, C., Treiner, E., & Lantz, O. (2011). Human MAIT cells are xenobiotic-resistant, tissue-targeted, CD161hi IL-17-secreting T cells. *Blood*, *117*(4), 1250–1259. https://doi.org/10.1182/blood-2010-08-303339

Ekhart, C., Doodeman, V. D., Rodenhuis, S., Smits, P. H. M., Beijnen, J. H., & Huitema, A. D. R. (2008). Influence of polymorphisms of drug metabolizing enzymes (CYP2B6, CYP2C9, CYP2C19, CYP3A4, CYP3A5, GSTA1, GSTP1, ALDH1A1 and ALDH3A1) on the pharmacokinetics of cyclophosphamide and 4-hydroxycyclophosphamide. *Pharmacogenetics and Genomics*, *18*(6), 515. https://doi.org/10.1097/FPC.0b013e3282fc9766

Ekhart, C., Rodenhuis, S., Smits, P. H. M., Beijnen, J. H., & Huitema, A. D. R. (2008). Relations between polymorphisms in drug-metabolising enzymes and toxicity of chemotherapy with cyclophosphamide, thiotepa and carboplatin. *Pharmacogenetics and Genomics*, *18*(11), 1009. https://doi.org/10.1097/FPC.0b013e328313aaa4

Elkon, K. B., & Wiedeman, A. (2012). Type I IFN system in the development and manifestations of SLE. *Current Opinion in Rheumatology*, *24*(5), 499–505. https://doi.org/10.1097/BOR.0b013e3283562c3e

Emadi, A., Jones, R. J., & Brodsky, R. A. (2009). Cyclophosphamide and cancer: Golden anniversary. *Nature Reviews Clinical Oncology*, *6*(11), 638–647. https://doi.org/10.1038/nrclinonc.2009.146

Engels, C., Schwab, C., Zhang, J., Stevens, M. J. A., Bieri, C., Ebert, M.-O., McNeill, K., Sturla, S. J., & Lacroix, C. (2016). Acrolein contributes strongly to antimicrobial and heterocyclic amine transformation activities of reuterin. *Scientific Reports*, *6*(1), 36246. https://doi.org/10.1038/srep36246

Episkopou, H., Kyrtopoulos, S. A., Sfikakis, P. P., Fousteri, M., Dimopoulos, M. A., Mullenders, L. H. F., & Souliotis, V. L. (2009). Association between transcriptional activity, local chromatin structure, and the efficiencies of both subpathways of nucleotide excision repair of melphalan adducts. *Cancer Research*, *69*(10), 4424–4433. https://doi.org/10.1158/0008-5472.CAN-08-3489

Erickson, L. C., Ramonas, L. M., Zaharko, D. S., & Kohn, K. W. (1980). Cytotoxicity and DNA cross-linking activity of 4-sulfidocyclophosphamides in mouse leukemia cells in vitro. *Cancer Research*, *40*(11), 4216–4220.

Fairbanks, L. D., Bofill, M., Ruckemann, K., & Simmonds, H. A. (1995). Importance of Ribonucleotide Availability to Proliferating T-lymphocytes from Healthy Humans: DISPROPORTIONATE EXPANSION OF PYRIMIDINE POOLS AND CONTRASTING EFFECTS OF DE NOVO SYNTHESIS INHIBITORS (∗). *Journal of Biological Chemistry*, *270*(50), 29682–29689. https://doi.org/10.1074/jbc.270.50.29682

Fanouriakis, A., Kostopoulou, M., Alunno, A., Aringer, M., Bajema, I., Boletis, J. N., Cervera, R., Doria, A., Gordon, C., Govoni, M., Houssiau, F., Jayne, D., Kouloumas, M., Kuhn, A., Larsen, J. L., Lerstrøm, K., Moroni, G., Mosca, M., Schneider, M., … Boumpas, D. T. (2019). 2019 update of the EULAR recommendations for the management of systemic lupus erythematosus. *Annals of the Rheumatic Diseases*, *78*(6), 736–745. https://doi.org/10.1136/annrheumdis-2019-215089

Feng, Y.-L., Xiang, J.-F., Liu, S.-C., Guo, T., Yan, G.-F., Feng, Y., Kong, N., Li, H.-D., Huang, Y., Lin, H., Cai, X.-J., & Xie, A.-Y. (2017). H2AX facilitates classical non-homologous end joining at the expense of limited nucleotide loss at repair junctions. *Nucleic Acids Research*, *45*(18), 10614. https://doi.org/10.1093/nar/gkx715

Fernández-Justel, D., Núñez, R., Martín-Benito, J., Jimeno, D., González-López, A., Soriano, E. M., Revuelta, J. L., & Buey, R. M. (2019). A Nucleotide-Dependent Conformational Switch Controls the Polymerization of Human IMP Dehydrogenases to Modulate their Catalytic Activity. *Journal of Molecular Biology*, *431*(5), 956–969. https://doi.org/10.1016/j.jmb.2019.01.020

Fernández-Justel, D., Peláez, R., Revuelta, J. L., & Buey, R. M. (2019). The Bateman domain of IMP dehydrogenase is a binding target for dinucleoside polyphosphates. *Journal of Biological Chemistry*, *294*(40), 14768–14775. https://doi.org/10.1074/jbc.AC119.010055

Fleer, R., & Brendel, M. (1982). Toxicity, interstrand cross-links and DNA fragmentation induced by “activated” cyclophosphamide in yeast: Comparative studies on 4-hydroperoxy-cyclophosphamide, its monofunctional analogon, acrolein, phosphoramide mustard, and nor-nitrogen mustard. *Chemico-Biological Interactions*, *39*(1), 1–15. https://doi.org/10.1016/0009-2797(82)90002-3

Fransen, J. H., van der Vlag, J., Ruben, J., Adema, G. J., Berden, J. H., & Hilbrands, L. B. (2010). The role of dendritic cells in the pathogenesis of systemic lupus erythematosus. *Arthritis Research & Therapy*, *12*(2), 207. https://doi.org/10.1186/ar2966

Frey, M. W., Nossal, N. G., Capson, T. L., & Benkovic, S. J. (1993). Construction and characterization of a bacteriophage T4 DNA polymerase deficient in 3’—>5’ exonuclease activity. *Proceedings of the National Academy of Sciences of the United States of America*, *90*(7), 2579–2583.

Friedberg, E. C., Walker, G. C., Siede, W., & Wood, R. D. (2005). *DNA Repair and Mutagenesis*. American Society for Microbiology Press.

Friedman, O. M., & Seligman, A. M. (1954). Preparation of N-Phosphorylated Derivatives of Bis-β-chloroethylamine1a. *Journal of the American Chemical Society*, *76*(3), 655–658. https://doi.org/10.1021/ja01632a006

Fujiyama, N., Miura, M., Kato, S., Sone, T., Isobe, M., & Satoh, S. (2010). Involvement of carboxylesterase 1 and 2 in the hydrolysis of mycophenolate mofetil. *Drug Metabolism and Disposition: The Biological Fate of Chemicals*, *38*(12), 2210–2217. https://doi.org/10.1124/dmd.110.034249

Fukuda, T., Goebel, J., Thøgersen, H., Maseck, D., Cox, S., Logan, B., Sherbotie, J., Seikaly, M., & Vinks, A. A. (2011). Inosine Monophosphate Dehydrogenase (IMPDH) Activity as a Pharmacodynamic Biomarker of Mycophenolic Acid Effects in Pediatric Kidney Transplant Recipients. *The Journal of Clinical Pharmacology*, *51*(3), 309–320. https://doi.org/10.1177/0091270010368542

Futer, O., Sintchak, M. D., Caron, P. R., Nimmesgern, E., DeCenzo, M. T., Livingston, D. J., & Raybuck, S. A. (2002). A mutational analysis of the active site of human type II inosine 5'-monophosphate dehydrogenase. *Biochimica Et Biophysica Acta*, *1594*(1), 27–39. https://doi.org/10.1016/s0167-4838(01)00277-1

Gaipl, U. S., Munoz, L. E., Grossmayer, G., Lauber, K., Franz, S., Sarter, K., Voll, R. E., Winkler, T., Kuhn, A., Kalden, J., Kern, P., & Herrmann, M. (2007). Clearance deficiency and systemic lupus erythematosus (SLE). *Journal of Autoimmunity*, *28*(2), 114–121. https://doi.org/10.1016/j.jaut.2007.02.005

Gaston, R. S., Kaplan, B., Shah, T., Cibrik, D., Shaw, L. M., Angelis, M., Mulgaonkar, S., Meier-Kriesche, H.-U., Patel, D., & Bloom, R. D. (2009). Fixed- or controlled-dose mycophenolate mofetil with standard- or reduced-dose calcineurin inhibitors: The Opticept trial. *American Journal of Transplantation: Official Journal of the American Society of Transplantation and the American Society of Transplant Surgeons*, *9*(7), 1607–1619. https://doi.org/10.1111/j.1600-6143.2009.02668.x

Gaudin, D., Guthrie, L., & Yielding, K. L. (1974). DNA Repair Inhibition: A New Mechanism of Action of Steroids with Possible Implications for Tumor Therapy. *Proceedings of the Society for Experimental Biology and Medicine*, *146*(2), 401–405. https://doi.org/10.3181/00379727-146-38114

Gensburger, O., Picard, N., & Marquet, P. (2009). Effect of Mycophenolate Acyl-Glucuronide on Human Recombinant Type 2 Inosine Monophosphate Dehydrogenase. *Clinical Chemistry*, *55*(5), 986–993. https://doi.org/10.1373/clinchem.2008.113936

Gensburger, O., Van Schaik, R. H. N., Picard, N., Le Meur, Y., Rousseau, A., Woillard, J.-B., Van Gelder, T., & Marquet, P. (2010). Polymorphisms in type I and II inosine monophosphate dehydrogenase genes and association with clinical outcome in patients on mycophenolate mofetil. *Pharmacogenetics and Genomics*, *20*(9), 537–543. https://doi.org/10.1097/FPC.0b013e32833d8cf5

Ginzler, E. M., Dooley, M. A., Aranow, C., Kim, M. Y., Buyon, J., Merrill, J. T., Petri, M., Gilkeson, G. S., Wallace, D. J., Weisman, M. H., & Appel, G. B. (2005). Mycophenolate mofetil or intravenous cyclophosphamide for lupus nephritis. *The New England Journal of Medicine*, *353*(21), 2219–2228. https://doi.org/10.1056/NEJMoa043731

Girard, P. M., Francesconi, S., Pozzebon, M., Graindorge, D., Rochette, P., Drouin, R., & Sage, E. (2011). UVA-induced damage to DNA and proteins: Directversusindirect

photochemical processes. *Journal of Physics: Conference Series*, *261*, 012002. https://doi.org/10.1088/1742-6596/261/1/012002

Giraud, C., Manceau, S., & Treluyer, J.-M. (2010). ABC transporters in human lymphocytes: Expression, activity and role, modulating factors and consequences for antiretroviral therapies. *Expert Opinion on Drug Metabolism & Toxicology*, *6*(5), 571–589. https://doi.org/10.1517/17425251003601953

Glander, P., Hambach, P., Braun, K.-P., Fritsche, L., Giessing, M., Mai, I., Einecke, G., Waiser, J., Neumayer, H.-H., & Budde, K. (2004). Pre-transplant inosine monophosphate dehydrogenase activity is associated with clinical outcome after renal transplantation. *American Journal of Transplantation: Official Journal of the American Society of Transplantation and the American Society of Transplant Surgeons*, *4*(12), 2045–2051. https://doi.org/10.1111/j.1600-6143.2004.00617.x

Glander, P., Sombogaard, F., Budde, K., van Gelder, T., Hambach, P., Liefeldt, L., Lorkowski, C., Mai, M., Neumayer, H. H., Vulto, A. G., & Mathot, R. A. (2009). Improved assay for the nonradioactive determination of inosine 5'-monophosphate dehydrogenase activity in peripheral blood mononuclear cells. *Therapeutic Drug Monitoring*, *31*(3), 351–359. https://doi.org/10.1097/FTD.0b013e31819c3f3d

Glander, P., Sommerer, C., Arns, W., Ariatabar, T., Kramer, S., Vogel, E.-M., Shipkova, M., Fischer, W., Zeier, M., & Budde, K. (2010). Pharmacokinetics and Pharmacodynamics of Intensified versus Standard Dosing of Mycophenolate Sodium in Renal Transplant Patients. *Clinical Journal of the American Society of Nephrology*, *5*(3), 503–511. https://doi.org/10.2215/CJN.06050809

Glavas, N. A., Ostenson, C., Schaefer, J. B., Vasta, V., & Beavo, J. A. (2001). T cell activation up-regulates cyclic nucleotide phosphodiesterases 8A1 and 7A3. *Proceedings of the National Academy of Sciences*, *98*(11), 6319–6324. https://doi.org/10.1073/pnas.101131098

Gollapalli, D. R., MacPherson, I. S., Liechti, G., Gorla, S. K., Goldberg, J. B., & Hedstrom, L. (2010). Structural Determinants of Inhibitor Selectivity in Prokaryotic IMP Dehydrogenases. *Chemistry & Biology*, *17*(10), 1084–1091. https://doi.org/10.1016/j.chembiol.2010.07.014

Good-Jacobson, K. L., Szumilas, C. G., Chen, L., Sharpe, A. H., Tomayko, M. M., & Shlomchik, M. J. (2010). PD-1 regulates germinal center B cell survival and the formation and affinity of long-lived plasma cells. *Nature Immunology*, *11*(6), 535–542. https://doi.org/10.1038/ni.1877

Gor, P. P., Su, H. I., Gray, R. J., Gimotty, P. A., Horn, M., Aplenc, R., Vaughan, W. P., Tallman, M. S., Rebbeck, T. R., & DeMichele, A. (2010). Cyclophosphamide- metabolizing enzyme polymorphisms and survival outcomes after adjuvant chemotherapy for node-positive breast cancer: A retrospective cohort study. *Breast Cancer Research : BCR*, *12*(3), R26. https://doi.org/10.1186/bcr2570

Grinyó, J. M., Ekberg, H., Mamelok, R. D., Oppenheimer, F., Sánchez-Plumed, J., Gentil, M. A., Hernandez, D., Kuypers, D. R., & Brunet, M. (2009). The pharmacokinetics of mycophenolate mofetil in renal transplant recipients receiving standard-dose or low-dose

cyclosporine, low-dose tacrolimus or low-dose sirolimus: The Symphony pharmacokinetic substudy. *Nephrology Dialysis Transplantation*, *24*(7), 2269–2276. https://doi.org/10.1093/ndt/gfp162

Groehler, 4th A., Villalta, P. W., Campbell, C., & Tretyakova, N. (2016). Covalent DNA-Protein Cross-Linking by Phosphoramide Mustard and Nornitrogen Mustard in Human Cells. *Chemical Research in Toxicology*, *29*(2), 190–202. https://doi.org/10.1021/acs.chemrestox.5b00430

Gurney, J., Stanley, J., & Sarfati, D. (2020). The inequity of morbidity: Disparities in the prevalence of morbidity between ethnic groups in New Zealand. *Journal of Comorbidity*, *10*, 2235042X20971168. https://doi.org/10.1177/2235042X20971168

Gurney, M. E. (2019). Genetic Association of Phosphodiesterases With Human Cognitive Performance. *Frontiers in Molecular Neuroscience*, *12*. https://www.frontiersin.org/articles/10.3389/fnmol.2019.00022

Hager, P. W., Collart, F. R., Huberman, E., & Mitchell, B. S. (1995). Recombinant human inosine monophosphate dehydrogenase type I and type II proteins. Purification and characterization of inhibitor binding. *Biochemical Pharmacology*, *49*(9), 1323–1329. https://doi.org/10.1016/0006-2952(95)00026-v

Hakkim, A., Fürnrohr, B. G., Amann, K., Laube, B., Abed, U. A., Brinkmann, V., Herrmann, M., Voll, R. E., & Zychlinsky, A. (2010). Impairment of neutrophil extracellular trap degradation is associated with lupus nephritis. *Proceedings of the National Academy of Sciences of the United States of America*, *107*(21), 9813–9818. https://doi.org/10.1073/pnas.0909927107

Hale, M. D., Nicholls, A. J., Bullingham, R. E., Hené, R., Hoitsma, A., Squifflet, J. P., Weimar, W., Vanrenterghem, Y., Van de Woude, F. J., & Verpooten, G. A. (1998). The pharmacokinetic-pharmacodynamic relationship for mycophenolate mofetil in renal transplantation. *Clinical Pharmacology and Therapeutics*, *64*(6), 672–683. https://doi.org/10.1016/S0009-9236(98)90058-3

Haroun, F., Al-Shaar, L., Habib, R. H., El-Saghir, N., Tfayli, A., Bazarbachi, A., Salem, Z., Shamseddine, A., Taher, A., Cascorbi, I., & Zgheib, N. K. (2015). Effects of CYP2B6 genetic polymorphisms in patients receiving cyclophosphamide combination chemotherapy for breast cancer. *Cancer Chemotherapy and Pharmacology*, *75*(1), 207–214. https://doi.org/10.1007/s00280-014-2632-4

Harris, G., Asbery, L., Lawley, P. D., Denman, A. M., & Hylton, W. (1982). Defective repair of 0(6)-methylguanine in autoimmune diseases. *Lancet (London, England)*, *2*(8305), 952–956. https://doi.org/10.1016/s0140-6736(82)90159-3

Hedstrom, L. (2009). IMP Dehydrogenase: Structure, Mechanism, and Inhibition. *Chemical Reviews*, *109*(7), 2903–2928. https://doi.org/10.1021/cr900021w

Helsby, N. A., Hui, C.-Y., Goldthorpe, M. A., Coller, J. K., Soh, M. C., Gow, P. J., de Zoysa, J. Z., & Tingle, M. D. (2010). The combined impact of CYP2C19 and CYP2B6 pharmacogenetics on cyclophosphamide bioactivation. *British Journal of Clinical Pharmacology*, *70*(6), 844–853. https://doi.org/10.1111/j.1365-2125.2010.03789.x

Helsby, N. A., Yong, M., van Kan, M., de Zoysa, J. R., & Burns, K. E. (2019). The importance of both CYP2C19 and CYP2B6 germline variations in cyclophosphamide pharmacokinetics and clinical outcomes. *British Journal of Clinical Pharmacology*, *85*(9), 1925–1934. https://doi.org/10.1111/bcp.14031

Hemendinger, R. A., & Bloom, S. E. (1996). Selective mitomycin C and cyclophosphamide induction of apoptosis in differentiating B lymphocytes compared to T lymphocytes in vivo. *Immunopharmacology*, *35*(1), 71–82. https://doi.org/10.1016/0162-3109(96)00124-5

Hemminki, K. (1987). DNA-binding products of nornitrogen mustard, a metabolite of cyclophosphamide. *Chemico-Biological Interactions*, *61*(1), 75–88. https://doi.org/10.1016/0009-2797(87)90020-2

Herrmann, M., Voll, R. E., Zoller, O. M., Hagenhofer, M., Ponner, B. B., & Kalden, J. R. (1998). Impaired phagocytosis of apoptotic cell material by monocyte-derived macrophages from patients with systemic lupus erythematosus. *Arthritis & Rheumatism*, *41*(7), 1241–1250. https://doi.org/10.1002/1529-0131(199807)41:7<1241::AID-ART15>3.0.CO;2-H

Heylmann, D., Bauer, M., Becker, H., Gool, S. van, Bacher, N., Steinbrink, K., & Kaina, B. (2013). Human CD4+CD25+ Regulatory T Cells Are Sensitive to Low Dose Cyclophosphamide: Implications for the Immune Response. *PLOS ONE*, *8*(12), e83384. https://doi.org/10.1371/journal.pone.0083384

Hilton, J. (1984). Role of Aldehyde Dehydrogenase in Cyclophosphamide-resistant L1210 Leukemia. *Cancer Research*, *44*(11), 5156–5160.

Hirayama, A. V., Gauthier, J., Hay, K. A., Voutsinas, J. M., Wu, Q., Gooley, T., Li, D., Cherian, S., Chen, X., Pender, B. S., Hawkins, R. M., Vakil, A., Steinmetz, R. N., Acharya, U. H., Cassaday, R. D., Chapuis, A. G., Dhawale, T. M., Hendrie, P. C., Kiem, H.-P., … Turtle, C. J. (2019). The response to lymphodepletion impacts PFS in patients with aggressive non-Hodgkin lymphoma treated with CD19 CAR T cells. *Blood*, *133*(17), 1876–1887. https://doi.org/10.1182/blood-2018-11-887067

Hom, G., Graham, R. R., Modrek, B., Taylor, K. E., Ortmann, W., Garnier, S., Lee, A. T., Chung, S. A., Ferreira, R. C., Pant, P. V. K., Ballinger, D. G., Kosoy, R., Demirci, F. Y., Kamboh, M. I., Kao, A. H., Tian, C., Gunnarsson, I., Bengtsson, A. A., Rantapää-Dahlqvist, S., … Behrens, T. W. (2008). Association of systemic lupus erythematosus with C8orf13-BLK and ITGAM-ITGAX. *The New England Journal of Medicine*, *358*(9), 900–909. https://doi.org/10.1056/NEJMoa0707865

Houssiau, F. A., Vasconcelos, C., D'Cruz, D., Sebastiani, G. D., Garrido Ed, E. de R., Danieli, M. G., Abramovicz, D., Blockmans, D., Mathieu, A., Direskeneli, H., Galeazzi, M., Gül, A., Levy, Y., Petera, P., Popovic, R., Petrovic, R., Sinico, R. A., Cattaneo, R., Font, J., … Cervera, R. (2002). Immunosuppressive therapy in lupus nephritis: The Euro-Lupus Nephritis Trial, a randomized trial of low-dose versus high-dose intravenous cyclophosphamide. *Arthritis and Rheumatism*, *46*(8), 2121–2131. https://doi.org/10.1002/art.10461

Hu, Q., Xie, Y., Ge, Y., Nie, X., Tao, J., & Zhao, Y. (2018). Resting T cells are hypersensitive to DNA damage due to defective DNA repair pathway. *Cell Death & Disease*, *9*(6), 662. https://doi.org/10.1038/s41419-018-0649-z

Hu, W., Liu, Z., Chen, H., Tang, Z., Wang, Q., Shen, K., & Li, L. (2002). Mycophenolate mofetil vs cyclophosphamide therapy for patients with diffuse proliferative lupus nephritis. *Chinese Medical Journal*, *115*(5), 705–709.

Huang, Y., Getahun, A., Heiser, R. A., Detanico, T. O., Aviszus, K., Kirchenbaum, G. A., Casper, T. L., Huang, C., Aydintug, M. K., Carding, S. R., Ikuta, K., Huang, H., Wysocki, L. J., Cambier, J. C., O'Brien, R. L., & Born, W. K. (2016). Γδ T Cells Shape Pre-Immune Peripheral B Cell Populations. *Journal of Immunology (Baltimore, Md. : 1950)*, *196*(1), 217–231. https://doi.org/10.4049/jimmunol.1501064

Hurd, E. R., & Giuliano, V. J. (1975). The effect of cyclophosphamide on B and T lymphocytes in patients with connective tissue diseases. *Arthritis and Rheumatism*, *18*(1), 67–75. https://doi.org/10.1002/art.1780180113

Hwang, M., Medley, S., Shakeel, F., Vanderwerff, B., Zawistowski, M., Kidwell, K. M., & Hertz, D. L. (2022). Lack of association of CYP2B6 pharmacogenetics with cyclophosphamide toxicity in patients with cancer. *Supportive Care in Cancer*, *30*(9), 7355–7363. https://doi.org/10.1007/s00520-022-07118-y

Ikegami, T., Natsumeda, Y., & Weber, G. (1985). Direct assay method for inosine 5'-monophosphate dehydrogenase activity. *Analytical Biochemistry*, *150*(1), 155–160. https://doi.org/10.1016/0003-2697(85)90454-3

International Consortium for Systemic Lupus Erythematosus Genetics (SLEGEN), Harley, J. B., Alarcón-Riquelme, M. E., Criswell, L. A., Jacob, C. O., Kimberly, R. P., Moser, K. L., Tsao, B. P., Vyse, T. J., Langefeld, C. D., Nath, S. K., Guthridge, J. M., Cobb, B. L., Mirel, D. B., Marion, M. C., Williams, A. H., Divers, J., Wang, W., Frank, S. G., … Kelly, J. A. (2008). Genome-wide association scan in women with systemic lupus erythematosus identifies susceptibility variants in ITGAM, PXK, KIAA1542 and other loci. *Nature Genetics*, *40*(2), 204–210. https://doi.org/10.1038/ng.81

Jahantigh, D., Salimi, S., Mousavi, M., Moossavi, M., Mohammadoo-Khorasani, M., Narooei-nejad, M., & Sandoughi, M. (2015). Association Between Functional Polymorphisms of DNA Double-Strand Breaks in Repair Genes XRCC5, XRCC6 and XRCC7 with the Risk of Systemic Lupus Erythematosus in South East Iran. *DNA and Cell Biology*, *34*(5), 360–366. https://doi.org/10.1089/dna.2014.2465

Jahrsdörfer, B., Vollmer, A., Blackwell, S. E., Maier, J., Sontheimer, K., Beyer, T., Mandel, B., Lunov, O., Tron, K., Nienhaus, G. U., Simmet, T., Debatin, K.-M., Weiner, G. J., & Fabricius, D. (2010). Granzyme B produced by human plasmacytoid dendritic cells suppresses T-cell expansion. *Blood*, *115*(6), 1156–1165. https://doi.org/10.1182/blood-2009-07-235382

Jain, J., Almquist, S. J., Ford, P. J., Shlyakhter, D., Wang, Y., Nimmesgern, E., & Germann, U. A. (2004). Regulation of inosine monophosphate dehydrogenase type I and type II isoforms in human lymphocytes. *Biochemical Pharmacology*, *67*(4), 767–776. https://doi.org/10.1016/j.bcp.2003.09.043

Jakes, R. W., Bae, S.-C., Louthrenoo, W., Mok, C.-C., Navarra, S. V., & Kwon, N. (2012). Systematic review of the epidemiology of systemic lupus erythematosus in the Asia-Pacific

region: Prevalence, incidence, clinical features, and mortality. *Arthritis Care & Research*, *64*(2), 159–168. https://doi.org/10.1002/acr.20683

Jakobsen Falk, I., Khan, M. S., Thunell, L., Nahi, H., & Green, H. (2012). Association of CYP2B6 Genotype with Survival and Progression Free Survival in Cyclophosphamide Treated Multiple Myeloma. *Journal of Cancer Therapy*, *3*(1), 20–27.

Jardine, I., Fenselau, C., Appler, M., Kan, M.-N., Brundrett, R. B., & Colvin, M. (1978). Quantitation by Gas Chromatography-Chemical Ionization Mass Spectrometry of Cyclophosphamide, Phosphoramide Mustard, and Nornitrogen Mustard in the Plasma and Urine of Patients Receiving Cyclophosphamide Therapy. *Cancer Research*, *38*(2), 408–415.

Ji, Y., Gu, J., Makhov, A. M., Griffith, J. D., & Mitchell, B. S. (2006). Regulation of the Interaction of Inosine Monophosphate Dehydrogenase with Mycophenolic Acid by GTP*. *Journal of Biological Chemistry*, *281*(1), 206–212. https://doi.org/10.1074/jbc.M507056200

Joerger, M., Huitema, A. D. R., Richel, D. J., Dittrich, C., Pavlidis, N., Briasoulis, E., Vermorken, J. B., Strocchi, E., Martoni, A., Sorio, R., Sleeboom, H. P., Izquierdo, M. A., Jodrell, D. I., Féty, R., de Bruijn, E., Hempel, G., Karlsson, M., Tranchand, B., Schrijvers, A. H. G. J., … Schellens, J. H. M. (2007). Population Pharmacokinetics and Pharmacodynamics of Doxorubicin and Cyclophosphamide in Breast Cancer Patients. *Clinical Pharmacokinetics*, *46*(12), 1051–1068. https://doi.org/10.2165/00003088-200746120-00005

Johns Hopkins Lupus Center. (2024). Treating Lupus with Steroids. *Johns Hopkins Lupus Center*. https://www.hopkinslupus.org/lupus-treatment/lupus-medications/steroids/

Johnson, G. G., Lin, K., Cox, T. F., Oates, M., Sibson, D. R., Eccles, R., Lloyd, B., Gardiner, L.-J., Carr, D. F., Pirmohamed, M., Strefford, J. C., Oscier, D. G., Castro, D. G. de, Else, M., Catovsky, D., & Pettitt, A. R. (2013). CYP2B6*6 is an independent determinant of inferior response to fludarabine plus cyclophosphamide in chronic lymphocytic leukemia. *Blood*, *122*(26), 4253–4258. https://doi.org/10.1182/blood-2013-07-516666

Johnson, L. A., Malayappan, B., Tretyakova, N., Campbell, C., MacMillan, M. L., Wagner, J. E., & Jacobson, P. A. (2012a). Formation of Cyclophosphamide Specific DNA Adducts in Hematological Diseases. *Pediatric Blood & Cancer*, *58*(5), 708–714. https://doi.org/10.1002/pbc.23254

Johnson, L. A., Malayappan, B., Tretyakova, N., Campbell, C., MacMillan, M. L., Wagner, J. E., & Jacobson, P. A. (2012b). Formation of cyclophosphamide specific DNA adducts in hematological diseases. *Pediatric Blood & Cancer*, *58*(5), 708–714. https://doi.org/10.1002/pbc.23254

Johnson, M. C., & Kollman, J. M. (2020). Cryo-EM structures demonstrate human IMPDH2 filament assembly tunes allosteric regulation. *ELife*, *9*, e53243. https://doi.org/10.7554/eLife.53243

Jorge, A., Wallace, Z. S., Lu, N., Zhang, Y., & Choi, H. K. (2019). Renal Transplantation and Survival Among Patients With Lupus Nephritis: A Cohort Study. *Annals of Internal Medicine*, *170*(4), 240. https://doi.org/10.7326/M18-1570

Joy, M. S., La, M., Wang, J., Bridges, A. S., Hu, Y., Hogan, S. L., Frye, R. F., Blaisdell, J., Goldstein, J. A., Dooley, M. A., Brouwer, K. L. R., & Falk, R. J. (2012). Cyclophosphamide

and 4-hydroxycyclophosphamide pharmacokinetics in patients with glomerulonephritis secondary to lupus and small vessel vasculitis. *British Journal of Clinical Pharmacology*, *74*(3), 445–455. https://doi.org/10.1111/j.1365-2125.2012.04223.x

Kagaya, H., Miura, M., Saito, M., Habuchi, T., & Satoh, S. (2010). Correlation of IMPDH1 Gene Polymorphisms with Subclinical Acute Rejection and Mycophenolic Acid Exposure Parameters on Day 28 after Renal Transplantation. *Basic & Clinical Pharmacology & Toxicology*, *107*(2), 631–636. https://doi.org/10.1111/j.1742-7843.2010.00542.x

Kahlenberg, J. M., Carmona-Rivera, C., Smith, C. K., & Kaplan, M. J. (2013). Neutrophil extracellular trap-associated protein activation of the NLRP3 inflammasome is enhanced in lupus macrophages. *Journal of Immunology (Baltimore, Md.: 1950)*, *190*(3), 1217–1226. https://doi.org/10.4049/jimmunol.1202388

Kaijser, G. P., Korst, A., Beijnen, J. H., Bult, A., & Underberg, W. J. (1993). The analysis of ifosfamide and its metabolites (review). *Anticancer Research*, *13*(5A), 1311–1324.

Kalich-Philosoph, L., Roness, H., Carmely, A., Fishel-Bartal, M., Ligumsky, H., Paglin, S., Wolf, I., Kanety, H., Sredni, B., & Meirow, D. (2013). Cyclophosphamide Triggers Follicle Activation and "Burnout"; AS101 Prevents Follicle Loss and Preserves Fertility. *Science Translational Medicine*, *5*(185), 185ra62. https://doi.org/10.1126/scitranslmed.3005402

Kalra, S., Kaur, R. P., Ludhiadch, A., Shafi, G., Vashista, R., Kumar, R., & Munshi, A. (2018). Association of CYP2C19*2 and ALDH1A1*1/*2 variants with disease outcome in breast cancer patients: Results of a global screening array. *European Journal of Clinical Pharmacology*, *74*(10), 1291–1298. https://doi.org/10.1007/s00228-018-2505-6

Kanakry, C. G., Ganguly, S., Zahurak, M., Bolaños-Meade, J., Thoburn, C., Perkins, B., Fuchs, E. J., Jones, R. J., Hess, A. D., & Luznik, L. (2013). Aldehyde Dehydrogenase Expression Drives Human Regulatory T Cell Resistance to Posttransplantation Cyclophosphamide. *Science Translational Medicine*, *5*(211), 211ra157-211ra157. https://doi.org/10.1126/scitranslmed.3006960

Karrar, S., & Cunninghame Graham, D. S. (2018). Abnormal B Cell Development in Systemic Lupus Erythematosus. *Arthritis & Rheumatology (Hoboken, N.j.)*, *70*(4), 496–507. https://doi.org/10.1002/art.40396

Kato, K., Takeuchi, A., Akashi, K., & Eto, M. (2020). Cyclophosphamide-Induced Tolerance in Allogeneic Transplantation: From Basic Studies to Clinical Application. *Frontiers in Immunology*, *10*. https://doi.org/10.3389/fimmu.2019.03138

Keppeke, G. D., Chang, C. C., Peng, M., Chen, L.-Y., Lin, W.-C., Pai, L.-M., Andrade, L. E. C., Sung, L.-Y., & Liu, J.-L. (2018). IMP/GTP balance modulates cytoophidium assembly and IMPDH activity. *Cell Division*, *13*(1), 5. https://doi.org/10.1186/s13008-018-0038-0

Kerr, J. F. R., Wyllie, A. H., & Currie, A. R. (1972). Apoptosis: A Basic Biological Phenomenon with Wide-ranging Implications in Tissue Kinetics. *British Journal of Cancer*, *26*(4), 239–257.

Khoury, T., Ademuyiwa, F. O., Chandraseekhar, R., Jabbour, M., DeLeo, A., Ferrone, S., Wang, Y., & Wang, X. (2012). Aldehyde dehydrogenase 1A1 expression in breast cancer is associated with stage, triple negativity, and outcome to neoadjuvant chemotherapy. *Modern*

Pathology : An Official Journal of the United States and Canadian Academy of Pathology, Inc, *25*(3), 388–397. https://doi.org/10.1038/modpathol.2011.172

Kim, D. H., & Lerner, A. (1998). Type 4 cyclic adenosine monophosphate phosphodiesterase as a therapeutic target in chronic lymphocytic leukemia. *Blood*, *92*(7), 2484–2494.

Kim, I.-W., Yun, H., Choi, B., Han, N., Kim, M. G., Park, S., & Oh, J. M. (2013). Population pharmacokinetics analysis of cyclophosphamide with genetic effects in patients undergoing hematopoietic stem cell transplantation. *European Journal of Clinical Pharmacology*, *69*(8), 1543–1551. https://doi.org/10.1007/s00228-013-1507-7

Kim, K., Bang, S.-Y., Joo, Y. B., Kim, T., Lee, H.-S., Kang, C., & Bae, S.-C. (2016). Response to Intravenous Cyclophosphamide Treatment for Lupus Nephritis Associated with Polymorphisms in the FCGR2B-FCRLA Locus. *The Journal of Rheumatology*, *43*(6), 1045–1049. https://doi.org/10.3899/jrheum.150665

Kim, S., Lee, W., Chun, S., Um, T. H., & Min, W.-K. (2014). Expression of IMPDH mRNA after Mycophenolate Administration in Male Volunteers. *BioMed Research International*, *2014*, 870209. https://doi.org/10.1155/2014/870209

Klaasen, R. A., Bergan, S., Bremer, S., Hole, K., Nordahl, C. B., Andersen, A. M., Midtvedt, K., Skauby, M. H., & Vethe, N. T. (2020). Pharmacodynamic assessment of mycophenolic acid in resting and activated target cell population during the first year after renal transplantation. *British Journal of Clinical Pharmacology*, *86*(6), 1100–1112. https://doi.org/10.1111/bcp.14218

Klein, M., Vaeth, M., Scheel, T., Grabbe, S., Baumgrass, R., Berberich-Siebelt, F., Bopp, T., Schmitt, E., & Becker, C. (2012). Repression of Cyclic Adenosine Monophosphate Upregulation Disarms and Expands Human Regulatory T Cells. *The Journal of Immunology*, *188*(3), 1091–1097. https://doi.org/10.4049/jimmunol.1102045

Kornberg, A., Lieberman, I., & Simms, E. S. (1955). Enzymatic Synthesis of Purine Nucleotides. *Journal of Biological Chemistry*, *215*(1), 417–427.

Kumaraswami, K., Katkam, S. K., Aggarwal, A., Sharma, A., Manthri, R., Kutala, V. K., & Rajasekhar, L. (2017). Epistatic interactions among CYP2C19*2, CYP3A4 and GSTP1 on the cyclophosphamide therapy in lupus nephritis patients. *Pharmacogenomics*, *18*(15), 1401–1411. https://doi.org/10.2217/pgs-2017-0069

Kurioka, A., Ussher, J. E., Cosgrove, C., Clough, C., Fergusson, J. R., Smith, K., Kang, Y.-H., Walker, L. J., Hansen, T. H., Willberg, C. B., & Klenerman, P. (2015). MAIT cells are licensed through granzyme exchange to kill bacterially sensitized targets. *Mucosal Immunology*, *8*(2), 429–440. https://doi.org/10.1038/mi.2014.81

Kuypers, D. R. J., Jonge, H. de, Naesens, M., Loor, H. de, Halewijck, E., Dekens, M., & Vanrenterghem, Y. (2008). Current target ranges of mycophenolic acid exposure and drug-related adverse events: A 5-year, open-label, prospective, clinical follow-up study in renal allograft recipients. *Clinical Therapeutics*, *30*(4), 673–683. https://doi.org/10.1016/j.clinthera.2008.04.014

Kuypers, D. R. J., Meur, Y. L., Cantarovich, M., Tredger, M. J., Tett, S. E., Cattaneo, D., Tönshoff, B., Holt, D. W., Chapman, J., & Gelder, T. van. (2010). Consensus Report on

Therapeutic Drug Monitoring of Mycophenolic Acid in Solid Organ Transplantation. *Clinical Journal of the American Society of Nephrology*, *5*(2), 341–358. https://doi.org/10.2215/CJN.07111009

Kwon, C. H., Maddison, K., LoCastro, L., & Borch, R. F. (1987). Accelerated decomposition of 4-hydroxycyclophosphamide by human serum albumin. *Cancer Research*, *47*(6), 1505–1508.

Laat, W. L. de, Appeldoorn, E., Jaspers, N. G. J., & Hoeijmakers, J. H. J. (1998). DNA Structural Elements Required for ERCC1-XPF Endonuclease Activity. *Journal of Biological Chemistry*, *273*(14), 7835–7842. https://doi.org/10.1074/jbc.273.14.7835

Lachmann, A., Torre, D., Keenan, A. B., Jagodnik, K. M., Lee, H. J., Wang, L., Silverstein, M. C., & Ma'ayan, A. (2018). Massive mining of publicly available RNA-seq data from human and mouse. *Nature Communications*, *9*(1), Article 1. https://doi.org/10.1038/s41467-018-03751-6

Lahita, R. G. (2011). Chapter 30—The Clinical Presentation of Systemic Lupus Erythematosus. In R. G. Lahita (Ed.), *Systemic Lupus Erythematosus (Fifth Edition)* (pp. 525–539). Academic Press. https://doi.org/10.1016/B978-0-12-374994-9.10030-0

Lande, R., Ganguly, D., Facchinetti, V., Frasca, L., Conrad, C., Gregorio, J., Meller, S., Chamilos, G., Sebasigari, R., Riccieri, V., Bassett, R., Amuro, H., Fukuhara, S., Ito, T., Liu, Y.-J., & Gilliet, M. (2011). Neutrophils activate plasmacytoid dendritic cells by releasing self-DNA-peptide complexes in systemic lupus erythematosus. *Science Translational Medicine*, *3*(73), 73ra19. https://doi.org/10.1126/scitranslmed.3001180

Lang, T., Klein, K., Fischer, J., Nüssler, A. K., Neuhaus, P., Hofmann, U., Eichelbaum, M., Schwab, M., & Zanger, U. M. (2001). Extensive genetic polymorphism in the human CYP2B6 gene with impact on expression and function in human liver. *Pharmacogenetics*, *11*(5), 399–415. https://doi.org/10.1097/00008571-200107000-00004

Langman, L. J., LeGatt, D. F., Halloran, P. F., & Yatscoff, R. W. (1996). PHARMACODYNAMIC ASSESSMENT OF MYCOPHENOLIC ACIDINDUCED IMMUNOSUPPRESSION IN RENAL TRANSPLANT RECIPIENTS. *Transplantation*, *62*(5), 666–672.

Langman, L. J., LeGatt, D. F., & Yatscoff, R. W. (1994). Blood distribution of mycophenolic acid. *Therapeutic Drug Monitoring*, *16*(6), 602–607. https://doi.org/10.1097/00007691-199412000-00012

Lao, C., White, D., Rabindranath, K., Van Dantzig, P., Foxall, D., Aporosa, A., & Lawrenson, R. (2023). Incidence and prevalence of systemic lupus erythematosus in New Zealand from the national administrative datasets. *Lupus*, 9612033231182204. https://doi.org/10.1177/09612033231182203

Le Bourhis, L., Dusseaux, M., Bohineust, A., Bessoles, S., Martin, E., Premel, V., Coré, M., Sleurs, D., Serriari, N.-E., Treiner, E., Hivroz, C., Sansonetti, P., Gougeon, M.-L., Soudais, C., & Lantz, O. (2013). MAIT Cells Detect and Efficiently Lyse Bacterially-Infected Epithelial Cells. *PLoS Pathogens*, *9*(10), e1003681. https://doi.org/10.1371/journal.ppat.1003681

Le Meur, Y., Borrows, R., Pescovitz, M. D., Budde, K., Grinyo, J., Bloom, R., Gaston, R., Walker, R. G., Kuypers, D., van Gelder, T., & Kiberd, B. (2011). Therapeutic drug monitoring of mycophenolates in kidney transplantation: Report of The Transplantation Society consensus meeting. *Transplantation Reviews*, *25*(2), 58–64. https://doi.org/10.1016/j.trre.2011.01.002

Le Meur, Y., Büchler, M., Thierry, A., Caillard, S., Villemain, F., Lavaud, S., Etienne, I., Westeel, P.-F., Hurault de Ligny, B., Rostaing, L., Thervet, E., Szelag, J. C., Rérolle, J.-P., Rousseau, A., Touchard, G., & Marquet, P. (2007). Individualized mycophenolate mofetil dosing based on drug exposure significantly improves patient outcomes after renal transplantation. *American Journal of Transplantation: Official Journal of the American Society of Transplantation and the American Society of Transplant Surgeons*, *7*(11), 2496–2503. https://doi.org/10.1111/j.1600-6143.2007.01983.x

Lee, H.-M., Sugino, H., Aoki, C., & Nishimoto, N. (2011). Underexpression of mitochondrial-DNA encoded ATP synthesis-related genes and DNA repair genes in systemic lupus erythematosus. *Arthritis Research & Therapy*, *13*(2), R63. https://doi.org/10.1186/ar3317

LeLeiko, N. S., Bronstein, A. D., Baliga, B. S., & Munro, H. N. (1983). De novo purine nucleotide synthesis in the rat small and large intestine: Effect of dietary protein and purines. *Journal of Pediatric Gastroenterology and Nutrition*, *2*(2), 313–319.

Lerner, M. R., & Steitz, J. A. (1979). Antibodies to small nuclear RNAs complexed with proteins are produced by patients with systemic lupus erythematosus. *Proceedings of the National Academy of Sciences of the United States of America*, *76*(11), 5495–5499.

Lertdumrongluk, P., Somparn, P., Kittanamongkolchai, W., Traitanon, O., Vadcharavivad, S., & Avihingsanon, Y. (2010). Pharmacokinetics of mycophenolic acid in severe lupus nephritis. *Kidney International*, *78*(4), 389–395. https://doi.org/10.1038/ki.2010.170

Levi, B. P., Yilmaz, Ö. H., Duester, G., & Morrison, S. J. (2009). Aldehyde dehydrogenase 1a1 is dispensable for stem cell function in the mouse hematopoietic and nervous systems. *Blood*, *113*(8), 1670–1680. https://doi.org/10.1182/blood-2008-05-156752

Li, H., Mager, D. E., Sandmaier, B. M., Storer, B. E., Boeckh, M. J., Bemer, M. J., Phillips, B. R., Risler, L. J., & McCune, J. S. (2014). Pharmacokinetic and Pharmacodynamic Analysis of Inosine Monophosphate Dehydrogenase Activity in Hematopoietic Cell Transplantation Recipients Treated with Mycophenolate Mofetil. *Biology of Blood and Marrow Transplantation*, *20*(8), 1121–1129. https://doi.org/10.1016/j.bbmt.2014.03.032

Li, Y. I., Knowles, D. A., Humphrey, J., Barbeira, A. N., Dickinson, S. P., Im, H. K., & Pritchard, J. K. (2018). Annotation-free quantification of RNA splicing using LeafCutter. *Nature Genetics*, *50*(1), Article 1. https://doi.org/10.1038/s41588-017-0004-9

Liang, L., Beshay, E., & Prud'homme, G. J. (1998). The phosphodiesterase inhibitors pentoxifylline and rolipram prevent diabetes in NOD mice. *Diabetes*, *47*(4), 570–575. https://doi.org/10.2337/diabetes.47.4.570

Lo, M. S. (2016). Monogenic Lupus. *Current Rheumatology Reports*, *18*(12), 71. https://doi.org/10.1007/s11926-016-0621-9

Lo, M. S., & Tsokos, G. C. (2018). Recent developments in systemic lupus erythematosus pathogenesis and applications for therapy. *Current Opinion in Rheumatology*, *30*(2), 222–228. https://doi.org/10.1097/BOR.0000000000000474

López-López, L., Nieves-Plaza, M., Castro, M. del R., Font, Y. M., Torres-Ramos, C., Vilá, L. M., & Ayala-Peña, S. (2014). Mitochondrial DNA damage is associated with damage accrual and disease duration in patients with Systemic Lupus Erythematosus. *Lupus*, *23*(11), 1133–1141. https://doi.org/10.1177/0961203314537697

Lutsiak, M. E. C., Semnani, R. T., De Pascalis, R., Kashmiri, S. V. S., Schlom, J., & Sabzevari, H. (2005). Inhibition of CD4+25+ T regulatory cell function implicated in enhanced immune response by low-dose cyclophosphamide. *Blood*, *105*(7), 2862–2868. https://doi.org/10.1182/blood-2004-06-2410

Lyons, P. A., McKinney, E. F., Rayner, T. F., Hatton, A., Woffendin, H. B., Koukoulaki, M., Freeman, T. C., Jayne, D. R. W., Chaudhry, A. N., & Smith, K. G. C. (2010). Novel expression signatures identified by transcriptional analysis of separated leucocyte subsets in systemic lupus erythematosus and vasculitis. *Annals of the Rheumatic Diseases*, *69*(6), 1208–1213. https://doi.org/10.1136/ard.2009.108043

Maccubbin, A. E., Caballes, L., Riordan, J. M., Huang, D. H., & Gurtoo, H. L. (1991). A cyclophosphamide/DNA phosphoester adduct formed in vitro and in vivo. *Cancer Research*, *51*(3), 886–892.

Madelian, V., & Vigne, E. L. (1996). Rapid regulation of a cyclic AMP-specific phosphodiesterase (PDE IV) by forskolin and isoproterenol in LRM55 astroglial cells. *Biochemical Pharmacology*, *51*(12), 1739–1747. https://doi.org/10.1016/0006-2952(96)00167-0

Madronich, S., McKenzie, R. L., Björn, L. O., & Caldwell, M. M. (1998). Changes in biologically active ultraviolet radiation reaching the Earth's surface. *Journal of Photochemistry and Photobiology. B, Biology*, *46*(1–3), 5–19. https://doi.org/10.1016/s1011-1344(98)00182-1

Magni, M., Shammah, S., Schiró, R., Mellado, W., Dalla-Favera, R., & Gianni, A. M. (1996). Induction of cyclophosphamide-resistance by aldehyde-dehydrogenase gene transfer. *Blood*, *87*(3), 1097–1103.

Mak, A., Cheak, A. A. C., Tan, J. Y. S., Su, H. C., Ho, R. C. M., & Lau, C. S. (2009). Mycophenolate mofetil is as efficacious as, but safer than, cyclophosphamide in the treatment of proliferative lupus nephritis: A meta-analysis and meta-regression. *Rheumatology*, *48*(8), 944–952. https://doi.org/10.1093/rheumatology/kep120

Manolakou, T., Nikolopoulos, D., Gkikas, D., Filia, A., Samiotaki, M., Stamatakis, G., Fanouriakis, A., Politis, P., Banos, A., Alissafi, T., Verginis, P., & Boumpas, D. T. (2022). ATR-mediated DNA damage responses underlie aberrant B cell activity in systemic lupus erythematosus. *Science Advances*, *8*(43), eabo5840. https://doi.org/10.1126/sciadv.abo5840

Maroz, N., & Segal, M. S. (2013). Lupus nephritis and end-stage kidney disease. *The American Journal of the Medical Sciences*, *346*(4), 319–323. https://doi.org/10.1097/MAJ.0b013e31827f4ee3

Marteijn, J. A., Lans, H., Vermeulen, W., & Hoeijmakers, J. H. J. (2014). Understanding nucleotide excision repair and its roles in cancer and ageing. *Nature Reviews. Molecular Cell Biology*, *15*(7), 465–481. https://doi.org/10.1038/nrm3822

Martis, S., Mei, H., Vijzelaar, R., Edelmann, L., Desnick, R. J., & Scott, S. A. (2013). Multi-ethnic Cytochrome-P450 Copy Number Profiling: Novel Pharmacogenetic Alleles and Mechanism of Copy Number Variation Formation. *The Pharmacogenomics Journal*, *13*(6), 558–566. https://doi.org/10.1038/tpj.2012.48

Masta, A., Gray, P. J., & Phillips, D. R. (1995). Nitrogen mustard inhibits transcription and translation in a cell free system. *Nucleic Acids Research*, *23*(17), 3508–3515.

Mayer, P. J., Lange, C. S., Bradley, M. O., & Nichols, W. W. (1991). Gender differences in age-related decline in DNA double-strand break damage and repair in lymphocytes. *Annals of Human Biology*, *18*(5), 405–415. https://doi.org/10.1080/03014469100001702

Mazur, D. J., & Perrino, F. W. (1999). Identification and expression of the TREX1 and TREX2 cDNA sequences encoding mammalian 3'—>5' exonucleases. *The Journal of Biological Chemistry*, *274*(28), 19655–19660. https://doi.org/10.1074/jbc.274.28.19655

McCune, J., Batchelder, A., Guthrie, K., Witherspoon, R., Appelbaum, F., Phillips, B., Vicini, P., Salinger, D., & McDonald, G. (2009). Personalized Dosing of Cyclophosphamide in the Total Body Irradiation–Cyclophosphamide Conditioning Regimen: A Phase II Trial in Patients With Hematologic Malignancy. *Clinical Pharmacology & Therapeutics*, *85*(6), 615–622. https://doi.org/10.1038/clpt.2009.27

McCune, J. S., Storer, B., Thomas, S., McKiernan, J., Gupta, R., & Sandmaier, B. M. (2018). Inosine Monophosphate Dehydrogenase Pharmacogenetics in Hematopoietic Cell Transplantation Patients. *Biology of Blood and Marrow Transplantation*, *24*(9), 1802–1807. https://doi.org/10.1016/j.bbmt.2018.04.006

McCurdy, D., Tai, L. Q., Frias, S., & Wang, Z. (1997). Delayed repair of DNA damage by ionizing radiation in cells from patients with juvenile systemic lupus erythematosus and rheumatoid arthritis. *Radiation Research*, *147*(1), 48–54.

McDiarmid, M. A., Iype, P. T., Kolodner, K., Jacobson-Kram, D., & Strickland, P. T. (1991). Evidence for acrolein-modified DNA in peripheral blood leukocytes of cancer patients treated with cyclophosphamide. *Mutation Research/Fundamental and Molecular Mechanisms of Mutagenesis*, *248*(1), 93–99. https://doi.org/10.1016/0027-5107(91)90091-2

McDonald, G., Cabal, N., Vannier, A., Umiker, B., Yin, R. H., Orjalo, A. V., Johansson, H. E., Han, J.-H., & Imanishi-Kari, T. (2015). Female Bias in Systemic Lupus Erythematosus is Associated with the Differential Expression of X-Linked Toll-Like Receptor 8. *Frontiers in Immunology*, *6*. https://www.frontiersin.org/articles/10.3389/fimmu.2015.00457

McGown, A. T., & Fox, B. W. (1986). A proposed mechanism of resistance to cyclophosphamide and phosphoramide mustard in a Yoshida cell line in vitro. *Cancer Chemotherapy and Pharmacology*, *17*(3), 223–226. https://doi.org/10.1007/BF00256688

Meas, R., Burak, M. J., & Sweasy, J. B. (2017). DNA repair and systemic lupus erythematosus. *DNA Repair*, *56*, 174–182. https://doi.org/10.1016/j.dnarep.2017.06.020

Melanson, S. E. F., Stevenson, K., Kim, H., Antin, J. H., Court, M. H., Ho, V. T., Ritz, J., Soiffer, R. J., Kuo, F. C., Longtine, J. A., & Jarolim, P. (2010). Allelic variations in CYP2B6 and CYP2C19 and survival of patients receiving cyclophosphamide prior to myeloablative hematopoietic stem cell transplantation. *American Journal of Hematology*, *85*(12), 967–971. https://doi.org/10.1002/ajh.21889

Merlo, L. M. F., & Mandik-Nayak, L. (2013). Chapter 3 - Adaptive Immunity: B Cells and Antibodies. In G. C. Prendergast & E. M. Jaffee (Eds.), *Cancer Immunotherapy (Second Edition)* (pp. 25–40). Academic Press. https://doi.org/10.1016/B978-0-12-394296-8.00003-8

Metz, D. K., Holford, N., Kausman, J. Y., Walker, A., Cranswick, N., Staatz, C. E., Barraclough, K. A., & Ierino, F. (2019). Optimizing Mycophenolic Acid Exposure in Kidney Transplant Recipients: Time for Target Concentration Intervention. *Transplantation*, *103*(10), 2012–2030. https://doi.org/10.1097/TP.0000000000002762

Mireles-Canales, M. P., González-Chávez, S. A., Quiñonez-Flores, C. M., León-López, E. A., & Pacheco-Tena, C. (2018). DNA Damage and Deficiencies in the Mechanisms of Its Repair: Implications in the Pathogenesis of Systemic Lupus Erythematosus. *Journal of Immunology Research*, *2018*. https://doi.org/10.1155/2018/8214379

Miyara, M., Amoura, Z., Parizot, C., Badoual, C., Dorgham, K., Trad, S., Nochy, D., Debré, P., Piette, J., & Gorochov, G. (2005). Global natural regulatory T cell depletion in active systemic lupus erythematosus. *Journal of Immunology (Baltimore, Md. : 1950)*, *175*(12). https://doi.org/10.4049/jimmunol.175.12.8392

Molinaro, M., Chiarelli, L. R., Biancone, L., Castagneto, M., Boschiero, L., Pisani, F., Sabbatini, M., Sandrini, S., Arbustini, E., Tinelli, C., Regazzi, M., Schena, F. P., & Segoloni, G. P. (2013). Monitoring of Inosine Monophosphate Dehydrogenase Activity and Expression during the Early Period of Mycophenolate Mofetil Therapy in De Novo Renal Transplant Patients. *Drug Metabolism and Pharmacokinetics*, *28*(2), 109–117. https://doi.org/10.2133/dmpk.DMPK-12-RG-048

Montero, C., Duley, J. A., Fairbanks, L. D., McBride, M. B., Micheli, V., Cant, A. J., & Morgan, G. (1995). Demonstration of induction of erythrocyte inosine monophosphate dehydrogenase activity in Ribavirin-treated patients using a high performance liquid chromatography linked method. *Clinica Chimica Acta; International Journal of Clinical Chemistry*, *238*(2), 169–178. https://doi.org/10.1016/0009-8981(95)06088-u

Motoyoshi, Y., Kaminoda, K., Saitoh, O., Hamasaki, K., Nakao, K., Ishii, N., Nagayama, Y., & Eguchi, K. (2006). Different mechanisms for anti-tumor effects of low- and high-dose cyclophosphamide. *Oncology Reports*, *16*(1), 141–146.

Munoz, L. E., van Bavel, C., Franz, S., Berden, J., Herrmann, M., & van der Vlag, J. (2008). Apoptosis in the pathogenesis of systemic lupus erythematosus. *Lupus*, *17*(5), 371–375. https://doi.org/10.1177/0961203308089990

Murray, A. W. (1971). The Biological Significance of Purine Salvage. *Annual Review of Biochemistry*, *40*(1), 811–826. https://doi.org/10.1146/annurev.bi.40.070171.004115

Nagai, M., Natsumeda, Y., & Weber, G. (1992). Proliferation-linked Regulation of Type II IMP Dehydrogenase Gene in Human Normal Lymphocytes and HL-60 Leukemic Cells. *Cancer Research*, *52*(2), 258–261.

Nakajima, M., Komagata, S., Fujiki, Y., Kanada, Y., Ebi, H., Itoh, K., Mukai, H., Yokoi, T., & Minami, H. (2007). Genetic polymorphisms of CYP2B6 affect the pharmacokinetics/pharmacodynamics of cyclophosphamide in Japanese cancer patients. *Pharmacogenetics and Genomics*, *17*(6), 431–445. https://doi.org/10.1097/FPC.0b013e328045c4fb

Namas, R., Renauer, P., Ognenovski, M., Tsou, P.-S., & Sawalha, A. H. (2016). Histone H2AX phosphorylation as a measure of DNA double-strand breaks and a marker of environmental stress and disease activity in lupus. *Lupus Science & Medicine*, *3*(1), e000148. https://doi.org/10.1136/lupus-2016-000148

Neuberger, M., Sommerer, C., Böhnisch, S., Metzendorf, N., Mehrabi, A., Stremmel, W., Gotthardt, D., Zeier, M., Weiss, K. H., & Rupp, C. (2020). Effect of mycophenolic acid on inosine monophosphate dehydrogenase (IMPDH) activity in liver transplant patients. *Clinics and Research in Hepatology and Gastroenterology*, *44*(4), 543–550. https://doi.org/10.1016/j.clinre.2019.12.001

Nguyen Thi, M. T., Capron, A., Mourad, M., & Wallemacq, P. (2013). Mycophenolic acid quantification in human peripheral blood mononuclear cells using liquid chromatography-tandem mass spectrometry. *Clinical Biochemistry*, *46*(18), 1909–1911. https://doi.org/10.1016/j.clinbiochem.2013.09.009

Nguyen Thi, M. T., Mourad, M., Capron, A., Musuamba Tshinanu, F., Vincent, M.-F., & Wallemacq, P. (2015). Plasma and intracellular pharmacokinetic–pharmacodynamic analysis of mycophenolic acid in de novo kidney transplant patients. *Clinical Biochemistry*, *48*(6), 401–405. https://doi.org/10.1016/j.clinbiochem.2014.12.005

Noble, P. W., Bernatsky, S., Clarke, A. E., Isenberg, D. A., Ramsey-Goldman, R., & Hansen, J. E. (2016). DNA-damaging autoantibodies and cancer: The lupus butterfly theory. *Nature Reviews. Rheumatology*, *12*(7), 429–434. https://doi.org/10.1038/nrrheum.2016.23

Noordam, L., Kaijen, M. E. H., Bezemer, K., Cornelissen, R., Maat, L. A. P. W. M., Hoogsteden, H. C., Aerts, J. G. J. V., Hendriks, R. W., Hegmans, J. P. J. J., & Vroman, H. (2018). Low-dose cyclophosphamide depletes circulating naïve and activated regulatory T cells in malignant pleural mesothelioma patients synergistically treated with dendritic cell-based immunotherapy. *OncoImmunology*, *7*(12), e1474318. https://doi.org/10.1080/2162402X.2018.1474318

Nowak, I., & Shaw, L. M. (1995). Mycophenolic acid binding to human serum albumin: Characterization and relation to pharmacodynamics. *Clinical Chemistry*, *41*(7), 1011–1017.

Ohmann, E. L., Burckart, G. J., Chen, Y., Pravica, V., Brooks, M. M., Zeevi, A., & Webber, S. A. (2010). Inosine 5'-monophosphate dehydrogenase 1 haplotypes and association with mycophenolate mofetil gastrointestinal intolerance in pediatric heart transplant patients. *Pediatric Transplantation*, *14*(7), 891–895. https://doi.org/10.1111/j.1399-3046.2010.01367.x

Okamoto, M., Wakabayashi, Y., Higuchi, A., Kadotani, Y., Ogino, S., Ushigome, H., Akioka, K., Kaihara, S., & Yoshimura, N. (2005). Therapeutic drug monitoring of mycophenolic acid in renal transplant recipients. *Transplantation Proceedings*, *37*(2), 859–860. https://doi.org/10.1016/j.transproceed.2004.12.238

Omori, K., & Kotera, J. (2007). Overview of PDEs and their regulation. *Circulation Research*, *100*(3), 309–327. https://doi.org/10.1161/01.RES.0000256354.95791.f1

Ong, L. M., Hooi, L. S., Lim, T. O., Goh, B. L., Ahmad, G., Ghazalli, R., Teo, S. M., Wong, H. S., Tan, S. Y., Shaariah, W., Tan, C. C., & Morad, Z. (2005). Randomized controlled trial of pulse intravenous cyclophosphamide versus mycophenolate mofetil in the induction therapy of proliferative lupus nephritis. *Nephrology*, *10*(5), 504–510. https://doi.org/10.1111/j.1440-1797.2005.00444.x

Patel, C. G., Ogasawara, K., & Akhlaghi, F. (2013). Mycophenolic Acid Glucuronide (MPAG) is Transported by Multidrug Resistance-Associated Protein 2 (MRP2) and this Transport is not Inhibited by Cyclosporine, Tacrolimus or Sirolimus. *Xenobiotica; the Fate of Foreign Compounds in Biological Systems*, *43*(3), 229–235. https://doi.org/10.3109/00498254.2012.713531

Patel, P. (2008). *Gene Expression Profiling to Understand the Alterations in the Monocyte Compartment of Pediatric Systemic Lupus Erythematosus*. Baylor University.

Paul, S., Singh, A. K., Shilpi, null, & Lal, G. (2014). Phenotypic and functional plasticity of gamma-delta (γδ) T cells in inflammation and tolerance. *International Reviews of Immunology*, *33*(6), 537–558. https://doi.org/10.3109/08830185.2013.863306

Peng, S. L., Szabo, S. J., & Glimcher, L. H. (2002). T-bet regulates IgG class switching and pathogenic autoantibody production. *Proceedings of the National Academy of Sciences of the United States of America*, *99*(8), 5545–5550. https://doi.org/10.1073/pnas.082114899

Petersen, A. B., Gniadecki, R., Vicanova, J., Thorn, T., & Wulf, H. C. (2000). Hydrogen peroxide is responsible for UVA-induced DNA damage measured by alkaline comet assay in HaCaT keratinocytes. *Journal of Photochemistry and Photobiology B: Biology*, *59*(1), 123–131. https://doi.org/10.1016/S1011-1344(00)00149-4

Picard, N., Yee, S. W., Woillard, J.-B., Lebranchu, Y., Le Meur, Y., Giacomini, K. M., & Marquet, P. (2010). The role of organic anion-transporting polypeptides and their common genetic variants in mycophenolic acid pharmacokinetics. *Clinical Pharmacology and Therapeutics*, *87*(1), 100–108. https://doi.org/10.1038/clpt.2009.205

Podhorecka, M., Skladanowski, A., & Bozko, P. (2010). H2AX Phosphorylation: Its Role in DNA Damage Response and Cancer Therapy. *Journal of Nucleic Acids*, *2010*, 920161. https://doi.org/10.4061/2010/920161

Podolska, M. J., Biermann, M. H., Maueröder, C., Hahn, J., & Herrmann, M. (2015). Inflammatory etiopathogenesis of systemic lupus erythematosus: An update. *Journal of Inflammation Research*, *8*, 161–171. https://doi.org/10.2147/JIR.S70325

Pontén, F., Jirström, K., & Uhlen, M. (2008). The Human Protein Atlas—A tool for pathology. *The Journal of Pathology*, *216*(4), 387–393. https://doi.org/10.1002/path.2440

Poulsen, C. B., Borup, R., Borregaard, N., Nielsen, F. C., Møller, M. B., & Ralfkiaer, E. (2006). Prognostic significance of metallothionein in B-cell lymphomas. *Blood*, *108*(10), 3514–3519. https://doi.org/10.1182/blood-2006-04-015305

Pourafshar, N., Karimi, A., Wen, X., Sobel, E., Pourafshar, S., Agrawal, N., Segal, E., Mohandas, R., & Segal, M. S. (2019). The utility of trough mycophenolic acid levels for the management of lupus nephritis. *Nephrology Dialysis Transplantation*, *34*(1), 83–89. https://doi.org/10.1093/ndt/gfy026

Povirk, L. F., & Shuker, D. E. (1994). DNA damage and mutagenesis induced by nitrogen mustards. *Mutation Research/Reviews in Genetic Toxicology*, *318*(3), 205–226. https://doi.org/10.1016/0165-1110(94)90015-9

Proffitt, R. T., Pathak, V. K., Villacorte, D. G., & Presant, C. A. (1983). Sensitive radiochemical assay for inosine 5'-monophosphate dehydrogenase and determination of activity in murine tumor and tissue extracts. *Cancer Research*, *43*(4), 1620–1623.

P. Sinha, R., & Häder, D.-P. (2002). UV-induced DNA damage and repair: A review. *Photochemical & Photobiological Sciences*, *1*(4), 225–236. https://doi.org/10.1039/B201230H

Pua, K. H., Stiles, D. T., Sowa, M. E., & Verdine, G. L. (2017). IMPDH2 Is an Intracellular Target of the Cyclophilin A and Sanglifehrin A Complex. *Cell Reports*, *18*(2), 432–442. https://doi.org/10.1016/j.celrep.2016.12.030

Qiu, Y., Fairbanks, L. D., Rückermann, K., Hawrlowicz, C. M., Richards, D. F., Kirschbaum, B., & Simmonds, H. A. (2000). Mycophenolic acid-induced GTP depletion also affects ATP and pyrimidine synthesis in mitogen-stimulated primary human T-lymphocytes. *Transplantation*, *69*(5), 890–897. https://doi.org/10.1097/00007890-200003150-00038

Raccor, B. S., Claessens, A. J., Dinh, J. C., Park, J. R., Hawkins, D. S., Thomas, S. S., Makar, K. W., McCune, J. S., & Totah, R. A. (2012). Potential Contribution of Cytochrome P450 2B6 to Hepatic 4-Hydroxycyclophosphamide Formation In Vitro and In Vivo. *Drug Metabolism and Disposition*, *40*(1), 54–63. https://doi.org/10.1124/dmd.111.039347

Rall-Scharpf, M., Friedl, T. W. P., Biechonski, S., Denkinger, M., Milyavsky, M., & Wiesmüller, L. (2021). Sex-specific differences in DNA double-strand break repair of cycling human lymphocytes during aging. *Aging (Albany NY)*, *13*(17), 21066–21089. https://doi.org/10.18632/aging.203519

Ramírez Sepúlveda, J. I., Bolin, K., Mofors, J., Leonard, D., Svenungsson, E., Jönsen, A., Bengtsson, C., Zickert, A., Björk, A., Bengtsson, A. A., Jönsen, A., Bengtsson, C., Sjöwall, C., Enocsson, H., Wetterö, J., Eriksson, P., Leonard, D., Svenungsson, E., Thorlacius, G. E., … the DISSECT consortium. (2019). Sex differences in clinical presentation of systemic lupus erythematosus. *Biology of Sex Differences*, *10*(1), 60. https://doi.org/10.1186/s13293-019-0274-2

Raphael, I., Nalawade, S., Eagar, T. N., & Forsthuber, T. G. (2015). T cell subsets and their signature cytokines in autoimmune and inflammatory diseases. *Cytokine*, *74*(1), 5–17. https://doi.org/10.1016/j.cyto.2014.09.011

Rastogi, R. P., Richa, Kumar, A., Tyagi, M. B., & Sinha, R. P. (2010). *Molecular Mechanisms of Ultraviolet Radiation-Induced DNA Damage and Repair* [Research article]. Journal of Nucleic Acids. https://doi.org/10.4061/2010/592980

Rees, F., Doherty, M., Grainge, M. J., Lanyon, P., & Zhang, W. (2017). The worldwide incidence and prevalence of systemic lupus erythematosus: A systematic review of epidemiological studies. *Rheumatology*, *56*(11), 1945–1961. https://doi.org/10.1093/rheumatology/kex260

Reha-Krantz, L. J., & Nonay, R. L. (1993). Genetic and biochemical studies of bacteriophage T4 DNA polymerase 3'—>5'-exonuclease activity. *Journal of Biological Chemistry*, *268*(36), 27100–27108.

Rekvig, O. P., Kalaaji, M., & Nossent, H. (2004). Anti-DNA antibody subpopulations and lupus nephritis. *Autoimmunity Reviews*, *3*(2), 1–6. https://doi.org/10.1016/S1568-9972(03)00081-8

Ren, S., Yang, J. S., Kalhorn, T. F., & Slattery, J. T. (1997). Oxidation of cyclophosphamide to 4-hydroxycyclophosphamide and deschloroethylcyclophosphamide in human liver microsomes. *Cancer Research*, *57*(19), 4229–4235.

Ren, Y., Tang, J., Mok, M. Y., Chan, A. W. K., Wu, A., & Lau, C. S. (2003). Increased apoptotic neutrophils and macrophages and impaired macrophage phagocytic clearance of apoptotic neutrophils in systemic lupus erythematosus. *Arthritis and Rheumatism*, *48*(10), 2888–2897. https://doi.org/10.1002/art.11237

Response to MMF Therapy for Lupus Nephritis Is Independent of Genetic Variation of Inosine Monophosphate Dehydrogenase. (n.d.). *ACR Meeting Abstracts*. Retrieved September 30, 2021, from https://acrabstracts.org/abstract/response-to-mmf-therapy-for-lupus-nephritis-is-independent-of-genetic-variation-of-inosine-monophosphate-dehydrogenase/

Rowland-Jones, S. L., & McMichael, A. J. (2000). *Lymphocytes: A Practical Approach*. Oxford University Press.

Roy, P., Yu, L. J., Crespi, C. L., & Waxman, D. J. (1999). Development of a Substrate-Activity Based Approach To Identify the Major Human Liver P-450 Catalysts of Cyclophosphamide and Ifosfamide Activation Based on cDNA-Expressed Activities and Liver Microsomal P-450 Profiles. *Drug Metabolism and Disposition*, *27*(6), 655–666.

Ruiz-Irastorza, G. (2021). Prednisone in systemic lupus erythematosus: Taper quickly, withdraw slowly. *Rheumatology*, *60*(12), 5489–5490. https://doi.org/10.1093/rheumatology/keab347

Saccoccia, P. A., & Miech, R. P. (1969). Inosinic Acid Dehydrogenase in Mammalian Tissues. *Molecular Pharmacology*, *5*(1), 26–29.

Sahay, M., Saivani, Y., Ismal, K., & Vali, Ps. (2018). Mycophenolate versus Cyclophosphamide for Lupus Nephritis. *Indian Journal of Nephrology*, *28*(1), 35–40. https://doi.org/10.4103/ijn.IJN_2_16

Sakura, M., Masuda, H., Matsuoka, Y., Yokoyama, M., Kawakami, S., & Kihara, K. (2009). Rolipram, a specific type-4 phosphodiesterase inhibitor, inhibits cyclophosphamide-induced haemorrhagic cystitis in rats. *BJU International*, *103*(2), 264–269. https://doi.org/10.1111/j.1464-410X.2008.07948.x

Sanquer, S., Breil, M., Baron, C., Dhamane, D., Astier, A., & Lang, P. (1999). Induction of inosine monophosphate dehydrogenase activity after long-term treatment with mycophenolate mofetil. *Clinical Pharmacology and Therapeutics*, *65*(6), 640–648. https://doi.org/10.1016/S0009-9236(99)90085-1

Sawamoto, T., Van Gelder, T., Christians, U., Okamura, N., Jacobsen, W., & Benet, L. (2001). Membrane transport of mycophenolate mofetil and its active metabolite, mycophenolic acid in MDCK and MDR1-MDCK cell monolayers. *The Journal of Heart and Lung Transplantation*, *20*(2), 234–235. https://doi.org/10.1016/S1053-2498(00)00525-8

Scalzotto, E., Corradi, V., Salin, A., Caprara, C., Skoumal, R., Neri, A., Cannone, M., Frigo, A., Chiaramonte, S., Ferrari, F., & Ronco, C. (2017). Single Nucleotide Polymorphism Profiles of Patients with Acute Renal Rejection to Personalize Immunosuppressive Therapy: Preliminary Results from An On-Going, Italian Study. *Journal of Organ Transplantation*, *1*(1), 17–31. https://doi.org/10.14302/issn.2576-9359.jot-17-1603

Schaier, M., Scholl, C., Scharpf, D., Schmitt, W. H., Schwenger, V., Zeier, M., & Sommerer, C. (2015). High interpatient variability in response to mycophenolic acid maintenance therapy in patients with ANCA-associated vasculitis. *Nephrology Dialysis Transplantation*, *30*(suppl_1), i138–i145. https://doi.org/10.1093/ndt/gfv065

Schütz, E., Armstrong, V. W., Shipkova, M., Weber, L., Niedmann, P. D., Lammersdorf, T., Wiesel, M., Mandelbaum, A., Zimmerhackl, L. B., Mehls, O., Tönshoff, B., & Oellerich, M. (1998). Limited sampling strategy for the determination of mycophenolic acid area under the curve in pediatric kidney recipients. German Study Group on MMF Therapy in Pediatric Renal Transplant Recipients. *Transplantation Proceedings*, *30*(4), 1182–1184. https://doi.org/10.1016/s0041-1345(98)00200-0

Senejani, A. G., Liu, Y., Kidane, D., Maher, S. E., Zeiss, C. J., Park, H.-J., Kashgarian, M., McNiff, J. M., Zelterman, D., Bothwell, A. L. M., & Sweasy, J. B. (2014). Mutation of POLB Causes Lupus in Mice. *Cell Reports*, *6*(1), 1–8. https://doi.org/10.1016/j.celrep.2013.12.017

Shao, W.-H., & Cohen, P. L. (2011). Disturbances of apoptotic cell clearance in systemic lupus erythematosus. *Arthritis Research & Therapy*, *13*(1), 202. https://doi.org/10.1186/ar3206

Shigesaka, M., Ito, T., Inaba, M., Imai, K., Yamanaka, H., Azuma, Y., Tanaka, A., Amuro, H., Nishizawa, T., Son, Y., Satake, A., Ozaki, Y., & Nomura, S. (2020). Mycophenolic acid, the active form of mycophenolate mofetil, interferes with IRF7 nuclear translocation and type I IFN production by plasmacytoid dendritic cells. *Arthritis Research & Therapy*, *22*, 264. https://doi.org/10.1186/s13075-020-02356-z

Shipp, M. A., Ross, K. N., Tamayo, P., Weng, A. P., Kutok, J. L., Aguiar, R. C. T., Gaasenbeek, M., Angelo, M., Reich, M., Pinkus, G. S., Ray, T. S., Koval, M. A., Last, K. W., Norton, A., Lister, T. A., Mesirov, J., Neuberg, D. S., Lander, E. S., Aster, J. C., & Golub, T. R. (2002). Diffuse large B-cell lymphoma outcome prediction by gene-expression profiling

and supervised machine learning. *Nature Medicine*, *8*(1), 68–74. https://doi.org/10.1038/nm0102-68

Shu, Q., Fan, Q., Hua, B., Liu, H., Wang, S., Liu, Y., Yao, Y., Xie, H., & Ge, W. (2021). Influence of SLCO1B1 521T>C, UGT2B7 802C>T and IMPDH1 −106G>A Genetic Polymorphisms on Mycophenolic Acid Levels and Adverse Reactions in Chinese Autoimmune Disease Patients. *Pharmacogenomics and Personalized Medicine*, *14*, 713–722. https://doi.org/10.2147/PGPM.S295964

Shu, W., Chen, L., Hu, X., Zhang, M., Chen, W., Ma, L., Liu, X., Huang, J., Pang, T., Li, J., & Zhang, Y. (2017). Cytochrome P450 Genetic Variations Can Predict mRNA Expression, Cyclophosphamide 4-Hydroxylation, and Treatment Outcomes in Chinese Patients With Non-Hodgkin's Lymphoma. *The Journal of Clinical Pharmacology*, *57*(7), 886–898. https://doi.org/10.1002/jcph.878

Shu, W., Guan, S., Yang, X., Liang, L., Li, J., Chen, Z., Zhang, Y., Chen, L., Wang, X., & Huang, M. (2016). Genetic markers in CYP2C19 and CYP2B6 for prediction of cyclophosphamide's 4-hydroxylation, efficacy and side effects in Chinese patients with systemic lupus erythematosus. *British Journal of Clinical Pharmacology*, *81*(2), 327–340. https://doi.org/10.1111/bcp.12800

Sibley, J. T., Haug, B. L., & Lee, J. S. (1989). Altered metabolism of poly(adp-ribose) in the peripheral blood lymphocytes of patients with systemic lupus erythematosus. *Arthritis & Rheumatism*, *32*(8), 1045–1049. https://doi.org/10.1002/anr.1780320815

Silva, I. U. D., McHugh, P. J., Clingen, P. H., & Hartley, J. A. (2000). Defining the Roles of Nucleotide Excision Repair and Recombination in the Repair of DNA Interstrand Cross-Links in Mammalian Cells. *Molecular and Cellular Biology*, *20*(21), 7980–7990. https://doi.org/10.1128/MCB.20.21.7980-7990.2000

Sládek, N. E., Kollander, R., Sreerama, L., & Kiang, D. T. (2002). Cellular levels of aldehyde dehydrogenases (ALDH1A1 and ALDH3A1) as predictors of therapeutic responses to cyclophosphamide-based chemotherapy of breast cancer: A retrospective study. *Cancer Chemotherapy and Pharmacology*, *49*(4), 309–321. https://doi.org/10.1007/s00280-001-0412-4

Smak Gregoor, P. J. H., de Sévaux, R. G. L., Hené, R. J., Hesse, C. J., Hilbrands, L. B., Vos, P., van Gelder, T., Hoitsma, A. J., & Weimar, W. (1999). EFFECT OF CYCLOSPORINE ON MYCOPHENOLIC ACID TROUGH LEVELS IN KIDNEY TRANSPLANT RECIPIENTS1. *Transplantation*, *68*(10), 1603.

Sobeck, A., Stone, S., Costanzo, V., de Graaf, B., Reuter, T., de Winter, J., Wallisch, M., Akkari, Y., Olson, S., Wang, W., Joenje, H., Christian, J. L., Lupardus, P. J., Cimprich, K. A., Gautier, J., & Hoatlin, M. E. (2006). Fanconi Anemia Proteins Are Required To Prevent Accumulation of Replication-Associated DNA Double-Strand Breaks. *Molecular and Cellular Biology*, *26*(2), 425–437. https://doi.org/10.1128/MCB.26.2.425-437.2006

Sobiak, J., Jóźwiak, A., Wziętek, H., Zachwieja, J., & Ostalska-Nowicka, D. (2020). The Application of Inosine 5′-Monophosphate Dehydrogenase Activity Determination in Peripheral Blood Mononuclear Cells for Monitoring Mycophenolate Mofetil Therapy in

Children with Nephrotic Syndrome. *Pharmaceuticals*, *13*(8), 200. https://doi.org/10.3390/ph13080200

Sobiak, J., Resztak, M., Zachwieja, J., & Ostalska-Nowicka, D. (2022). Inosine monophosphate dehydrogenase activity and mycophenolate pharmacokinetics in children with nephrotic syndrome treated with mycophenolate mofetil. *Clinical and Experimental Pharmacology and Physiology*, *49*(11), 1197–1208. https://doi.org/10.1111/1440-1681.13706

Sommerer, C., Müller-Krebs, S., Schaier, M., Glander, P., Budde, K., Schwenger, V., Mikus, G., & Zeier, M. (2010). Pharmacokinetic and pharmacodynamic analysis of enteric-coated mycophenolate sodium: Limited sampling strategies and clinical outcome in renal transplant patients. *British Journal of Clinical Pharmacology*, *69*(4), 346–357. https://doi.org/10.1111/j.1365-2125.2009.03612.x

Souliotis, V. L., Vougas, K., Gorgoulis, V. G., & Sfikakis, P. P. (2016). Defective DNA repair and chromatin organization in patients with quiescent systemic lupus erythematosus. *Arthritis Research & Therapy*, *18*. https://doi.org/10.1186/s13075-016-1081-3

Staatz, C. E., & Tett, S. E. (2007). Clinical Pharmacokinetics and Pharmacodynamics of Mycophenolate in Solid Organ Transplant Recipients. *Clinical Pharmacokinetics*, *46*(1), 13–58. https://doi.org/10.2165/00003088-200746010-00002

Stern, S. T., Tallman, M. N., Miles, K. K., Ritter, J. K., Dupuis, R. E., & Smith, P. C. (2007). Gender-related differences in mycophenolate mofetil-induced gastrointestinal toxicity in rats. *Drug Metabolism and Disposition: The Biological Fate of Chemicals*, *35*(3), 449–454. https://doi.org/10.1124/dmd.106.012013

Stojan, G., & Petri, M. (2018). Epidemiology of Systemic Lupus Erythematosus: An update. *Current Opinion in Rheumatology*, *30*(2), 144–150. https://doi.org/10.1097/BOR.0000000000000480

Struck, R. F., Kirk, M. C., Witt, M. H., & Russell, W. L. (1975). Isolation and mass spectral identification of blood metabolities of cyclophosphamide: Evidence for phosphoramide mustard as the biologically active metabolite. *Biomedical Mass Spectrometry*, *2*(1), 46–52. https://doi.org/10.1002/bms.1200020109

Sugiyama, K., Isogai, K., Toyama, A., Satoh, H., Saito, K., Nakagawa, Y., Tasaki, M., Takahashi, K., Saito, N., & Hirano, T. (2008). Pharmacodynamic Parameters of Immunosuppressive Drugs Are Not Correlated with Age, Duration of Dialysis, Percentage of Lymphocytes or Lymphocyte Stimulation Index in Renal Transplant Recipients. *Biological and Pharmaceutical Bulletin*, *31*(11), 2146–2149. https://doi.org/10.1248/bpb.31.2146

Sutherland, J. C., & Griffin, K. P. (1981). Absorption Spectrum of DNA for Wavelengths Greater than 300 nm. *Radiation Research*, *86*(3), 399–410. https://doi.org/10.2307/3575456

Sweeney, C., Ambrosone, C. B., Joseph, L., Stone, A., Hutchins, L. F., Kadlubar, F. F., & Coles, B. F. (2003). Association between a glutathione S-transferase A1 promoter polymorphism and survival after breast cancer treatment. *International Journal of Cancer*, *103*(6), 810–814. https://doi.org/10.1002/ijc.10896

Swiecki, M., & Colonna, M. (2010). Unraveling the functions of plasmacytoid dendritic cells during viral infections, autoimmunity, and tolerance. *Immunological Reviews*, *234*(1), 142–162. https://doi.org/10.1111/j.0105-2896.2009.00881.x

Swift, L. H., & Golsteyn, R. M. (2014). Genotoxic anti-cancer agents and their relationship to DNA damage, mitosis, and checkpoint adaptation in proliferating cancer cells. *International Journal of Molecular Sciences*, *15*(3), 3403–3431. https://doi.org/10.3390/ijms15033403

Szczypka, M. (2020). Role of Phosphodiesterase 7 (PDE7) in T Cell Activity. Effects of Selective PDE7 Inhibitors and Dual PDE4/7 Inhibitors on T Cell Functions. *International Journal of Molecular Sciences*, *21*(17), 6118. https://doi.org/10.3390/ijms21176118

Takada, K., Arefayene, M., Desta, Z., Yarboro, C. H., Boumpas, D. T., Balow, J. E., Flockhart, D. A., & Illei, G. G. (2004). Cytochrome P450 pharmacogenetics as a predictor of toxicity and clinical response to pulse cyclophosphamide in lupus nephritis. *Arthritis & Rheumatism*, *50*(7), 2202–2210. https://doi.org/10.1002/art.20338

Takahashi, K., Ochiai, T., Uchida, K., Yasumura, T., Ishibashi, M., Suzuki, S., Otsubo, O., Isono, K., Takagi, H., & Oka, T. (1995). Pilot study of mycophenolate mofetil (RS-61443) in the prevention of acute rejection following renal transplantation in Japanese patients. RS-61443 Investigation Committee—Japan. *Transplantation Proceedings*, *27*(1), 1421–1424.

Tan, E. M., Cohen, A. S., Fries, J. F., Masi, A. T., Mcshane, D. J., Rothfield, N. F., Schaller, J. G., Talal, N., & Winchester, R. J. (1982). The 1982 revised criteria for the classification of systemic lupus erythematosus. *Arthritis & Rheumatism*, *25*(11), 1271–1277. https://doi.org/10.1002/art.1780251101

Tan, T. C., Fang, H., Magder, L. S., & Petri, M. A. (2012). Differences between Male and Female Systemic Lupus Erythematosus in a Multiethnic Population. *The Journal of Rheumatology*. https://doi.org/10.3899/jrheum.111061

Tang, J., de Winter, B. C., Hesselink, D. A., Sombogaard, F., Wang, L., & van Gelder, T. (2017). The pharmacokinetics and pharmacodynamics of mycophenolate mofetil in younger and elderly renal transplant recipients. *British Journal of Clinical Pharmacology*, *83*(4), 812–822. https://doi.org/10.1111/bcp.13154

Tang, M., Wang, H., Hu, Y., Chen, W.-S., Akao, M., Feng, Z., & Hu, W. (2011). Acrolein induced DNA damage, mutagenicity and effect on DNA repair. *Molecular Nutrition & Food Research*, *55*(9), 1291–1300. https://doi.org/10.1002/mnfr.201100148

Tektonidou, M. G., Dasgupta, A., & Ward, M. M. (2016). Risk of End-Stage Renal Disease in Patients With Lupus Nephritis, 1971–2015: A Systematic Review and Bayesian Meta-Analysis. *Arthritis & Rheumatology*, *68*(6), 1432–1441. https://doi.org/10.1002/art.39594

Thanei, S., & Trendelenburg, M. (2016). Anti-C1q Autoantibodies from Systemic Lupus Erythematosus Patients Induce a Proinflammatory Phenotype in Macrophages. *Journal of Immunology (Baltimore, Md.: 1950)*, *196*(5), 2063–2074. https://doi.org/10.4049/jimmunol.1501659

Thapa, P., & Farber, D. L. (2019). The role of the thymus in the immune response. *Thoracic Surgery Clinics*, *29*(2), 123–131. https://doi.org/10.1016/j.thorsurg.2018.12.001

Thomas, E. C., Gunter, J. H., Webster, J. A., Schieber, N. L., Oorschot, V., Parton, R. G., & Whitehead, J. P. (2012). Different characteristics and nucleotide binding properties of inosine monophosphate dehydrogenase (IMPDH) isoforms. *PloS One*, *7*(12), e51096. https://doi.org/10.1371/journal.pone.0051096

Thomas, R., & Jawad, A. S. (2022). Systemic lupus erythematosus: Rarer in men than women but more severe. *Trends in Urology & Men's Health*, *13*(5), 11–14. https://doi.org/10.1002/tre.876

Tian, M., Song, X., Dong, L., Xin, X., & Dong, J. (2017). Systematic evaluation of different doses of cyclophosphamide induction therapy for lupus nephritis. *Medicine*, *96*(51). https://doi.org/10.1097/MD.0000000000009408

Timm, R., Kaiser, R., Lötsch, J., Heider, U., Sezer, O., Weisz, K., Montemurro, M., Roots, I., & Cascorbi, I. (2005). Association of cyclophosphamide pharmacokinetics to polymorphic cytochrome P450 2C19. *The Pharmacogenomics Journal*, *5*(6), 365–373. https://doi.org/10.1038/sj.tpj.6500330

Tisdale, M. J. (1977). Interaction of cyclophosphamide and its metabolites with adenosine 3',5'-monophosphate binding proteins. *Biochemical Pharmacology*, *26*(16), 1469–1474. https://doi.org/10.1016/0006-2952(77)90417-8

Traverso, I., Fenoglio, D., Negrini, S., Parodi, A., Battaglia, F., Kalli, F., Conteduca, G., Tardito, S., Traverso, P., Indiveri, F., & Filaci, G. (2012). Cyclophosphamide inhibits the generation and function of CD8(+) regulatory T cells. *Human Immunology*, *73*(3), 207–213. https://doi.org/10.1016/j.humimm.2011.12.020

Tsai-Turton, M., Luong, B. T., Tan, Y., & Luderer, U. (2007). Cyclophosphamide-induced apoptosis in COV434 human granulosa cells involves oxidative stress and glutathione depletion. *Toxicological Sciences: An Official Journal of the Society of Toxicology*, *98*(1), 216–230. https://doi.org/10.1093/toxsci/kfm087

Tulsyan, S., Agarwal, G., Lal, P., & Mittal, B. (2014). Significant role of CYP450 genetic variants in cyclophosphamide based breast cancer treatment outcomes: A multi-analytical strategy. *Clinica Chimica Acta*, *434*, 21–28. https://doi.org/10.1016/j.cca.2014.04.009

Uhlen, M., Karlsson, M. J., Zhong, W., Tebani, A., Pou, C., Mikes, J., Lakshmikanth, T., Forsström, B., Edfors, F., Odeberg, J., Mardinoglu, A., Zhang, C., von Feilitzen, K., Mulder, J., Sjöstedt, E., Hober, A., Oksvold, P., Zwahlen, M., Ponten, F., … Brodin, P. (2019). A genome-wide transcriptomic analysis of protein-coding genes in human blood cells. *Science (New York, N.Y.)*, *366*(6472), eaax9198. https://doi.org/10.1126/science.aax9198

Uwai, Y., Motohashi, H., Tsuji, Y., Ueo, H., Katsura, T., & Inui, K. (2007). Interaction and transport characteristics of mycophenolic acid and its glucuronide via human organic anion transporters hOAT1 and hOAT3. *Biochemical Pharmacology*, *74*(1), 161–168. https://doi.org/10.1016/j.bcp.2007.03.024

Uzair, B., Khan, B. A., Sharif, N., Shabbir, F., & Menaa, F. (2018). Phosphodiesterases (PDEs) from Snake Venoms: Therapeutic Applications. *Protein and Peptide Letters*, *25*(7), 612–618. https://doi.org/10.2174/0929866525666180628160616

Valente, E. J., Chan, K. K., & Servis, K. L. (1984). Proton magnetic resonance studies of the decomposition of 4-hydroxycyclophosphamide, a microsomal metabolite of cyclophosphamide. *Pharmaceutical Research*, *1*(2), 89–92. https://doi.org/10.1023/A:1016307515811

Valeri, A., Radhakrishnan, J., Estes, D., D'Agati, V., Kopelman, R., Pernis, A., Flis, R., Pirani, C., & Appel, G. B. (1994). Intravenous pulse cyclophosphamide treatment of severe lupus nephritis: A prospective five-year study. *Clinical Nephrology*, *42*(2), 71–78.

van Gelder, T., Hilbrands, L. B., Vanrenterghem, Y., Weimar, W., de Fijter, J. W., Squifflet, J. P., Hené, R. J., Verpooten, G. A., Navarro, M. T., Hale, M. D., & Nicholls, A. J. (1999). A randomized double-blind, multicenter plasma concentration controlled study of the safety and efficacy of oral mycophenolate mofetil for the prevention of acute rejection after kidney transplantation. *Transplantation*, *68*(2), 261–266. https://doi.org/10.1097/00007890-199907270-00018

van Hest, R. M., van Gelder, T., Vulto, A. G., & Mathot, R. A. A. (2005). Population Pharmacokinetics of Mycophenolic Acid in Renal Transplant Recipients. *Clinical Pharmacokinetics*, *44*(10), 1083–1096. https://doi.org/10.2165/00003088-200544100-00006

van Kan, M., Burns, K. E., Browett, P., & Helsby, N. A. (2019). A higher throughput assay for quantification of melphalan-induced DNA damage in peripheral blood mononuclear cells. *Scientific Reports*, *9*(1), 1–8. https://doi.org/10.1038/s41598-019-55161-3

Veal, G. J., Cole, M., Chinnaswamy, G., Sludden, J., Jamieson, D., Errington, J., Malik, G., Hill, C. R., Chamberlain, T., & Boddy, A. V. (2016). Cyclophosphamide pharmacokinetics and pharmacogenetics in children with B-cell non-Hodgkin's lymphoma. *European Journal of Cancer*, *55*, 56–64. https://doi.org/10.1016/j.ejca.2015.12.007

Vethe, N. T., Ali, A. M., Reine, P. A., Andersen, A. M., Bremer, S., Line, P.-D., Rootwelt, H., & Bergan, S. (2014). Simultaneous Quantification of IMPDH Activity and Purine Bases in Lymphocytes Using LC-MS/MS: Assessment of Biomarker Responses to Mycophenolic Acid. *Therapeutic Drug Monitoring*, *36*(1), 108–118. https://doi.org/10.1097/FTD.0b013e3182a13900

Vethe, N. T., Bremer, S., Rootwelt, H., & Bergan, S. (2008). Pharmacodynamics of Mycophenolic Acid in CD4+ Cells: A Single-Dose Study of IMPDH and Purine Nucleotide Responses in Healthy Individuals. *Therapeutic Drug Monitoring*, *30*(6), 647–655. https://doi.org/10.1097/FTD.0b013e31818955c3

Vigone, G., Shuhaibar, L. C., Egbert, J. R., Uliasz, T. F., Movsesian, M. A., & Jaffe, L. A. (2018). Multiple cAMP Phosphodiesterases Act Together to Prevent Premature Oocyte Meiosis and Ovulation. *Endocrinology*, *159*(5), 2142–2152. https://doi.org/10.1210/en.2018-00017

Villanueva, E., Yalavarthi, S., Berthier, C. C., Hodgin, J. B., Khandpur, R., Lin, A. M., Rubin, C. J., Zhao, W., Olsen, S. H., Klinker, M., Shealy, D., Denny, M. F., Plumas, J., Chaperot, L., Kretzler, M., Bruce, A. T., & Kaplan, M. J. (2011). Netting neutrophils induce endothelial damage, infiltrate tissues, and expose immunostimulatory molecules in systemic lupus erythematosus. *Journal of Immunology (Baltimore, Md.: 1950)*, *187*(1), 538–552. https://doi.org/10.4049/jimmunol.1100450

Voelcker, G. (2017). Enzyme Catalyzed Decomposition of 4-Hydroxycyclophosphamide. *The Open Conference Proceedings Journal*, *8*(1), 44–51. https://doi.org/10.2174/2210289201708010044

Voelcker, G., Bielicki, L., & Hohorst, H. J. (1981). Evidence for enzymatic toxification of activated cyclophosphamide (4-hydroxycyclophosphamide). *Journal of Cancer Research and Clinical Oncology*, *99*(3), A58–A59. https://doi.org/10.1007/BF00405237

von Eitzen, U., Meier-Tackmann, D., Agarwal, D. P., & Goedde, H. W. (1994). Detoxification of cyclophosphamide by human aldehyde dehydrogenase isozymes. *Cancer Letters*, *76*(1), 45–49. https://doi.org/10.1016/0304-3835(94)90132-5

von Vietinghoff, S., Ouyang, H., & Ley, K. (2010). Mycophenolic acid suppresses granulopoiesis by inhibition of interleukin-17 production. *Kidney International*, *78*(1), 79–88. https://doi.org/10.1038/ki.2010.84

Vukovic, V., Karan-Djurasevic, T., Antic, D., Tosic, N., Kostic, T., Marjanovic, I., Dencic-Fekete, M., Djurasinovic, V., Pavlovic, S., & Mihaljevic, B. (2019). Association of SLC28A3 Gene Expression and CYP2B6*6 Allele with the Response to Fludarabine Plus Cyclophosphamide in Chronic Lymphocytic Leukemia Patients. *Pathology & Oncology Research*. https://doi.org/10.1007/s12253-019-00613-4

WANG, H., REN, Y., CHANG, J., GU, L., & SUN, L.-Y. (2017). A Systematic Review and Meta-analysis of Prevalence of Biopsy-Proven Lupus Nephritis. *Archives of Rheumatology*, *33*(1), 17–25. https://doi.org/10.5606/ArchRheumatol.2017.6127

Wang, J., Figurski, M., Shaw, L. M., & Burckart, G. J. (2008). The impact of P-glycoprotein and Mrp2 on mycophenolic acid levels in mice. *Transplant Immunology*, *19*(3–4), 192–196. https://doi.org/10.1016/j.trim.2008.05.009

Wang, J., Yang, J. W., Zeevi, A., Webber, S. A., Girnita, D. M., Selby, R., Fu, J., Shah, T., Pravica, V., Hutchinson, I. V., & Burckart, G. J. (2008). IMPDH1 gene polymorphisms and association with acute rejection in renal transplant patients. *Clinical Pharmacology and Therapeutics*, *83*(5), 711–717. https://doi.org/10.1038/sj.clpt.6100347

Wang, J., Zeevi, A., Webber, S., Girnita, D. M., Addonizio, L., Selby, R., Hutchinson, I. V., & Burckart, G. J. (2007). A novel variant L263F in human inosine 5'-monophosphate dehydrogenase 2 is associated with diminished enzyme activity. *Pharmacogenetics and Genomics*, *17*(4), 283–290. https://doi.org/10.1097/FPC.0b013e328012b8cf

Wang, P., Wu, P., Ohleth, K. M., Egan, R. W., & Billah, M. M. (1999). Phosphodiesterase 4B2 is the predominant phosphodiesterase species and undergoes differential regulation of gene expression in human monocytes and neutrophils. *Molecular Pharmacology*, *56*(1), 170–174. https://doi.org/10.1124/mol.56.1.170

Weeda, G., Donker, I., de Wit, J., Morreau, H., Janssens, R., Vissers, C. J., Nigg, A., van Steeg, H., Bootsma, D., & Hoeijmakers, J. H. J. (1997). Disruption of mouse ERCC1 results in a novel repair syndrome with growth failure, nuclear abnormalities and senescence. *Current Biology*, *7*(6), 427–439. https://doi.org/10.1016/S0960-9822(06)00190-4

Wei, D., Fabris, D., & Fenselau, C. (1999). Covalent Sequestration of Phosphoramide Mustard by Metallothionein—An In Vitro Study. *Drug Metabolism and Disposition*, *27*(7), 786–791.

Wieland, E., Shipkova, M., Schellhaas, U., Schütz, E., Niedmann, P. D., Armstrong, V. W., & Oellerich, M. (2000). Induction of cytokine release by the acyl glucuronide of mycophenolic acid: A link to side effects? *Clinical Biochemistry*, *33*(2), 107–113. https://doi.org/10.1016/S0009-9120(99)00101-0

Winnicki, W., Weigel, G., Sunder-Plassmann, G., Bajari, T., Winter, B., Herkner, H., & Sengoelge, G. (2010). An inosine 5′-monophosphate dehydrogenase 2 single-nucleotide polymorphism impairs the effect of mycophenolic acid. *The Pharmacogenomics Journal*, *10*(1), Article 1. https://doi.org/10.1038/tpj.2009.43

Winoto, J., Song, H., Hines, C., Nagaraja, H., & Rovin, B. H. (2011). Cytochrome P450 polymorphisms and the response of lupus nephritis to cyclophosphamide therapy. *Clinical Nephrology*, *75*(05), 451–457. https://doi.org/10.5414/CN106886

Wolff, N. A., Burckhardt, B. C., Burckhardt, G., Oellerich, M., & Armstrong, V. W. (2007). Mycophenolic acid (MPA) and its glucuronide metabolites interact with transport systems responsible for excretion of organic anions in the basolateral membrane of the human kidney. *Nephrology Dialysis Transplantation*, *22*(9), 2497–2503. https://doi.org/10.1093/ndt/gfm219

Wu, L., Adams, M., Parton, S., & Schafer, P. (2012). Phosphodiesterase 4 Expression in Rheumatoid Arthritis Synovium and Anti-Inflammatory Effects of Apremilast On Synovial Fibroblasts. *ACR Meeting Abstracts*, A51.

Wu, T.-Y., Peng, Y., Pelleymounter, L. L., Moon, I., Eckloff, B. W., Wieben, E. D., Yee, V. C., & Weinshilboum, R. M. (2010). Pharmacogenetics of the mycophenolic acid targets inosine monophosphate dehydrogenases IMPDH1 and IMPDH2: Gene sequence variation and functional genomics. *British Journal of Pharmacology*, *161*(7), 1584–1598. https://doi.org/10.1111/j.1476-5381.2010.00987.x

Xie, H., Griskevicius, L., Ståhle, L., Hassan, Z., Yasar, Ü., Rane, A., Broberg, U., Kimby, E., & Hassan, M. (2006). Pharmacogenetics of cyclophosphamide in patients with hematological malignancies. *European Journal of Pharmaceutical Sciences*, *27*(1), 54–61. https://doi.org/10.1016/j.ejps.2005.08.008

Xie, H.-J., Yasar, Ü., Lundgren, S., Griskevicius, L., Terelius, Y., Hassan, M., & Rane, A. (2003). Role of polymorphic human CYP2B6 in cyclophosphamide bioactivation. *The Pharmacogenomics Journal*, *3*(1), 53–61. https://doi.org/10.1038/sj.tpj.6500157

Xiong, Y., Liu, T., Wang, S., Chi, H., Chen, C., & Zheng, J. (2017). Cyclophosphamide promotes the proliferation inhibition of mouse ovarian granulosa cells and premature ovarian failure by activating the lncRNA-Meg3-p53-p66Shc pathway. *Gene*. https://doi.org/10.1016/j.gene.2016.10.011

Yan, B., Ye, S., Chen, G., Kuang, M., Shen, N., & Chen, S. (2008). Dysfunctional CD4+,CD25+ regulatory T cells in untreated active systemic lupus erythematosus secondary to interferon-alpha-producing antigen-presenting cells. *Arthritis and Rheumatism*, *58*(3), 801–812. https://doi.org/10.1002/art.23268

Yao, S., Sucheston, L. E., Zhao, H., Barlow, W. E., Zirpoli, G., Liu, S., Moore, H. C. F., Budd, G. T., Hershman, D. L., Davis, W., Ciupak, G. L., Stewart, J. A., Isaacs, C., Hobday, T. J., Salim, M., Hortobagyi, G. N., Gralow, J. R., Livingston, R. B., Albain, K. S., … Ambrosone, C. B. (2014). Germline genetic variants in ABCB1, ABCC1, and ALDH1A1 and risk of hematological and gastrointestinal toxicities in a SWOG Phase III trial S0221 for breast cancer. *The Pharmacogenomics Journal*, *14*(3), 241–247. https://doi.org/10.1038/tpj.2013.32

Yap, D. Y. H., Tang, C. S. O., Ma, M. K. M., Lam, M. F., & Chan, T. M. (2012). Survival analysis and causes of mortality in patients with lupus nephritis. *Nephrology, Dialysis, Transplantation: Official Publication of the European Dialysis and Transplant Association - European Renal Association*, *27*(8), 3248–3254. https://doi.org/10.1093/ndt/gfs073

Yee, J., Hwang, H. S., Chung, J. E., Park, J. Y., Lee, K. E., Kim, Y. J., & Gwak, H. S. (2019). Effects of PDE4 gene polymorphisms on efficacy and adverse drug events of ritodrine therapy in preterm labor patients: A prospective observational study. *European Journal of Clinical Pharmacology*, *75*(10), 1379–1386. https://doi.org/10.1007/s00228-019-02719-9

Yigitaslan, S., Ozatik, O., Ozatik, F. Y., Erol, K., Sirmagul, B., & Baseskioglu, A. B. (2014). Effects of tadalafil on hemorrhagic cystitis and testicular dysfunction induced by cyclophosphamide in rats. *Urologia Internationalis*, *93*(1), 55–62. https://doi.org/10.1159/000352095

Yildirim-Toruner, C., & Diamond, B. (2011). Current and Novel Therapeutics in Treatment of SLE. *The Journal of Allergy and Clinical Immunology*, *127*(2), 303–314. https://doi.org/10.1016/j.jaci.2010.12.1087

Yin, S., Mao, Y., Li, X., Yue, C., Zhou, C., Huang, L., Mo, W., Liang, D., Zhang, J., He, W., & Zhang, X. (2015). Hyperactivation and in situ recruitment of inflammatory Vδ2 T cells contributes to disease pathogenesis in systemic lupus erythematosus. *Scientific Reports*, *5*, 14432. https://doi.org/10.1038/srep14432

Yoshida, A. (1992). Molecular genetics of human aldehyde dehydrogenase. *Pharmacogenetics*, *2*(4), 139–147.

Zhang, J., Tian, Q., Chan, S. Y., Li, S. C., Zhou, S., Duan, W., & Zhu, Y.-Z. (2005). Metabolism and Transport of Oxazaphosphorines and the Clinical Implications. *Drug Metabolism Reviews*, *37*(4), 611–703. https://doi.org/10.1080/03602530500364023

Zhang, N., & Bevan, M. J. (2011). CD8+ T Cells: Foot Soldiers of the Immune System. *Immunity*, *35*(2), 161–168. https://doi.org/10.1016/j.immuni.2011.07.010

Zhao, J., Cao, Y., Lei, Z., Yang, Z., Zhang, B., & Huang, B. (2010). Selective Depletion of CD4+CD25+Foxp3+ Regulatory T Cells by Low-Dose Cyclophosphamide Is Explained by Reduced Intracellular ATP Levels. *Cancer Research*, *70*(12), 4850–4858. https://doi.org/10.1158/0008-5472.CAN-10-0283

Zhou, J., Tao, M.-J., Jin, L.-R., Sheng, J., Li, Z., Peng, H., Xu, L., & Yuan, H. (2020). Effectiveness and safety of common therapeutic drugs for refractory lupus nephritis: A network meta-analysis. *Experimental and Therapeutic Medicine*, *19*(1), 665–671. https://doi.org/10.3892/etm.2019.8257

Zhou S., Qin L., Liu S., Liu L., Zhang Y., Zhang H., Wang C., Huang M., & Li J. (2018). Associations of IMPDH1 polymorphisms with pharmacodynamics of mycophenolic acid in renal transplant patients. *Acta Pharmaceutica Sinica*, 765–770.

Zon, G., Ludeman, S. M., Brandt, J. A., Boyd, V. L., Ozkan, G., Egan, W., & Shao, K. L. (1984). NMR spectroscopic studies of intermediary metabolites of cyclophosphamide. A comprehensive kinetic analysis of the interconversion of cis- and trans-4-hydroxycyclophosphamide with aldophosphamide and the concomitant partitioning of aldophosphamide between irreversible fragmentation and reversible conjugation pathways. *Journal of Medicinal Chemistry*, *27*(4), 466–485. https://doi.org/10.1021/jm00370a008